UNIVERSITY OF OKLAHOMA

GRADUATE COLLEGE

DIMENSIONAL STABILITY OF CONCRETE SLABS ON GRADE

A DISSERTATION

SUBMITTED TO THE GRADUATE FACULTY

in partial fulfillment of the requirements for the

Degree of

DOCTOR OF PHILOSOPHY

By

SHIDEH SHADRAVAN
Norman, Oklahoma
2011

DIMENSIONAL STABILITY OF CONCRETE SLABS ON GRADE

A DISSERTATION APPROVED FOR THE
SCHOOL OF CIVIL ENGINEERING AND ENVIRONMENTAL SCIENCE

BY

____
Dr. Christopher C. Ramseyer, Chair

____
Dr. Curtis C. Mc Knight

____
Dr. Jinsong Pei

____
Dr. Thomas H. Kang

____
Dr. Lisa M. Holliday

DEDICATION

To my parents who raised both me and my children, and who provided substantial encouragement to me throughout my pursuit for education. Also to my loving husband and my dearest sons who gave me continuous support. And to my brother who has always been there for me. Without their support, this work would not have been possible.

ACKNOWLEDGMENTS

I would like to thank everyone who offered guidance and encouragement to me during this study.

First, I wish to express my deep gratitude to Dr. Chris Ramseyer, my research advisor, for his enormous support, valuable comments, interest, helpful guidance, and inspiring discussions encouraging my work, and above all, for his faith in my effort and in my success as a PhD candidate. I am forever grateful to my advisor, Dr. Ramseyer.

I would like to express my sincere thanks to Dr. Curtis Mc Knight, for the guidance extended to me with his field of expertise. My appreciation is extended to Dr. Jinsong Pei, Dr. Thomas Kang, and Dr. Lisa Holliday, not only for serving as members of my PhD committee, but also for their assistance, valuable ideas, and constant encouragement and support. I would also appreciate Dr. Kyran Mish for his support during my PhD program. I will always be thankful for their help.

Sincere thanks are due to CTS Cement Manufacturing Corporation for providing funding for lab construction and the materials for this study, also for all encouraging and supporting me through this research.

I would also like to thank to the CEES faculty and staff, especially to Dr. Robert Knox, Dr. Amy Cerato, Ms. Susan Williams, Ms. Brenda Clouse and Ms. Audre Carter for their continuous help in many aspects throughout my PhD candidature.

I would like to thank Mike Schmitz the facility manager of Fears Structural Engineering Laboratory for helping and training me to use the lab equipment. My appreciation is extended to Patrick Crowder, Mark Emde, Chris Davis, David Frank, Chris Hill, Michael Rice, and Carlos Rincon who helped me build the Advanced Concrete Research Lab and for their help in the lab during the past three years of this research. My sincere thanks go to Dr. Priyantha Wijesinghe, Dr. Woosuk Kim, and Dr. Krisda Piyawat for their friendship and support during my PhD program.

Also, special thanks and appreciation to my mother, Maleehe Ragheb, and my father Bahram Shadravan for their love and hope, assistance, encouragement, and their support in every step of my achievements.

I wish to thank my caring husband Mahoor Pezeshkian and my two loving sons, Hamidreza and Pouria for supporting and encouraging me in this accomplishment. Last but not least, I would like to thank my dear brother whose advice and support has come a very long way for me.

I offer my regards and blessings to all of those who supported me in many ways during the completion of my dissertation. Without their constant support and encouragement this endeavor would not have been successful.

TABLE OF CONTENTS

LIST OF TABLES

LIST OF FIGURES

ABSTRACT

Drying shrinkage is one of the major causes of cracking in concrete slabs on grade. The moisture difference between the top and bottom surface of the slabs causes a dimensional or “shrinkage” gradient to develop through the depth of the slabs. This can cause cracks and warping which result in serviceability and performance problems for concrete slabs on grade. There have been numerous analytical and experimental investigations to characterize drying shrinkage as a material property. However, there have not been significant improvements in terms of validation and calibration to provide engineers with a reliable evaluation of the strains and stresses within a concrete element subjected to moisture gradients and restrained shrinkage.

This test program characterizes the dimensional properties of selected concrete materials, evaluating their performance as real slabs-on-grade in that they are exposed to ground moisture on the bottom surface and drying conditions on the top surface. The concrete mix designs examined included low and high strength concrete (PCC and HPC), typical Portland cement using two common types of shrinkage reducing admixtures (SRA+PCC), and Calcium sulfoaluminate cement (CSA). The data includes standard concrete material characterization tests, joint opening measurements, internal relative humidity and temperature in ½ in. increments through the depth of the slab, prism tests and compression test results. It was found that CSA is very stable, with no long term shrinkage, cracking or warping while typical PCC and HPC continue to show crack growth at over 600 days of age. Shrinkage Reducing Admixtures have a minor impact at early age but do not impact long term sectional stability. The SRA concrete exhibited

shrinkage, cracking and warping nearly similar to typical PCC but slightly better than HPC.

CHAPTER 1

Introduction

1.1. Background

Concrete has been used in United States since the 18th century. It has been utilized extensively in slabs, columns, and beams in buildings, dams and bridges. In the 1950's, concrete was used extensively to help build the strategic highway system and public roads. As cities grew, the American suburbs expanded and the use of automobiles increased. Consequently, automobile traffic has grown, and the need for additional interconnected ride systems to supplement the existing has become more important. In 2008, the United States had 4.04 million miles of highways, 3.9 million miles of public road, and 600,000 bridges (FHA, ARRA 2009). As construction of new roads developed the cost of maintaining existing roads has increased.

One of the major maintenance and repair problems with slabs on grade is caused by volumetric distortion of the slab and the subsequent cracking of the slab. The volumetric distortion of a slab on grade is caused by two types of environmental loads: curling (due to uneven temperature through the slab) and warping (due to uneven moisture through the slab). For this dissertation the following definitions will be used throughout: Curling is due to a temperature gradient through the depth of a slab and Warping is due to a moisture gradient through the depth of a slab. Please note that these definitions are typical to the research community even though the American Concrete Institute (ACI) refers to both phenomena as curling.

In the field of transportation engineering, volumetric distortion is a major problem because most of the states have both curling and warping problems with highway panels cast on grade. Curling and warping slowly degrades the ride characteristics and repeated vehicle forces on a curled and warped section generally will cause cracks to occur. Cracking and warping seriously reduces the productive and performance value of both indoor and outdoor slabs on grade. Consequently, cracking and warping affect the long-term strength and durability of slabs on grade. Hundreds of millions of dollars are being spent annually to repair the distortion of slab on grade and decks in bridges due to warping and cracking. An entire industry using diamond grinding and dowel bar retro-fitting has developed to address the symptoms of volumetric distortion.

Grinding the deformation is one of the common methods used to repair the symptoms of indoor and outdoor slab distortion. But grinding reduces the section depth and this can cause further problems such as poor serviceability in the future and it does not address the cause of the slab distortion. Over one hundred million dollars is spent on grinding each year. For instance, the state of California has the worst Interstate Highways, with 16.3 percent of rural and 24.7 percent of urban Interstates in poor or mediocre condition (FHA, ARRA 2009). The state of California spent over $ 31,000,000 for grinding in just one year treating the symptoms of volumetric distortion. Drying shrinkage, warping and joint opening of slabs-on-grade is a major concern in Oklahoma and across the country.

Drying shrinkage is one of the major causes of cracking in a concrete slab. Drying shrinkage is very difficult to predict because many parameters affect this phenomenon. Although many studies have been completed on concrete materials, there is very little data to provide a reliable evaluation of strains and stresses of restrained concrete slabs on grade. Additionally, there is not an acceptable method to evaluate drying shrinkage and warping tendency of a concrete slab on grade. Generally, the unrestrained length change method (ASTM C157) is used to evaluate concrete drying shrinkage, but this test ignores early age shrinkage, only evaluates a dry prism of concrete and as such does not provide any information concerning warping.

This research project provides a unique opportunity to improve our understanding of warping and our ability to predict its effects. This work provides an understanding of drying shrinkage, warping and joint opening performance of slab-on-grade pavement systems.

1.2. Research Objectives

The general objectives of this research are:

- to provide reliable warping data under controlled conditions for:
    - typical portland cement concrete
    - High Performance Concrete (HPC)
    - Portland cement concrete with two types of shrinkage reducing admixtures, and
    - calcium sulfoaluminate (CSA) cement
- to investigate a representative selection of shrinkage magnitudes for concrete

- to develop a better understanding of some of the tests being used to evaluate the properties of cementitious materials
    - Such as the ASTM C 157 length change test vs. ASTM C 879 length change test vs. the “shrinkage from time zero” test
- to characterize reliable performance criteria for the selection of materials used in slabs-on-grade where shrinkage effects, especially warping, are a concern.

1.3. Definitions

Before studying the warping of slab-on-grade, some basics regarding concrete shrinkage must be defined. Since warping depends on differential shrinkage in the slab, as shrinkage is minimized, differential shrinkage will also be minimized and consequently warping will be reduced in the slab. The first step towards a better understanding of shrinkage of a slab on grade is to define the different types of shrinkage in concrete. The second step towards a good understanding of the shrinkage process is to define the warping mechanism of concrete slabs-on-grade.

1.3.1. Types of Concrete Shrinkage

The change of concrete volume resulting from structural and environmental factors is one of the most detrimental material properties of concrete. Volume change in concrete is important because it induces the volumetric distortion of concrete which results in cracks in concrete. This is particularly evident in floors and pavements where the surface area is large when compared to the depth. Cracks can cause serious performance and serviceability problems in concrete.

Shrinkage is one of the major factors, if not the most common factor which causes the volumetric distortion of slabs on grade and resulting cracks in the concrete. Shrinkage most often occurs due to loss of moisture. Shrinkage does not begin at the time of loading or drying; it starts immediately after cement and water come in contact during the concrete mix (Holt, 2001, Ramseyer, 1999). Concrete shrinkage is sub-divided into the following classifications: plastic shrinkage, autogeneous shrinkage, carbonate shrinkage and drying shrinkage.

1.3.1.1. Plastic Shrinkage

Plastic shrinkage occurs when the concrete is still in the plastic state after the concrete is placed in the forms. The main causes of the plastic shrinkage are loss of water by evaporation of water on the surface of the freshly placed concrete and by absorption of water by the aggregates or subgrade. Water loss due to evaporation can be caused by exposing the concrete surface to drying winds or the hot sun. For instance, in the case of floors and pavements, when the concrete mix cannot retain all the mixing water, bleeding occurs and if the water evaporates faster than bleeding on the surface of concrete, plastic shrinkage occurs (Neville, 2000). Capillary tension is induced inside the concrete and produces a microscopic volume reduction. Plastic shrinkage is non-uniform due to restraining factors such as depth of section, reinforcement, ties, forms, etc. and due to the non uniform nature of the loss of water. This uneven plastic shrinkage causes surface cracking to occur in the concrete (Neville, 2000). Simply preventing the rapid loss of water from the surface of the concrete can significantly reduce plastic shrinkage. For this reason, properly curing the concrete immediately after the finishing operation is very important. The curing process can include covering the surface with a polyethylene sheet, fog spraying, using a curing sealer (generally wax based) or the use of a small quantity of aluminum powder.

1.3.1.2. Autogenous Shrinkage

Autogenous shrinkage is the shrinkage of the cement paste and concrete that occurs at an early age. When cement comes in contact to water, cement is hydrated. Generally, the volume of hydrated cement is less than that of the initial products (cement and water). As the concrete is still unhardened, this phenomenon causes a macroscopic and external volume change in the concrete. Some of water is contained in the capillary pores at this stage. Then, as the concrete is hardening, the water contained in the capillary pores is used for hydration resulting in a decrease in the relative humidity within the paste. This causes a tension in the pores and resulting compression in the concrete solid phase (Bissonnette, 1996). This phenomenon is called autogenous shrinkage and is more common in low water/cement ratio [under approximately 0.42 (Holt, 2001)] concretes or high performance concrete. Thus, autogenous shrinkage is generally very small in typical concrete and is not generally considered.

1.3.1.3. Carbonate Shrinkage

When the concrete is exposed to air containing carbon dioxide, carbonate shrinkage occurs. Carbon dioxide present in the atmosphere reacts in the presence of water with the hydrated (hardened) cement. Carbonation on cementitious composites causes a loss of alkalinity, which protects reinforcement from corrosion by passivation.

The chemical reaction of carbonation increases the weight and concrete undergoes carbonation shrinkage. Carbonation shrinkage can cause superficial cracks that increase the carbonation rate (Houst, 1997). Carbon dioxide generally penetrates 0.5 in. or less into high quality concrete with low porosity, is time dependent and is generally only an issue in Carbon dioxide rich environments. Due to these issues carbonation shrinkage is not a major component in the overall shrinkage of most concrete structures (ACI 224R-01) in a normal environment. Though structures exposed to high carbon dioxide, such as parking garages, enclosed tanks and sewer lines may experience a higher degree of carbonation shrinkage.

1.3.1.4. Drying Shrinkage

Drying shrinkage is defined as a reduction in the volume of concrete caused by the loss of water. As concrete dries, free water, which is not used in cement hydration, evaporates from the surfaces of the concrete (Figure 1.1). Losing moisture causes the concrete to shrink. If the shrinkage is restrained, tensile stresses develop within the concrete. Since the tensile strength of concrete is low, roughly 10% of the compressive strength of concrete, cracks can occur due to the restrained shrinkage of concrete if these stresses are not relieved by creep.

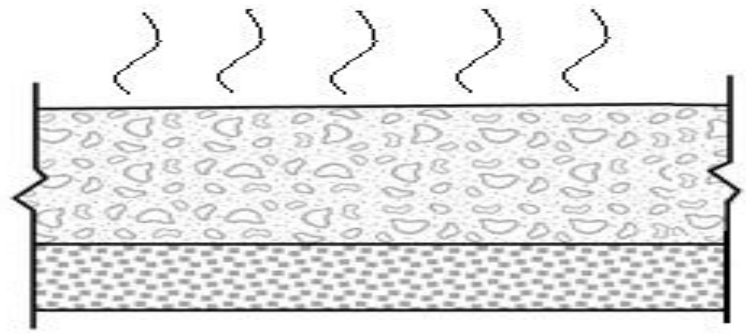

Figure 1.1 Water evaporation from the top surface of concrete slab

Drying shrinkage can continue for years before reaching equilibrium because the loss of water from hardened concrete is diffusion controlled (ACI 224R-2001). The ultimate amount of shrinkage in concrete is a function of the shrinkage potential of the paste, the volume fraction of the paste, the stiffness of the aggregate and the strength of the bond between the paste and the aggregate (Newberry, 2001).

Since many parameters affect drying shrinkage, predicting drying shrinkage is very difficult. The major factors controlling drying shrinkage of concrete are concrete composition, source of aggregate, ambient relative humidity, specimen geometry, ratio of the exposed surface to the volume of the structural element, and the slow development of shrinkage. This has led to a lack of knowledge for predicting and controlling shrinkage (ACI 224R-01).

Prediction of shrinkage cracking caused by restraining shrinkage depends on the interaction of following factors: free shrinkage, creep relaxation, material stiffness, fracture resistance, environmental conditions, time dependence, and degree of restraint (Shah et al, 1997). This makes the prediction and control of restrained shrinkage even more of a challenge.

1.3.2. Drying Shrinkage Mechanism for Slabs on Grade

Drying shrinkage is one of the major causes of cracks in concrete particularly in slabs on grade. Since the top surface of a concrete slab is exposed to the environment, the top surface loses moisture and shrinks due to drying shrinkage. The core and bottom surface of the slab does not tend to lose moisture and to shrink as much as the top surface. This creates differential shrinkage through the depth of the slab. This results in restraining shrinkage near the top surface due to the core and bottom surface of the concrete. Self-equilibrating internal stresses are created with tension stress on the top surface and compression stresses in the core and bottom surface. A combination of shrinkage and restraint induces a tensile stress in the top or near the top surface with balancing compressive stress in the core or near the bottom surface of the concrete slabs. When the internal tensile stress exceeds the concrete tensile strength, cracks appear, these are generally on the top surface of the concrete.

If the concrete slab is not restrained, the slab will simply shrink and contract to a smaller, but stable volume. In the real world, there is always some sort of external and internal restraint acting on the slab which induces internal stresses. According to ACI 224R, the final shrinkage strain of concrete in a typical structure is approximately 600 x 10^{-6} in/in, while the concrete tensile strain capacity is 150 x 10^{-6} in/in or less. Thus, cracks always occur, as the shrinkage is restrained in concrete.

Slabs can also shrink due to changes in the slab temperature from the time of slabs were initially placed. Thermal movement due to the change in slabs temperature should be considered in floors where the concrete is cast at a significantly different temperature than normal operating temperature. According to ACI 360R-06, thermal contraction of concrete is calculated by using a thermal expansion coefficient of $5.5x10^{-6}$ per ºF. Therefore, a 50º F variation in temperature between casting and typical operation will produce a thermal shrinkage of 275×10^{-6} in/in or 0.028%.

1.3.3. Factors that Restrain Shrinkage of Slabs on Grade

Shrinkage and expansion of concrete slabs on grade is restrained due to several factors. Concrete slabs on grade can be restrained by the foundation, friction between subbase and slab, not having a level and uniform surface to the subbase, adjacent structural elements, and reinforcing steel (ACI 224R-01). As previously mentioned, restrained volume change of concrete is the main reason for cracks in slabs on grade, thus, it is important to isolate slabs as much as possible from anything that could restrain the contraction or expansion in slabs on grade to reduce the possibility of generating the stresses that cause cracks.

1.3.4. Volumetric Distortion of Slabs on Grade

Drying shrinkage is one of the main factors causing the volumetric distortion of slabs on grade. The volumetric distortion of slabs on grade due to environmental loads is essentially due to two mechanisms: curling and warping.

1.3.5. Curling and Warping

Curling and warping are defined as vertical movement of concrete slabs at the edges and corners. According to the American Concrete Institute (ACI), the definition of curling is the upward movement of a slab's corners and edges due to differences in moisture content or temperature between the top and bottom of a slab. The top dries or cools and contracts more than the wetter or warmer bottom. Because of the reduced subgrade support, cracks often develop parallel to the joints or cracks and at the corners where joints intersect.

The academic community defines volumetric distortion of slabs due to environmental loads as curling (due to temperature gradient through the slab) and warping (due to moisture gradient through the slab). [Note: This research uses the academic definition of curling and warping and focuses on warping due to moisture gradient through the slab. Thus, in this research, temperature differentials through the depth of a slab induce concrete slab curling and moisture differential between the top and bottom surfaces of the slab causes concrete slab warping]. The most important reason for curling and warping of concrete slab is restraint stresses within the concrete slab.

Curling and warping could be upward or downward. When the slab curls or warps upward, compressive stress develops at the top surface and tensile stress at the bottom surface of slab and vice versa when the slab curls or warps downward.

Upward curling occurs when the top surface of slab shrinks due to a cooler surface at the top in compared to the bottom surface. Upward warping occurs when the top surface of concrete is drier than bottom surface, thus, the top surface shrinks. Upward curling and warping typically occur in internal slabs (Figure 1.2).

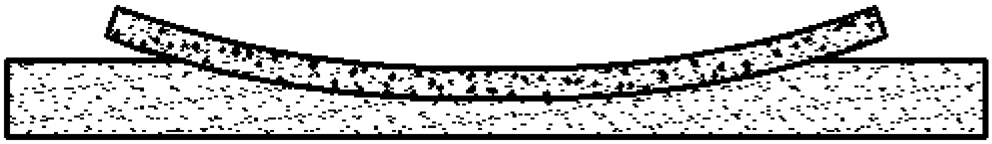

Figure 1.2 Upward curling or warping

Downward curling occurs when the top surface of slab expands due to a higher temperature at the top than the bottom surface. Downward warping occurs when the top surface exposed to a higher relative humidity in comparison to the bottom surface, thus, the top surface expands. Downward curling and warping are typical for external slabs (Figure 1.3).

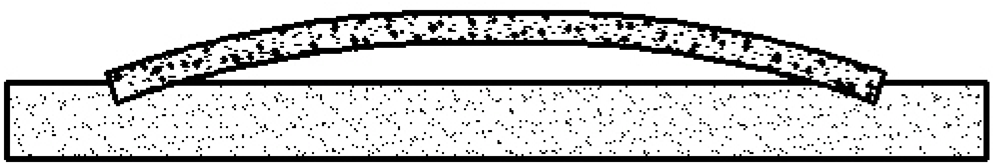

Figure 1.3 Downward curling or warping

1.3.6. More Details Regarding the Curling and Warping Mechanism

Temperature gradient through depth of a slab causes changes in the volume of the slab (expansion and contraction) called a shrinkage gradient. The shrinkage gradient due to developing temperature gradients produces curling moments to the slab. If top surface is cooler than the bottom surface and curling moment is greater than weight of slab plus any load that can be resisted, the slab tends to lift off the ground and act as cantilever. As a result, slabs corners or edges will deflect upward (Figure 1.4).

A moisture gradient due to loss of moisture at the top surface of a slab causes shrinkage to occur near the top surface of the concrete slab (Carlson, 1938). Typically a concrete slab losses moisture significantly only in the top 2 in. of the slab depending on the specimen size (Suprnant, 2002). Therefore, a shrinkage gradient is produced within the slab depth. The shrinkage gradient applies a warping moment to the slab. If the warping moment is greater than weight of the slab plus any other loads applied to the slab, the slab will deflect upward (Figure 1.4). According to the study by Walker and Holland (1999), curling/warping stresses can range from 200 to 450 psi.

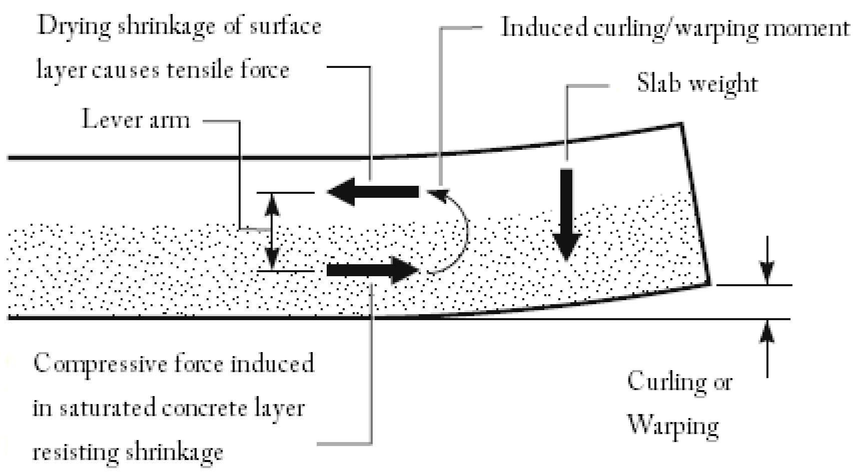

Figure 1.4 Upward curling or warping of slab caused by differential drying shrinkage
(Cement Concrete and Aggregates, 2006)

The self-weight of the slab and other loads react against the upward forces due to warping and induce internal stresses (Figure 1.5). The internal stresses can cause cracks if they exceed the concrete tensile strength unless the internal stresses can be relieved by creep.

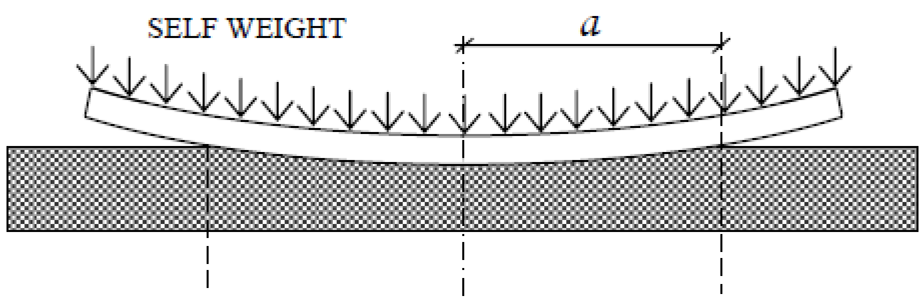

Figure 1.5 Internal stresses caused by self-weight on a curled concrete slab [Mailvaganam et al., 2002]

Cracks can increase permeability of the concrete and cause subsequent corrosion and durability problems. Consequently, cracks reduce the load capacity of a structure, fatigue strength, wear resistance and durability, and the aesthetic aspect of slabs on grade.

1.4. Dissertation Layout

This dissertation consists of six chapters. Chapter 2 contains the literature review in which the mechanism of drying shrinkage, curling and warping, effect of shrinkage reducing admixture, high performance, expansive cement concrete, and reviewing ACI 360R in expansive cement concrete and drying shrinkage are discussed. The 3rd chapter consists of the testing program, initial tests, main tests procedure, and additional test procedure. Chapter 4 presents the test results. Chapter 5 discussed the results. At the end, chapter 6 represents the conclusions.

CHAPTER 2

Literature Review

2.1. Background

Drying shrinkage is one of the main reasons for cracking in concrete slabs. Generally, shrinkage of concrete slabs is not considered in design; however structural designers know that this phenomenon occurs when concrete dries. One reason that shrinkage is not considered is that adequate test data is not available (Perenchio, 1997). Also the slow process of drying shrinkage does not lend itself to easy evaluation which has limited the research in this area. This has resulted in a lack of data for predicting and controlling shrinkage. It has been shown that even when concrete is dried from both surfaces it requires 28 months to reach an internal relative humidity of 50% at mid-depth in a 6 in. thick concrete member with 35% relative humidity on both surfaces (Spears, 1983).

There are many references which point out the factors influencing concrete shrinkage. The amount of water per unit volume of concrete has a significant effect on shrinkage of concrete (Hart, 1928; Washa, 1955; Powers, 1959; Tremper and Spellman, 1963; Meininger, 1966), It has been shown that the water demand of the materials used in the production of concrete is one of the main factors affect drying shrinkage (Powers, 1959; Meininger, 1966; Tremper and Spellman, 1963). Portland cement with low C_3A content and largest possible maximum sized coarse aggregate use less water reducing the drying shrinkage and curling of concrete (Powers, 1959; Meininger, 1966; Tremper and Spellman, 1963). The source of the course aggregate has a significant influence on the shrinkage of concrete (Meininger, 1966; Tremper and Spellman, 1963). The amount of cement per unit volume is one of the most important factors affect increasing shrinkage (Troxell et al, 1968; ACI 224R)].

This literature review is organized under several sections. The first section discusses the mechanism of drying shrinkage and curling or warping, factors affect on drying shrinkage and curling/warping as it is understood by researchers today. In addition, different techniques to control and repair these problems mostly focusing on concrete slabs on grade are proposed. The next three sections focus briefly on effects of shrinkage reducing admixture, high-performance cement and expansive cement on drying shrinkage of concrete based on previous researchers' studies. The final section summarizes ACI 360-06 documents regarding to the controlling warping and curling and also reviewing use of shrinkage compensating cement concrete slabs-on-grade.

2.2. Drying Shrinkage

The smoothness of concrete a slab is one of the first requirements of a good floor. According to Hart (1928), low shrinkage concrete floor toppings and toweled concrete floor finish are two methods that can be used to provide a smooth concrete floor. Hart concluded that using finer sand and a high percentage of extreme fines in the concrete floor topping increases shrinkage and cracking of concrete slabs. He recommended lowering the water cement ratio, using thoroughly washed aggregate, and delaying troweling until there is no danger of drawing up excessive quantities of inert fines as methods of providing a smooth concrete slab floor. Based on Hart's research, curling or warping of concrete floors occurs due to differential drying of extremely rich concrete mixes on the top surface and excessively lean mixes at the bottom surface. He suggested the following procedure to reduce curling: using the coarsest aggregate possible, reducing the amount of mixing water, reducing the number of joints, wet curing for at least for ten days, and avoiding high temperature and low relative humidity during the first few days following the moist curing.

Freyssinet (1929) was the first person to explain the shrinkage mechanisms by using the capillary stress theory (Baron and Satery, 1982). This theory postulates that while the concrete dries the larger pores are emptied first and then the smaller pores are emptied. At the time pores are being emptied, they are partially saturated and menisci are formed between the liquid and gas interface. As a result, a hydrostatic tension is induced in the liquid phase and a compressive force is generated in the solid skeleton. These forces produce a contraction in the concrete and are defined as shrinkage.

Carlson (1938) performed an experimental study on the drying shrinkage of concrete. He studied three different cements and two types of aggregates. For 600 days he measured moisture loss and shrinkage of the specimens at various depths through the slab, measuring from the exposed concrete surface. Carlson's work concluded that the top surface of concrete lost more moisture than the bottom surface, and shrinkage occurred near the top surface. Carlson research showed moisture content differences between top and bottom of the slabs on grade. Carlson concluded that this change in moisture content causes a shrinkage gradient to occur. This phenomenon creates a curling moment to the slab. Carlson showed that the greater the moisture-content differences between the top and bottom of slab surfaces, the larger the shrinkage gradient and the larger the induced curling moment will be. And, the larger the applied curling moment, the greater the deflections will be. Carlson also showed that for given moisture gradient, the shrinkage gradients differ for different cements or concrete materials in the same environment. In addition, he showed that different concrete materials have different shrinkage gradients in the same environment.

Tremper and Spellman (1963) studied the shrinkage of concrete highway pavements. They conducted displacement profilograms and developed data for slab curling of three full size highway pavement projects. They compared the data to the shrinkage of laboratory specimens made with the same concrete. Tremper and Spellman showed that the top surface of the concrete slab is always dryer than that in the bottom surface. This induces differential moisture to occur through the depth of the slab and causes an upward curling at the edges of the highway pavements. As the top surface of the pavement is exposed to the sun, higher temperature at the top surface of slab may offset part of the upward curling of pavement but rising temperature during the day is not enough to cause downward curling in daytime. At night the upward curling increased and reached to the maximum point because of dryer and lower temperature at the top surface of the concrete slab. Because these three projects have different variables such as subgrade or subbase stiffness and drying environments, it was difficult to show the correct relation between curling deflection and drying shrinkage. However, they showed that curling or warping of concrete highway slabs is directly related to the drying shrinkage or moisture loss of the slab concrete (Figure 2.1). Table 2.1 shows the average curl, in inches, is three times the drying shrinkage, in percent (Suprenant, 2002). Therefore, it can be concluded that in some cases if the drying shrinkage decreases, the curling deflection decreases with a higher rate. The profilograms shows that curling is not increased after 40 days of casting the slab concrete. According to their research, water content significantly affects drying shrinkage and curling of concrete. Also, the factors reduce the water content in concrete can be coarser sand, aggregates with no clay and other fine materials, coarser ground cement, cement with low C_3A content, largest possible maximum sized coarse aggregate, shortest travel time from central mix plant to job, fewest agitating revolutions after complete mixing is achieved, and lowest temperature.

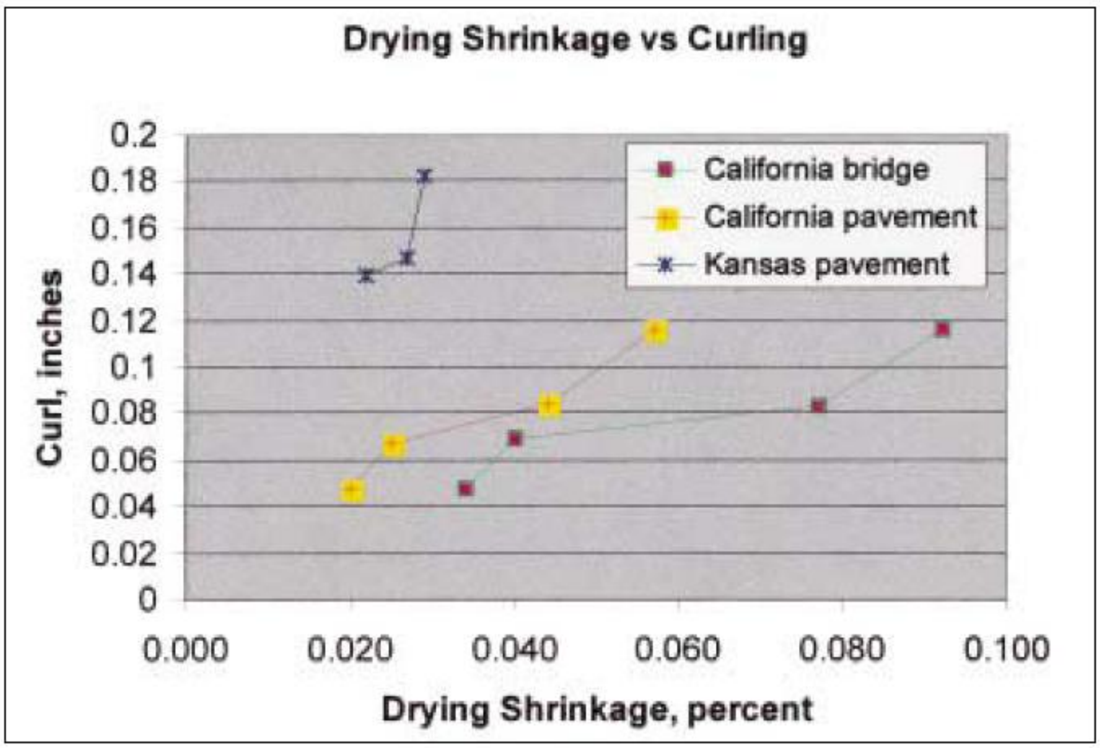

Figure 2.1 Relationship between drying shrinkage of test specimens and the amount of curling deflection of full-size test slabs for three different slabs (Suprement, 2002)

Table 2.1 Drying shrinkage of specimens versus curling of full-size slabs (Suprement, 2002)

Drying shrinkage of prisms, %	Slab curling, in.	Ratio of curl, in., to shrinkage, %	Tremper and Spellman reference
0.020	0.048	2.4	California pavement
0.022	0.139	6.3	Kansas pavement
0.025	0.067	2.7	California pavement
0.027	0.147	5.4	Kansas pavement
0.029	0.182	6.3	Kansas pavement
0.034	0.048	1.4	California bridge
0.040	0.069	1.7	California bridge
0.044	0.084	1.9	California pavement
0.057	0.116	2.0	California pavement
0.077	0.083	1.1	California bridge
0.092	0.116	1.3	California bridge
		Avg. 3.0	

Meininger (1966) studied the factors affecting drying shrinkage of concrete. He concerned the effect of aggregates, cement source, and water needs in concrete mix on shrinkage. Based on the test results, he found coarse and fine aggregate very effective on concrete shrinkage. Additionally, a change in both coarse and fine aggregate causes shrinkage to increase 150 percent over a control concrete. Also, decreasing maximum aggregate size from 2 ½ in. to a 3/8 in. increases shrinkage 25%. He was not in agreement with Tremper and Spellman (1963), and Powers (1959) for maximum size of aggregate to reduce the shrinkage. Meininger states: "not much advantage would be gained in going from a 3/8 in. (19 mm) maximum to 1 ½ in. (38 mm) maximum". He also states that using washed aggregates in concrete mix reduces shrinkage (up to 20%) in compare to the concrete made with "as received" aggregates. He reported that cement source has only about 15% effect on shrinkage, changing amount of cement from 517 to 705 Ib of cement per cubic yard has only effect about 10% on shrinkage, changing slump from 2-3 in. to a 6-7 in. only increases shrinkage about 2% for the higher shrinkage aggregate and only 5% for the stock aggregate, and curing concrete for 7 days instead of 3 days reduces shrinkage up to 5 percent. Effect of grading of sand was not mentioned in his report.

Powers (1968) studied the shrinkage mechanism of concrete. Based on his investigation, water contained between two plane surfaces cannot be adsorbed freely when the distance between those surfaces is less than 3.0 nm. As a result, the water contained in these areas which is called areas of hindered adsorption is compressed and it is in balance with the attraction forces of the CSH. Powers concluded that the water loss in the concrete initially occurs in capillary pores and the adsorbed water is transferred toward the capillarity pores to maintain the hygrometric balance. Therefore, the water contained in the area hindered adsorption moves to the free adsorbed zone. This transferring water causes the disjoining pressure between the solid particles decreases and a volume contraction occurs in the concrete element.

Nagataki (1970) studied on shrinkage restraints in concrete pavement. He tested three 4x4x20-in. concrete specimens. The specimens were cured for 7 days, and then they were exposed in 75 ºF and 50% relative humidity. One specimen was dried in all four sides, one specimen was dried only from top, and the last specimen was exposed to drying only at top, and its bottom placed on wet sand with 10 % moisture content. He showed that the specimen with all sides drying had the lowest shrinkage gradient. The specimen with top exposed drying had a much larger shrinkage gradient. The largest shrinkage gradient occurs in the specimens placed on the moist sand because of the expansion in the bottom of specimen when exposed to the wet sand. The specimen with larger shrinkage gradient had greater applied curling. Nagataki showed that the moisture content of the subbase has an important effect on drying shrinkage and curling moment of concrete. As Nagataki's tests were not included a dry subbase to compare with the slab placed on a vapor retarder, he provided another test with a 10 x 32 x 408 in. concrete pavement placed on a heavy sheet of paper. The concrete was cured with wet burlap for 10 days. He used Carlson-type strain gages and provided a plot for shrinkage gradients at various distances from the free ends. His work proved that the slab placed on vapor retarder curls more than that when placed on a granular subbase.

Carrier et al. (1975) measured the moisture contents of a pavement and two bridge decks. One of the bridge decks was formed on plywood forms which were removed after the deck was placed and cured, and another bridge deck was formed on metal forms which were stayed in place. The moisture gradient profiles for each of the structure are shown in Figure 2.2. It can be seen that the moisture loss occurs significantly in top few inches of slabs which are exposed to the ambient.

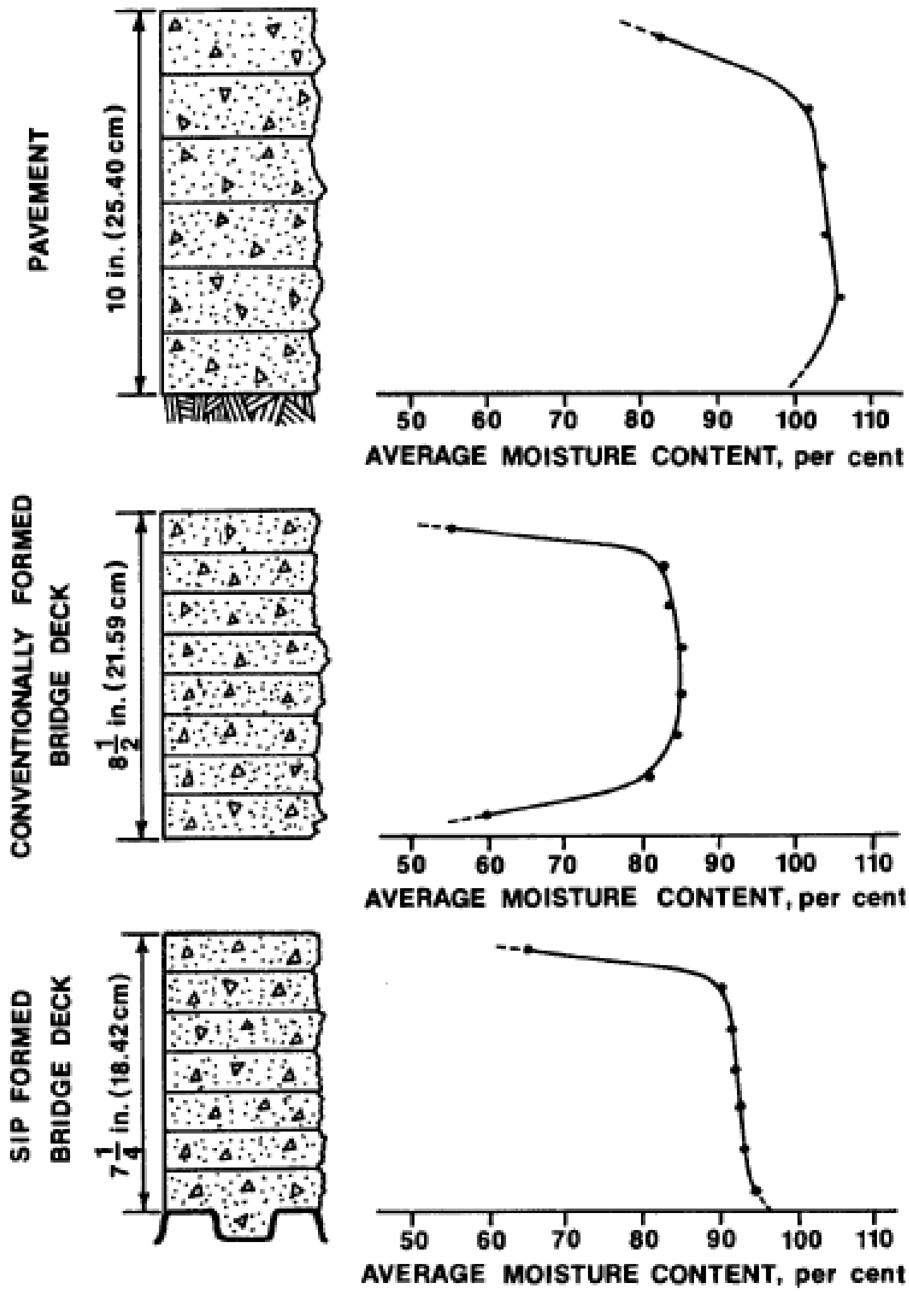

Figure 2.2 Moisture distributions in a pavement and in bridge decks (Carrier et al., 1975)

Keeton (1979) studied shrinkage drying of slabs on grade for relative humidity from 20% to 100%. Based on his research, a lower relative humidity causes a larger shrinkage gradient. The large rate of shrinkage gradient increases the moment curling of the slab and causes it to deflect upward at a greater rate. He concluded that when the slab is exposed to a lower relative humidity, it will lose moisture faster and it will curl earlier than the slab exposed to a higher humidity environment.

Nicholson (1981) studied the effect of vapor barriers on cracking and strength of slab on grade. In his experimental study, he cast the concrete over polyethylene sheeting, a 3-inch sand layer with no vapor barrier, and a 3-inch sand-cement layer with no vapor barrier. The water-cement ratio of the concrete mixes was different (0.697, 0.753, and 0.801) and the slumps were 8, 8, and 9 inches respectively. The results show that extensive cracking in the slabs placed on polyethylene and little cracking in the slabs placed over sand or cement-treated sand. He concluded that the sand base absorbed the concrete mix water, thus the effect of sand base is more important for the high water-cement ratios than low water-cement ratio. He also cored the concrete slabs of his experimental study and he found that the concrete placed over sand bed was stronger than concrete placed on the polyethylene. According to Nicholson et al. (1976), the strength of concrete slab cast over sand bed is more than 30% stronger than concrete cast on the polyethylene.

Hansen (1985) studied on shrinkage and weight loss of Portland cement past. His study focused shrinkage mechanisms of Portland cement paste. For the purpose of this research, shrinkage, weight loss, and pore structure measurements using nitrogen sorption and mercury intrusion porosimetry (MIP) were applied. Hansen followed the test procedure of Parrott et al. with some modifications. He casted type I Portland cement into thin slabs (2.3 mm) with *w/c* ratios of 0.4 and 0.6. Then the shrinkage specimens were cut from the slabs with 76 mm length. The specimens were dried in desiccators conditioned at 75%, 50%, 11%, and 0% related humidity using aqueous solution of sulfuric acid. The desiccators were kept in an environmental chamber at 24 ± 3℃. Two active stress mechanisms were identified based on the equilibrium shrinkage verses calculated increase in surface free energy curves. The two active stress mechanisms are the Gibbs-Bangham (surface free energy) and capillary tension mechanisms. The Gibbs is active in the RH range from 100% to 0%, while the capillarity stresses mechanism are only activate in the RH range above 25%. From the elastic modulus calculation, Hansen works proved that the Gibbs-Bangham theory can explain only about one third of the total shrinkage deformation when the relative humidity is below 40% and the rest of the total shrinkage deformation may be caused by decreasing in interlayer spacing due to Gibbs and capillary induced stresses. In addition, Hansen found that nitrogen can measure the external surface area, and using both nitrogen and MIP measurements obtain the total external pore volume. Hansen (1987) also showed that the water/cement ratio has an important influence in the drying shrinkage process.

Ytterberg (1987-part I and II) studied the shrinkage and curling of slabs on grade, particularly slabs located inside the buildings. His study and conclusions were based on reviewing the previous investigations. According to his references, the common causes for shrinkage cracking and upward curling in enclosed industrial floor slabs on grade are moist subgrade, low relative humidity (dry air) on the top surface of slab, and free water which is used only for concrete workability. These factors cause the top surface is drier than the bottom surface of slab and this results a differential shrinkage through depth of the slab and causes upward curling or warping (Figure 2.3). Ytterberg illustrates the long term relative humidity in the surface of the slabs has a significant effect on the moisture gradient. Therefore, lower ambient relative increases drying shrinkage that results larger upward curling of slabs on grade. Downward curling may occur in slabs exposed to the sun (Figure 2.3).

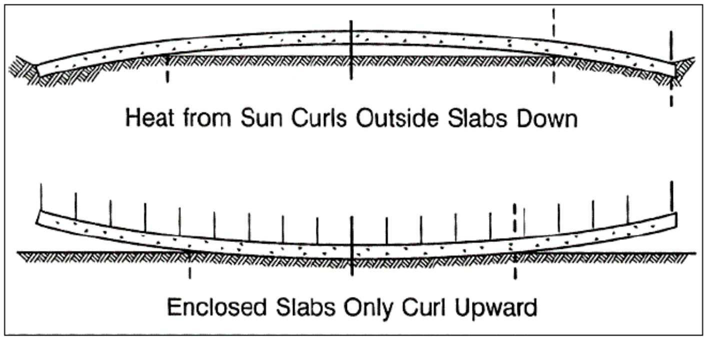

Figure 2.3 Outdoor slabs exposed to the sun curl downward and enclosed slabs curl only upward (Ytterberg, 1987)

According to Powers (1959), Meininger (1966), and Termper and Spellmand (1963) water demand of the separate concrete ingredients has a major effect on shrinkage of concrete (Ytterberg, 1987). Although, it was assumed that high-range water reducers (HRWRs) or superplasticizers reduces shrinkage as they reduce water in concrete mix, Ytterburg states that high-range water reducers (HRWRs) do not reduce shrinkage of concrete (Whiting, 1979; Rixom, 1981; Gebler, 1982). Ytterberg does not agree with PCA (1983) which states: "Slab made of low-slump concrete properly cured in a moist environment, with or without reinforcement, will have minimum shrinkage and few cracks." Ytterberg cited that designers should specify concrete materials with low shrinkage and stony concrete mixes with large maximum sized coarse aggregate instead of considering low slump. Note that larger aggregate increases the modulus of elasticity *E* of concrete that can develop warping problem in slab. He also states that cement source has an effect on shrinkage of concrete. For instance, low C_3A cement reduces the shrinkage. Ytterberg recommends not using high strength concrete for the purpose of minimizing slab thickness, because high strength concrete increases shrinkage in concrete slab. Ytterberg extended Leonards and Harr table related to moisture gradients of enclosed slabs on grade. Ytterberg (Table 2.2) shows: “the great magnitude of shrinkage strain differences between the top and bottom of slabs caused by a drying shrinkage gradient equal to a temperature gradient of 3 to 5 deg F per inch of slab thickness”.

Table 2.2 Drying shrinkage gradients expressed as equivalent temperature gradients (Leonards and Harr, 1959)

Shrinkage strain gradient through slab (millionths)	Equivalent temperature gradient through slab (° F)	Equivalent temperature gradient for various slab thicknesses (° F per in.)		
		6 in.	8 in.	10 in.
275	50	–	–	5.0
220	40	–	5.0	4.0
165	30	5.0	3.8	3.0
110	20	3.3	–	–

Ytterberg also stated that subgrade moisture and modulus have influence on vertical curling deflection of concrete. He refers to ACI (1982) that dry subgrade causes lesser curling deflection than saturated subbase (Figure 2.4). Also, high subgrade modulus causes the slabs cannot depress into the subgrade when the upward curling occurs, thus the unsupported length of slab edges increases. In addition, weight of slab causes a large stress to develop in slabs on grade when they warp or curl. This stress increases as length of slabs increases but only up to a certain distance.

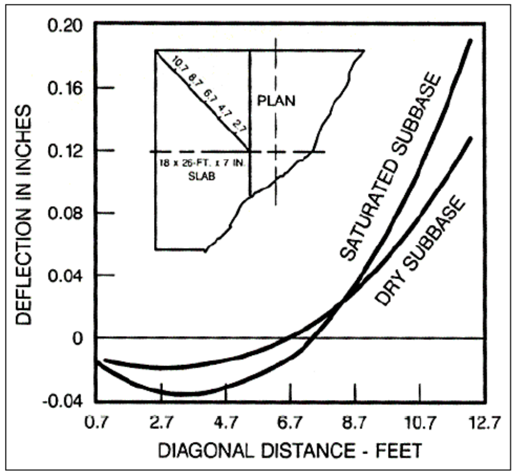

Figure 2.4 Upward curling deflection of a slab during its initial drying cycle on a dry subbase, compare with deflection of the same slab on a saturated subbase (ACI, 1982)

Ytterberg did not agree with the recommendation from Portland Cement Association (PCA), 1978, for adding joints to reduce shrinkage cracking. He states that curling and break down of joint edges increase maintenance problems and its cost.

Ytterberg (1993, part III) recommends the followings for controlling cracks in concrete: using distributed reinforcement, using shrinkage-compensating concrete, using post tensioning in the slab, and removing factors that restrain shrinkage or expansion.

- *Distributed reinforcement:* PCA's "Concrete Floors on Ground" suggests using plain concrete for slabs on grade with joints at common spacing (10 to 20 feet apart based on the idea that normal unreinforced concrete cracks every 15 feet due to drying shrinkage) or using distributed reinforcement in slabs on grade. The subgrade drag formula is used with the greater distances for joint.

$$A_s = \frac{F\,L\,w}{2\,f_s} \qquad (2.1)$$

A_s= area of steel at cross section, in square inches per lineal foot of slab width

F= subgrade friction coefficient (1.5 or 2.0 are used for pavements by designer; 1.5 is recommended to use for concrete slab on grade)

L= Slab length (or width, if appropriate) between free ends, in feet

w= weight of slab, in pounds per square foot (designers use 12.5 pounds per inch floor thickness for regular-weight concrete)

f_s= allowable stress of reinforcement, in psi (0.67 or 0.75 yield strength of the steel)

According to Ytterberg, the steel calculated based on subgrade drag formula shall not be less than 0.15% by cross section area of the concrete. Besides, steel shall be located at top half of the slab because slab lose its moisture from its top surface and shrinks at top, but steel shall not be closer than 1 ½ in. to the top surface for the purpose of steel coverage. In addition, minimum diameter of steel shall not be less than 0.4 inch for sufficient stiffness and the steels should be spaced at least 15 inches on center to permit workers to step between and not on the steel.

- *Shrinkage-compensating concrete:* This type of concrete expands in the top half in a higher rate than the bottom half. Therefore, when the top surface is losing free water and shrinks, the shrinkage reduces the initial expansion and shrinkage and expansion will be in equilibrium. As a result, curling is reduced due to reducing drying shrinkage.
- *Post tensioning:* post tensioned slabs keep shrinkage cracks closed. Therefore, joints can be spaced far enough.

- *Removing restrains:* the slab shall be separate from anything that can restrain it. Slab should be allowed to move with no restrained from foundation, pit wall, columns, and other materials can restraint slab from shrinkage or expansion.

Schrader and McKinnon (1989) illustrated Roller Compacted Concrete (RCC) is an efficient concrete and has an economical design and construction technique for heavy duty pavements. However, it is assumed that slab thickness can be reduced with higher strength concrete, but there is no guarantee that the concrete has higher strength. For this reason, it is recommended to substitute an alternative for higher strength concrete in slab on grade. Thus, Schrader and McKinnon suggest thicker pavement of RCC with lower strength that can cause less curling and curl stress in practice. Due to lower strength, it has also less shrinkage and fewer joints and cracks appearances.

Suprenant (1992) studied using vapor barriers under concrete slabs. His study was based on the previous research and ACI Committee 302. Vapor barrier can be placed in two locations: concrete cast directly over vapor barrier, or vapor barrier placed under sand layer and concrete cast over sand layer. According to this study, the location of the vapor barrier for interior slabs is not as important as exterior slabs while using a high-quality concrete with low water content and water-cement ratio and finishing concrete correctly. He recommended casting concrete over an aggregate layer if concretes have high water contents and high water-cement ratios. This way, it reduces the finishing time, increases strength, and reduces the curling and finishing defect of the slab concrete.

Rollings (1993) analyzed curling problems in concrete airport pavement using steel-fiber-reinforced. The pavements were relatively thin with large plan dimensions. Analysis showed that curling of large, relative thin slabs are influenced slightly with the differential shrinkage between top and bottom of the slab. Differential shrinkage was mostly caused by early-age shrinkage due to autogenous and temperature-induced shrinkage and drying shrinkage at later ages. Joint spacing was found more likely a cause of longitudinal cracking. Therefore, Rollings recommended using low-friction interfaces between slabs and underlying material and reducing joint spacing to reduce curling problems in the concrete slab.

Dobson (1995) studied the problems on concrete floor slabs. Based on his study, slab curling caused by shrinkage can be minimized by applying his five advices. As water content has a significant effect on shrinkage and curling of concrete, His first recommendation was using a proper mix design with fewer fines to reduce water content. Secondly, he suggested use of permeable sub grade like sand cushion to allow free water of concrete exit from the bottom surface of concrete, resulting reduction of differential shrinkage between top and bottom of slab. He also recommended balancing temperature between top and bottom surface of slab and starting with a slightly dampened subbase without free standing water. Finally he suggested a properly curing immediately after finishing the concrete.

Fitzpatrick (1996) studied designing industrial floor slabs. He provided some recommendations concerning the mix design and the field work. Based on his study, replacing 10% to 20% of the cement with fly ash can affect increasing the ultimate strength of concrete and reducing the heat produced during hydration. He cited the role of air entrainment to improve concrete durability and reduce thermal cracking. In addition, using fiber in concrete provides a tensile strength during the early hydration period which can reduce the potential for cracks in concrete. He recommended providing a uniform, well compacted, and reasonable degree of flatness for subgrade. He stated that however vapor barrier prevents transferring moisture from subgrade into the slab but it should not be used to compensate for inadequate drainage of the subgrade. In addition, using reinforcement is not required in slabs-on-grade because there is no possibility to maintain reinforcement in the upper third of slab depth. The reinforcements are pushed down to the bottom in practice by workers, floating and vibrating operation. He also recommended lightly spraying the concrete surface with water after finishing concrete slab until curing slab with wet burlaps. He suggested 48 to 72 hours of curing to be adequate for finishing hydration process in concrete.

Bissonnette (1996) studied the problems of concrete repairs. He focused effects of the paste volume, water to cement ratio, aggregates, admixture and ambient relative humidity on drying shrinkage of concrete. Bissonnette showed that water to cement ratio for concrete has a less significant effect on shrinkage because of using aggregates in concrete. He tested concrete with a constant paste volume. The results showed that water to cement ratio reduction (0.34 to 0.65) does not have a significant effect on drying shrinkage. Thus, he concluded that water to cement ratio has an effect on concrete shrinkage but it might not be as important as it is often considered to be. He showed that adding silica fume to cement paste has a benefit effect on shrinkage. Using silica fume reduces the water to cement ratio and hence results a reduction in shrinkage. According to Bissonnette, evaporation rate does not have primarily influence on drying shrinkage, but diffusion rate has a direct influence on this phenomenon. Thus, the time to reach a given shrinkage deformation is related to the volume to surface ratio. Bissonnette concluded that the time needed for shrinkage deformation is proportional to the square of the volume to surface ratio. He showed that the rigidity of aggregate has a direct effect on magnitude of shrinkage. Based on his study, using softer aggregates causes the shrinkage magnitude increases three times larger than that in rigid aggregates. Also, aggregate shape and grading do not have direct effect on shrinkage, but they change the mix proportions and have an effect on shrinkage of concrete. Bissonnette's work on shrinkage reducing admixture specifically alcohol-based admixtures showed that shrinkage reducing admixtures reduce the surface tension of water contained in the concrete pores and alcohol-based admixtures reduce the shrinkage by about 30 to 50%. He also showed that relative humidity of environment has an important effect on drying shrinkage of concrete. As the environment relative humidity decreases, shrinkage increases.

Roy Reiterman (1996) studied the effect of reinforcement in concrete slab. He had a personal views in his article based on developing extensive cracking over the unreinforced concrete slab in practice. Based on his study, using steel reinforced concrete slab has advantages due to simple placement, reducing random cracking, reducing and controlling crack width, reducing curling of slab, increasing strength of concrete, and helping maintain aggregate interlock. In addition, using reinforcement in slab is economical for owners because using reinforcement for strength of slabs increases mechanical properties especially moment capacity of slab and can reduce thickness of slab and increase control joint spacing. Reiterman disagreed with advertises in substituting reinforcement with admixture and using plain concrete and said that admixtures cannot be used as an alternative to steel reinforcement. He cited that admixture and steel reinforcement are two materials and do different things in the concrete, thus there is no substitute for steel reinforcement in concrete slab.

Perenchio (1997) studied drying shrinkage mechanism for concrete slab and its effects. Based on his study, drying shrinkage is a major cause of failures at filled joints, slab curling, and excessive cracking. Curling occurs in slab on grade when the top surface of the slab is exposed to the atmosphere. The top surface dries and consequently shrinks while the bottom surface does not tend to dry as much as the top surface. Therefore, the top surface will be shorter than bottom surface, and this causes the slab curls upward, as shown in Figure 2.5. The magnitude of curling at the corners of slabs is greater than the sides because the corners are subjected to the shrinkage along both of the sides adjacent to the corners. According to Perenchio, because the slab edges deflected upward and not in contact with the subbase, the weight of the concrete near the edges causes an uplifting force at the slab center. Figure 2.6 shows the contact area between slab and subbase. In this figure, the open area at the perimeter represents the portion of the slab not in contact with the subbase, the cross-hathched represents the area in contact with the subbase, and the shaded area at the slab center shows the portion of the slab that is in contact with the subbase. The center ares is in pressure due to cantilevered slab force. Perenchio cited that the amount of curling is significantly affected by thickness of slab. This opinion is in contrast with Ytterburg (1987) who suggested using thicker slab to reduce slab curling. Perenchio recommends filling the joints not sooner than 90 days because the concrete slabs on grade reach to their ultimate drying shrinkage in long term. Also spacing joints shall not be farther than 15 feet to reduce cracking of slab.

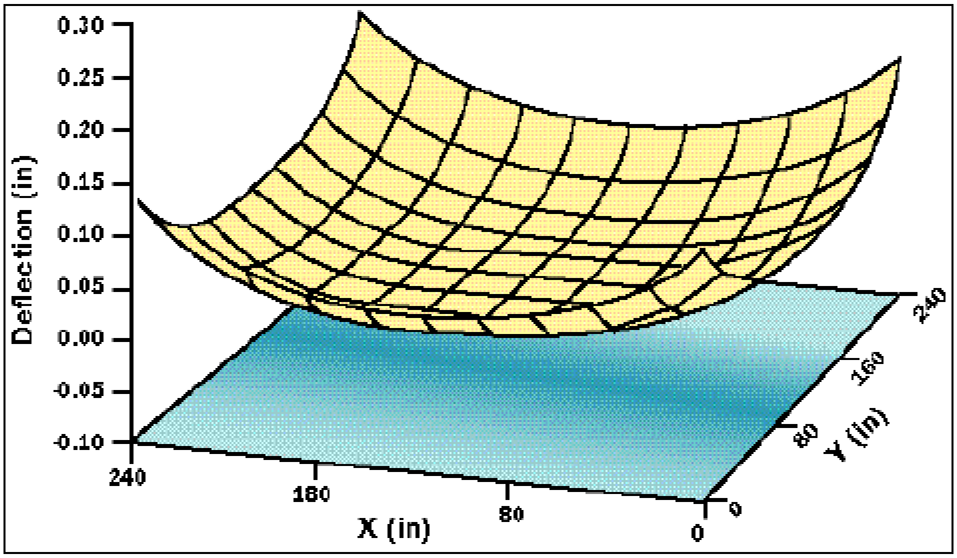

Figure 2.5 Top surface deflection of a 20x20-foot, 6-inch thick warped slab with free edges
(Al-Nasra and Wang, 1994)

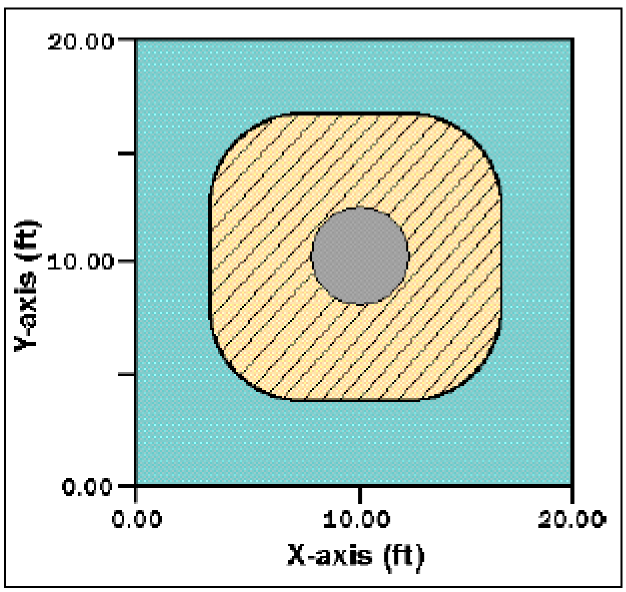

Figure 2.6 Contact areas between the slab and subbase
(Al-Nasra and Wang, 1994)

Kiamco (1997) illustrated placing reinforcement close to the bottom of slab is proactive in preventing cracks at the top surface of slab. Also, placing reinforcement close to the top surface of slab is reactive in trying to control the deep cracks.

Weiss and Shah (1997) studied on reducing shrinkage cracking in concrete pavements. They recommended use of fiber reinforcement, shrinkage compensating concrete, and a newly developed shrinkage reducing admixture to reduce cracking in pavement mostly caused by drying shrinkage.

Weiss et al. (1998) studied on shrinkage cracking of restrained concrete slab. In this research, an experimental method and theoretical model were developed to provide a better understanding of shrinkage cracking for restrained concrete structures. They used normal and high strength concrete and they added Silica fume slurry to produce high strength concrete. They also used a commercially available solution of modified naphthalene sulfonate known as type F admixture based on ASTM C-494 (1996) in a 0, 1, and 2 %. The tests were performed in two parts. In the first tests, thin specimens were made, and a 5 in. thick steel plate with grooves was used to provide restrained concrete. The plate was found insufficient due to debonding and bending occurred in specimens. Therefore, in the final test, a solid base using a steel tube 3in. x 4in. with a wall thickness of about 4 in. was used to present a sufficient resistance against bending. In addition, the specimens were restrained axially with the horizontal threaded bars. In the theoretical modeling, fracture mechanics with energy balance considerations were used as a method to predict the behavior of the concrete. From this research, it was found that reducing admixture delays the cracking as well as reducing in the free shrinkage of concrete, the high strength concrete cracks earlier than normal concrete, and experimental method and theoretical model results showed a favorable correlation.

Suprenant and Malisch (1998) studied moisture loss of concrete slabs. They measured the moisture-emission rates of concrete slabs for three months. They found that the moisture-emission rates reduce with time at the similar rates for slabs 2-, 4-, 6-, and 8-inch thick. They repeated their measurements for four different concrete mixtures and found that drying occurs in the top few inches of slab, and it is not affected by slab thickness or environment.

Daimler Chrysler Corp. (1998) developed its factory based on Windsor, Ontario. The goal of company was to build a high quality slabs-on-grade. A project team of the company researched the recent project experiences to provide the best design and construction practices (Shashaani et al., 2000). They produced a specification, a test slab evaluation program and a 24-step checklist for a high qualify floor slab. In the first eight steps, they focused management and cost reduction without reducing quality and safety. In the next 12 steps, a concrete mix design is suggested. They recommended the following issues to present a high quality slabs-on-grade: a) not use fly ash to replace Portland cement because it causes increasing concrete shrinkage, b) use a concrete mix with 30 MPa compression strength, a minimum cement content of 330 kg/m^3, a water/cement ratio of 0.45, and a 50- to-50 ratio of 1 ½ inches and 3/8 inches aggregates, c) keep the cement content consistent to reduce further adjustment to sand proportions, d) use trap rock and liquid sealer/hardener to provide a better surface durability, e) use steel fiber reinforced concrete to increase tensile strength, toughness and ductility of concrete slab, f) isolate columns and control irregular shrinkage cracks with using a pinwheel contraction joint pattern, g) use a ½ in. choker lime screening as a slip-sheet between the slab-on-grade and subgrade, h) use a compactable granular material, i) reduce construction cost and controlling curling at joints with a proper thickness design and providing fewer construction joints. Finally, at the last 4 steps, they focused on providing a uniform compacted subgrade and subbase. They recommend maintaining a smooth well-graded and compacted subgrade and subbase surface however it might be difficult.

Supernant and Malisch (1999) studied the methods of repairing curled slabs. However several repair methods available that contractors, engineers, and owners must evaluate the feasibility, cost, benefits, and limitation of each. The best time for repairing curling is concerned since curling continues for months due to moisture cycle of concrete slab. The first issue concerned in repairing is waiting and hoping. This means to measure curling during the time and hope that the curling decreases. Based on this study, curling decreases as slab dries and moisture gradient becomes more uniform. Wetting the top surface of the slab is another method of repairing curled slab. Test results from laboratory study by Childs and Kapernick, 1958, showed that since curling is due to drier surface at top of slab than the bottom of slab, wetting top surface of slab reverse the curling. But when water was removed, and the slab dried, the curling returned to its original level. Therefore PCA (1997) suggested ponding slab until it reaches its level and provideing additional control joints at the location of curling. Based on this research, cutting additional joints is most successful methods for the curled floors that do not have forklift traffic and are covered with carpet. Grinding is a common method to repair curled floors. In this method, the slab edges and corners are diamond grind to achieve a desired profile. Also, grout and grind is a method typically used on floors with forklift traffic. In this method, in addition to grinding, one to two inch diameter holes are drilled around joints and corners of slabs. Then inject the grout inside the holes and fill the under slab void. Installing dowel bars across a curl joint are the last method recommended in this research. Steel dowels can be installed at joints with some steps before the concrete is placed, or at existing joints to repair curled floors. Dowel bars are typically used in floors with heavy forklift traffic because they improve load transfer and minimize differential movement under traffic.

Neville (2000) studied properties of concrete. He showed that the type and fineness of cement do not have an important effect on concrete shrinkage. According to his study, the water/cement ratio has an important influence in the drying shrinkage process. Also, the cement paste shrinkage is directly proportional to water/cement ratio in the ratio between 0.20 and 0.60. Indeed, the relation between shrinkage and water/cement ratio would be also true for concrete however other parameters have influence in the concrete shrinkage. Neville also studied the effect of aggregate in shrinkage, and he showed that maximum aggregate size does not have a direct effect on shrinkage, but the use of larger aggregate causes a leaner mix and a lower shrinkage. In addition, relative humidity of environment has an important effect on drying shrinkage of concrete. Indeed, concrete shrinks when relative humidity is less than 94%, and it swells when it is 100%. Many studies agree that the paste volume influence in the concrete shrinkage (Bissonnette et al., 1999; Hansen, 1987). Thus, the higher the paste volume is, the higher the shrinkage will be.

Silfwerbrand and Paulsson-Tralla (2000) studied a construction method to reduce shrinkage cracking and curling in slab-on-grade. They used lifting and lowering technique to provide a uniform drying between the top and bottom faces of the slab-on-grade and to prevent restraining shrinkage during a certain time. Airbags are placed under the slab parallel to the short side of the slab to achieve a uniform drying and unrestraint shrinkage. A thin polymer film is put under the pipes to prevent friction with concrete and is spaced based on the characteristics of the slab (thickness, strength, etc.). The concrete slab is cast in parts to prevent restriction of slab-on-grade in the total length. After 3 to 5 days of curing, the pipes are filled with compressed air and the slab is lifted. With this method, the slab is not restrained from shortening caused by shrinkage and facilitates the bilateral desiccation if spaces between airbags are properly ventilated. Then, after a few weeks of treatment, the air is removed from the pipes and slab is returned to its initial position (Figure 2.7).

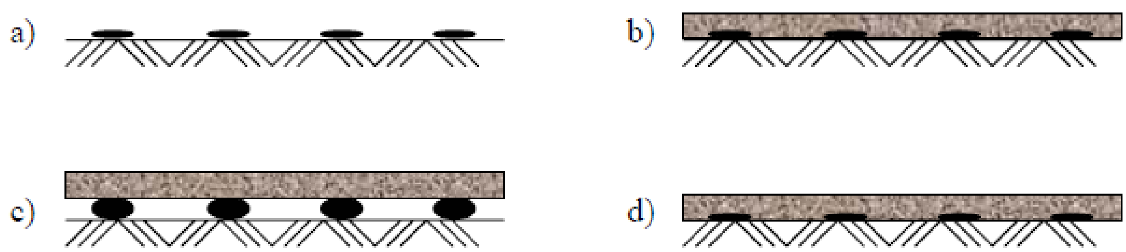

Principle of the construction technique: a) empty airbag on leveled subgrade, b) newly-cast concrete floor, c) air-filled airbags lifting concrete floor, d) lowered concrete floor resting on subgrade.

Figure 2.7 Principle of the lifting and lowering construction technique (Silfwerbran and Paulsson-Tralla, 2000)

It was concluded that this technique reduces the effective drying time and curling with providing a uniform shrinkage distribution which are caused by bilateral desiccation. This technique also causes the shrinkage to be restrained-free. Therefore it can reduce shrinkage cracking and in the meanwhile reduce the required reinforcements and increases joint spacing to control cracking of slabs-on-grade. This method was found having a major disadvantage. The problem is the slab cannot be subjected to a heavy load while the slab is lifted. Thus, the slab cannot be used for the first few months.

Mailvaganam et al. (2000) recommend a careful control of concrete mix composition. He states that handling can minimize curling however many techniques are available to repair most slabs regarding to curling problem.

Gilbert (2001) presented a model for predicting the shrinkage strain in normal and high strength concrete and the time-dependent behavior of plain concrete and reinforced concrete, with and without restrains. Gilbert states that high strength concrete causes a smaller drying shrinkage due to less free water after hydration, but endogenous shrinkage is significantly higher for high strength concrete due to less water to cement ratio in the concrete mix. Also, moist curing delays drying and may cause concrete to reach to the sufficient tensile stress and resist unsightly surface concrete. He provided an analytical procedure to estimate the final width and spacing of the flexural cracks and direct tension cracks. He concluded that the final average cracks spacing and average crack width depend on the quantity and distribution of reinforcement, the quality of bond between the concrete and steel, the amount of shrinkage, and the concrete strength. Gilbert (1986) analyzed shrinkage of unrestrained reinforced concrete member. However, there is no external restrains to shrinkage, but reinforcement embed in concrete restrains shrinkage internally. He considered a simply-supported concrete beam with no restrain and a row of reinforcing close to the bottom of the beam. Figure 2.8.a shows the beam and a small segment of beam (Δx). Figures 2.8.b and c show the stresses and strains due to shrinkage on an uncracked and a cracked cross-section, respectively. When the concrete shrinks, the reinforcement will be under compression and provides an equal and opposite tensile restraining force (ΔT) on the concrete at the level of the steel. Due to eccentricity of the tensile force to the centroid of the concrete cross section, the beam slightly warps and crack appears in an uncracked member or the existing crack width is increased in the cracked member. As Figures 2.8.b and c show ΔT is much larger on the uncracked section than the cracked section. If the compressive reinforcement is placed at the top of the sections in addition to the bottom steel, the eccentricity of resultant tension reduces and shrinkage warping is reduced. He concluded that the cracked beam shows larger shrinkage warping due to the load in compare to the uncracked beam and also shrinkage strain is not depend on stress. Furthermore, when the reinforcement is not placed symmetrically in the beam or slab, shrinkage causes a significant deflection even in unloaded member.

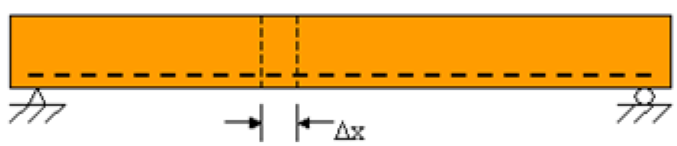

(a) Beam elevation

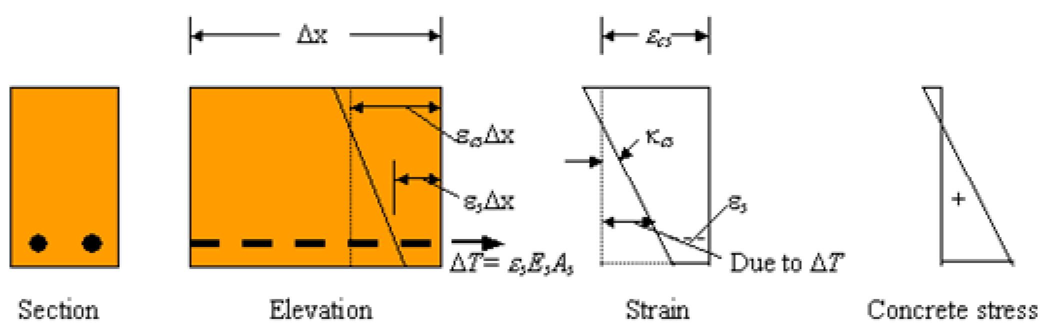

(b) Deformation and stresses in an uncracked segment

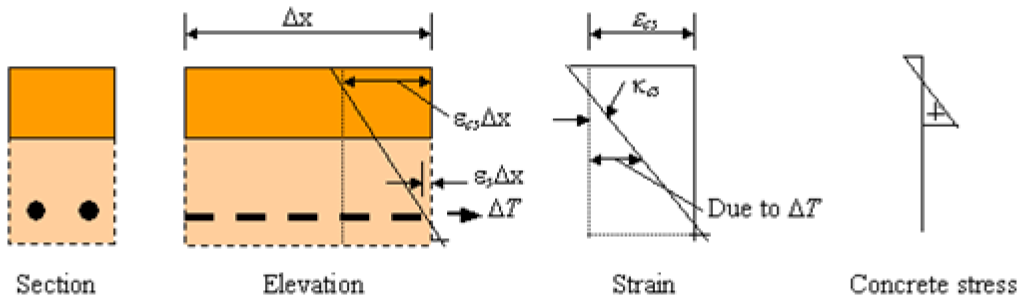

(c) Deformation and stresses in a fully-cracked segment

Figure 2.8 Shrinkage warping in a singly reinforced beam (Gilbert, 2001)

Gilbert (1988) analyzed shrinkage in unrestrained and unreinforced concrete. He considered a plain concrete slab exposed to drying at both the top and bottom surfaces of slab. The slab is unloaded and unrestrained. Figure 2.9 shows the self equilibrating stresses that produce the elastic and creep strains required to restore compatibility. ε_{cs} is defined as average contraction or mean shrinkage strain, $\Delta\varepsilon_{cs}$ as non-linear strain and is portion of the shrinkage strain developing internal stresses. The elastic and creep strains relieve shrinkage $\Delta\varepsilon_{cs}$ and result a linear total strain distribution (Figure 2.9.c).

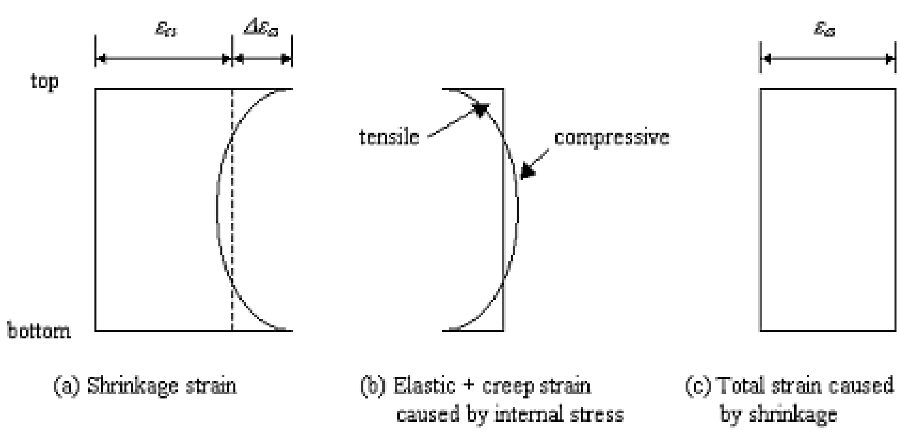

Figure 2.9 Strain components caused by shrinkage in a plain concrete slab (Gilbert, 2001)

Gilbert (1992) analyzed shrinkage in a restrained reinforced concrete member. He considered a fully-restrained member. Based on his analysis, the restraining force, N(t), increases as concrete shrinks Figure 2.10.a until the first crack occurs at N(t)=$A_c f_t$. At this point, restraining force reduces to N_{cr}. As Figure 2.10.b shows, the concrete on both sides of the crack shrinks elastically and width of the crack increases to *w*. While steel continues through the crack, the entire N_{cr} is carried by the steel and concrete does not carry stresses at the crack location. Gilbert defined two regions to carry stresses by steels and concrete. Distance S_0 on each side of the crack is defined as region 2. In this region, the crack does not influence the concrete and steel stresses anymore. In Region 1, the concrete and steel stresses are σ_{c1} and σ_{s1}, respectively. When crack occurs, the steel is in tension, but as member is fully restrained, steel cannot be elongated. Thus, steel must be compressive (σ_{s1}) at S_0 distance from the crack. The steel compressive stress creates a tensile stress in the concrete in region 1. Equilibrium requires that the sum of the forces carried by the concrete and the steel on any cross section is equal to the restraining force. As Figure 2.10.c shows the concrete stress is zero at the crack and reaches to σ_{c1} at the S_0 distance from the crack. From Figure 2.10.d the steel is in tension σ_{s2} at the crack and changes to compressive (σ_{s1}) at the S_0 distance from the crack. Gilbert calculated the concrete and steel stresses and restraining force immediately after first cracking, and approximated S_0 distance from the crack. Finally he presented calculations to predict long term behavior of concrete.

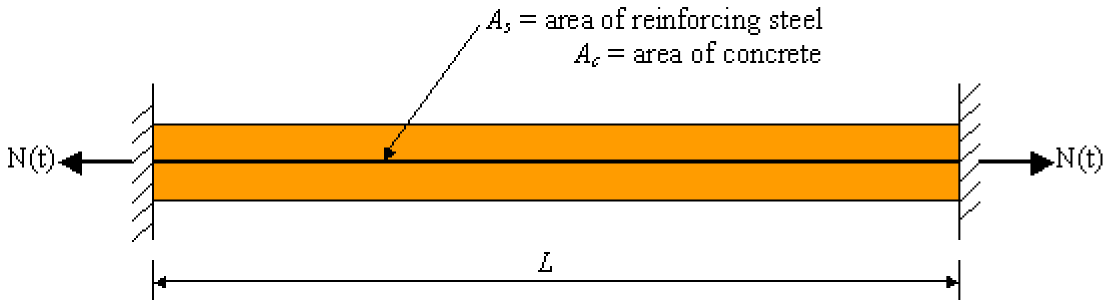

(a) Just prior to first cracking

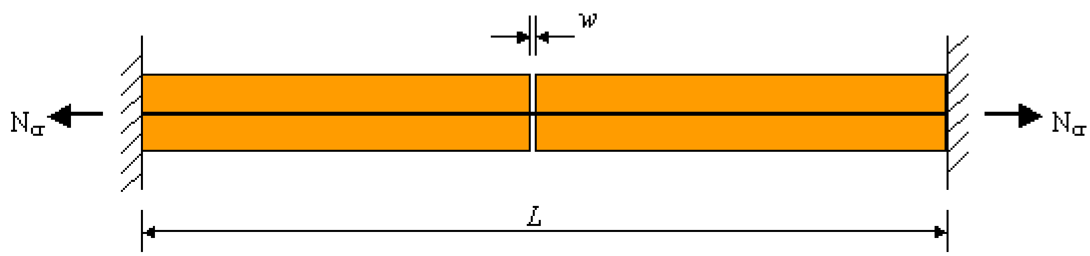

(b) Just after cracking

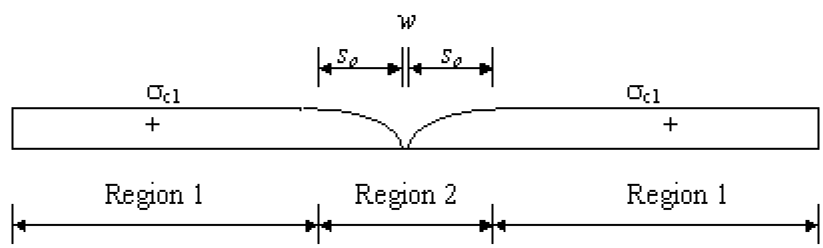

(c) Average concrete stress just after first cracking

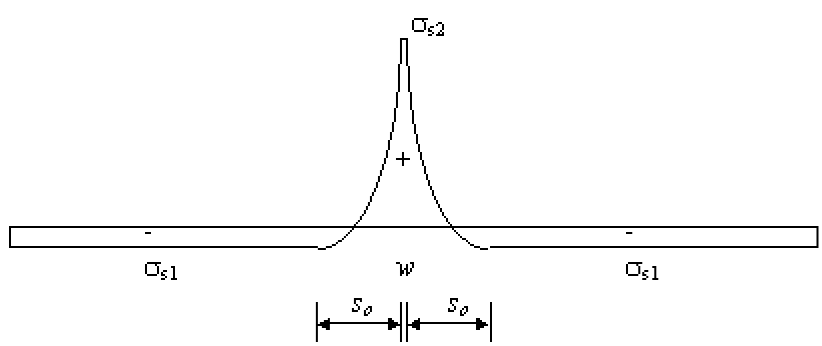

(d) Steel stress just after first cracking

Figure 2.10 First cracking in a restrained member by direct tension rather than by flexural tension
(Gilbert, 2001)

Gilbert referred to Favre et al. (1983) for estimating S_0 when deformed bar or welded wire mesh is used:

$$S_0 = d_b/10\ \rho \qquad (2.2)$$

d_b is the bar diameter, and ρ is the reinforcement ratio A_s/A_c .

Gilbert determined the concrete and steel stresses immediately after first crack appears as following equations:

$$\sigma_{c1} = \frac{N_{cr} - \sigma_{s1} A_s}{A_c} = \frac{N_{cr}\,(1 + C_1)}{A_c} \qquad (2.3)$$

$$\sigma_{s1} = \frac{2\,S_0}{3L - 2\,S_0} \frac{N_{cr}}{A_s} = -C_1 \frac{N_{cr}}{A_s} \qquad (2.4)$$

$$\sigma_{s2} = \frac{N_{cr}}{A_s} \qquad (2.5)$$

$$C_1 = 2\,S_0/(3L - 2\,S_0) \qquad (2.6)$$

Restraining force immediately after first crack: $N_{cr} = \frac{n\,\rho\,f_t A_c}{C_1 + n\,\rho(1 + C_1)}$ (2.7)

$n = E_s/E_c$ *(modular ratio)* (2.8)

Gilbert calculated the long-term behavior of concrete as shrinkage continues. His prediction equations are based on the theory states that concrete loses the fully restrained as first crack appears. After first cracking, concrete is partially restrained. As shrinkage strain continues to increase, additional cracks may appear in concrete.

Final shrinkage induced restraining force: $N(\infty) = -\frac{n^* A_s}{C_2}(\sigma_{av} + \varepsilon_{cs}^*\,E_e^*)$ (2.9)

ε_{cs}^* : final shrinkage strain

E_e^*: final effective modulus of the concrete

$E_e^* = E_c/(1 + \Phi^*)$, Φ^*: final creep coefficient (2.10)

n^* : effective modular ratio (E_s/E_c) (2.11)

$C_2 = 2\,S_0/(3S - 2\,S_0)$ (2.12)

σ_{av}: average stress in the uncracked concrete ($\sigma_{c1} + f_t)/2$ (2.13)

Maximum crack spacing: $s = \frac{2\,S_0(1+\xi)}{3\xi}$ (2.14)

$$\xi = \frac{-n^*\,\rho(\sigma_{av} + \varepsilon_{cs}^*\,E_e^*)}{n^*\,\rho(\sigma_{av} + \varepsilon_{cs}^* E_e^*) + f_t} \quad (2.15)$$

Final steel stress at each crack : $\sigma_{s2}^* = N(\infty)/A_s$ (2.16)

Note: Steel quantity is not small and steel does not yield at the crack.

Final concrete stress in region 1 : $\sigma_{c1}^* = N(\infty)(1 + C_2)/A_c < f_t$ (2.17)

Final crack width: $w = -\left[\frac{\sigma_{c1}^*}{E_e^*}\left(s - \frac{2}{3}\,s_0\right) + \varepsilon_{cs}^*\,s\right]$ (2.18)

If steel quantity is small, steel yields at first cracking, resulting uncontrolled and unserviceable cracking and crack width is wide. In this case:

$\sigma_{s1}^* = \frac{n^*\rho f_y - \varepsilon_{cs}^* E_s}{1+n^*\rho}$ (2.19); $\sigma_{s2}^* = f_y$ (2.20); and $\sigma_{c1}^* = \frac{f_y A_s - \sigma_{s1}^* A_s}{A_c}$ (2.21)

Final crack width : $w = -\frac{\sigma_{s1}^*(3L-2S_0) + 2S_0 f_y}{3E_s}$ (L: length of the restrained member)

(2.22)

Lee et al. (2002) had study on curling of unreinforced concrete toping laid over wood floor system using finite element simulations. The model showed a reasonable agreement with the curling of a full-sized wood floor with a thin concrete topping. In this research, the finite analysis had two following parts: calculating the relative humidity distribution with respect to the time and determining the topping curling deformation based on modulus of elasticity, density, and shrinkage of the concrete. It was found that topping thickness and relative humidity of the environment have a significant influence on curling of slab.

Suprenant (2002-part I) reviewed the previous research related to curling mechanism and the effect of moisture and shrinkage gradients on the amount of curling. According to Suprenant, vertical deflection or curling of slabs occurs when a combination of temperature and moisture differences develop between the top and bottom surface of slab. In the other hand, when the top surface of slab is drier, it shrinks more than the bottom surface, and when the top surface is cooler, it contracts more than the bottom and hence slabs edges and corners curl upward. Both shrinkage and temperature differences between the top and bottom surface of slab affect stress distribution and apply curling moment to the slab resulting a deflection that occur mostly at the construction joints, sawcut joints and random cracks. When the slab exposed to a low relative humidity, shrinkage gradient develops greater than that slab exposed to a high relative humidity. Therefore it was concluded that the relative humidity has an important effect on shrinkage gradient. Also, drying mostly occurs in top few inches not considering the slab thickness or external environment. Subbase has also a significant effect on shrinkage and curling of the slabs. Moist subbase increases shrinkage gradient and curling in slabs on grade. It was also concluded that the same concrete may have different amount of curling in different environments (Suprenant and Malisch, 1998). Suprenant's final conclusion states: "Factors related to the slab's final environment-temperature and relative humidity at the surface, and moisture content in the subbase or subgrade if it's in contact with concrete-can affect the amount of curl as much as the concrete properties. However, we usually attempt to control curling by modifying the concrete."

Suprenant (2002-part II) studied the factors affecting the amount of curling such as drying shrinkage, modulus of subgrade reaction, concrete strength and modulus of elasticity, reinforcement, slab thickness, joint spacing, and curing. Based on previous studies, Suprenant concluded that a) curling has direct relation to drying shrinkage and can increase by 10% with increasing modulus of subgrade reaction (*k*) between 100-200 Ib/in^3 (Al-Nasra and Wang, 1994), b) increasing the concrete compressive strength by 1000 psi increases curling about 10% (Leonards and Harr, 1959), c) curling significantly reduces with using reinforcement in the top third of the slab thickness and perpendicular to the slab edge or joint (table 2.3, Abdul-Wahab and Jaffar, 1983), d) 1% reinforcement is recommended by ACI 302 to reduce the curling potential by 60-80%, e) using 0.1-0.15% distributed steel is for crack-width control and do not have a significant effect to reduce curling, f) increasing thickness of slab decreases curling deflection (ACI Committee 360 based on work of Childs and Kapernick ,1958), g) decreasing joint spacing may reduce curling deflection, but increasing the number of joints increases the joint maintenance (Ytterberg, 1987) thus designer should use their judgment choosing a joint opening, h) longer curing only delay drying shrinkage and curling, i) finally the most important factors resulting curling deflection are the rate of moisture migration and the resulting relaxation of concrete.

Table 2.3 Effect of reinforcement on curling deflection (Suprenant, 2002- Part II)

Reinforcement, %	Reduction in deflection (compared with unreinforced)
0.46	30%
0.92	60%
1.38	100%
1.74	Negative deflection (opposite direction)

Miltenberger and Attiogbe (2002) proposed a design model for slabs-on-grade to predict the joint spacing in slabs-on-grade. The model was based on ASTM C157 drying shrinkage and environmental parameters. They formulated joint spacing based on using the following parameters for the model: shrinkage, tensile creep, tensile strength, reinforcement ratio in the slab, subgrade friction and slab geometry. They analyzed the slab with three different restraining effects taken into account. The slab is restricted by the moisture gradient through depth of the slab, friction between the slab and the subgrade, and distributed reinforcement through thickness of slab. It is assumed that the strain distribution through depth of slab is linear, and the moisture gradient restraint at top is represented as ε_{sr}. The restriction caused by friction between the slab and subgrade is represented as $\varepsilon_{\mu r}$. The restriction caused by the reinforcement is represented as ε_{rr}. Figure 2.11 shows the combination of the three restraint factors through depth of slab (h). The net shrinkage strain at the top and the bottom surfaces of slab concrete are represented as ε_{nt} and ε_{nb} respectively and free shrinkage strains at the top and bottom surfaces of slab concrete represented as ε_{ft} and ε_{fb} respectively.

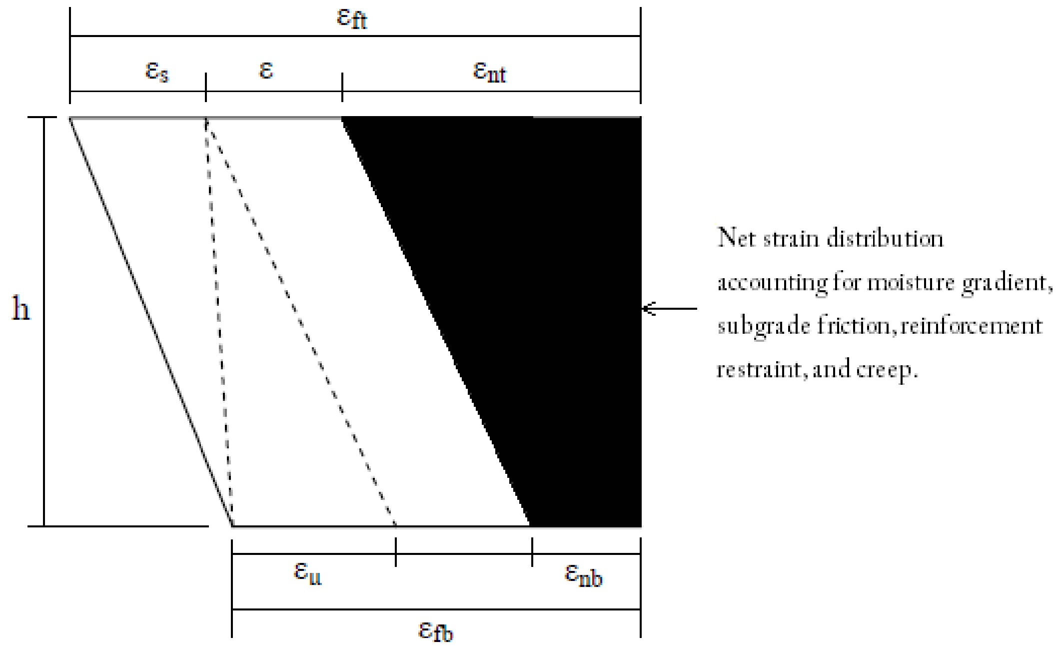

Figure 2.11 Schematic of net strain gradient in slab-on-grade (Miltenberger and Attiogbe, 2002)

Three formulas that include creep are used:

$$\varepsilon_{sr} = \alpha_{sr}\, \varepsilon_{sr}^{e} = R_{sr}(1 + k_{sr}C)\, \varepsilon_{sr}^{e} \qquad (2.23)$$

$$\varepsilon_{\mu r} = \alpha_{\mu r}\, \varepsilon_{\mu r}^{e} = R_{\mu r}(1 + k_{\mu r}C)\, \varepsilon_{\mu r}^{e} \qquad (2.24)$$

$$\varepsilon_{rr} = \alpha_{rr}\, \varepsilon_{rr}^{e} = R_{rr}(1 + k_{rr}C)\, \varepsilon_{rr}^{e} \qquad (2.25)$$

In these formulas, (R) is the degree of restraint and (k) is the creep modification factor, (C) is the creep coefficient, (ε^{e}) is maximum elastic strains. [Note: For each types of restraint, a different value is used for the parameters]. The maximum elastic strains are calculated for the moisture gradient restraint, the friction restraint and the reinforcement restraint as following equations:

$$\varepsilon_{sr}^{e} = \varepsilon_{ft} - \varepsilon_{fb} \qquad (2.26)$$

$$\varepsilon_{\mu r}^{e} = \frac{\mu \rho_c L}{E_c} \qquad (2.27)$$

$$\varepsilon_{rr}^{e} = \frac{A_s f_s}{b h E_c} \qquad (2.28)$$

In these formulas, (ε_{sr}^{e}) is the maximum elastic strain provided by the full differential shrinkage restraint, ($\varepsilon_{\mu r}^{e}$) is the maximum elastic strain provided by frictional restraint between the slab concrete and subgrade, (ε_{rr}^{e}) is the maximum elastic strain provided by reinforcement restraint. (ρ_c) is the unit weight of concrete, (L) is the control-joint spacing, (E_c) is the modulus of elasticity of concrete, (A_s) is the cross-sectional area of reinforcement, (f_s) is the elastic stress in reinforcement, and (bh) is sectional area of the concrete slab. Equation (2.26) shows that the difference in free shrinkage between top and bottom surfaces is equal to the maximum elastic strain provided by the differential shrinkage restraint. From equation (2.27), ($\varepsilon_{\mu r}^{e}$) is a function of the coefficient of subgrade friction (μ), the unit weight of concrete (ρ_c) , the control-joint spacing (L), and the modulus elasticity of concrete (E_c). From equation (2.28), (ε_{rr}^{e}) is a function of the elastic stress in reinforcement (f_s), the cross-sectional area of the reinforcement (A_s), the cross-sectional area of the concrete (bh) and the modulus of elasticity of concrete (E_c). Finally the maximum joint spacing is calculated for a given standard shrinkage (Equ. 2.29) based on the evaluation of different restraint types.

$$L_{crack} = \frac{w_{cr}}{K\ \varepsilon_{std}\left[1-\alpha_{rr}\left(\frac{\rho n}{\rho n+1}\right)\right]} \qquad (2.29)$$

In this formula,(L_{crack}) represents the control-joint spacing based on maximum crack width. (K) is used for adjustments of the curing period, the drying period, the volume to surface ratio, and the relative humidity. w_{cr} is the maximum crack width at top surface of the slab, and ε_{std} is the shrinkage obtained at 28 days based on ASTM C157. (n) is the steel modulus of elasticity to concrete modulus of elasticity ratio, (ρ) is the reinforcement ratio, and α_{rr} is defined in equation (2.25). Also, when the slab curls upward, it acts cantilever at the corners and edges. Sometimes, self weight can cause cracks occurs in the slab. Therefore, a maximum joint spacing corresponding to curling is calculated as following equation:

$$L_{curling} = \sqrt{\frac{2\varphi f_r'\left(1-\frac{1}{F.S.}\right)h^2}{3(\rho_c h\beta+\sigma_{rr})\Delta\varepsilon}} \qquad (2.30)$$

In this formula, (φ) is the strength reduction factor, (f_r') is the specified flexural strength of concrete, (*F.S.*) is the factor of safety, (h) is the slab thickness, (ρ_c) is the concrete density, (β) is a function of the relative stiffness between slab and soil, (σ_{rr}) is the restrained stress provided by the reinforcement, and ($\Delta\varepsilon$) is the difference of deformation between top and bottom of slab surfaces.

Milvaganam et al. (2002) studied curling mechanism and factors affect curling in concrete of industrial floors and also curling repairing. They found shrinkage the most important factor affects on curling of slabs. Humidity or temperature difference between top and bottom surface of the slab causes a differential strain through depth of the slab, resulting curling at the edges of the slabs due to volume changes. For instance, upward curling occurs at the joints locations in the heat buildings due to long length of joints spacing or filling the joints with incompressible materials. Based on this research, the factors that affect the amount of curling are concrete mix characteristics such as type of aggregate and water to cement ratio, environment such as winter with low relative humidity, subbase materials, and handling of the concrete and in-service conditions of slab after constructions. It was recommended that prevention is preferable than repairing however some methods were provided to repair curling. In this research, the following methods are suggested for minimizing shrinkage and curling: using concrete mix with low water/cement ratio (but not lower than 0.30), replacing blast furnace slag or fly ash, appropriate construction methods and providing protection. Milvaganam et al. recommended the following repair options based on service conditions: waiting until slab dries to the point that moisture content becomes more uniform, cutting additional joints at slab corners or panel centerlines for the floors that do not have forklift traffic, grinding for areas with no forklift traffic, patching for area with forklift traffic, grouting and grinding for floors subjected to heavy forklift, and installation of dowels for floors subjected to heavy forklift. The time for repairing must be considered after curling is almost stopped; otherwise repairing curling may cause it to be worst.

Siddique et al. (2003) had an experimental study the effect of curling on as-constructed and short-term smoothness of PCC pavements and also the factors that affect curling and roughness. In this study, the profile data was collected on six test sections on three newly built Portland cement concrete pavements (PCCP) projects in Kansas at four months intervals. All sections have 4 in. stabilized drainable subbase (cement and cement-fly ash binder), and 6 in. lime-treated subgrade (fine and plastic materials). The International Roughness Index (IRI) and a digital method were used for the smoothness statistic and for separating curling from the measured profiles using Fast Fourier Transform (FFT) respectively. It was found that curling has a significant effect on smoothness of at early life of concrete slab. Also, as-constructed and early age curling is a function of the slab thickness, stiff base, stronger concrete, and vertical grade.

Springfield (2003) illustrated the use of floor can cause lose of surface flatness. Also, differential shear between the replacement slab and the original slab causes shear to transfer across control joints, resulting cracks at the joint edges as traffic pass the joints. Therefore, Springfield recommended installing shear dowels in to the sawcut edges.

Harrison (2003) illustrated the higher shrinkage materials increase shrinkage restrain, resulting random cracks. Also higher shrinkage materials increase curling and warping caused by differential drying at cracks, floor joints, or other slab separations.

Kim et al. (2003) developed a computer program, CRCP-10 based on finite element formulations, transformed field domain analysis, and probability theories to analyze the behavior of continuously reinforced concrete pavement. The model concerns many variables such as pavement geometry, concrete and steel material properties, bond-slip relationships between concrete and steel bars and concrete and base layers, environmental (temperature and drying shrinkage through depth of the concrete slab) and external wheel loads, finite element types, and creep parameters. According to Kim et al., this program can solve real problems related to reinforced concrete pavement more efficiently. The program can also predict crack spacing distributions and punch-out failures. However, performing the future calibration of the program with field data is recommended to provide more accurate results.

Simpson (2004) had some idea for controlling cracks in slab concrete. He stated the requirements of placing the crack control reinforcement at top surface of suspended industrial floors.

Phelan (2004) found Athletic Concrete a successful way in industry. Athletic concrete has shown a very good quality of hardened concrete at reduced cost.

Jeong and Zoollinger (2004) studied effects of temperature, moisture, and creep on curling and warping behavior of jointed concrete pavements under different curing condition. They cured half of the slab tests with standard curing component and the other half with mat-cured. The half slab cured with mat showed much less shrinkage and creep before comparing the final set with the other half slab using standard curing. Shrinkage and creep were increased significantly after removing mat curing. Also, mat cured half showed a larger magnitude of shift in tensile strain with time in compare to membrane-cured half. A linear relationship was found among vertical corner displacements, concrete strain differences, and dowel bending moment. It was concluded that a) as concrete exposed to the ambient climatic conditions, the concrete water evaporates, b) drying concrete causes drying shrinkage occurs in concrete slab, c) if drying shrinkage is uniformly distributed through the depth of concrete slab, the slab movement would be accommodated by saw-cut joints, d) slab dimensions and subbase stiffness are the main factors for restraining the concrete slabs.

Lange et al. (2006) studied curling problem of concrete slabs for Airfield Applications. The purpose of this research was predicting moisture curling according to a set of material models for aging concrete. The material models set include the material models for elastic, creep, hygrothermal and thermal behavior of concrete. The total strain of concrete was obtained from following equation (2.31) based on combining elastic (ε_{EL}), creep (ε_{CR}), hygrothermal (ε_{HT}) and thermal strains (ε_{T}).

$$\varepsilon = \varepsilon_{EL} + \varepsilon_{CR} + \varepsilon_{HT} + \varepsilon_{T} \qquad (2.31)$$

A computer simulation modeling and a series of laboratory experiments were conducted and compared in this research. The computer model of the curling was based on measuring temperature and internal relative humidity profiles for a tested single slab to validate the material model set and the finite element implementation. The measurements in the experimental section included mechanical properties, internal relative humidity and temperature at three different depths (6.25 mm, 25 mm, and 50 mm from the surface), drying shrinkage and creep. It was found that the numerical simulation with the material model set has a very good agreement with the laboratory experimental measurements. Thus, it could be concluded that the prediction method can be used for concrete pavement design.

Tarr et al. (2006) studied the flatness of concrete slabs and how to maintain the flatness of the slab. They found that warping and warping relaxation are the phenomenon that creates humps, severely damaging the slab. Measured warping results show that as the moisture gradient reduced in covered floors compare to uncovered floors, the warping magnitude decreased from 0.80 in. for uncovered floors to 0.18 in. for covered floors (Figure 2.12). From the measured concrete relative humidity plot, the moisture content is almost 100% in bottom surface of slab for both covered and uncovered slab, and also the moisture content drops about 20% and 12% as close to top surface of uncovered and covered slab respectively (Figure 2.13).

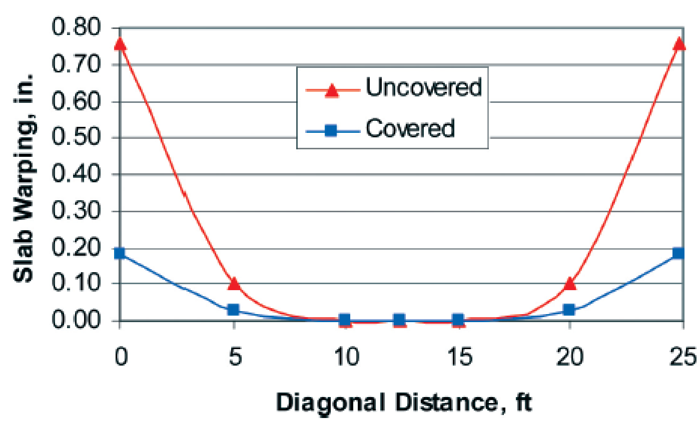

Figure 2.12 Relative Warping profile between uncovered and covered slab panels (Concrete Repair Bulletin, 2006)

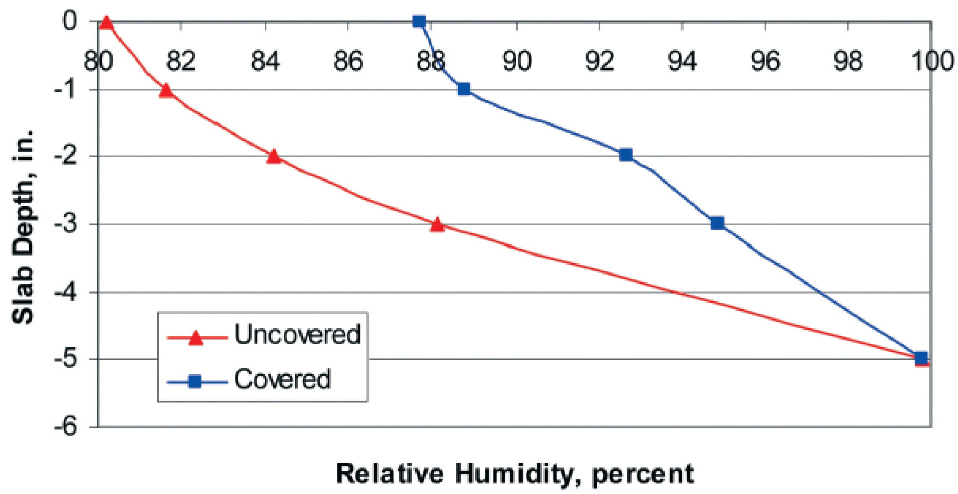

Figure 2.13 Relative Moisture Gradient between uncovered and covered portions of a slab (Concrete Repair Bulleten, 2006)

According to this research however, post tensioning, shrinkage compensating, and reinforcement (generally > 1%) can prevent warping but they are not an absolute remedy for upward warping and cracks that are caused by drying shrinkage. Thus, the minimizing of the w/c ratio is recommended in order to reduce the shrinkage potential of concrete. Additionally, it is recommended that the surface of concrete is sub-sealed prior to surface grinding in order to mitigate the risk of warping relaxation.

Wong et al. (2007) had an experimental study on drying shrinkage and creep of concrete. They used two methods, using Brag grating (FBG) as a fiber-optic device (Lee, 2003), and standard mechanical method using strain gage. The fiber-optic sensor was embedded in core of concrete and used to measure the strain change of the core in concrete. In mechanical measurement, a length comparator (Wykehan Farrance) with 295 mm (Mitutoyo 167-112 MB-300) and a Demec were used to find the surface strain of concrete. The length comparator has a resolution of 0.002 or about 7 με. Drying shrinkage is obtained from the optical measurements from the embedded FBG sensors and the mechanical device using a reference bar to find the fractional length change of the prisms. Creep strain is obtained from the loaded specimens immediately after loading. In this experiment, two types of mould rectangular prism and cylinder were used based on AS 1012.2 (1994) and AS 1012.8. (2000). The rectangular prisms (75x75x280 mm) were used for the drying shrinkage tests and the cylinders (100 mm diameter and 200 mm height) were used for creep experiments. The concrete mix composed of cement, sand, coarse aggregate with a maximum size of 19 mm and water-to-cement ratio of 0.57. The specimens were demoulded after 24 hours and cured in a fog room with the (T=23 ºC and relative humidity (RH) =100%) for 7 days. Then they were kept in a drying room with the (T=23 ºC and RH=50%). Data were collected for 56 days to follow up the drying shrinkage and creep of specimens. Then the long-shrinkage and creep prediction were analyzed based on the available experimental data. The AS does not have any formula for shrinkage prediction, therefore a formula (2.32) for a normal weight concrete in a drying environment and normal temperature was used to predict shrinkage of concrete for long term (Neville and Brooks 2004).

$$\varepsilon_{\text{shr}}(\text{t}) = \varepsilon_{\text{shr},28} + 100\sqrt{3.61.\ln\ (t) - 12.05} \qquad (2.32)$$

Where ε_{shr} is the drying shrinkage strain, $\varepsilon_{shr,28}$ is the measured shrinkage after 28 days of drying, and t > 28 days is the time since the start of drying.

The following equation from AS 1012.16 (1996) was used to predict creep of concrete:

$$C_T(t) = F(K).\ln(t+1) + \left(\frac{1}{E(t_0)}\right) \qquad \text{Long term prediction} \quad (2.33)$$

Where $C_T(t)$ is the specific total strain at time t (in με/MPa), F(K) is the rate of creep (in με/MPa/day), and $E(t_0)$ is the instantaneous elastic modulus (in με/MPa). From the test results, the embedded FBG sensors and the standard mechanical strain gages have a good agreement with a high degree of correlation. In the both methods, shrinkage values increased fast in the first week, and then increased more slowly afterwards. Also, the creep increased fast after loading in the first week, and it increased more slowly after one month. Therefore, both methods have the same trends. The drying shrinkage and creep were predicted after one year by using expression, and it was found that the prediction has an agreement with actual measurements. Also, the FBG was found a better method to study the time-dependent properties of concrete.

Walker and Holland (2007) investigated use of dowels at the joint locations on floors that are designed to sustain heavy traffic such as lift truck. They analyzed the forces in the dowels via computer models and they found the relative differential deflection between the slab panels. The assumptions for the model were close to a common condition for slab on ground. In this research, design graphs were developed for dowel plate. The graphs help designers find the most economical dowel size and space for industrial floors where lift trucks will be used.

Duran-Herrera et al. (2007) studied the effect of substituting 20% of normal sand by an equal mass of light sand on shrinkage of high-performance concrete with a 0.35 water/binder ratio (w/b). Based on this research theory, autogenous shrinkage of high-performance concrete with low w/b can be mitigated with internal curing. In high w/b ration, drying shrinkage is large and autogenous shrinkage can be neglected while in low w/b ration autogenus shrinkage can be as large as drying shrinkage. Four concrete samples of 100x100x400 mm (4x4x16 in.) were tested. The four samples received the same curing for the first 23 to 25 hours, and then they were demolded. Two of the samples were sealed with self-adhesive aluminum foil to prevent any exchange of humidity between the concrete and environment and a closed curing system was represented. Another two samples were cured under water for 6 days. After removing these two samples from water, they were maintained at 23 ºC (73 ºF) and a 50% relative humidity environment. Vibrating wire gauges cast at the center of the specimens to monitor shrinkage. The concrete contained some light weight sand swelled slightly more and for a longer time during the first 23-25 hours staying in the molds because of the better hydration condition than the normal sand concrete. The results showed that a 20% substitution of normal weight by lightweight sand reduces autogenous and drying shrinkage of high-performance concrete with a 0.35 w/b. Also, cementitious matrix showed low chloride ion permeability in accordance with ASTM C 1202 at the age of 56 days results. In addition, light weight sand did not have a significant effect on 28-day compressive strength.

Bissonnet et al. (2007) studied drying shrinkage, curling, and joint opening of slabs-on-grade. The purpose of their investigation was to characterize the curling and joint opening of concrete slabs in a controlled environment. The variables of their experimental slab tests were concrete mix and amount of steel reinforcement. Two concrete mixtures were used in this research: normal-strength concrete with a water-cement ratio of 0.53, and high-strength concrete with a water-cement ratio of 0.36. A water-reducing admixture and a high-range water-reducing admixture were used in both mixtures. The 3 x 40 x 240 inch slabs were cast over a concrete warehouse floor on a vapor barrier and 4 inches of moist compacted sand and were conditioned in a controlled environment at a 30% RH and 23ºC (73.4 ºF) temperature. Slabs were restrained in longitudinal direction with three stiff channels (CSA C 200x28 channels). The channels were tied with welded transverse reinforcing bars to transfer load from the concrete slab. The amount of steel reinforcement investigated were ρ_s=0, 0.08, and 0.23%. Welded wire fabric reinforcements were installed at mid height of slab. Slab monitoring which began after 7-day moist curing consisted of the curvature of slab, axial strains, join movements, surface cracking, and RH. It was found that curling and joint opening develop early and they relate to drying shrinkage. In other words, the rate of developing curling is proportional to that of drying shrinkage and curling has a direct influence on joint opening. It was also found that with increasing reinforcement ratio, cracking is observed most at mid-span between joints. Therefore, Bissonnette concluded that high stiffness reinforcement can promote cracks.

Poppoff (2008), a concrete contractor, submitted an article based on his experience on a 6 in. thick concrete floor for a new warehouse and office building. The purpose of his experiment was a research to provide a flat and level floor for many years with minimizing curling and cracking of slabs. A low-shrinkage, athletic concrete were used in this research. Also diamond dowels were used at all construction joints and load plate baskets at all sawcuts joints. The joints located at 25 ft x 20 ft x 10 in. According to Poppoff, the results were excellent. He found the floor almost flat with little cracks after fourteen months. He concluded that the proper base preparation, planning, execution, and use of a low-shrinkage, fiber-rich mixture helped them to provide an excellent floor. As a contractor, they use the same mixture, with entrained air, for their other jobs and also for the exterior paving jobs with no extreme problem. Table 2.4 shows the mixture used in this experiment.

Table 2.4 Mixture proportions and physical properties for the floor concrete [Mike Poppoff, 2008]

Mixture proportions	
Cement	517 lb/yd³ (307 kg/m³)
Fine aggregate	1296 lb/yd³ (769 kg/m³)
3/4 in. (19 mm) maximum size coarse aggregate	1250 lb/yd³ (742 kg/m³)
1-1/2 in. (38 mm) maximum size coarse aggregate	750 lb/yd³ (445 kg/m³)
Water	270 lb/yd³ (160 kg/m³)
High-range water-reducing admixture	10 oz/100 lb cement (650 mL/100 kg cement)
Macropolymeric synthetic fibers	4.0 lb/yd³ (2.4 kg/m³)
w/cm	0.51
Physical properties	
Air content	1.3%
Slump	6 in. (150 mm)
Shrinkage	0.038% at 28 days

2.3. Shrinkage Reducing Admixture (SRA)

Researchers and engineers have used several techniques to control shrinkage and consequently cracking of concrete. Shrinkage reducing admixture (SRA) is one the approaches used to control concrete shrinkage. SRA has been discussed in the literature for more than two decades by numerous authors. Shrinkage reducing admixtures (SRAs) are designed to decrease the effects of drying shrinkage by reducing the surface tension in these pores. It is expected that SRA can be dispersed in the concrete during mixing and it remains in the pores and continues to reduce the surface tension effects even after concrete hardens. Thus, SRA can attribute to the reduction in the evaporation rate, delay of the peak capillary pressure due to the development of menisci in the pores and lower settlement. Although, it has been many studies based on using ASTM C 157 method to find out the effects of SRAs on drying shrinkage of concrete, but it is not still clear whether SRAs reduce shrinkage cracking in large scale concrete structures. The SRAs discussions are based on behavior of cement while it is hydrated. A hydrated cement paste loses moisture from its extremely small pores. The remaining water provides a surface tension that tends to pull the pores together and consequently loss of volume over the time and resulting shrinkage of cement paste. This shrinkage mechanism does not occur in pores larger than 50 nanometers (0.00000004 inches) because the tensile force in the water is too small to cause shrinkage (Balogh, 1996).

Shah et al. (1992) studied the effects of three different types and amount of shrinkage reducing admixture (SRA) on restrained shrinkage cracking of concrete. They performed Free-shrinkage tests and restrained- shrinkage tests. Then the results of tests using SRA were compared with concrete reinforced with steel and polypropylene fibers and wire mesh. The results showed that SRA significantly reduces free shrinkage and also crack width.

Balogh (1996) studied effects of shrinkage reducing admixture (SRA) on concrete shrinkage. The experimental tests were conducted according to ASTM C 157-93, and ASTM C 494-92. Based on the lab and field test results, Balogh showed that SRA is affected by three following major factors: water-cement ration, type of cement, and level of curing. It was shown that generally the percentage of shrinkage reduction increases with lowering the water-cement ration. Also, different cements affect an admixture's performance. Longer wet curing has a positive effect on admixture especially in early-age concrete and it also reduces the ultimate levels of shrinkage. It was also found that SRA reduces the compressive strength of concrete. Balogh stated that the provided tests data in this and previous research are not enough to confirm the effect of SRA on shrinkage cracking and curling of slab concrete used in the field.

Folliard and Berke (1997) studied the effect of shrinkage reducing admixture (SRA) on properties of high-performance concrete. They found shrink reducing admixture effective in reducing shrinkage of high-performance concrete and also SRA reduces the restrained shrinkage cracking.

Nmai et al. (1998) studied shrinkage reducing admixture. Their work was based on minimizing drying shrinkage by reducing concrete water content as low as possible. According to this research, reducing water content can be obtained by using high content of free clay, stiff, and rigid aggregates, and by using mid-range and high range water-reducing admixture. It was concluded that shrinkage-reducing admixtures effectively reduce drying shrinkage and cracking of concrete.

Shah and Weiss (2000) had experimental tests regarding to using shrinkage reducing admixture. They found that shrinkage reducing admixture (SRA) have a similar or slightly lower chloride penetration index and reduced cracking potential with similar or lower strength.

Newberry (2001) illustrated shrinkage reducing admixture reduces the surface tension of water within the capillaries and pores within the cement past. Therefore, using SRA in concrete mix slows down early age shrinkage and also it reduces long-term shrinkage. Thus, SRA provides crack-free watertight structures for water retaining structures and prevents movement along joints in concrete slabs. However SRA reduces the compressive strength of concrete.

Weiss and Berke (2003) reviewed the recent research on the use of non-expansive shrinkage reducing admixtures. They concluded that using SRA in concrete mixtures reduces strength, modulus, and fracture properties of concrete. SRA also reduces overall magnitude of the shrinkage and consequently cracking of the concrete.

Gettu and Roncero (2005) studied drying shrinkage behavior of concrete using glycol-based SRA for one year. They used SRA with 1.5% of the cement weight. The specimens were maintained at 50% relative humidity and 20 ºC temperature after 28 days of curing. The results showed a 22% reduction of drying shrinkage and also reduction of the compressive strength which is not significant in compare with reduction of drying shrinkage.

Jian-Guo and Pei-Yu (2006) illustrated SRA has a potential to decrease autogenous shrinkage and drying shrinkage of concrete. They states: “SRA delays setting time of concrete to a tolerable degree and slightly improves its strength development expect those in early age”. They concluded that SRA reduces restrained shrinkage stress, resulting in a decrease of cracking in concrete under restrained condition.

Zhibin et al. (2008) studied the effect of shrinkage reducing admixtures (SRAs) on autogenous shrinkage and drying shrinkage of cement paste. Their results show that SRA effectively reduces the autogenous and drying shrinkage. It was found that SRA slightly delays the hydration of cement, resulting in delaying the time of exothermic peak, and reducing the peak value and hydration heat of cement.

2.4. High Performance Concrete

Use of high-performance concrete (HPC) has significantly been increased in structures since 1990. Although HPC has superior strength and low permeability, it is sensitive to early-age cracking (Cusson et al., 2005). High strength concrete often called high-performance concrete since compressive strength is practically the parameter to describe the quality of concrete. It is generally assumed that high strength of concrete increases the long-term durability; however it may not always be true. The high strength concrete is sensitive to shrinkage cracking. Early contraction distortion of high-performance concrete is more complex than that of ordinary concrete (Meng, 2011). Sensitivity to early age cracking can cause premature reinforcement corrosion, concrete deterioration, and higher maintenance costs and reduced service life of concrete structures.

Mechanical properties and durability properties are a function of material porosity, both pore volume and distribution. Mechanical properties are defined as strength and stiffness of materials and durability properties are defined as permeability of materials. Concrete has a wide range of pore sizes that have influence performance characteristics of concrete differently. Many researchers have studied the relation between porosity and performance of concrete. According to Young (1986) study, volumetric stability or shrinkage is related to the small capillary and gel pores. Brown et al. (1991) showed that permeability of concrete is related to the capillary pore size and distribution. Takahashi et al. (1997) found that as pore size and volume reduce, strength and ion penetration resistance increase. He also stated that cracking resistance of concrete is related to maximum pore size or total pore volume.

El Hindy et al. (1994) measured shrinkage of two different types of high-performance concrete (HPC). They found that longer curing time and lower the water to cement ratio reduce drying shrinkage.

De Larrad et al. (1994) studied silica fume which has been recently used in concrete to increase strength and durability of concrete. Based on this research, however, it was shown that silica fume increases the strength of concrete due to pozzalanic reactions and increased particle packing density; it may show increasing free shrinkage due to pore refinement.

Wiegrink et al. (1996) studied the restrained shrinkage cracking on several levels of concrete focusing on high- strength concrete. In the test procedure, high strength concrete was obtained with replacing cement partially by silica fume and reducing water content. Ring-type specimens were used to provide restrained shrinkage cracking tests. Free shrinkage, creep, weight loss, compressive, and splitting tensile strength were considered in this research. It was found that water content and weight loss do not have effect on free shrinkage of concrete. Furthermore, high strength silica fume concrete showed higher shrinkage and lower creep. Also, high strength silica fume showedt cracks develop faster and significantly wider in compare to the normal-strength concrete.

Shah et al. (1997) studied the effects of mix proportions on compressive strength, shrinkage, creep, and brittleness. The focuses of this research was to understand and characterize early age cracking in high performance concrete. Effects of various percentages of silica fume and shrinkage reducing admixture on several material compositions were investigated. In addition to experimental specimens stored in an environmental chamber, a model was provided based on fracture mechanics concepts in conjunction with coupling the effects of shrinkage stress and creep relaxation. The model was used to predict the age of the first cracking. The results showed that early age cracking occurs in high performance concrete quicker than normal strength concrete and using silica fume significantly reduces the effect of creep. Also, use of 2% of shrinkage reducing admixture (SRA) reduces free shrinkage in 42% at 50 days. Furthermore, delaying shrinkage cracking significantly reduce crack opening. Finally, a favorable comparison is observed between the model predictions and the experimental observations.

Li et al. (1999) studied the crack width of high performance concrete using ring-type tests to restrain the shrinkage of specimen. They found that increasing silica fume, fly ash, and calcium nitrite inhibitor in concrete mixture causes the crack width increases. Additionally, based on their numerical analysis of the experimental results, restrained shrinkage causes the damage of the restrained surface contributes significantly to the crack width.

Shah and Weiss (2000) used two methods for the purpose of improving the performance of concrete and five mixtures to illustrate compressive strength, chloride permeability, and potential of restrained shrinkage cracking. The methods included decreasing the w/c ratio (0.5, 0.4, and 0.3) with using two admixtures, and adding silica fume to reduce chloride penetrability. They found that reducing the water to cement ratio (w/c) of concrete improve the strength, stiffness, chloride penetration resistance, and drying shrinkage. However lowering w/c ratio increases autogenous shrinkage especially at early ages when the material is gaining strength. Furthermore, silica fume reduces chloride penetrability, improves strength and stiffness while may cause an early ages cracking. Based on this research, it was concluded: “high performance materials may relay on the ability to manipulate the microstructure (pore size and distribution) of cementitous materials to optimize the performance of concrete for a given application”.

Qi et al. (2002) had an experimental study on effects of three types of chemical admixtures, calcium nitrite inhibitor (CNI), retarder (D-17) and superplasticizer (W-19) on free shrinkage and restrained shrinkage cracking of high performance concrete. It was found that with the same water to binder ratio (0.4), free shrinkage and shrinkage cracking width reduces with mixtures using D-17 of 0.25 percent or higher ratio of W-19 (2.76 percent). Mixture containing CNI showed an increase in free shrinkage and shrinkage cracking width.

Lee et al. (2003) showed that the early age autogenous shrinkage of HPC is developed more rapidly than that of normal-strength concrete. Although, partially replacement of cement by fly ash has a direct effect on reducing autogenouse shrinkage, it might not prevent early age cracking.

Nassif et al. (2003) studied three curing methods consisted of air-dry curing, burlap or moist curing, and use of a curing compound. The results show that using moist (burlap) curing within one hour after the placement of concrete improves early-age performance of the concrete.

Ye et al. (2009) showed the effect of three fine aggregates composed of superfine, medium, mixed and manufactured sand on high performance concrete (HPC). The HPC with superfine sand produced a higher initial shrinkage than mixed or medium sand. They found that an optimal sand percentage is required to reduce shrinkage cracking of HPC with mixed or medium sand.

Gupta et al. (2009) provided an experimental investigation to evaluate shrinkage of high strength concrete. They used different types of coarse and fine aggregates such as sand stone and Granite (12.5 mm size) and Yamuna and Badarpur Sand, 1:0.8:2.2 of the mix proportion of concrete, water to cement ratio of 0.3, 2% by cement weight of Suerplasticizer . Fly ash and silica fume were used as portion of High Strength Concrete. It was found that the shrinkage strain of concrete increases with time, and also fly ash and silica fume increases shrinkage strain of concrete. Also, 90 days shrinkage strain results showed that concrete with Badarpur sand has slightly less shrinkage strain (10%) than concrete with Yamuna sand. In addition, shrinkage strain of concrete with granite aggregate is slightly less (0.7%) than shrinkage strain of concrete with sandstone aggregate.

Soliman and Nehdi (2010) investigated the effects of drying conditions on autogenous shrinkage of ultra-high performance concrete (UHPC) at early ages. The specimens were exposed to different temperature (10, 20 and 40 ºC) and relative humidity (RH) from 40 to 80%. The tests indicate the effects of shrinkage reducing admixture (SRA) and superabsorbent polymer (SAP) using as shrinkage mitigation method in sealed and drying conditions. It was found that autogenous and drying shrinkage are dependent phenomena. Both SRA and SAP have a significant effect in reducing autogenous shrinkage under sealed conditions. SRA reduces drying shrinkage in drying conditions while SAP increases drying shrinkage in drying conditions. Furthermore, adequate curing is very effective in reducing shrinkage in UHPC even with using any type of shrinkage mitigation method.

2.5. Expansive Cement Concrete

Expansive cements reduce the shrinkage of concrete that causes cracks to occur in conventional concrete. Both expansive cements and ordinary Portland cement have similar strengths with same quantities. Also, design of expansive cement is similar to the ordinary Portland cement [Simms (1966)]. Expansive cement causes the concrete to expand during the first two or three days. This expansion is caused by forming anhydrous calcium sulfoaluminate from sulfoaluminate admixtures using limestone, bauxite and gypsum. Concrete expansion causes tensile strength is developed in steel reinforcements and consequently the concrete to be in compression (ACI 224R-01). Maximum value of expansion of concrete is 0.04 to 0.5 % and does not bend forms (Architectural Record, 1966).

Pinkerton et al. (1972) studied expansive cement concrete type K. In this research, the field length change measurement in one project was compared with library restrained expansion test for 90 days. The similar results were found in both field and laboratory tests. The conclusion was that a longer joint spacing can be performed in use of expansive cement in compare to the regular Portland cement.

Folliard and Berke (1997) illustrated abundance of ettringite formed during the early hydration stages can cause Rapid slump loss with in expansive cement concrete. They referred to Mahta (1973) study and stated that the addition of 0.05 percent citric acid by weight of cement delayed the ettringite and gypsum formation at early age. Thus, they concluded that citric acid provides a solution to the slump loss problem in expansive cements.

Rubin (1973) illustrated expansive cements need more water of hydration in compare to the normal Portland cement. Also, expansive cements are more sensitive to high temperatures.

Russell (1973) showed that three types of commercially available shrinkage compensating cements (Types M, S, and K) have the same structural behavior. The compensation of these cements is mainly dependent upon the restraint within and adjoining the slab. Russell mentioned that based on structural design details, type of cement, type of external restraint, percentage and position of reinforcement and type of concrete aggregates have influence the degree of shrinkage compensation. In addition, type of cement, type of external restraint, percentage and position of reinforcement, and type of concrete aggregates are details that influence the degree of shrinkage compensation.

Hanson et al. (1973) compared Type M shrinkage compensating cement (SCC) with Type I Portland cement in the library. It was found that both concretes have the same properties for both plastic and hardened conditions. Both concretes were restrained against shrinkage and expansion. During the expansion, compressive stress of type M concrete was increased up to 120 psi and creep affected this stress to be dissipated in 12-18 hours. Furthermore, tensile stresses were developed in both concretes as drying shrinkage increased and "self-induced" failure occurs in all restrained specimens. Hanson compared drying shrinkage curves for the two types of concrete. He concluded that the curves are parallel for both type I and type M but offset by the initial expansion of type M concrete.

Liljestrom (1976) studied shrinkage-compensating cement concrete (SCC). He referred to ACI 223 report that identified three types of shrinkage-compensating cements K, S, and M. Liljestrom drew a conclusion based on ACI 223 report and said that the main purpose of using SCC is offsetting the amount of drying shrinkage of concrete. Figure 2.14 shows volume changes to be expected with shrinkage-compensating concrete are compared with those for Type I and II Portland cement concrete for mixes containing 537 pounds of cement per cubic yard. It showed that SCC and Type I and II Portland Cement concrete have same characteristics in the plastic condition. Furthermore, shrinkage-compensating concretes are more cohesive and have fewer tendencies to segregate in compare to the conventional concrete. Also, bleed water does not occur with SCC concrete. SCC concrete is sensitive to extreme temperature either hot or cold. It sets faster in high temperature and slower in low temperature. SCC is also sensitive to mixing time. If mixing time significantly increased, it will increase slump loss. Liljestrom provided following guidelines based on SCC concrete characteristic, to obtain full advantages from the properties of shrinkage-compensating cement concrete:

- For the slab made with SCC, concrete contraction joins are not needed when construction joints are used at intervals of 40 to 120 feet.
- Subgrade should be wet cured in case of slab on grade made with Shrinkage-compensating cement concrete.
- Do not place slab on grade made with shrinkage-compensating cement concrete directly over a vapor barrier. If it is required, at least 1 to 3 inches of sand should be placed over the vapor barrier and the pre-wetted sand.

- Location of reinforcement is important for slab on grade made with shrinkage-compensating cement concrete. The reinforcement should be placed in the upper half of the slab, preferably at about 1/3 the thickness of the slab.
- Avoid delaying in discharging the concrete from transit mixers at the job site.
- In hot, dry and windy weather, provide continues fog sprays to reduce the high rate of evaporation on the surface.
- At least seven days of curing is required for the concrete made with SCC to achieve the best results.

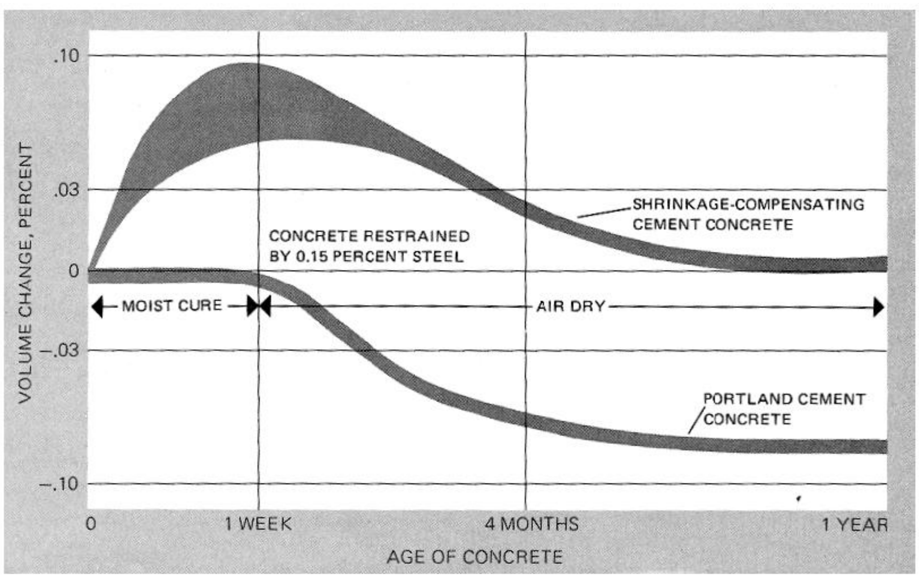

Figure 2.14 Volume changes of Portland cement and shrinkage-compensating cement concrete (Liljestrom, 1976)

Cohen and Mobasher (1988) illustrated almost all of the researchers who study the expansive cement focus on the expansion behavior rather than on shrinkage behavior. Therefore there is a lack of research on shrinkage behavior of expansive cement.

Generally shrinkage of expansive cements is greater than Portland cements especially if expansive cements are not cured at least 7 days.

Keith et al. (1996) studied a pavement project using shrinkage compensating concrete (SCC). Atlanta Bonded Warehouse Corporation (ABW), the owner of this project, asked for less maintenance, drain well, keeping joints and cracks to a minimum. In order to prevent spalling and keeping surface runoff from reaching the subgrade, minimizing joint widths, and eliminating significant upward edge curl. Using shrinkage compensating concrete easily met ABW expectations. The paving drains very well and has no significant "bird baths". Using shrinkage compensating concrete in this project showed significantly reduction of curling, cracking, and number of pavement joints.

Pera and Ambroise (2004) studied the utilization of calcium sulfoaluminate cement. This study is a limited work based on the chemical formula of calcium sulfoalominate. The main parts of sulfoaluminate cements are the belite (C_2S), yeelimite or tetracalcuim trialuminate sulfate($C_4A_3\bar{S}$), and gypsum ($C\bar{S}H_2$). Sulfoaluminate cements also include additional components such as : C_4AF, $C_{12}A_{37}$, C_3A, and C_6AF_2 (Su et al. , 1997; Zhang and Glasser , 1999; Chatterjee, 2002). Two following reactions [Odler, 2000] illustrate how ettringite ($C_6A\bar{S}_3H_{32}$) is produced when the CSA cement hydrates.

$C_4A_3\bar{S} + 2C\bar{S}H_2 + 36H \Rightarrow C_6A\bar{S}_3H_{32} + 2AH_3$ (Calcium hydroxide or lime is **not** present) (2.34)

$C_4A_3\bar{S} + 8C\bar{S}H_2 + 6CH + 74H \Rightarrow 3C_6A\bar{S}_3H_{32}$ (Calcium hydroxide or lime is present) (2.35)

According to the research by Metha (1973), the microstructure of ettringite depends on the presence of lime. Therefore, the ettrinigite produced from equation 2.34 provides a high early strength, and it is nonexpendable (Beretka, 1997). And the ettrinigite formed from equation 2.35 is expansive and it is used to reduce shrinkage (Su, 1992). Pera and Ambroise developed a high early strength concrete and designed self-leveling screed with limiting curling and self leveling repair mortar based on these two important properties of ettringite in CSA. They also found that using glass-fiber-reinforced cement can be demolded 4 hours after casting and it provides high ductility and durability after aging in different weathering condition.

Bondy (2010) studied four projects using shrinkage compensating concrete. He found this type of concrete one of the most successful solutions to the restraint to shortening (RTS) problem encounter with the post-tensioning industry.

2.6. American Concrete Institute (ACI 360R-06)

ACI 360R-06 has provided information to design slabs-on-ground made with unreinforced concrete, reinforced concrete, shrinkage-compensating concrete, post-tensioned concrete, fiber-reinforced concrete, and slab on ground in refrigerated buildings. This document presents the general advantages and disadvantages of each of these slab designs and concerns minimizing curling and cracking of slabs-on-ground [Note: The document is presented in ACI 360R-6 table titled “general comparison of slab types”]. ACI 360 does not specifically address the design of roadway pavements, airport pavements, parking lots, and mat foundations. ACIs do not include a single design technique for all slab applications. Rather, there are a number of identifiable construction concepts and a number of design methods. Each combination should be selected based on the requirements of the specific application.

2.6.1. Reducing Effects of Slab Shrinkage and Curling

ACI referred to previous research (Ytterberg ,1987; Walker and Holland, 1999) for reducing effect of the drying shrinkage and curling (warping) in slabs-on-ground. According to ACI, approximately half of the water used in concrete mix is only for workability of concrete and it is not used for cement hydration. The additional or free water evaporates from the upper surface of the concrete slabs and a moisture gradient is created between the top and bottom of the slabs. Moist subgrade and low relative humidity at the top surface of slab causes the moisture gradient increases between the top and bottom surface of the slabs. Thus, upper half of the surface shrinks while lower half does not tend to shrink same as upper half. The difference in drying shrinkage between the top and bottom surfaces of slab causes curling occurs at the corners and edges of the slabs. Drying shrinkage and curling of slabs should be considered in design as they affect serviceability, durability and performance of concrete slabs on grade. In accordance with ACI, the followings can increase shrinkage and curling potential of concrete slabs on grade: a) increasing moisture gradient between the top and bottom of slab due to placing concrete slab on high moisture content subgrades, b) increasing water content in concrete with using more finely ground cements, smaller maximum size coarse aggregates, and gap- graded aggregates, c) increasing modulus of elasticity of concrete by using higher compressive strength that means increasing cement past (volume of water and cement per cubic yard) causes brittleness increases and curl relaxation due to creep decreases, d) restraining shrinkage of concrete slabs by the adjacent structures and friction between subgrade and slab. ACI provided a list for designers to be considered in design of concrete slabs-on-ground and reduce shrinkage cracking and shrinkage curling. The list is summarized as: a) providing smoothness, dryness, and permeable with a low moisture content base and subgrade, b) using vapor retarder/barrier is not recommended unless controlling moisture transmission is required, c) thickening slab edges, d) in the case of using reinforcement, use at least 14 in. spacing and 3/8 in. diameter, e) placing reinforcement in the upper half of the slab to decrease sawcut contraction joints, f) use dimond-plate or rectangular-plate dowel systems for transferring vertical load and eliminating longitudinal and transverse restraint, g) eliminate slab restraints as many as possible, h) using adequate size for base plate using for rack posts, i) using shrinkage compensating concrete or post-tensioning system for slabs-on-grade, j) using the largest practical maximum size of coarse aggregate and minimize aggregate gap-grading, k) using minimum cement paste with the lowest required, also using mineral or metallic harder or topping is recommended if surface durability is concerned, l) testing shrinkage of various cement, aggregate gradations, and concrete mixtures, m) specifying cement type and brand, n) ensuring the uniformity of water demand and shrinkage with daily check of aggregate gradation and considering plant inspection.

2.6.2. Design of Shrinkage-Compensating Concrete Slabs

This section is a discussion concrete slabs-on-ground made with shrinkage-compensating cement concrete based on ACI 360R-06 according to experimental results from ASTM C 878 prism test specimens.

ACI 360R-06 defines shrinkage-compensating concrete as expansive cement concrete that expanse equally or slightly greater than predicted drying shrinkage when the concrete is restrained by the proper reinforcement. When the concrete cements expand, tensile strain develops in reinforcements and this produces a compressive stress in the concrete. The tensile stress caused by drying shrinkage will be offset with the residual compressive stress in concrete and consequently shrinkage cracking and curling are reduced. Typically, the drying shrinkage characteristics are similar for both shrinkage-compensating cement and Portland cement concretes. Also, drying shrinkage of both shrinkage-compensating cement and Portland cement concretes is affected by the same factors including water content of the concrete mixture, type of aggregate, aggregate gradation, and cement content. Figure 2.15 shows the typical length change characteristics of shrinkage-compensating and Portland-cement concretes based on

ASTM C 878 prism specimens tests (ACI 223). According to ASTM C 878 test results, the minimum concrete expansion for slab-on-ground is 0.03%.

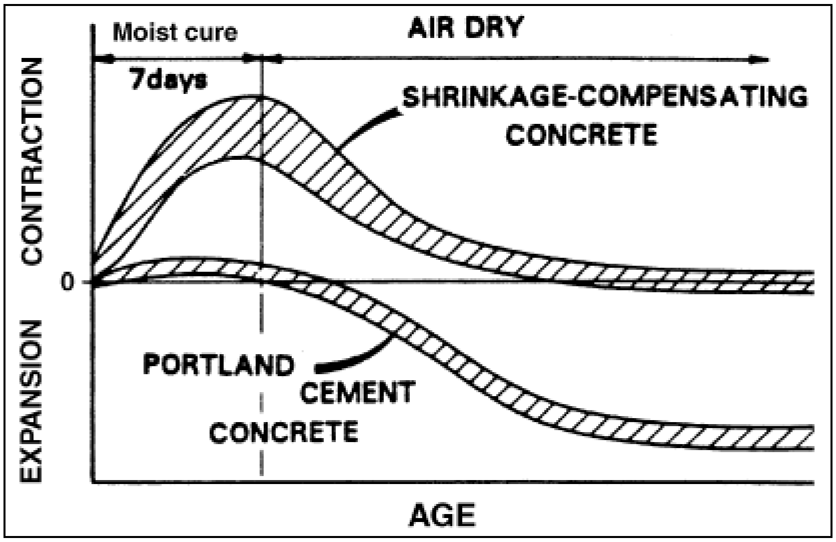

Figure 2.15 Typical length change characteristics of shrinkage-compensating and Portland-cement concretes (ACI Committee 223, 1970)

Based on ACI 360R-06 design method of slabs-on-grade containing the slab thickness required by imposed loading is the same for both using shrinkage-compensating cement and Portland cement.

It is recommended to use a minimum ratio of reinforcement to gross area of 0.0015 in each direction for the concrete using shrinkage-compensating cement. Furthermore, maximum required reinforcement is approximately 0.6% (Kesler et al., 1973) based on the theory says restrained expansion strains are equal to restrained shrinkage strains at 0.6% reinforcements. Note that minimum and maximum ratios do not depend on the yield strength of the steel reinforcements. The location of the steel reinforcement in concrete is very important for the slab behavior and internal concrete stress with use of shrinkage-compensating cement. ACI 223 recommends placing steel reinforcement at 1/3 of depth from top surface of the concrete slab.

CHAPTER 3

Testing Program

3.1. Description

There is no accepted test method to evaluate the warping tendency of a concrete slab on grade. Generally, the only available data relating to concrete shrinkage problems is the ASTM C 157 unrestrained length change results normalized at one day. However, even with better shrinkage data there is little published experimental information relating linear shrinkage of concrete to warping strains. Other properties such as the elastic modulus, creep and permeability are also likely to play a significant role and are generally not available. To develop procedures for accurately predicting the behavior of concrete elements exposed to nonsymmetrical drying (i.e. warping) data must be obtained in realistic conditions and related to the basic dimensional or material properties of concrete. A state of the art warping protocol was recently developed by Bissonnette et al. (2007) in which they outlined a realistic test procedure for reasonably sized slabs-on-grade specimens. This research generally follows Bissonnette's test protocol for the phase III of this research. This allows a comparison between the two research programs and helps increase the amount of data available.

This project is intended to improve our understanding of warping and our ability to predict its affect. This experimental program is designed to characterize the warping of slab as a function of various parameters and establish correlations with basic properties, especially shrinkage as measured by ASTM C 157 test method, expansion measured by ASTM C 878 test method and the "shrinkage from time zero" test method.

3.2. Method of Investigation

This research has five phases. Phase I was building the lab structure. The lab which is called the "Advanced Concrete Research Laboratory" is a unique facility for testing seven, sixty square foot, slabs on grade. Phase II consisted of the initial tests used to select mix designs for the slab specimens. A variety of concrete mixes were batched and tested to select the concrete mix designs to be used in phase III.

Phase III consisted of casting seven slab specimens on the ground in the controlled environment lab (Advanced Concrete Research Laboratory) and the testing and monitoring of them for long term (600+ days). This section generally followed the Bissonnette et al. (2007) test procedure with the major exception that the slabs were cast on grade and the specimen were exposed to a moisture gradient for the entire testing period. The specimen mix designs were selected based on the mix designs results from Phase II.

Phase IV includes additional tests for "shrinkage from time zero" to provide additional data for shrinkage of prism specimens using the same concrete mixes from phase III. Dial gages are used for measuring expansion and shrinkage from time zero of the specimens. The results from phase IV are compared with the slab specimens' results from phase III.

Phase V included reducing the relative humidity of the lab from 60% to 30%. All monitoring, measurements and tests are continued to characterize shrinkage and warping in low relative humidity at the top surface of the slab while the bottom of the slab is exposed to the ground relative humidity.

3.3. Phase I: Building the Lab Structure

Phase I included building the lab structure. The research lab is a 1,800 ft^2 building sponsored by CTS Cement Manufacturing Corp. This building was built by CEES students at Fears Lab under the mentorship of Dr. Ramseyer (Figure 3.1, 3.2, and 3.3). They did everything from laying the foundation and erecting the framework, to paneling the walls and ceiling. The only sub-contracted work was the casting of the interior slab and the electrical work. The lab is a unique project and has been named the Advanced Concrete Research Laboratory. This lab consists of seven test beds for studying the long-term behavior of concrete slabs on grade. The test beds allow 3-foot-by-20-foot slabs to be tested with full restraint at each end of the specimen while the top surface is exposed to a controlled environment and the bottom surface is exposed to soil temperature and moisture.

Figure 3.1 Lab construction

Figure 3.2 Exterior view of lab construction

Figure 3.3 Advanced Concrete Research Lab

3.4. Phase II: Initial Tests

Phase II included initial tests to select mix designs for the slab specimens. A variety of concrete mixes (over 20 mixes) were batched and tested for months to select the concrete mix designs to be used in the construction of the slab specimens. Various tests such as the flow table test based on ASTM C230 (Figure 3.4), compression strength of concrete test based on ASTM C39 (Figure 3.5), length change of hardened hydraulic cement mortar and concrete in accordance with ASTM C157 (Figure 3.6), and restrained expansion of shrinkage-compensating concrete according to ASTM C878 (Figure 3.6) were performed on these specimen. Appendix I includes the test results for 13 batches using shrinkage compensating concrete. The appendix also includes some of the test results for the flow table tests.

Figure 3.4 Flow table test (ASTM C 230)

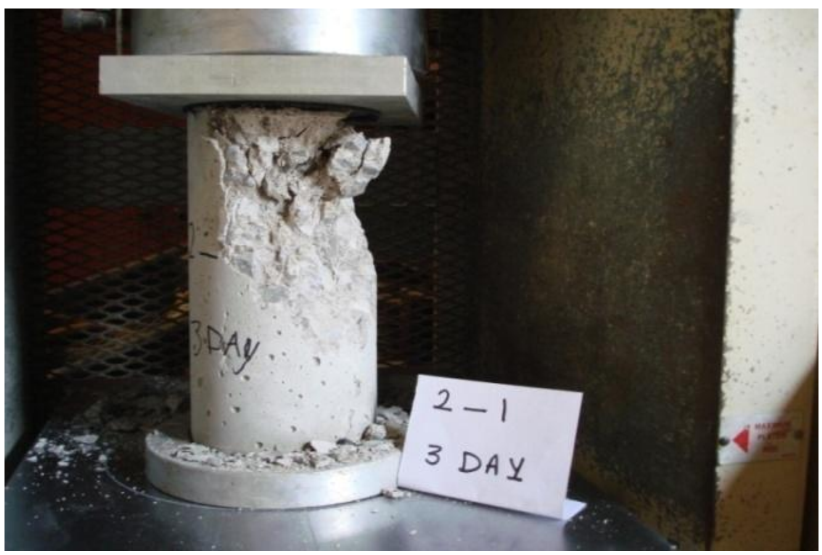

Figure 3.5 Compressive strength test (ASTM C 39)

Figure 3.6 Length change test (ASTM C 157, ASTM C 878)

3.4.1. Materials

The concrete mixture of the initial thirteen tests is provided in Table 3.1. Since this research focuses on shrinkage compensating cement (Calcium SulphoAluminate - Komp I), the initial tests materials and results using shrinkage compensating cement are included in this dissertation. In the first three tests, WRDA 64 was used as a water reducing admixture. It showed a low slump and high shrinkage results. As tests were conducted in the hot summer (over 100 °F), ice was used as 1/3 of the weight of the required water in the mix. Polyheed 1020 was also used as a shrinkage reducing admixture due to help address the very low workability. Appendix I includes the preliminary tests results of the thirteen mix designs.

Table 3.1 Concrete mixes for the initial thirteen tests

	Portlan Cement							Type I Cement					
	WRDA 64			POLYHEED 1020									
	Water			2/3 Water+1/3 Ice									
Materials	**# 1**	**#2**	**#3**	**# 4**	**# 5**	**# 6**	**# 7**	**# 8**	**# 9**	**# 10**	**# 11**	**# 12**	**# 13**
Komp I	100	120	140	140	140	130	120	110	100	130	120	110	100
P. C	470	470	470	470	470	430	390	350	310	430	390	350	310
C. Agg.	1750	1750	1750	1750	1750	1750	1750	1750	1750	1750	1750	1750	1750
Sand	1406	1361	1315	1315	1315	1315	1315	1315	1315	1315	1315	1315	1315
Water	285	295	305	335.5	323.3	296.8	270.3	243.8	217.3	308	280.5	253	225.5
MR/cwt	10	14.39	14.39	11.65	12	12	12	12	12	12	12	12	12
W/C	0.5	0.5	0.5	0.55	0.53	0.53	0.53	0.53	0.53	0.55	0.55	0.55	0.55

3.5. Phase III: Testing Slabs on Grade

This phase tested concrete slabs exposed to nonsymmetrical drying warping in a realistic condition. This work followed Bissonnett's protocol with some exceptions. These exceptions include: an improved test bed, which is truly "on grade" helping to maintain a moisture gradient through the slab, measurement of relative humidity at 13 mm(1/2 in.) increments through the depth of the slab allowing measurement of the moisture gradient influencing the warping, and measurements of temperature at 13 mm(1/2 in.) increments through the depth of the slab allowing measurement of the temperature gradient to verify that a temperature gradient does not exist which would cause curling (Note- curling is not addressed by this research).

3.5.1. Materials

The concrete mixes used in phase III of this research are provided in Table 3.2. Calcium SolfoAluminate (Komp I) cement were used in two slabs and Rapid Set cement concrete in one slab. DOLESE Company provided concrete for four slabs. Based on a DOLESE Company report, Pozzolith 80 was used as mid-range and high-range water reducer (MRWR) for all of the mixes they provided. DOLESE expected compression strength of 3,500 psi at 28 days (typical performance concrete) for three of the slabs and 5,000 psi (high performance concrete) for one of the slab mixes. Two types of common shrinkage reducing admixture, Eclipse and Tetragaurd, were added to the DOLESE mixes with typical compressive strength.

Table 3.2 Concrete mixes for slabs specimens

Materials (per cubic yard)	SRA#1	SRA#2	PCC	HPC	CTS Shrinkage Compensating Cement		Rapid Set
					#1	#2	
Komp I	-	-	-	-	120	120	-
P C	356	355	355	543	370	370	-
Flyash	88	88	88	180	-	-	-
Rapid Set Cement	-	-	-	-	-	-	658
Citric Acid	-	-	-	-	-	-	5
Course Aggregate 57	1850	1850	1850	1850	1750	1750	1772
Sand	1463	1463	1463	1196	1315	1315	1307
Water	266	266	266	264	270	272	290
MR (Polyheed (oz))	-	-	-	-	64	64.6	52.6
MR (Pozzolith 80 (oz))	13	14	14	29	-	-	-
Eclipse (oz)	128	-	-	-	-	-	-
Tetraguard (oz)	-	128	-	-	-	-	-
W/C ratio	0.60	0.60	0.60	0.37	0.55	0.55	0.44

3.5.2. Experimental Program

Seven slab test specimens 75 mm x 900 mm x 6000 mm (3 in x 3 ft x 20 ft) were cast on 4 in. moist compacted sand on the ground (Figure 3.7). The specimens were located in the test facility specifically built as a controlled environmental chamber in Phase I. The slabs were cast in specially designed pits, truly on-grade.

Figure 3.7 Interior view of Adveanced Concrete Research Lab

The idea of this portion of the research is while the base is kept moist by ground water, the top of the slabs are exposed to the low ambient relative humidity environment in the lab; this will increase the moisture gradient in the slab and will increase warping. The Advanced Concrete Research Lab is situated adjacent to a geotechnical testing site at Fears Lab that includes several observation well sites. During the last five years the water table in these wells has varied from a depth of 1.5 m to 4 m (5 feet to 14 feet) from the surface, which is fairly typical for this area of Oklahoma.

As previously mentioned shrinkage compensating cement (Komp I) is used for two of the slabs concrete mix, Rapid set cement is used for one slab, and portland cement is used for four slab specimens. The portland cement concrete includes high performance concrete (HPC), low performance concrete (PCC), and two different common shrinkage reducing admixtures (SRA) Eclipse and Tetraguard. The slabs were cast on 4 inches of moist compacted sand on ground. The moisture transfers from ground to the sand and to the bottom of the slab. The lab relative humidity and temperature is controlled and it is generally 60% and 70ºF. In this way, the bottom of the slab was exposed to the ground moisture and the top of the slab was exposed to the controlled environment. This created a moisture gradient through the slab depth. The minimum required longitudinal reinforced steel for temperature (ρ_s =0.0015, ACI 360 R) was used for all of the slabs. The slabs were fully restrained longitudinally by casting the test slabs around a transverse steel truss that was attached to the edges and the test pits.

This restrained the slabs against movement or changing its length due to shrinkage or expansion. The steel trusses transfer all the loads to two #8 rebar, cast previously in the existing floor along each edge of the test. The test slab ends were thickened to 230 mm (9 in.) to accommodate this detail. After casting the slabs, contraction joints were saw cut 1 inch deep at 5 feet from each end to provide a 10 ft long central test section. The longitudinal reinforcement (4 No. 2) are continuous through the joints. All the slab specimens except the one made with Rapid set cement were cured with wet burlap and a plastic sheet for 7 days. The slab made with Rapid set was cured with water for about 4-5 hours after casting.

The slabs using Komp I and Rapid Set cement were made in a mixer at Fears Lab and delivered to the testing site (Testing facility) in a “Georgia” Buggy. During the evaluation, slab monitoring consisted of: visual observation of cracking, surface strain and joint opening measurements using Demec strain gages, internal slab temperature and relative humidity, ambient temperature and RH. Additionally, a laboratory testing program was conducted which consisted of the compression strength of the cylinder specimens based on ASTM C 39, and the length changes of the prism specimens based on ASTM C878 and ASTM C157.

3.5.3. Slab on Grade Test Setup

As previously mentioned, slab specimens were located on 4 in wet compacted sand on ground. Also, for the purposes of this research, length change of the slab specimens must be restrained. [Note: No loads except environmental loads apply to the slabs test specimen]. To limit changes in length, steel trusses were made by welding #7 reinforcing bar and placed at the ends of the slab specimens. The following work was performed:

1) Made the testing beds ready for casting
    - The slabs were cast on 4 in. moist compacted sand (Figure 3.8).
        - Removed the existing soil by an amount to allow for 4 inches of sand
        - Placed 4 in. sand in layers and made it flat (Figure 3.8 and 3.9).
        - Watered sand to make it moist and to compact it (Figure 3.10)
    - Placed 1 in. thick foam around the edge of the test slab location, except the ends of the slab. The foam was used as a form for concrete test slab and to ensure the slabs did not bond or bind on the test beds. The, surface of the sand bed was once again leveled and moisted (Figure 3.9 and 3.10).

Figure 3.8 Making sand ready for slab on grade

Figure 3.9 Four inches moist compacted sand

Figure 3.10 Watering sand

2) Sloped sand to make the 9 in. thick end of the test slab to accommodate restraining the slab (Figure 3.12).

3) Restrained volume change of slab by using steel trusses

- Welded #7 reinforcing bar and made two trusses for each slab specimen. Steel trusses are placed at both ends of the slabs (Figure 3.11). [Note: The size of the steel trusses was designed based on tensile strength of concrete and the tributary area which transfer the loads to the trusses].
- Made 1”x3”x12” plates with two 13/16” holes 9” apart at mid height of the plates (Figure 3.12). The bolts diameters (Φ) are 3/4 in, and they fasten the plates to the existing slab.
- Drilled two holes (1”) into the existing slabs for the bolts.

- Used epoxy around the 3/4”Φ Bolts to fasten the end plate completely to the existing slab.
- Grouted the gap between the plates and the existing slab to make a full attachment (Figure 3.13).
- Welded the steel trusses at the mid- height (1.5 in.) of the plates (Figure 3.14).

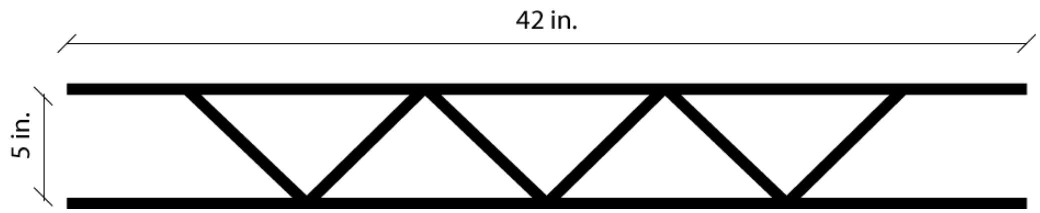

Figure 3.11 Steel trusses are placed at both ends of slab specimens

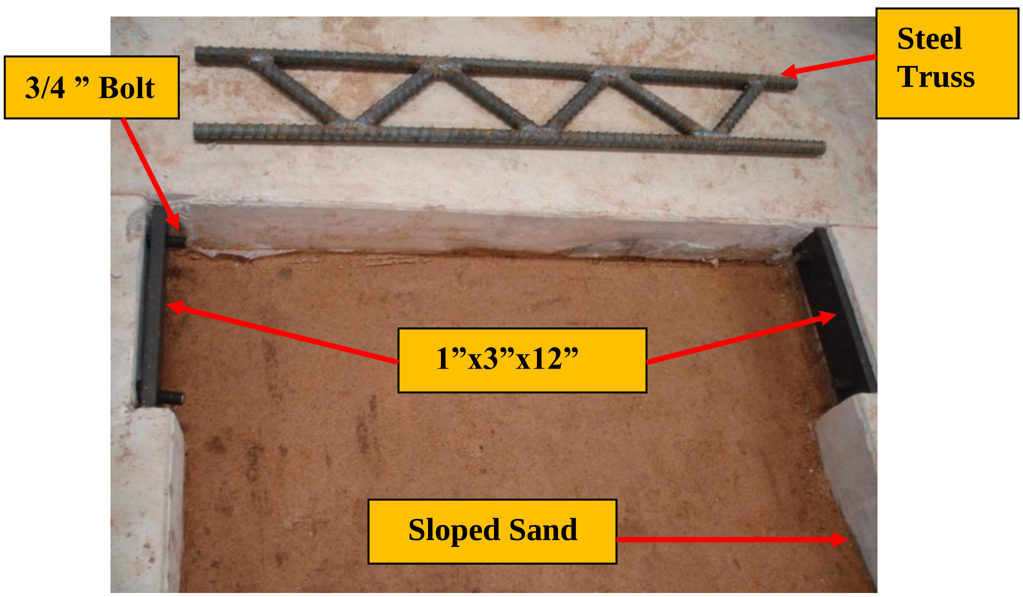

Figure 3.12 End of slab before welding the steel truss

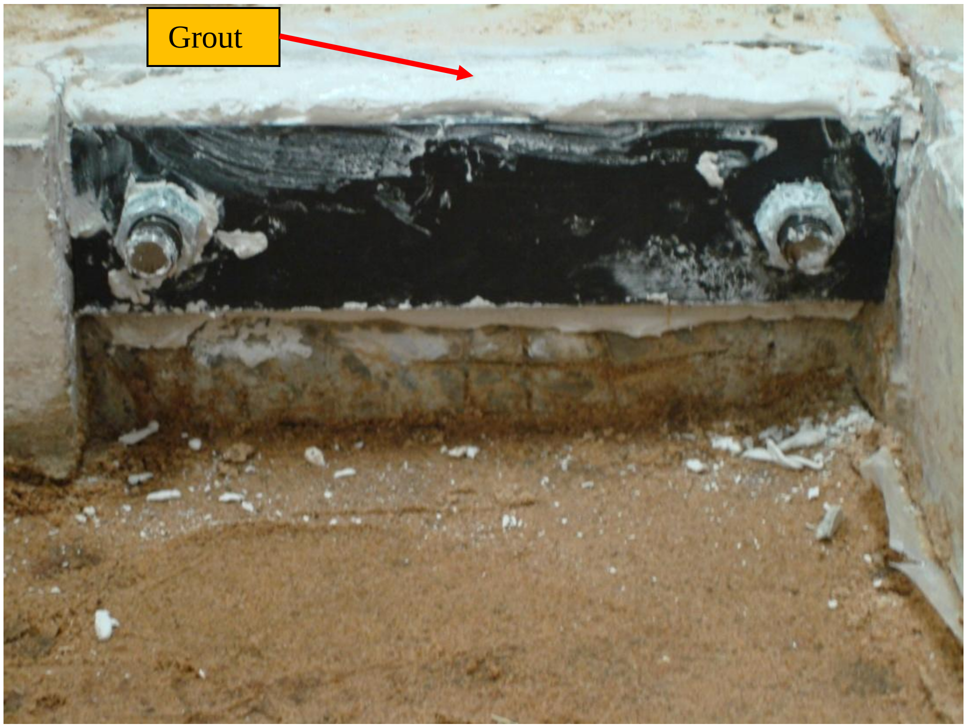

Figure 3.13 Grout in gap between plate and existing slab

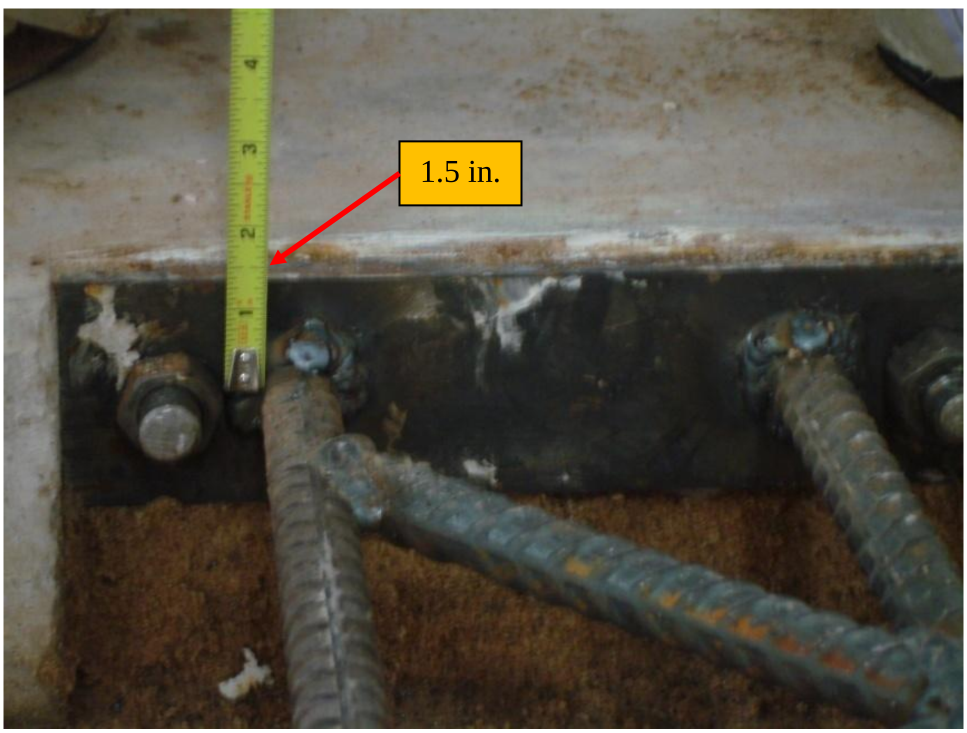

Figure 3.14 Welded truss at mid-height of the plate

4) The thickness of the concrete at the slab ends is 9 in.; therefore to provide the form for the end of the slab, 1 in. thick foam is cut, place at the end, and taped over the holes around the truss (Figure 3.15 and 3.16).

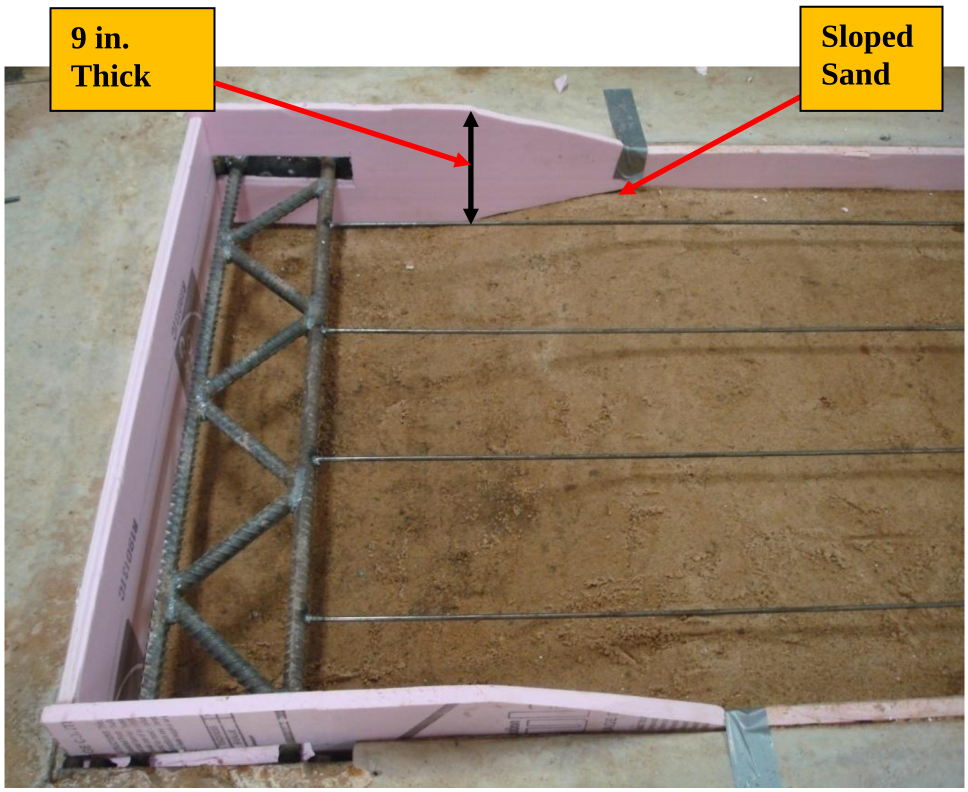

Figure 3.15 Nine inches end foam

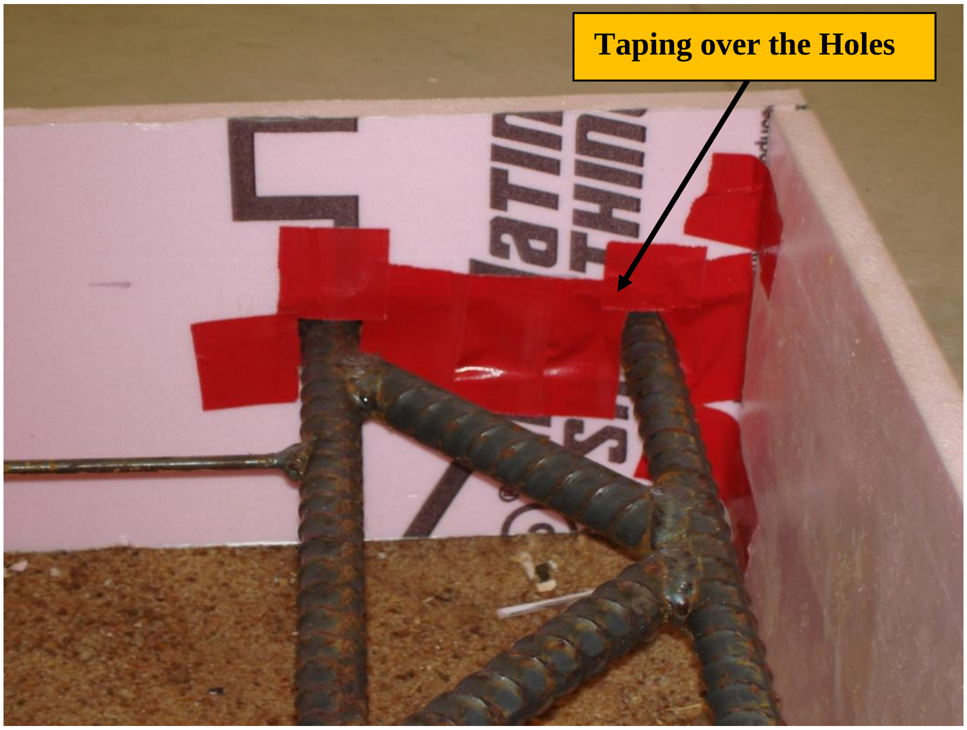

Figure 3.16 End truss

5) Welded (4) 1/4”Φ @ 9 in. rebar longitudinally to the steel trusses. The bars are located at the mid-height of the 3 inches slab (Figure 3.17). The steel rebar restrains shrinkage of the concrete. [Note: The bars continue at the joint locations].

6) Place chairs below the rebar to keep reinforcements at the required elevation while casting concrete (Figure 3.17). The chairs are placed on an aluminum plate sheet to prevent depressing the chairs into the sand.

7) The intersection of the rebar and chair is epoxy to keep them at their locations while casting concrete.

8) The wood forms are placed at top of the ends of the slabs to provide 9 in. support at the end of the test slab (Figure 3.18).

9) At this point, the slab is ready to be cast (Figure 3.18).

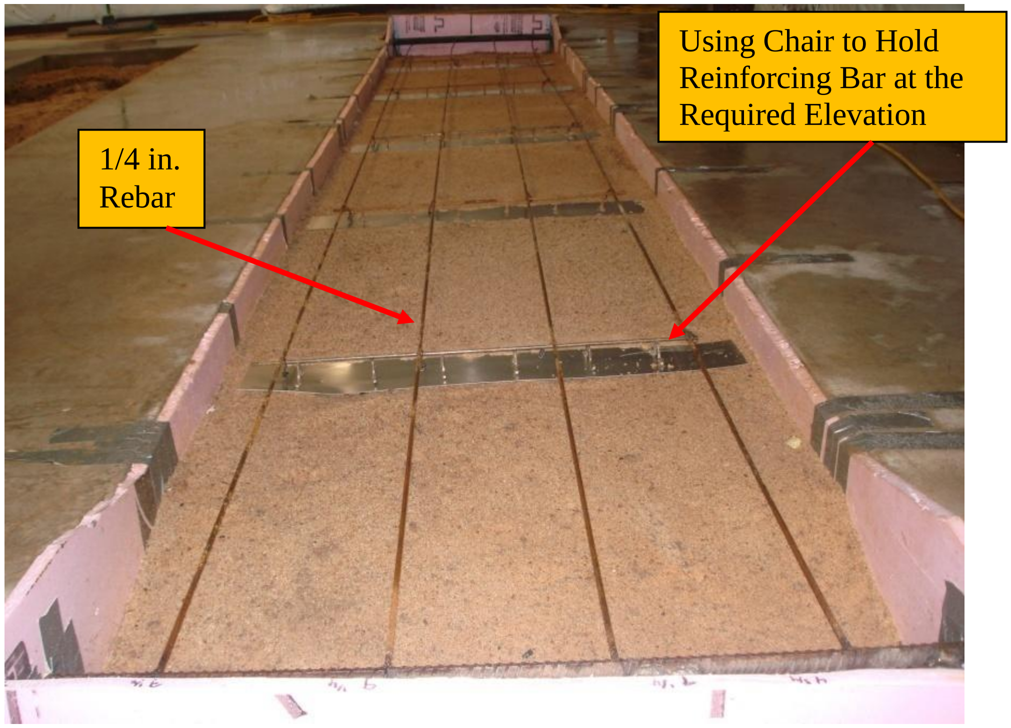

Figure 3.17 Longitudinal reinforcement

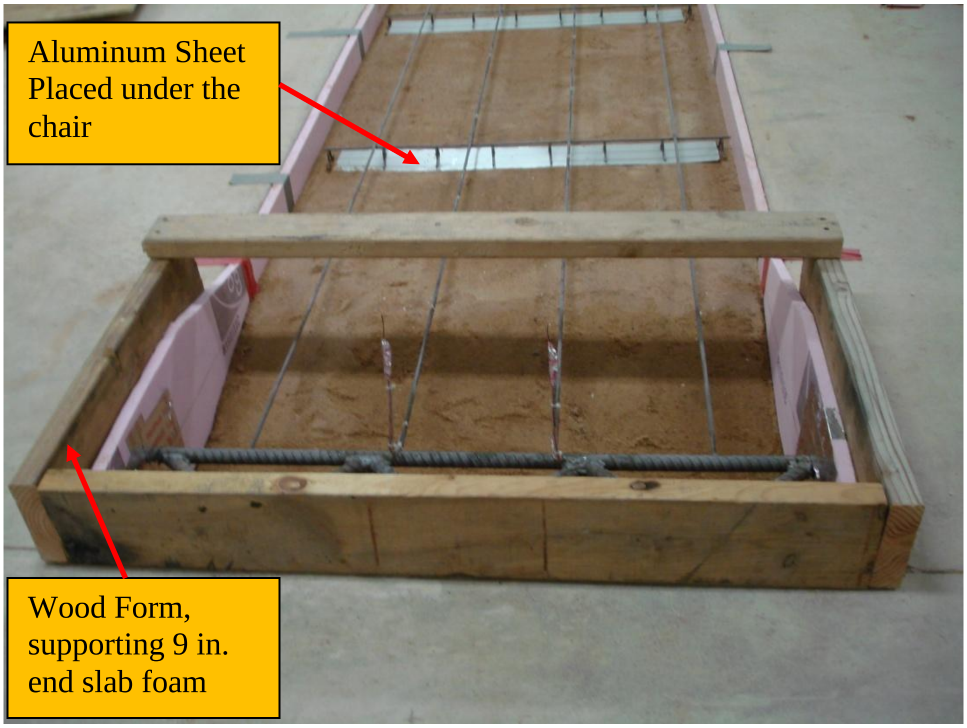

Figure 3.18 Slab is ready to be cast

Three of the concrete slabs were batched in a mixer at Fears lab. Then, concrete was delivered to the testing site with a "Georgia" Buggy (Figure 3.19). Four of the concrete slabs were delivered by DOLESE Company (Figure 3.20). After casting the concrete slab in place (Figure 3.21), a finishing crew finished the concrete surface (Fig. 3.22, 3.23 and 3.24). A vibrator was not used while casting concrete slabs to ensure the sand bed below the concrete was not disturbed. Cylinders and prism test specimens were filled with the concrete from each batch following ASTM standard test methods (ASTM C 39, ASTM C 157, and ASTM C 878) (Appendix D includes picture of prism test specimens).

Figure 3.19 Mixer and delivery machine

Figure 3.20 Delivered concrete by DOLESE Company

Figure 3.21 Casting concrete slab

Figure 3.22 Finishing concrete surfaces at end of the slab

Figure 3.23 Finishing concrete surface

Figure 3.24 Finished concrete slab specimens

After casting the slabs in place, the following work was completed:

1. Curing the slabs specimens with wet burlap and a plastic sheet for 7 days (Figure 3.25 and 3.26). [Note: Rapid set cement was cured with water spray for 4-5 hours]. The purpose of curing is to develop concrete strength by following good concrete practices and delay shrinkage and warping.
2. Provide contraction joints with saw cut method at 24 hours (Figure 3.27).
    - Joint depths are 1 in.
    - Joints were located at 5 ft from each end, the west and east sides, to provide a 10 ft long central test section between the joints (Figure 3.28).

Figure 3.25 Moist cured slab

Figure 3.26 Wet burlap and plastic sheet used for curing concrete slab

Figure 3.27 One inch sawcut joint

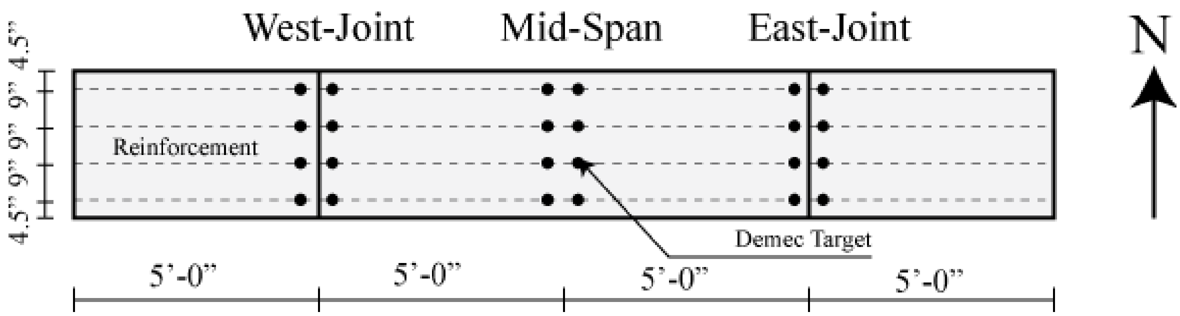

Figure 3.28 Demec target placed at top of the reinforcements' location on surface of the slab (Top View)

3. Attach Demec targets on the rebar location at joints and mid span using epoxy after finishing curing time. [Note: Demec target could not be attached and fixed on the surface of slab during the curing period due to the wet concrete]. Figure 3.29 shows Demec target attached to the surface of concrete slab at mid-span and joint opening. In this way, the strain is measured at mid-span with no cracks and strain across the crack at joint opening which allows calculating the width of cracks. Figure 3.30 shows the strain gage measuring surface strain on Demec target. Additional pictures are included in Appendix D.
4. Weekly slab monitoring began after 7 days curing. Slab using Rapid Set was started to be monitored on the second day since it was cured for only 4-5 hours after placing concrete.
5. Monitoring and measurement of slab specimens are:
    - Regular visual observations for surface cracking
    - Surface strain and joint opening measurement using Demec target strain gauges with 7 in. gauge length

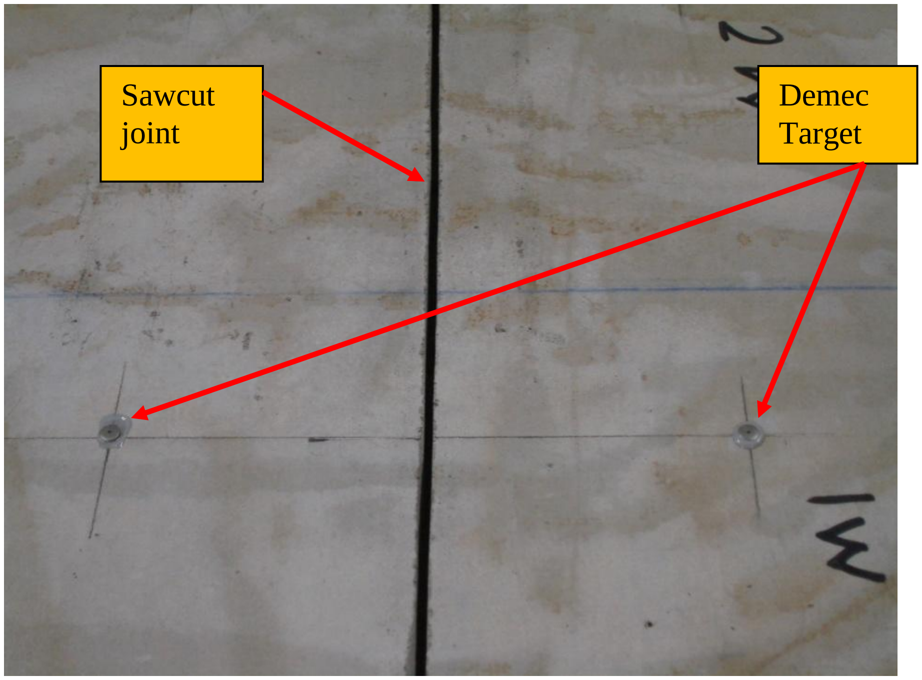

Figure 3.29 Demec target located at saw cut joint

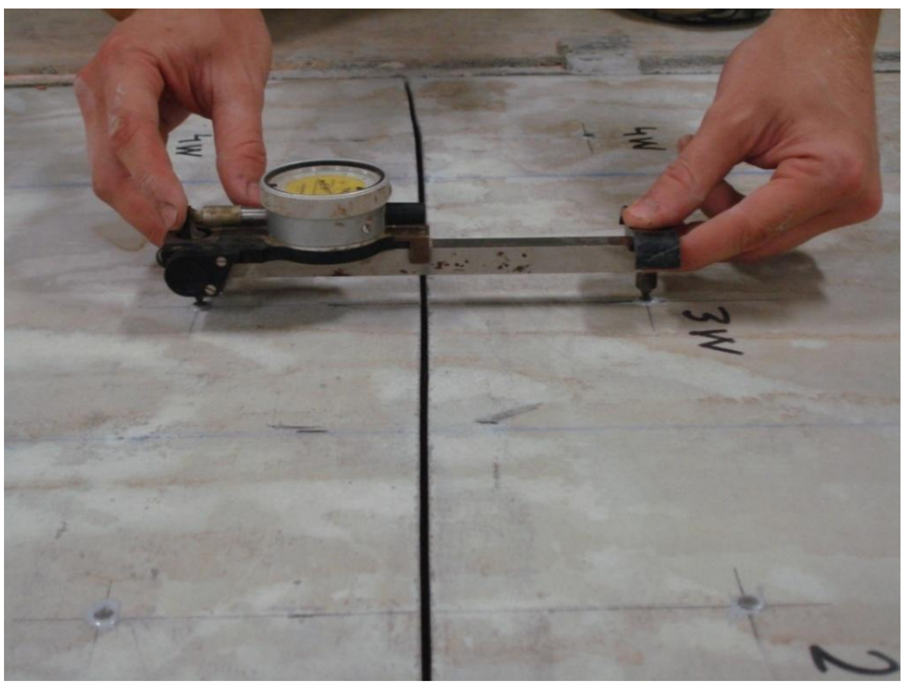

Figure 3.30 Monitoring slab length changes (shrinkage or expansion) using demec strain gage

- Testing cylindrical concrete specimens (4 in. Diameter x 8 in. Height) to provide compressive strength of slab specimens based on ASTM C 39 (Figure 3.31). Test specimens were kept at the lab (Advanced Concrete Research Lab) where the large scale slab specimens were located.

Figure 3.31 Cylinder specimens placed for testing the compressive strength of concrete

- Length change tests measurements (3x3x10 in. specimens) based on ASTM C 157 (Figure 3.32).
- Restrained expansion tests measurements based on ASTM C 878 (Figure 3.32).

  Note: All test specimens were kept at the Advanced Concrete Research lab.

Figure 3.32 Testing Prism length change

- Internal relative humidity (ASTM F 2170) at 1/2 in. increments through the depth of the slab (Figure s3.33 and 3.37).
- Internal temperature at 1/2 in. increments through depth of the slab (Figures 3.33 and 3.37)
- Ambient relative humidity. Generally, lab relative humidity is 60% (Figure 3.34).
- Ambient temperature. Generally, lab temperature is set on 70 ºF (Figure 3.34).

Figure 3.33 Slab internal temperature and moisture meter

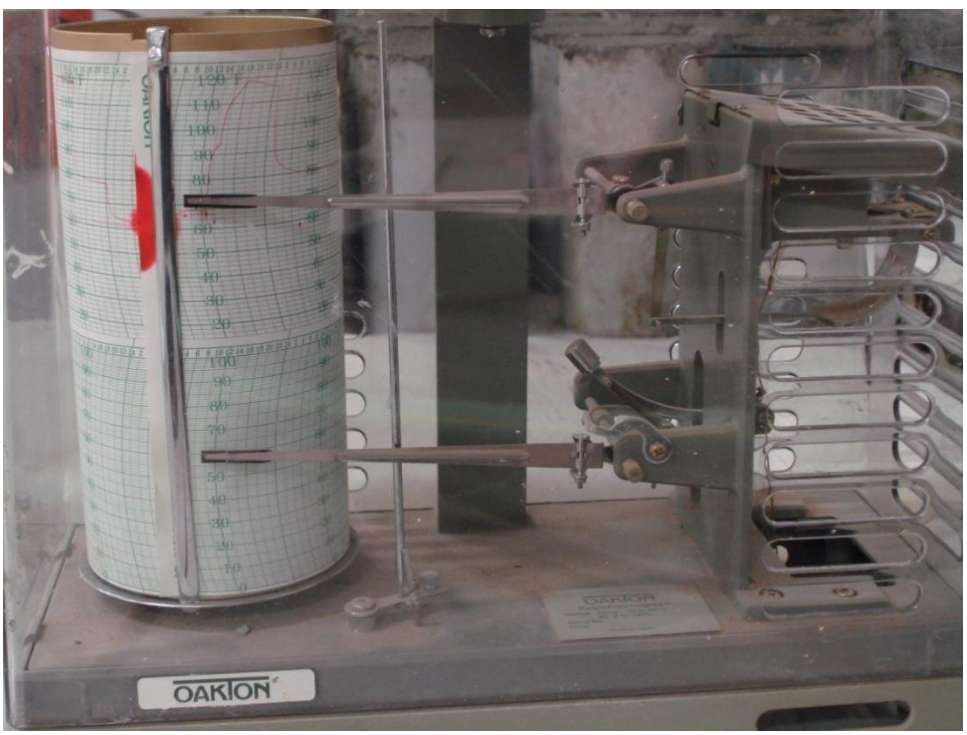

Figure 3.34 Ambient temperature and moisture meter

6. The one inch foam edges used as forms for the concrete slab were removed one week after placing concrete slab. Then, a 1 in. flexible Backer Rod was placed all around the slab specimens at two layers. The Backer rod seals the gap or crack between the slab specimens and concrete floor of the lab .Backer rod was used to maintain the moisture in the sand and then below. The two layer backer rod to prevent transferring moisture from bottom to top surface of the slab and from top to bottom surface of the slab. Therefore, top surface of concrete slab is enclosed to the air and bottom surface of concrete slab is exposed to the sand moisture. (Figure 3.35).

7. Drill 5 holes close to the Mid-Span for installing the device to measure interior temperature and relative humidity at 1/2 in. increments through the depth of the slab (Figure 3.33). Holes are provided at 2.5, 2, 1.5, 1, and 0.5 inch depth respectively at the Mid-Span of the slab.

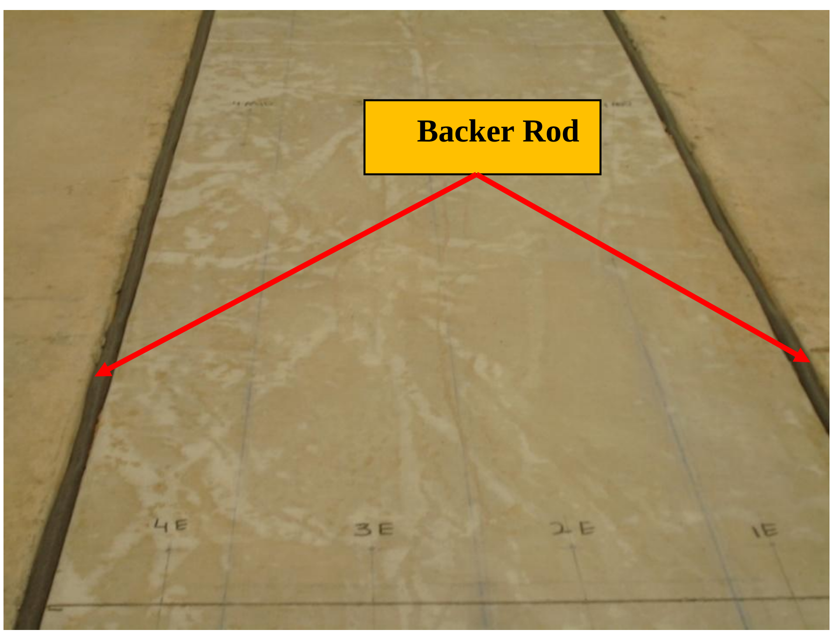

Figure 3.35 One inch Backer Rod placed at two layers around the slab specimen

Figure 3.36 shows interior view of the controlled environment lab. It can be seen that the slab specimens located on ground and also the prism test and cylinder test specimens were kept in the same lab environment.

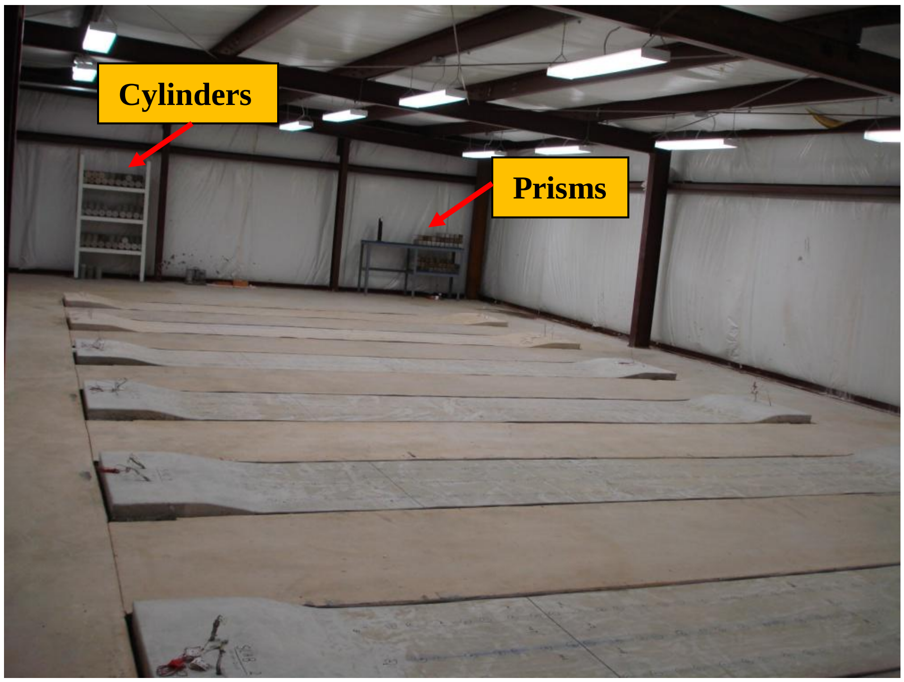

Figure 3.36 Controlled environment lab facilities

Figure 3.37 is an overall slab plan view. It shows the location of demec target and RH meter. Figure 3.38 shows a profile of the slab deformation due to warping. It represents the behavior of slab exposed to the low relative humidity environment at the top surface and a high relative humidity environment at the bottom surface of the slab. It can be seen that the slab is restrained at the ends and warping occurs at the joint locations. More pictures are available in Appendix D, pages 296-306.

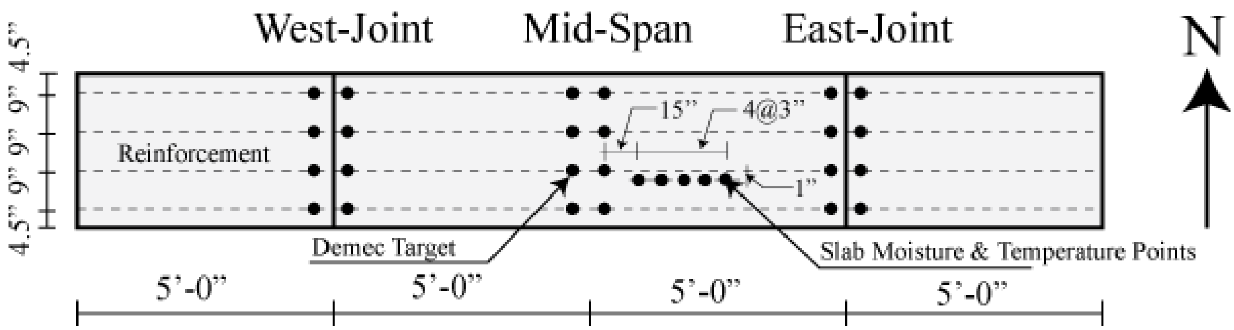

Figure 3.37 Top view of slab specimen

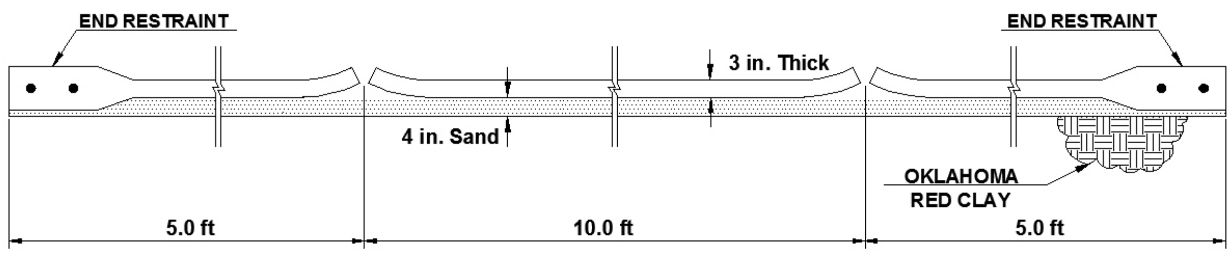

Figure 3.38 Profile of slab deformation due to warping

3.6. Phase IV: Additional Tests

According to ASTM C878 standard test method it is only used for measuring expansion of prism tests specimens using shrinkage compensating concrete; therefore, additional tests are needed to provide more data for shrinkage of prism tests using shrinkage compensating concrete (CSA). However, 110 days of additional tests in Phase IV did not provide adequate data for shrinkage of prisms made with CSA. A further purpose of additional tests is to use other method "shrinkage from time zero", provide data based on the new method and compare the results. In this phase, Demec target strain gages and dial gages are used to measure shrinkage m time zero of concrete specimens. Demec target strain gages measurements were not possible due to the unlevel surface of the specimens. Therefore, the results from dial gage measurements are compared with the results from Phase III. The test specimens were made similar to the large scale slab concrete specimens from Phase III. Figure 3.39 shows the form for prism test (3 x 3 x 13 in.) ready for casting concrete. A one inch plastic block is places at one end of the form. Therefore, concrete is free to move for shrinkage and concrete expansion is restrained by steel plate at this end (Figure 3.39, 3.40, and 3.41). The other end is fixed with steel form; thus, concrete is restrained to shrinkage and expansion at this end. Two bolts are screwed to the ends. The bolts are 11 inches apart (Figure 3.39) which is used as original length of specimens for calculating strain of the specimens. A plastic sheet and grease cover inside the steel mold to reduce friction between concrete and steel mold (steel form). In this manner, there is no restraint between the concrete specimens and the steel forms. The specimens are placed in the chamber at 72º F temperature and 60 % relative humidity. They are isolated to prevent transferring temperature and humidity from the concrete floor of the chamber to the concrete specimens.

Next dial gages are installed at the free end (the end with plastic block) of each specimen (Figure 3.40 and 3.41) and the dial gage is read at this time which is time “Zero”. The dial gage is connected to the bar and bar goes through the hole and touches the back of the nut (bolt). The dial gage is placed at the free end and it measures how the free end moves related to the fix end. Shrinkage/expansion measurements are begun at time zero and continued for 28 days. The specimens are wet cured from top surface of specimens for 7 days. Then, they are demolded from the sides (not the ends) and demec target are placed at top surface of the specimens (Figure 3.42, 3.43).

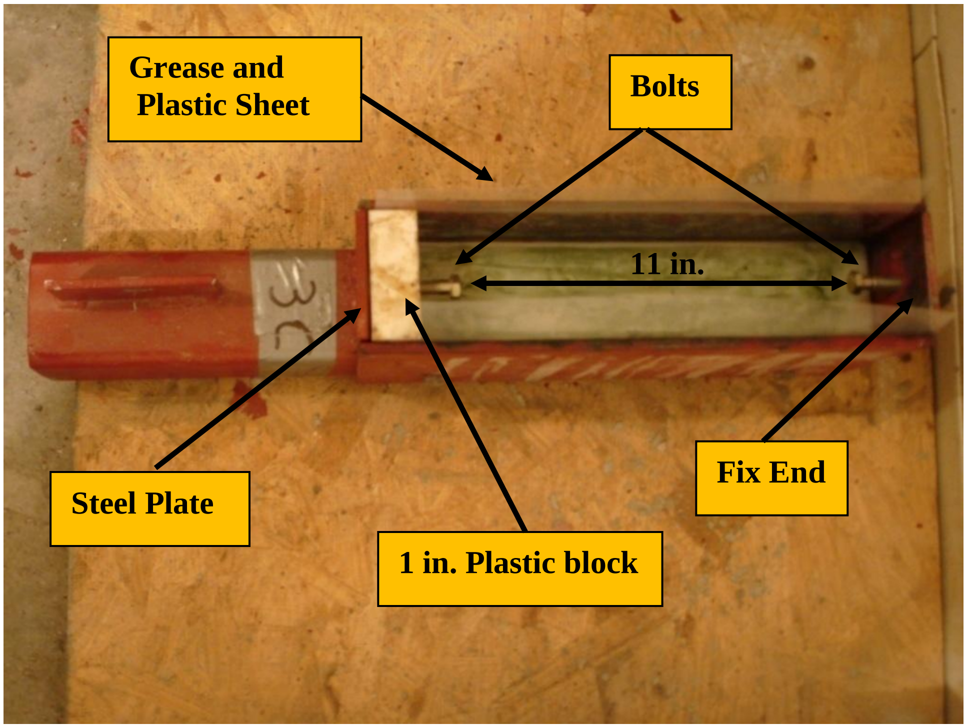

Figure 3.39 Prism form is ready for concrete

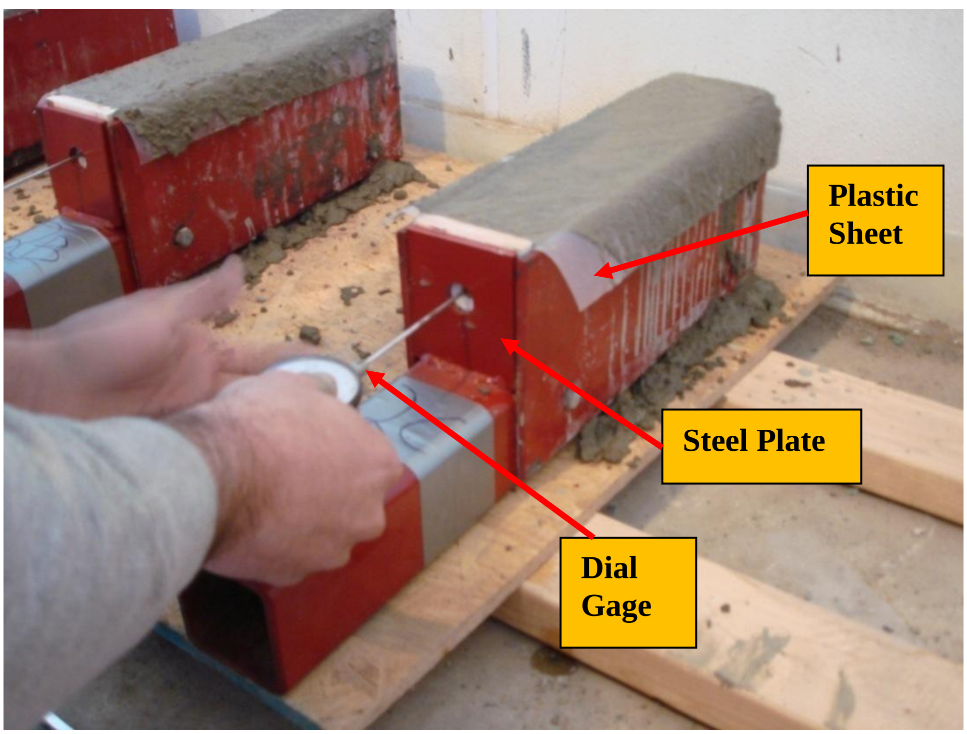

Figure 3.40 Placing dial gage into the specimens

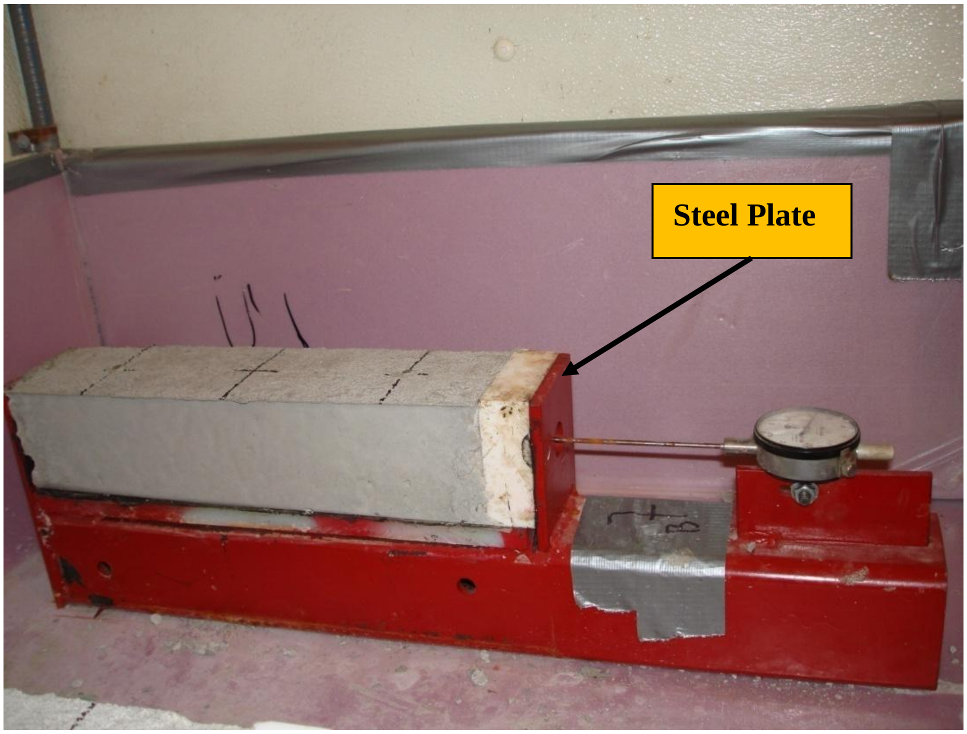

Figure 3.41 Side view of specimen

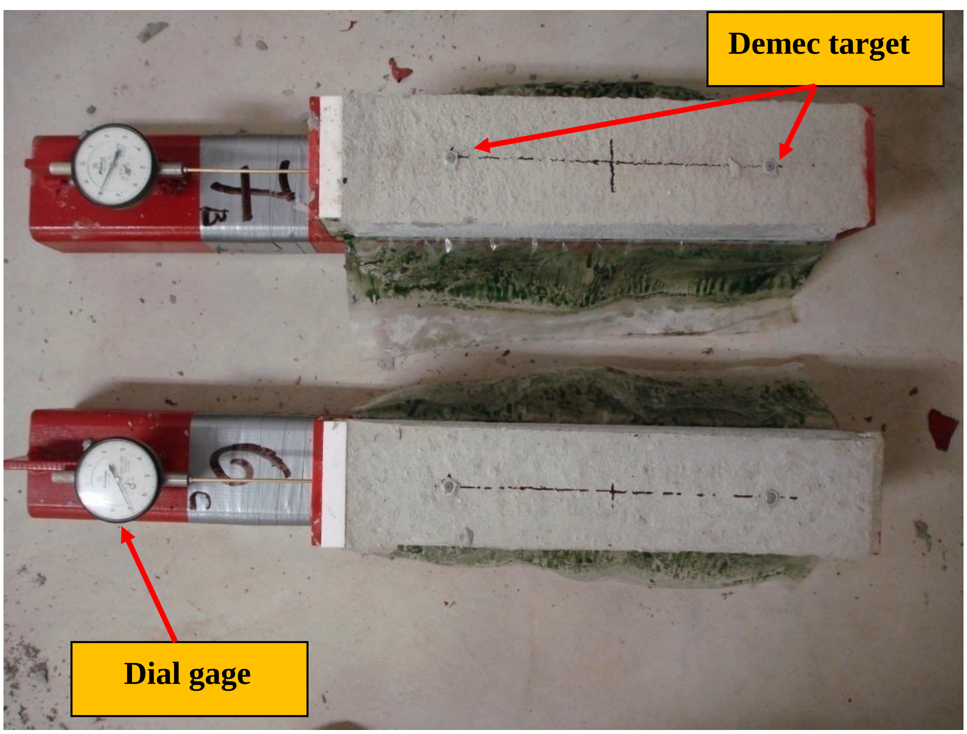

Figure 3.42 Placing demec target on the top surface of the prism specimen

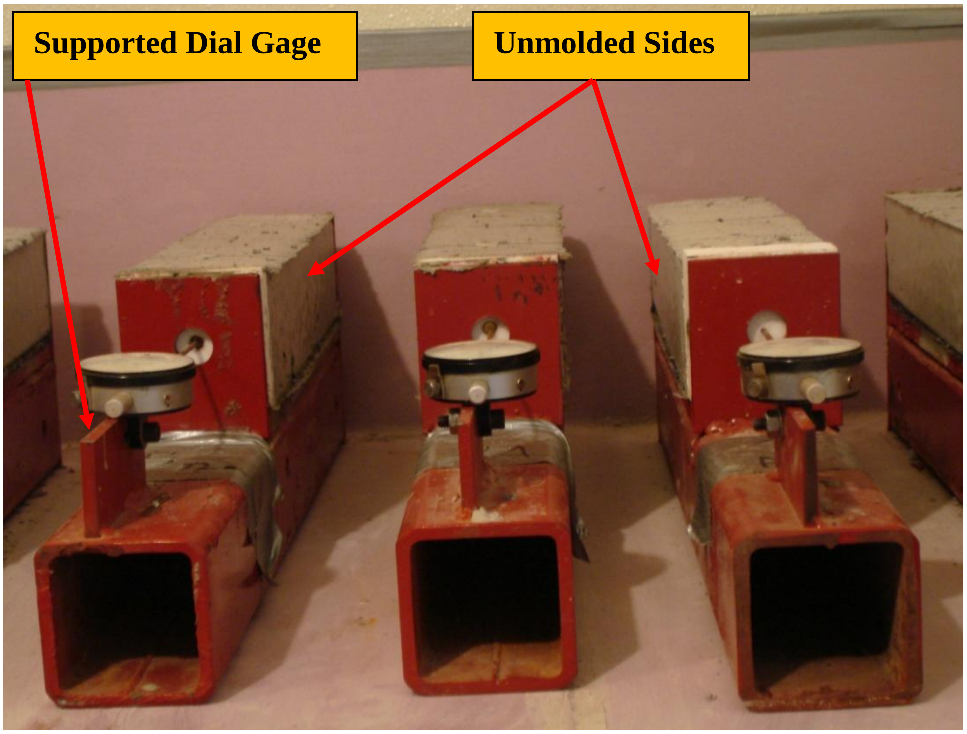

Figure 3.43 Supporting dial gages and unmolded sides

In addition to shrinkage/expansion of concrete, slump and compressive strength of concrete are measured (Figures 3.44 and 3.45). More pictures are available in Appendix D, page 307 and 308.

Figure 3.44 Measuring concrete Slump

Figure 3.45 Cylinder specimens for testing compressive strength of concrete

3.7. Phase V: Reducing Ambient Relative Humidity

The relative humidity of the lab is reduced from 60% to 30%. Figure 3.46 shows the instruments used to reduce lab RH. The purpose of this Phase is to increase the moisture gradient through slab due to a lower relative humidity at the top surface of the slab. All monitoring, measurements and tests are continued to allow comparison with the results at 60% ambient relative humidity.

Figure 3.46 Dehumidifier used to reduce the ambient relative humidity

CHAPTER 4

Test Results

This chapter presents a selection of general test results for phases III- V. These results are presented in the form of tables and graphs. The complete test results (phase II-V) are presented in Appendixes A, B, and C in the following order:

Appendix A represents the initial test results for phase II. This appendix includes flow table test results (ASTM C 230) for type K cement. Also, compressive strength test results (ASTM C 39) and length changes of prism specimens (ASTM C 878) for thirteen different concrete mixes are presented in Appendix A. The thirteen initial batches were made with shrinkage compensating cement concrete Komp I.

Appendix B (pages 186-271) presents entire test results for large scale slab on grade specimens (phases III and V). The results are based on material characterization and slab monitoring for each slab, then comparing the results. Material characterization includes all the test results based on ASTM C 39, ASTM C 157, and ASTM C 878. Slab monitoring represents behavior of slab on grade based on control joint expansion, surface strain measurements, and interior slab temperature and relative humidity.

- Results for each slab are represented Appendix B (pg. 188-206).
- Comparisons of results are represented Appendix B (pg. 207-233).
- Internal temperature at 1/2 in. increments through depth of the slab Appendix B (pg. 234-246)
- Internal relative humidity at 1/2 in. increments through the depth of the slab Appendix B (pages 247-271)

Appendix C represents 28 days and 110 days test results for additional tests based on shrinkage from time zero method. The results for shrinkage from time zero are compared with the results for ASTM C 157, ASTM C 878, and slabs.

- Concrete materials and compressive strength test results Appendix C (pg. 273-274)
- Strain of test specimens for 28 days (pg. 275-278)
- Comparing 28 days shrinkage from time zero with ASTM C 157 and C-878 (pg. 279-281)
- Comparing 28 days shrinkage from time zero with slab on grade (pg. 282-284)
- Strain of test specimens for 110 days (pg. 285-288)
- Comparing 110 days shrinkage from time zero with ASTM C 157 and C-878 (pg. 289-291)
- Comparing 110 days shrinkage from time zero with slab on grade (pg. 292-294)

4.1. Phase III and IV: Test Results

Followings are abbreviation used in tables and graphs:

PC: Portland Cement

PCC: Portland Cement Concrete

HPC: High Performance Concrete

RSCC: Rapid Set Cement Concrete

SCC: Shrinkage Compensating Cement Concrete

CSA: Calcium SulphoAlominate

SRA: Shrinkage Reducing Admixture

MR: Moisture Reducing Admixture (Water Reducer)

W/C ratio: water to cement ratio

C. Agg. : Course Aggregate 57

4.1.1. Concrete Mix and Compressive Strength Test Results

Table 4.1 presents concrete mixes used for the large scale slabs-on-grade tests. Cylinder concrete specimens were made from each batch of the concrete slabs and they were used to measure the compressive strength of the concrete slabs in accordance with ASTM C 39. The cylinders' diameter and height are 4 in. and 8 in. respectively. A Forney machine was used to measure compressive strength of the concrete used to construct the slabs. Table 4.2 and Figure 4.1 illustrate one year compressive strength test results for seven slab specimens. As expected, the compression test results show that Rapid Set concrete gains its strength in the first hours. Rapid Set concrete reached 3,500 psi in 7 hours, and 5,550 psi in one day.

Table 4.1 Seven slabs tests concrete mixes

Materials (per cubic yard)	SRA#1	SRA#2	PCC	HPC	CTS Shrinkage Compensating Cement		Rapid Set
					#1	#2	
Komp I	-	-	-	-	120	120	-
P C	356	355	355	543	370	370	-
Flyash	88	88	88	180	-	-	-
Rapid Set Cement	-	-	-	-	-	-	658
Citric Acid	-	-	-	-	-	-	5
Course Aggregate 57	1850	1850	1850	1850	1750	1750	1772
Sand	1463	1463	1463	1196	1315	1315	1307
Water	266	266	266	264	270	272	290
MR (Polyheed (oz))	-	-	-	-	64	64.6	52.6
MR (Pozzolith 80 (oz))	13	14	14	29	-	-	-
Eclipse (oz)	128	-	-	-	-	-	-
Tetraguard (oz)	-	128	-	-	-	-	-
W/C ratio	0.60	0.60	0.60	0.37	0.55	0.55	0.44

Table 4.2 Compressive strength of seven slab specimens

	Compressive Strength (psi)						
	SRA #1	SRA #2	PCC	HPC	Shrinkage Comp.		Rapid set
Day					#1	#2	
6 Hours	-	-	-	-	-	-	2750
7 Hours	-	-	-	-	-	-	3400
1	650	650	750	1650	1900	-	5550
3	1800	1900	1900	3850	3900	2350	6600
7	2700	2750	2800	5100	4900	3950	7500
14	-	-	-	-	5650	-	8850
28	3800	3450	3150	5250	5950	5650	10000
60	-	-	-	-	-	-	10350
90	3550	3750	3400	5750	6950	6350	10750
365	3450	3800	3000	4900	6500	7100	10700

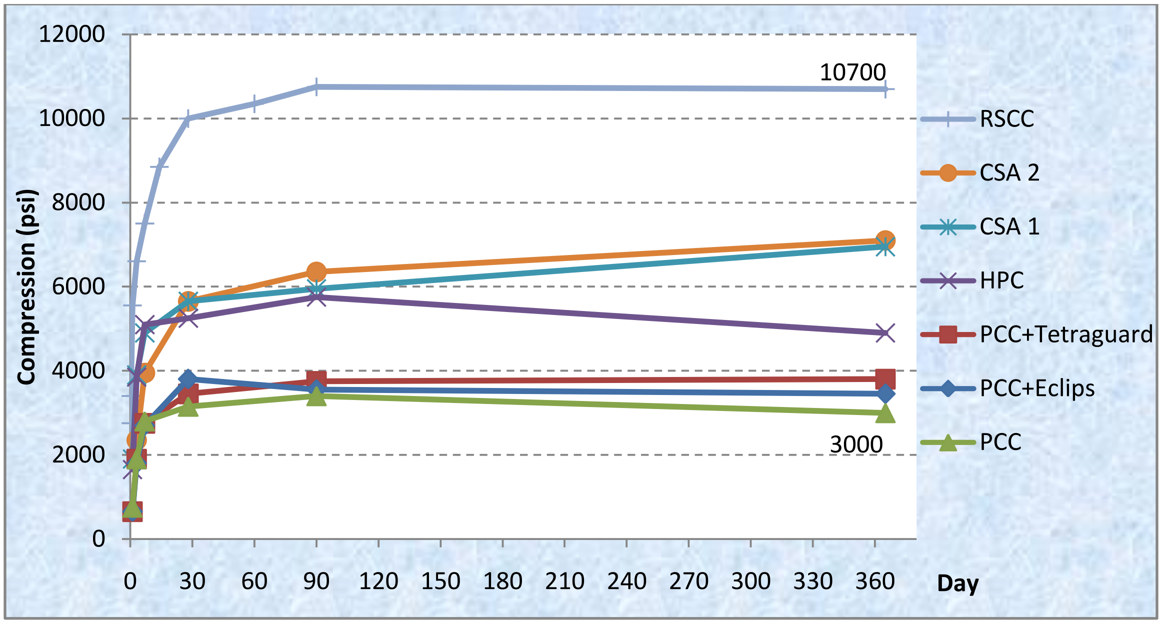

Figure 4.1 Compressive Strength vs. Time for all seven slab specimens

4.1.2. Length Changes of Prism Test Specimens

Based on ASTM C 157 and C 878 test methods, prism specimens sized 3 x 3 x 12 in. and were made from each concrete slab mix. ASTM C 157 is a standard test method for length change of hardened hydraulic-cement mortar and concrete and ASTM C 878 is a standard test method for restrained expansion of shrinkage compensating concrete. Upon curing the specimens into the limestone and water (saturated water with lime) for 7 days, measurement of length variations was initiated.

Note: Shrinkage compensating cement concrete (CSA) was used for two of the concrete slab specimens, and both concrete mixes were similar. Therefore, all the results showing CSA is the average of the two concrete specimens using CSA.

Figure 4.2 shows general strain test results (ASTM C 157) for the slab using Portland cement concrete. Figure 4.3 presents general strain test results (ASTM C 878) for the slab using shrinkage compensating cement concrete. Expansion is represented as positive number and shrinkage is as negative number in graphs. All the results are presented in Appendix B.

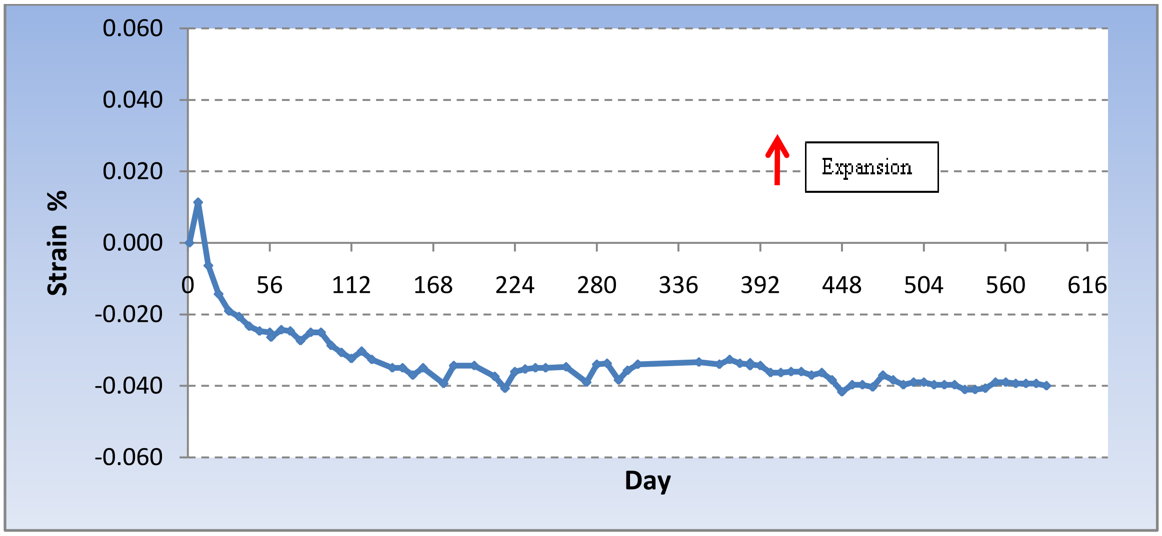

Figure 4.2 Unrestrained Expansions (ASTM C 157) vs. Time for PCC with 355 PCYcement and 0.60 w/c ratio

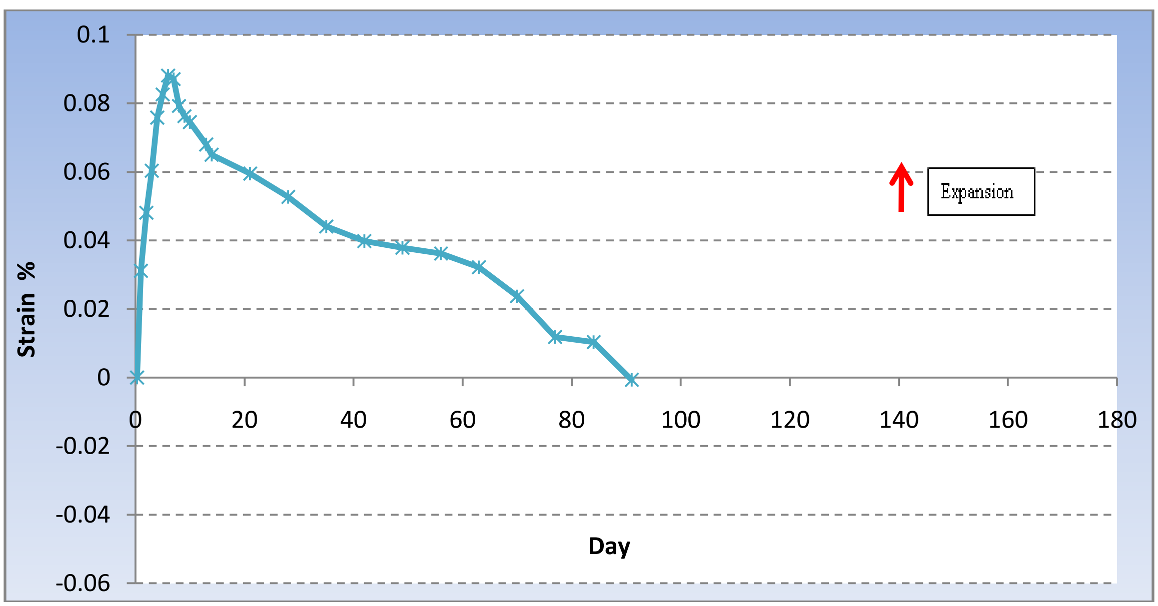

Figure 4.3 Restrained Expansions (ASTM C 878) vs. Time for shrinkage compensating concrete (CSA), Komp I

Figure 4.4 shows prism test results for PCC verses PCC with Eclipse (SRA). It can be seen that SRA has *minimal impact* on shrinkage at short and almost *No impact* at long term. Therefore, it can be concluded that using shrinkage reducing admixture does not have a noticeable improvement on reducing shrinkage.

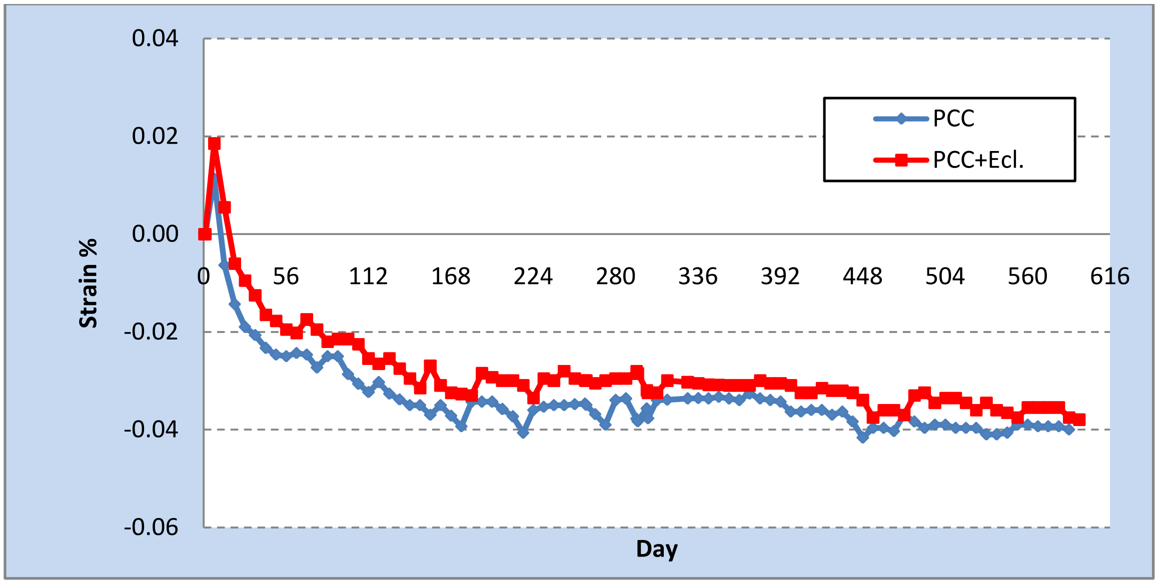

Figure 4.4 Unrestrained Expansions (ASTM C 157) vs. Time for PCC and PCC + Eclipse (SRA)

Figure 4.5 represents prism test results for HPC verses Portland cement with Eclipse (SRA). It can be seen that using SRA has *minor impact* on shrinkage at both short and long term when compared with HPC. Figure 4.6 represents prism test results for PCC verses HPC. It shows that HPC shrinkage is greater than PCC.

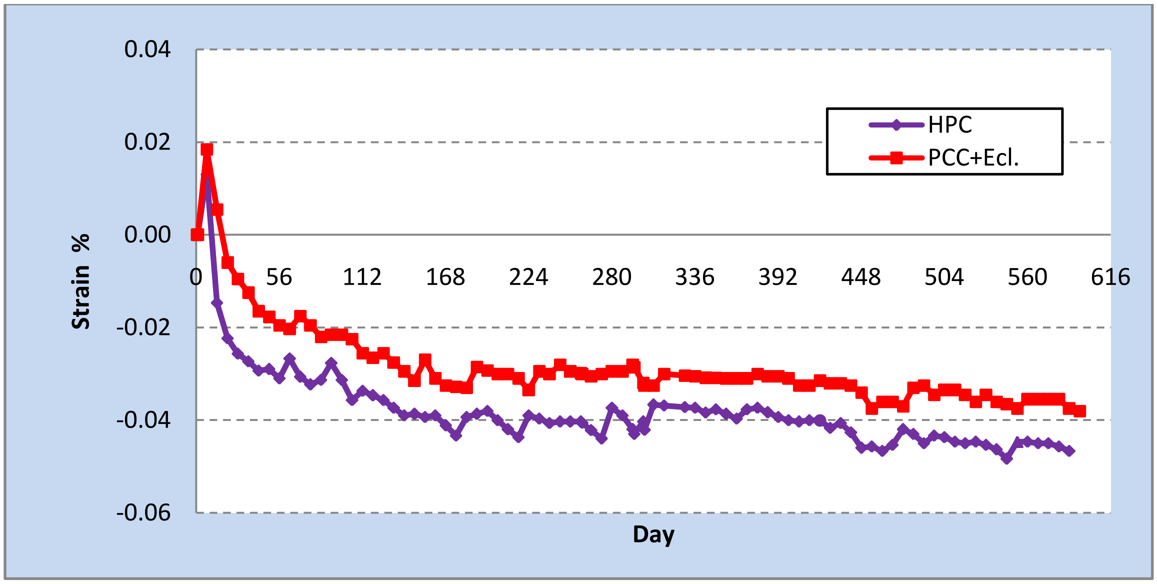

Figure 4.5 Unrestrained Expansions (ASTM C 157) vs. Time for HPC and PCC + Eclipse (SRA)

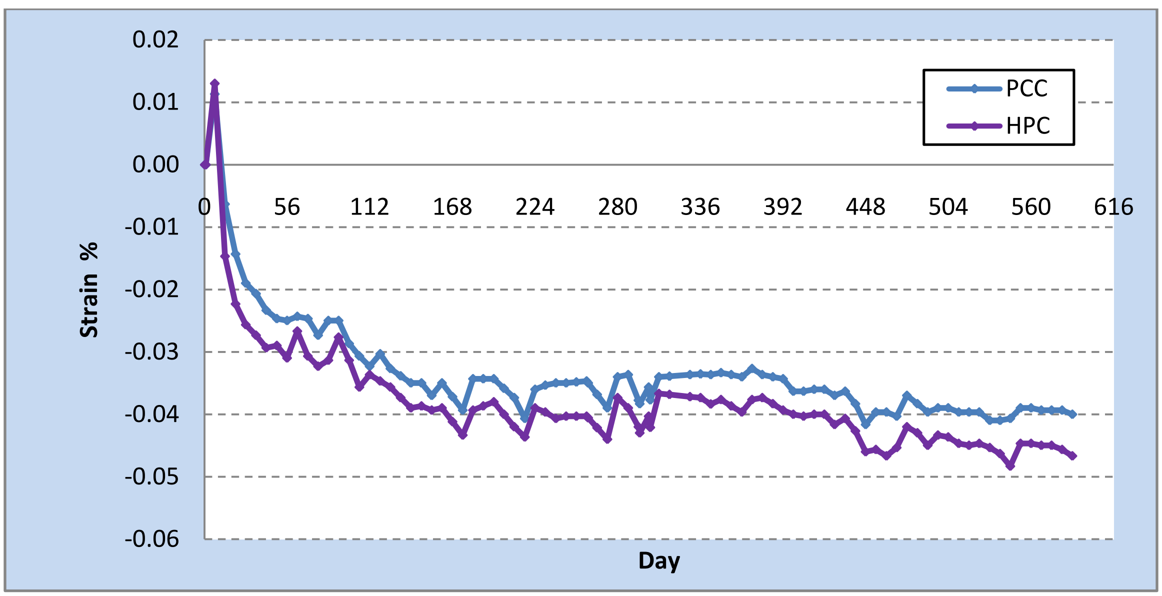

Figure 4.6 Unrestrained Expansions (ASTM C 157) vs. Time for PCC and HPC

Figure 4.7 shows the results for prism tests based on ASTM C 157 and C 878 for all the slab mixes. It appears that HPC has the greatest shrinkage at both short and long terms, and shrinkage compensating cement concrete (CSA) has the largest expansion (about four times larger than the other mixes expansion) during the first few days of curing. It can be expected that the large expansion of CSA is able to offset the restrained shrinkage caused by drying shrinkage of concrete at the long term. [Note: ASTM C 878 method provides data only for expansion of CSA. Therefore, additional tests are provided in phase IV to provide data for shrinkage from time zero. This way, comparing data for both methods is possible]. Appendix B (pg. 207-211) represents comparison of results for all the mixes based on ASTM C 157 and C 878.

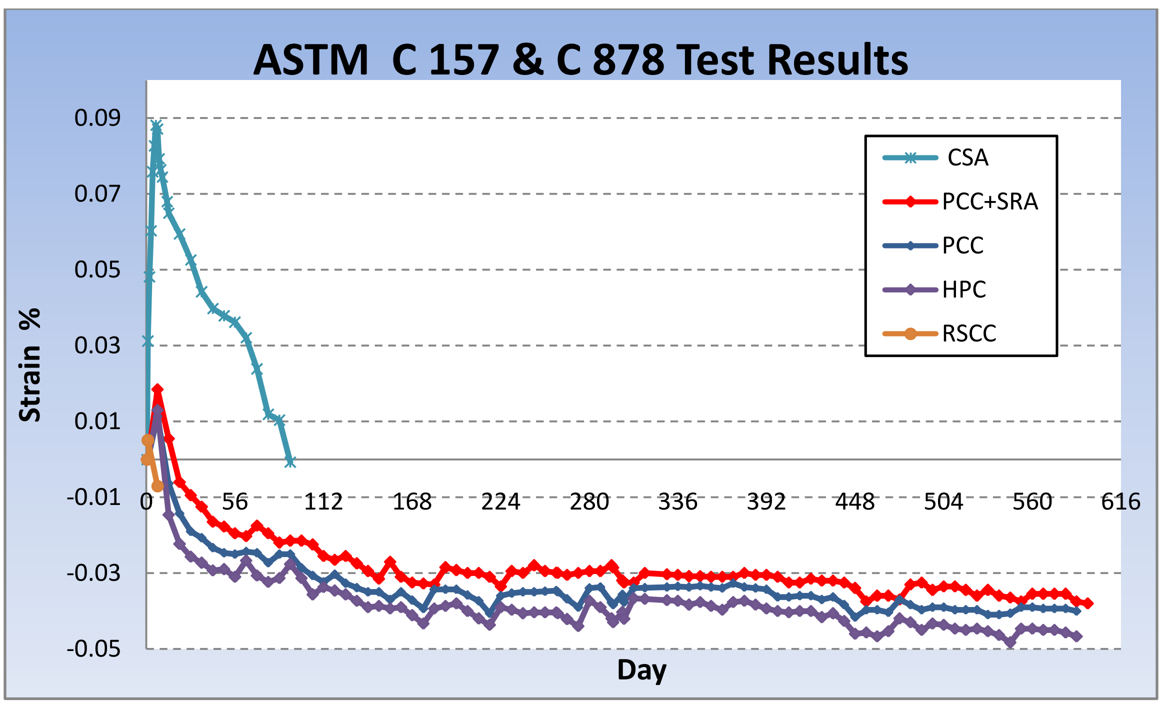

Figure 4.7 Restrained (ASTM C 878) and Unrestrained (ASTM C 157) Expansions vs. Time for all slab test specimens

4.1.3. Joint Openings and Surface Strain Measurements

As previously mentioned (in chapter 3), demec targets were installed on the slab across each joint to monitor their movement in the longitudinal direction. Each slab has two control joints located 5 ft. from the ends to provide a 10 ft. central length test. Four pairs of targets spaced as previously shown in Figure 3.39 (4.5, 9.0, 9.0, 9.0, and 4.5 in. apart) to measure surface strain across the joint or crack at longitudinal direction. Demec target were also installed with the same configuration at mid-length of the slabs to monitor surface strains with no crack at longitudinal direction. This way width of joint opening or crack can be calculated.

Surface Strain Calculation Method

The averages of four targets located at the control joints and at mid-span are calculated respectively. Each division of the demec gage is multiplied by 0.81×10^{-5} to obtain strain (based on the demec gage direction). The strain is converted to micro strain by being multiplied by 10^{-6}. The shrinkage was measured from the point of initial set and continued for 600 days.

Figures 4.8 and 4.9 show expansion at joint opening. Figures 4.10 and 4.11 present strain of control joints and mid-span of the slabs using PCC and using CSA respectively. Appendix B presents complete results for strain of surface for all of the slabs (Pg. 189, 192,195,198,202, and 205).

Note: Expansions are shown as positive numbers and shrinkages as negative numbers. Comparing the expansion of the control joints and shrinkage at mid-span from Figures 4.10 and 4.11, it can be seen that joint opening expansion and slab shrinkage at mid span made with PCC are much greater than the slab specimens made with CSA. Appendix B represents comparing the strain at control joints and mid-span for all of the slabs (pg. 220-233).

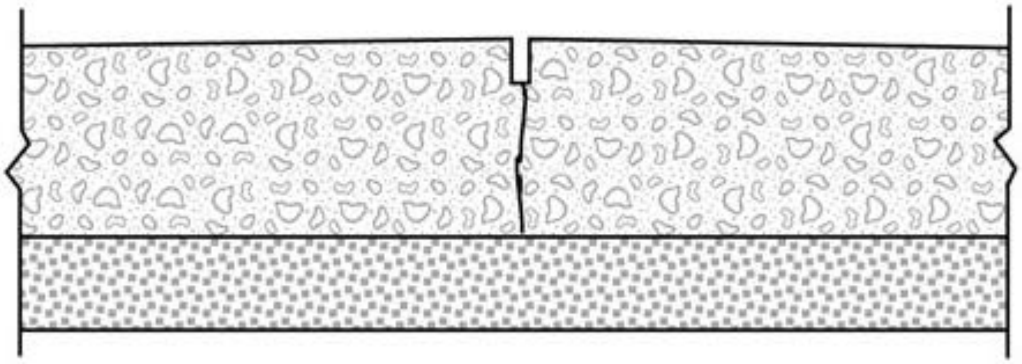

Figure 4.8 Schematic side view at joint opening

Figure 4.9 Top View of joint opening expansion or crack at large scale slab specimen

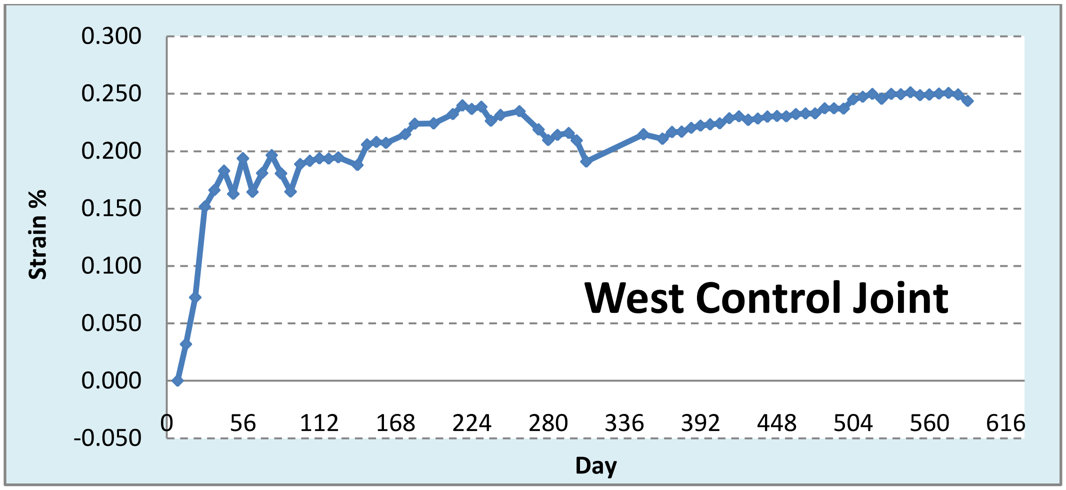

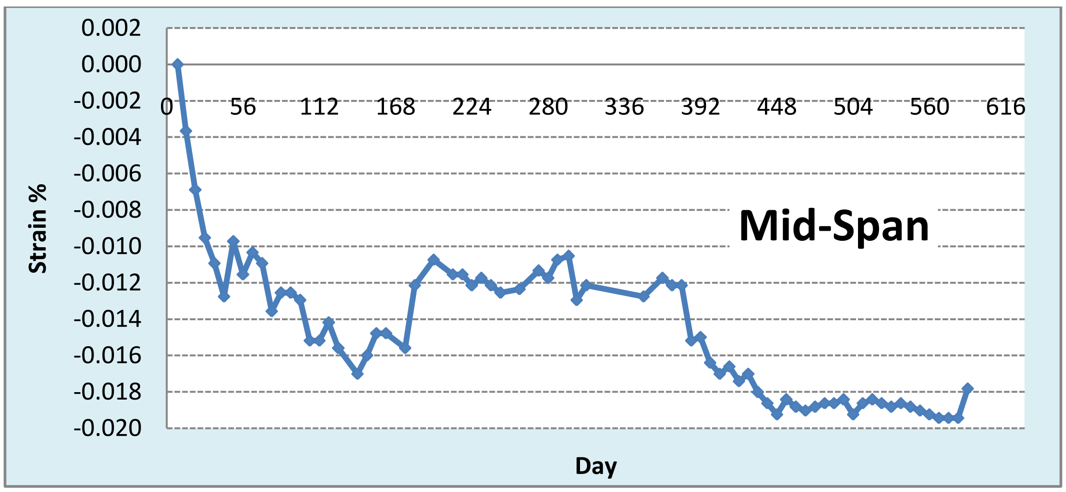

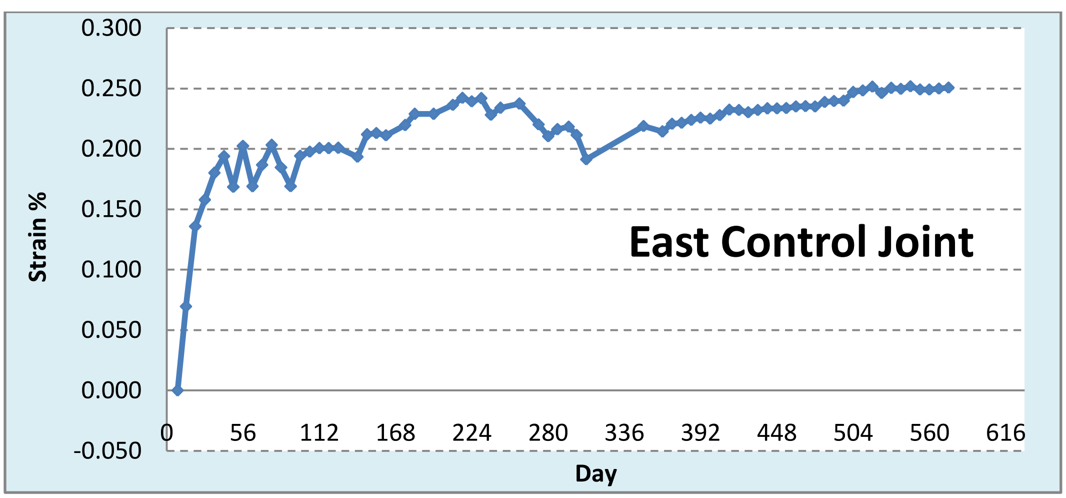

Figure 4.10 Demec Expansion vs. Time for slab using PCC with 355 PCY cement and 0.60 w/c ratio

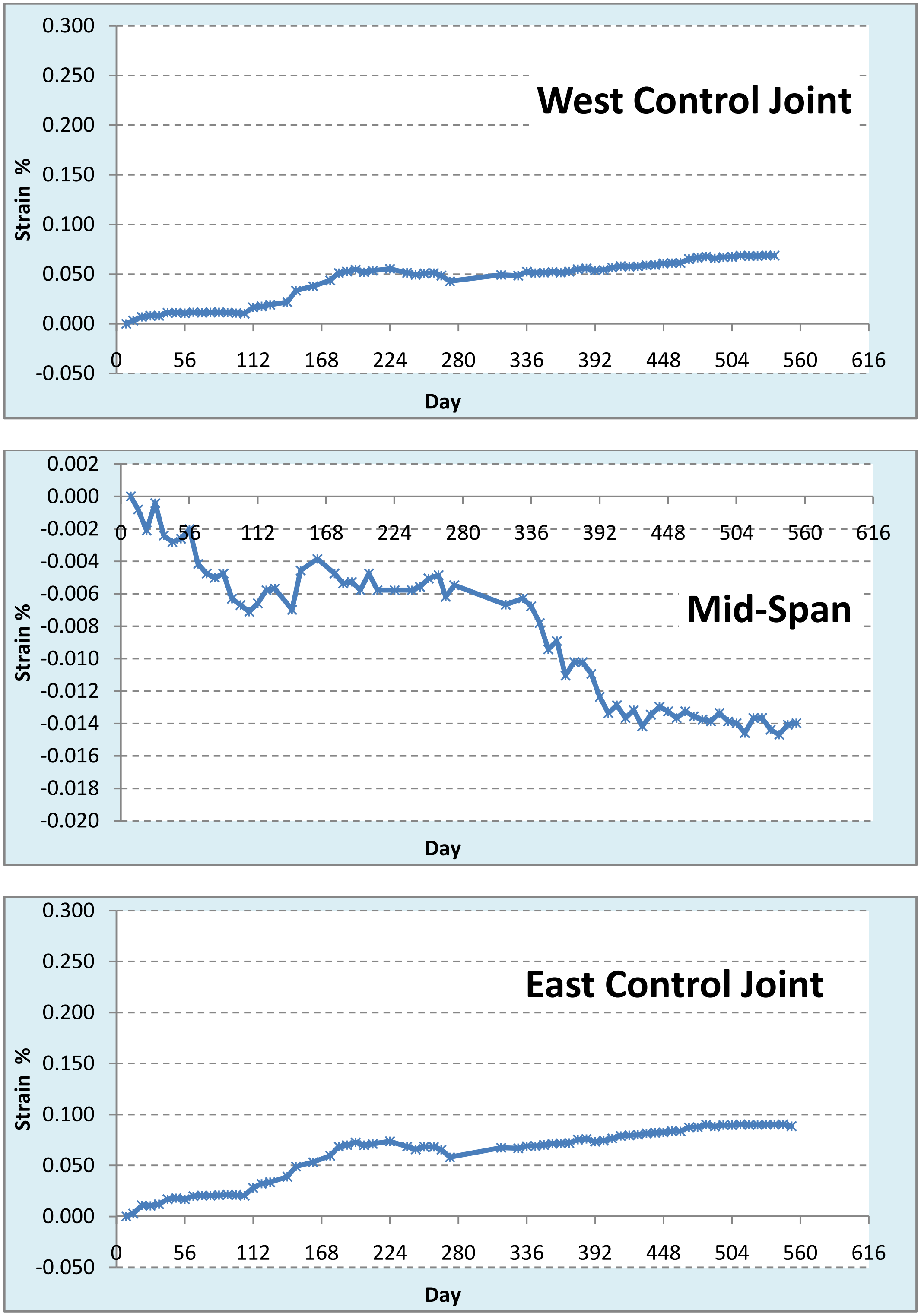

Figure 4.11 Demec Expansion vs. Time for slab using CSA, Komp I

4.1.4. Width of Joint Opening at Control Joint

Calculation of Width of Joint Openings

Expansion of joint opening ($\Delta\varepsilon$) is calculated based on strain at joint (A) and strain at mid-span or center line (C) during the time (Figure 4.12).

$\Delta\varepsilon = \mathrm{A} - \mathrm{C}$ Joint Opening (Crack) = A − C

A: $\varepsilon_{sh\ (No\ Crack\ +\ Crack)} = \frac{\Delta L1}{L}$ + Crack Strain of shrinkage with no crack + crack

(Strain at control joint)

C: $\varepsilon_{sh\ (No\ Crack)} = \frac{\Delta L1}{L}$ Strain of shrinkage with no crack * at center line

(Strain at mid-span)

* These measurements are not equal to ASTM C 157 and C 878 because the bottom of slab is exposed to the moisture in the soil and the top of slab is exposed to the low relative humidity of controlled environment while for ASTM C 157 and C 878 all sides of the specimens are exposed to the environment relative humidity.

$\Delta\varepsilon = \left(\frac{\Delta L1}{L} + \text{Crack}\right) - \frac{\Delta L1}{L} = \text{Crack}$

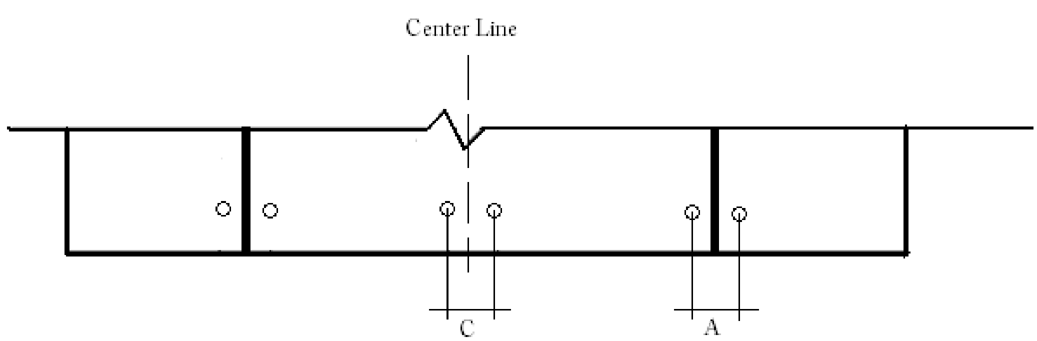

Figure 4.12 Joint opening and mid-span

Figures 4.13 and 4.14 present a general strain/expansion at both control joints (West and East sides). As expected, both control joints of each slab show nearly the same expansion width [Appendix B (pg. 190, 193, 196, 199, and 203)]. Comparing joint opening for different concrete mixes is discussed in next chapter. [Note: The average of west and east joint opening strains are used as test results].

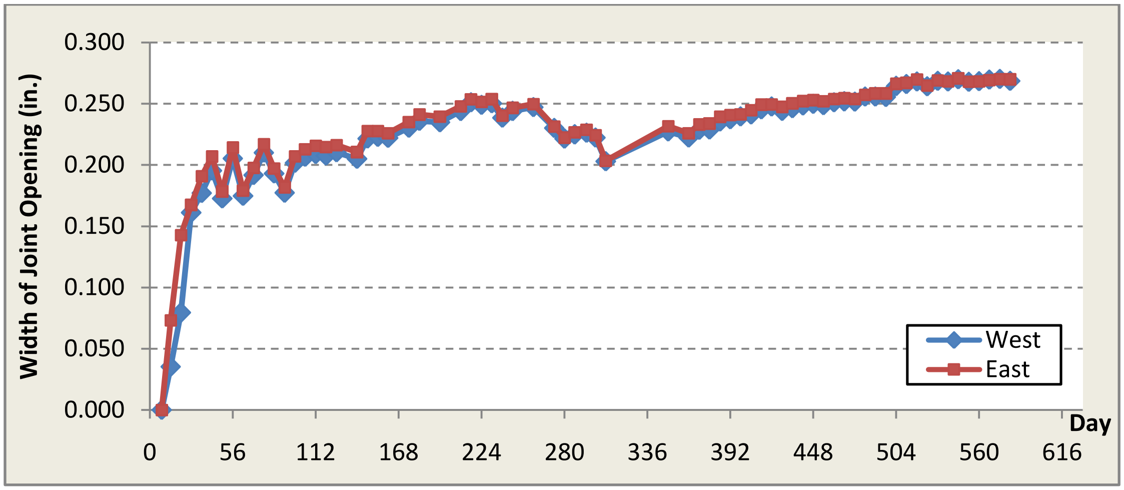

Figure 4.13 Width of Joint Opening vs. Time for slab using PCC with 355 PCY cement and 0.6 w/c ratio

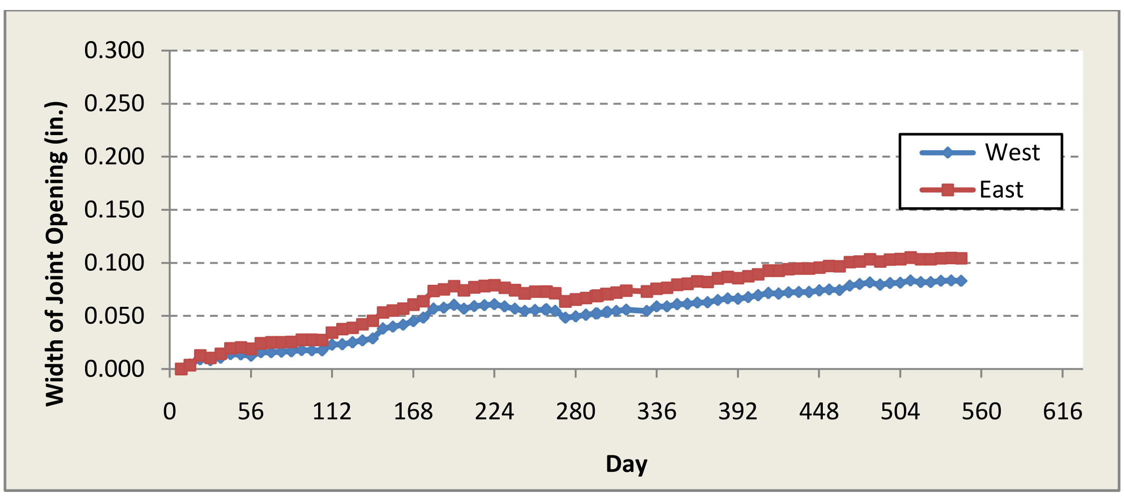

Figure 4.14 Width of Joint Opening vs. Time for slab using CSA, Komp I

Figures 4.15 represent the average strain at control joint for the normal concrete (PCC) versus PCC+SRA, and Figure 4.16 show the expansion or width of joint opening for (PCC) verses normal concrete using shrinkage reducing admixture (PCC+SRA). It can be seen that using SRA only reduces shrinkage in the first week. The rest of the slop curve are the same for normal concrete and concrete using SRA; the curves are only shifted (both curves are parallel with Offset, by the initial reduced shrinkage of the SRA concrete). The two graphs, with exception to the first few days, are positively correlated. Figure 4.17 represents the behavior of the material in the slab with no crack at mid-span. It can be seen that there is a minor impact on reducing shrinkage with using SRA at short term and almost no impact at long term in compare to the concrete slab using PCC. Also, using SRA delays the shrinkage for the first few days, then concrete cracks (Figures 4.15. 4.16, and 4.17). This means that SRA saves the concrete slab to crack for the first few days when PCC cracks at early age.

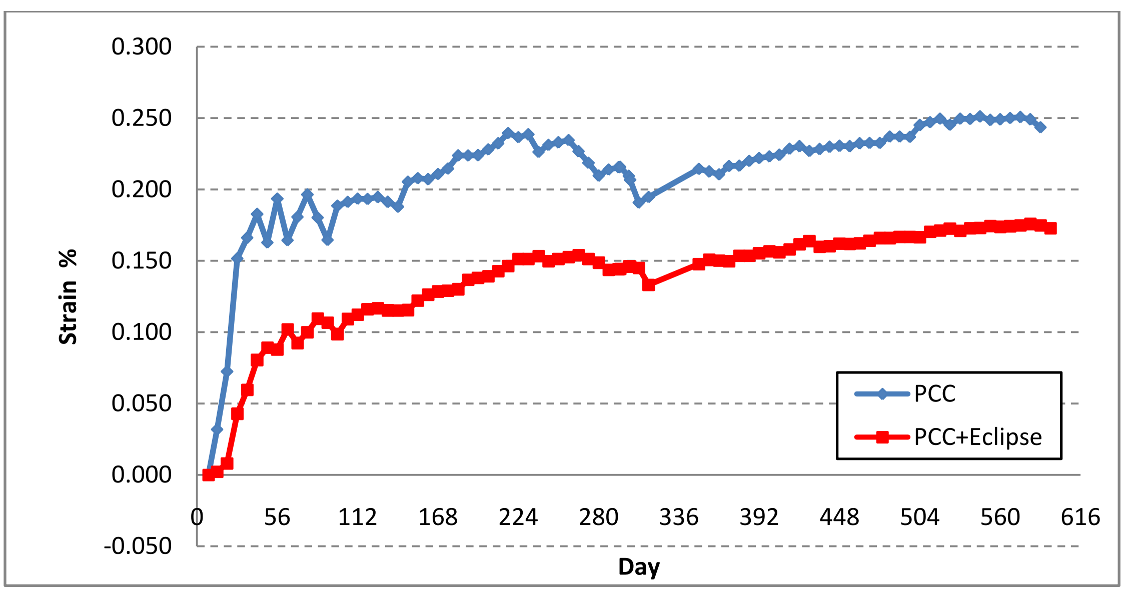

Figure 4.15 Strain at Joint Opening vs. Time for slab using PCC and slab using (PCC+ Eclipse)

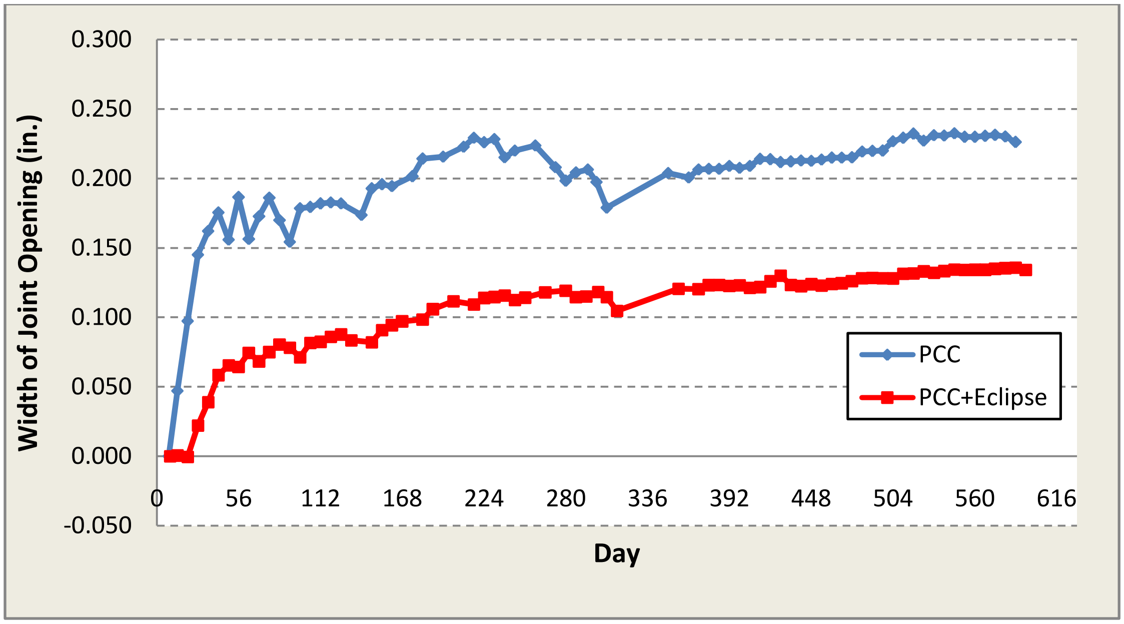

Figure 4.16 Width of Joint Opening vs. Time for slab using PCC and slab using (PCC+ Eclipse)

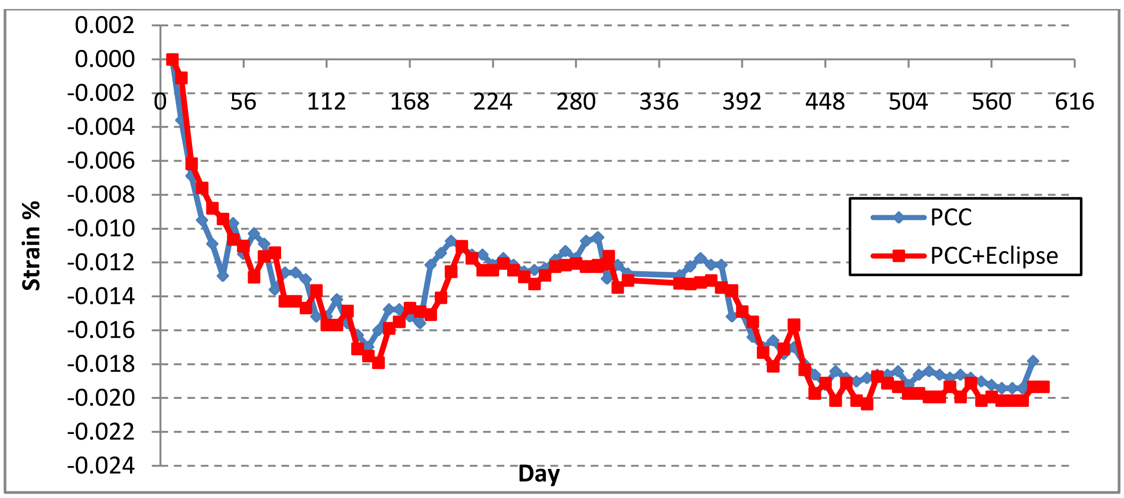

Figure 4.17 Strain at Mid-Span vs. Time for slab using PCC and slab using (PCC+ Eclipse)

Figure 4.18 shows the behavior of the material in the slab with no crack at mid-span for HPC vs. PCC+ Eclipse. It can be seen that there is a minor impact on reducing shrinkage with using SRA at short and long term in compare to the concrete slab using HPC.

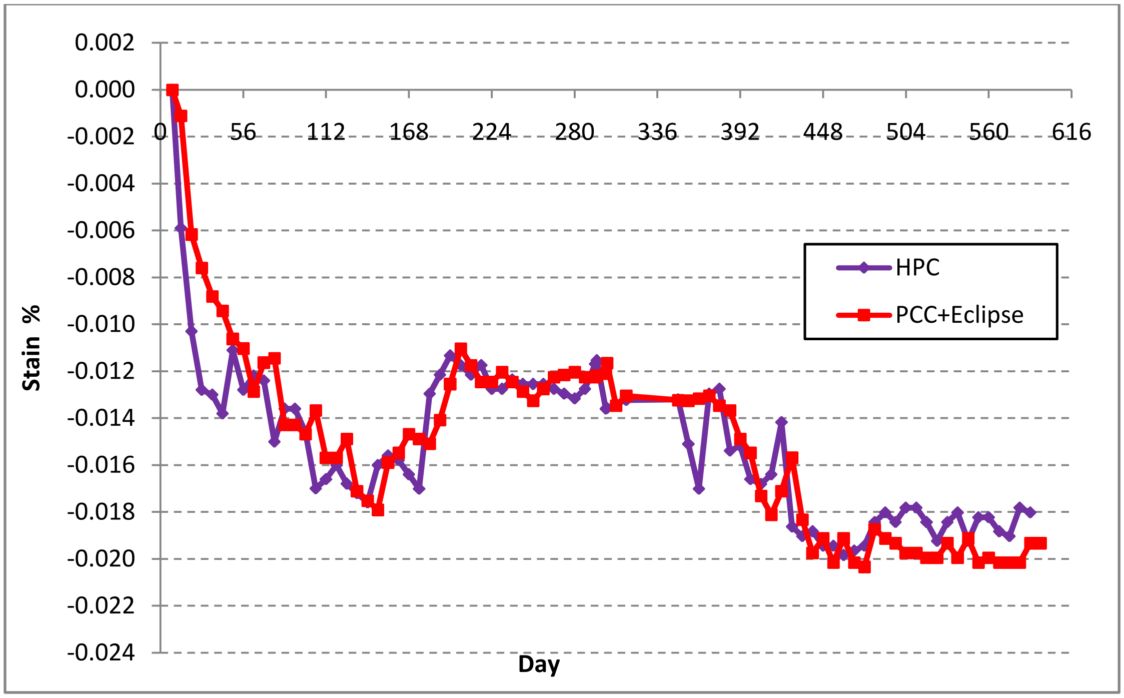

Figure 4.18 Strain at mid-span vs. Time for slab using HCC and slab using (PCC+ Eclipse)

Figure 4.19 presents expansion or crack at the joint opening (calculated by taking the average of west and east sides joint openings) for all of the slabs. The results show that the slab with HPC has the largest expansion or crack at the joints and slab with CSA has the smallest expansion or crack at the joints. Also, it can be seen that joint opening expansion continues for long term (600 days) with slab using PCC and HPC. Comparing HPC and PCC shows that HPC cracks are wider than PCC.

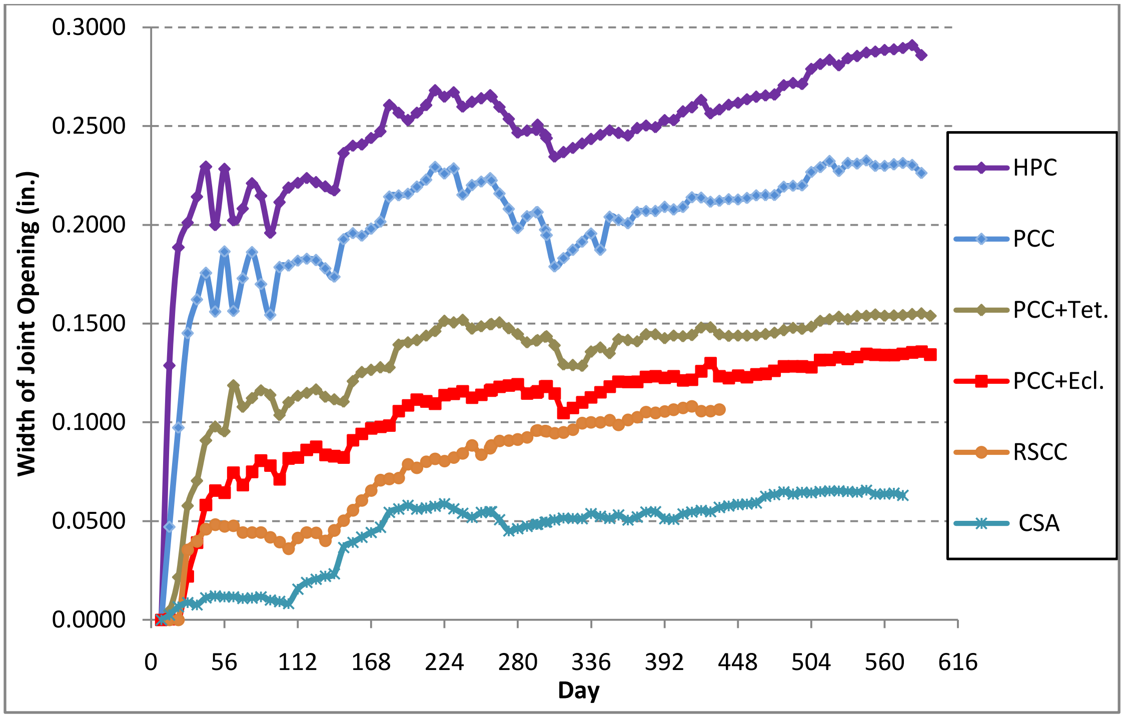

Figure 4.19 Width of Joint Opening vs. Time for slab using CSA, Komp I

Figure 4.20 demonstrates the strain of control joints for normal concrete (PCC) verses high performance concrete (HPC). It shows that HPC shrinks quicker than normal concrete. And shrinkage of HPC occurs at a faster rate during the first few weeks (early age) after curing compared with the normal concrete. Additionally, HPC and PCC shrinkage growth continues for the long term.

Figure 4.21 shows the strain of control joints for shrinkage compensating cement concrete (CSA) verses PCC+ Eclipse (SRA). It can be seen that shrinkage compensating concrete has a positive effect on reducing shrinkage of concrete at both short and long terms in compare to the SRA. Comparing width of joints for all the slabs are represented in Appendix B (pg. 212-219) and comparing strain at mid-span and control joints are presented in Appendix B (pg. 220-233)

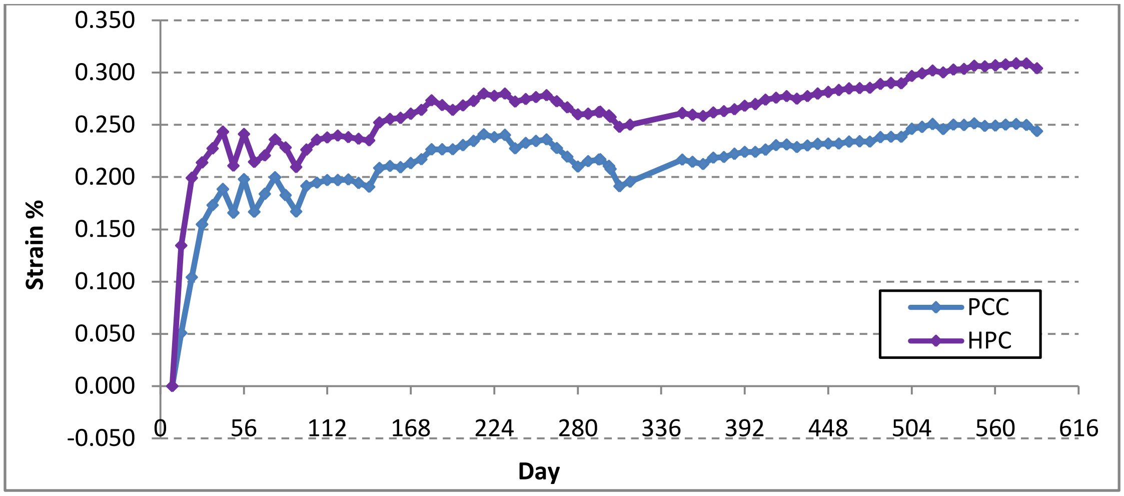

Figure 4.20 Average strain at control joints vs. Time for slab using PCC and slab using HPC

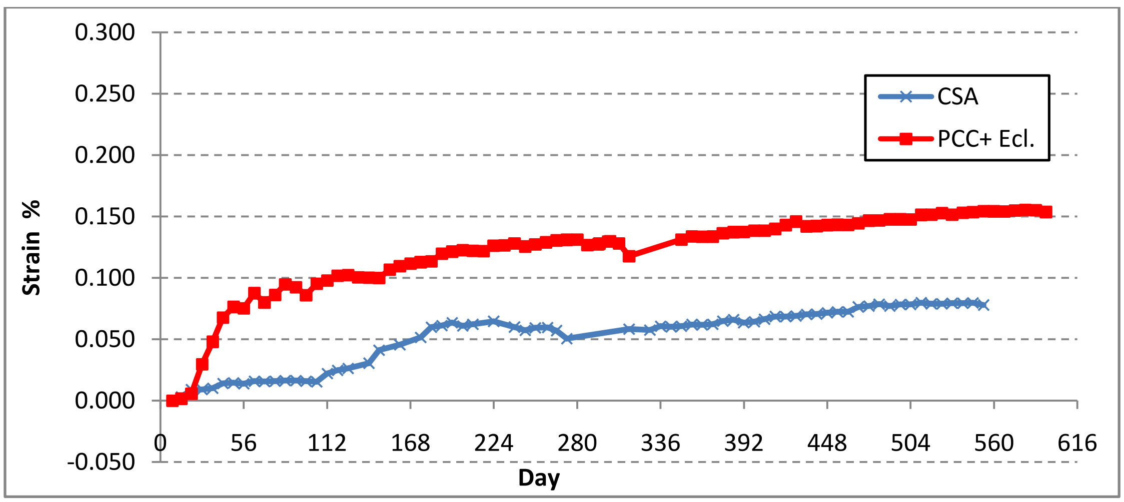

Figure 4.21 Average strain at control joints vs. Time for slab using CSA and slab using (PCC+ Eclipse)

4.1.5. Comparing Slab Test Results with ASTM C 157

Figure 4.22, 4.23, and 4.24 compare slab behavior at mid-span (no crack) with ASTM C 157 method using PCC+ Eclipse, PCC, and HPC respectively. It can be seen that there are significant differences in the results between slab behavior and ASTM C-

157 results. Thus, it can be concluded that ASTM C 157 does not provide an accurate results for predicting slab behavior.

Note: It is not possible to compare slab shrinkage behavior with ASTM C 878 method because ASTM C 878 is only used for expansion and is not acceptable for shrinkage.

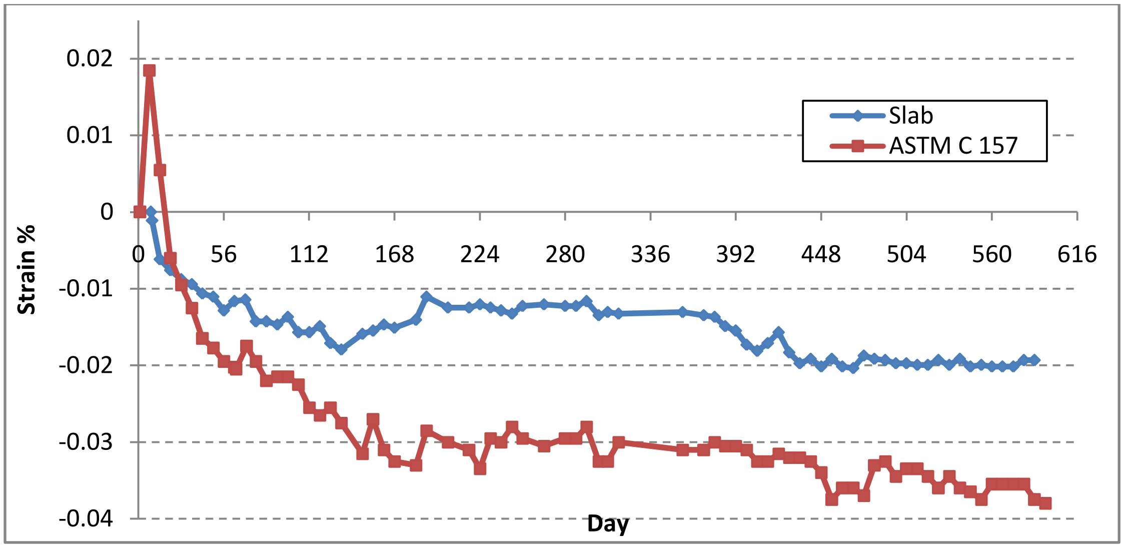

Figure 4.22 Strain at mid-span vs. ASTM C 157 method using PCC+Eclipse

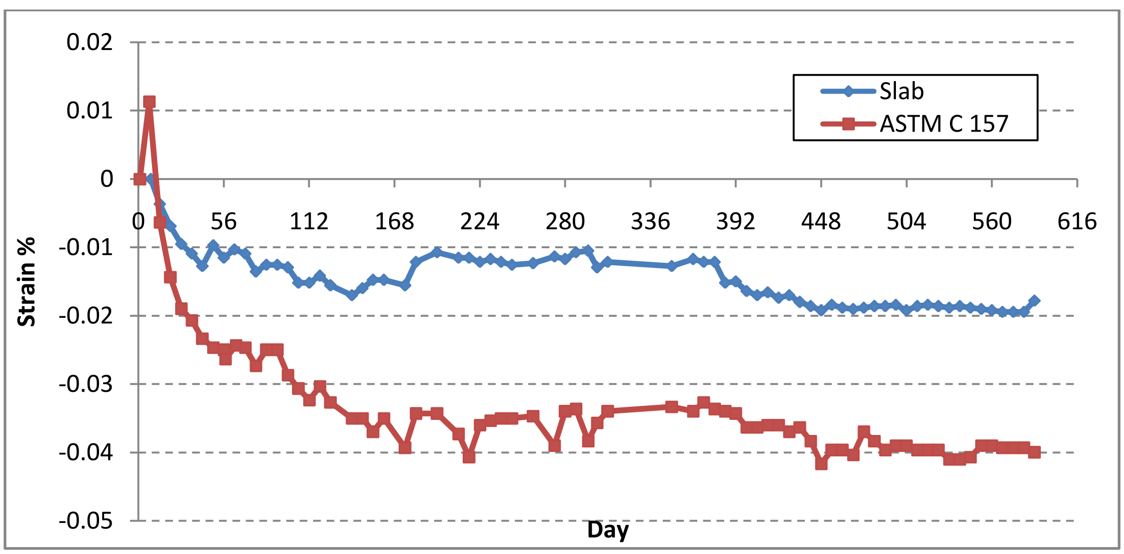

Figure 4.23 Strain at mid-span vs. ASTM C 157 method using PCC

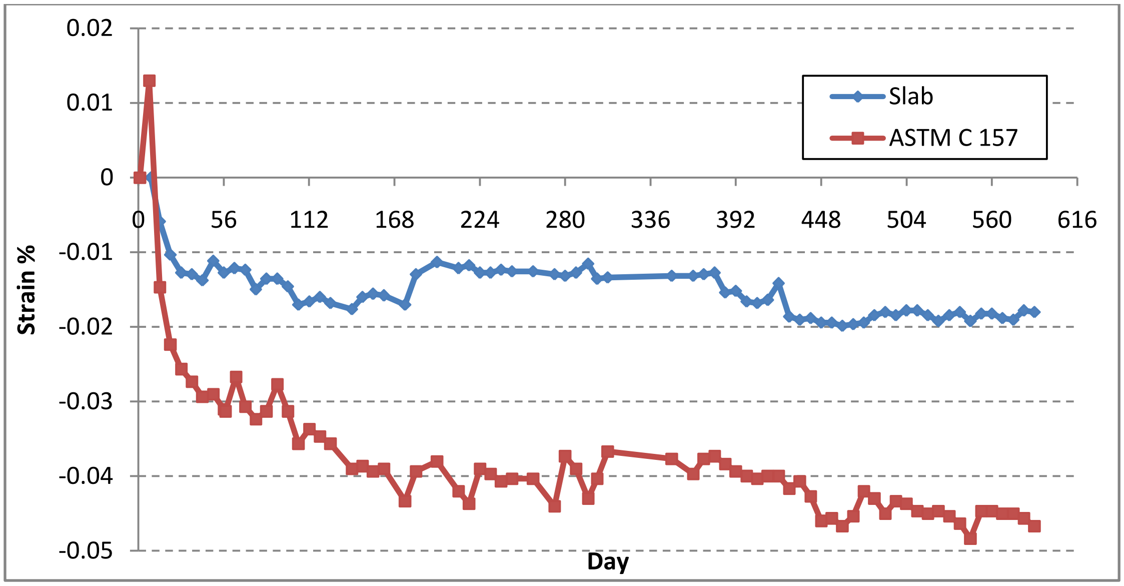

Figure 4.24 Strain at mid-span vs. ASTM C 157 method using HPC

Note: This investigation did not have any visual cracks on the slabs on grade except for a few shallow hairline cracks that occurred at the surface of the slabs using shrinkage compensating concrete (SCC) and Rapid Set cement concrete (RSCC). These shallow cracks appeared soon after casting the concrete and are caused by uncompleted initial cement hydration due to incomplete mixing and the cracks did not grow and increase.

4.1.6. Slab Temperature and Relative Humidity

Temperature and relative humidity were monitored at each concrete slab, throughout using calibrated probes, installed at ½ in. increments through the depth of the slabs. The calibrated probes were located at mid-span as previously shown in Figure 3.34 and 3.37. A general result for temperature and relative humidity of slabs on day 7/13/2010 are presented in Tables 4.3 and 4.4 and also Figures 4.25 and 4.26. Table 4.3 and Figure 4.25 show that there is no temperature changes through depth of the slabs which means the ambient temperature remained constant. Table 4.4 and Figure 4.26 represent how vary relative humidity is through depth of the slabs. It can be seen that the slab with HPC has the greatest moisture gradient and slab with CSA has the smallest moisture gradient and other mixes are between HPC and CSA. In addition, there are almost no changes in the moisture content past 2.5 in. depth in the slab. Also, moisture content changes only within 1.5-2.0 inches from top surface of the slab. Discussion is presented in the next chapter and results are displayed in Appendix B; slabs' interior temperature (pg. 234-246) and slabs' interior relative humidity (pg. 247-271).

Table 4.3 Slabs interior temperature (7/13/2010)

7/13/2010	**Slab Temperature (ºF)**					
Depth (in.)	**PCC+ Eclipse**	**PCC+ Tetraguard**	**PCC**	**HPC**	**Average CSA**	**RSCC**
0						
-0.5	71	71	71	71	71	72
-1	71	71	71	71	71	71
-1.5	71	71	71	71	71	71
-2	71	71	71	71	72	72
-2.5	71	71	71	71	72	72
-3						

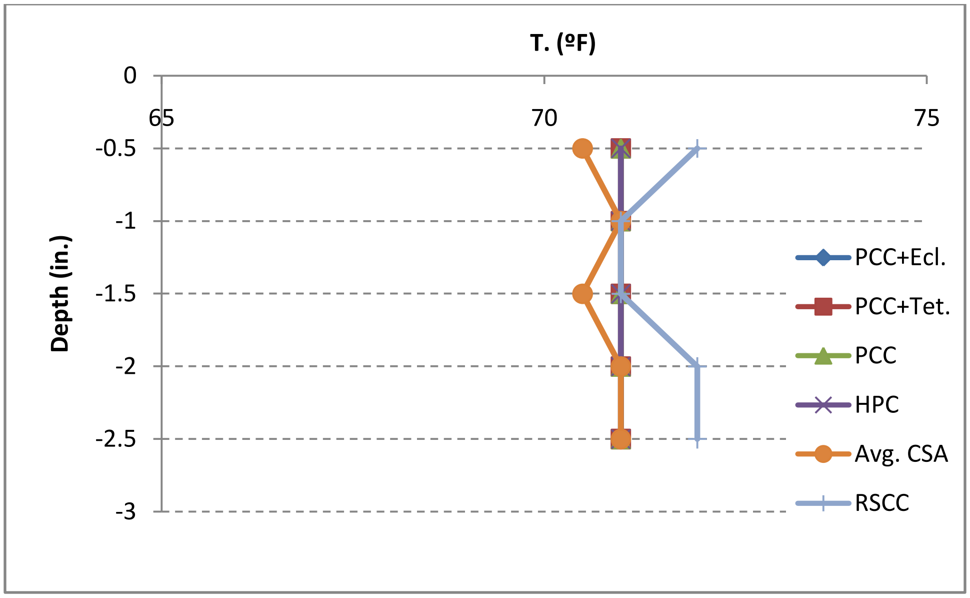

Figure 4.25 Interior slabs temperature in depth vs. Time (7/13/2010)

Table 4.4 Slabs interior relative humidity (7/13/2010)

7/13/2010	Slab Relative Humidity (%)					
Depth (in.)	**PCC+ Eclipse**	**PCC+ Tetraguard**	**PCC**	**HPC**	**Average CSA**	**RSCC**
0						
-0.5	68	70	73	63	81	61
-1	75	71	76	68	92	82
-1.5	87	82	84	76	97	91
-2	94	91	90	80	100	96
-2.5	100	97	96	100	100	100
-3						

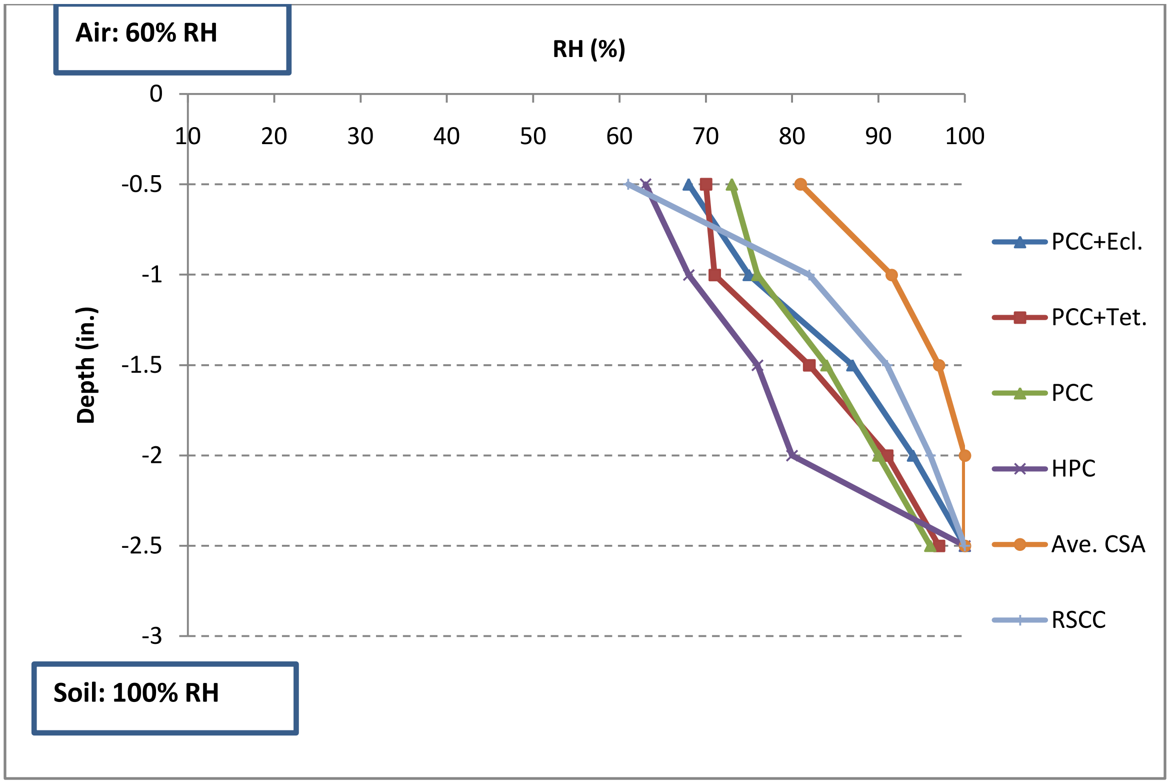

Figure 4.26 Interior slabs relative humidity in depth vs. Time (7/13/2010)

Figure 4.27 shows interior slabs RH vs. depth on day 3/15/2011. The ambient relative humidity was reduced to 30% for a few months by then. The figure presents the RH of the slabs within the top 0.5 in. of concrete slab in comparison to the higher ambient relative humidity (Figure 4.23), but the same relationship exists; the slab with HPC has the greatest moisture gradient and slab with CSA has the smallest moisture gradient and the other mixes are between HPC and CSA.

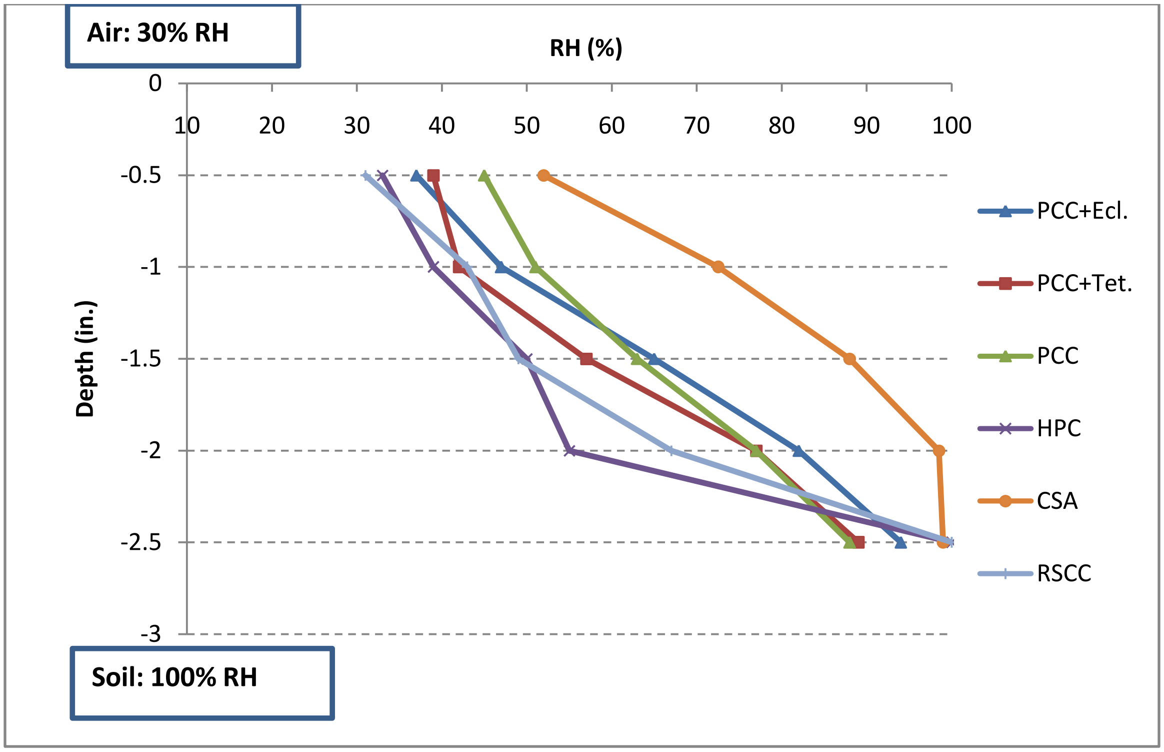

Figure 4.27 Interior slabs relative humidity in depth vs. Time (3/15/2010)

4.1.7. Ambient Temperature and Relative Humidity

Ambient temperature and relative humidity are presented in Figures 4.28 and 4.29 respectively. As it is shown, temperature is mostly 70 ºF and relative humidity is mostly 60%. The relative humidity was reduced to 30% (phase V) for the last few months of testing and monitoring.

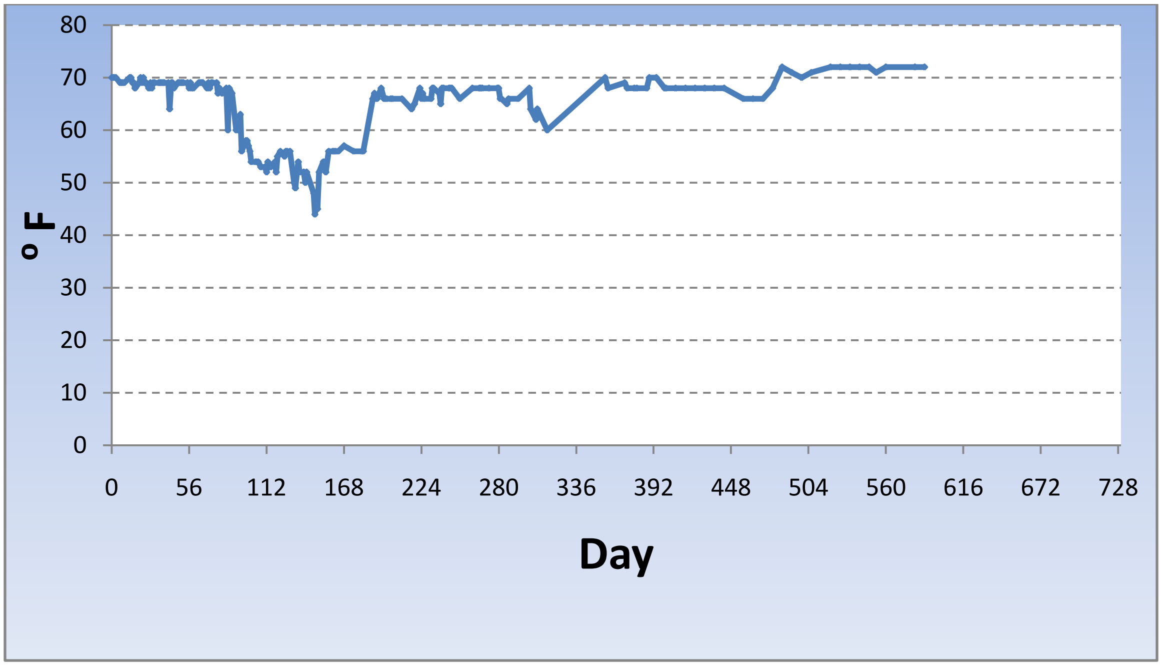

Figure 4.28 Advanced Concrete Research Lab ambient temperature

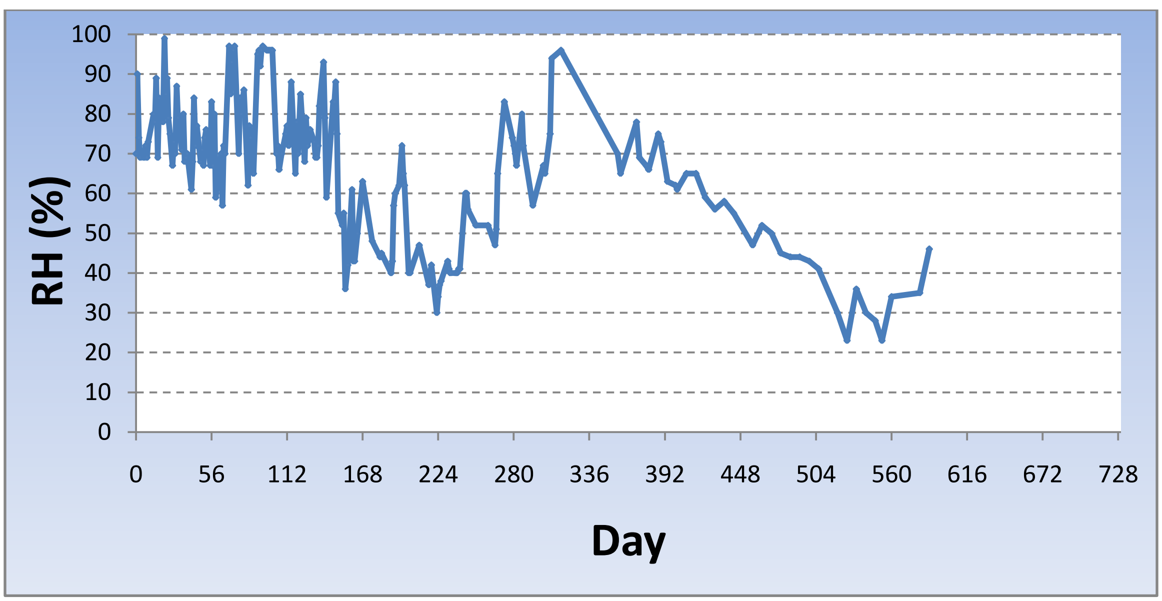

Figure 4.29 Advanced Concrete Research Lab ambient relative humidity

4.2. Phase IV: Test Results for Additional Tests

As previously mentioned a dial gage was used for measuring the length change of the time zero specimens. The concrete mixes are the same, with the minor exception being the type of water reducer on 4 of the samples (Appendix C). The results are presented in two sections; results for 28 days (Appendix C, section C.2) and results for 110 days (Appendix C, section C.3). This helps to provide the data clearly for the first 28 days tests and then for the longer period of the time (110 days).

Figure 4.30 represents 28 days “shrinkage from time zero” test results for the additional tests in phase IV. This shows the behavior of the concrete from time zero. It can be seen that CSA expands during the first 7 days of curing and has the largest expansion, and HPC has the greatest early age shrinkage and the largest shrinkage in 28 days compared with the other concrete mixes. The other mixes shrinkage is very close to each other and are between CSA and HPC. Note that SRAs still show shrinkage, but not as much.

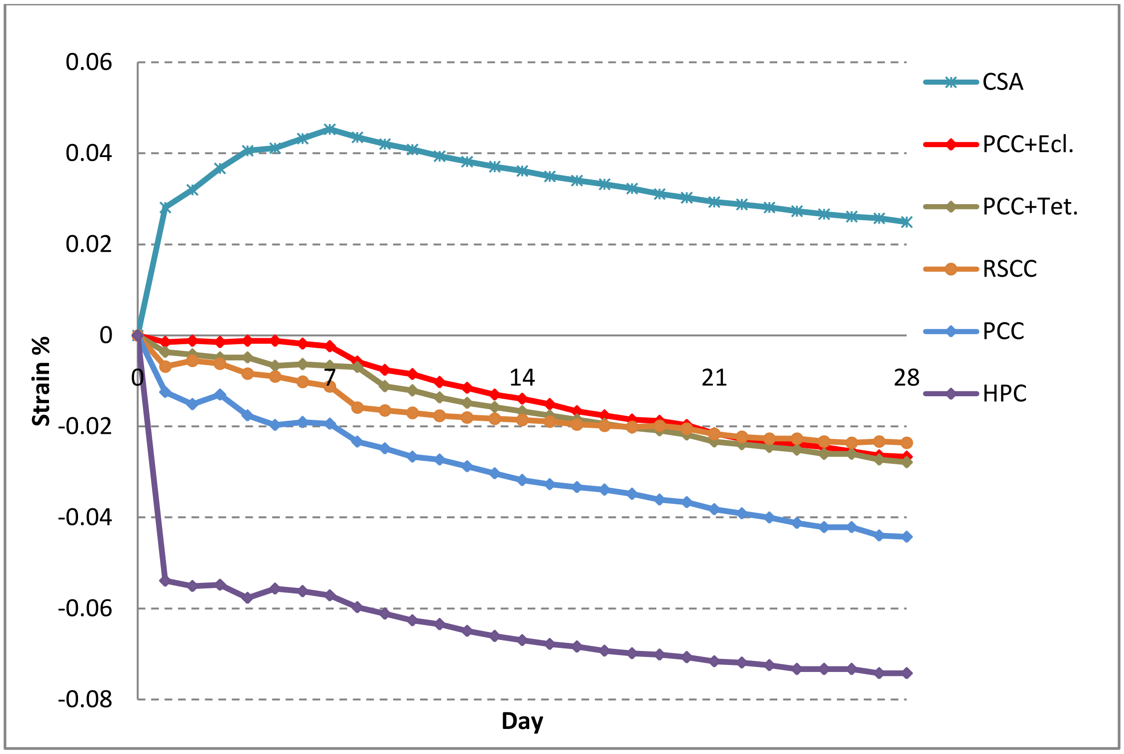

Figure 4.30 Shrinkage from time zero for all the specimens (Phase IV) for 28 days

Figure 4.31 represents test results for shrinkage from time zero in comparison to the unrestrained expansion ASTM C 157 with (PCC+Eclipse). It can be seen that there is no expansion in concrete using the "shrinkage from time zero" method because the expansion is restraind due to the steel plate at free end of the specimens while the expansion is unrestrained for ASTM C 157 method. Also, curing process for ASTM C 157 was different from that for shrinkage from time zero method. But it can be noted that the trend is the same for both testing methods.

Note: ASTM C 157 and C 878 curing method was diferent with curing for shrinkage from time zero. All sides of the concrete specimens were placed into the saturated limewater for the ASTM C 157 and C 878 methods. Only top surfaces of the concrete specimens were wet cured by putting the concrete pad saturated moisture on top of the specimens for the shrinkage from time zero method (Appendix D, pg. 305 and 307).

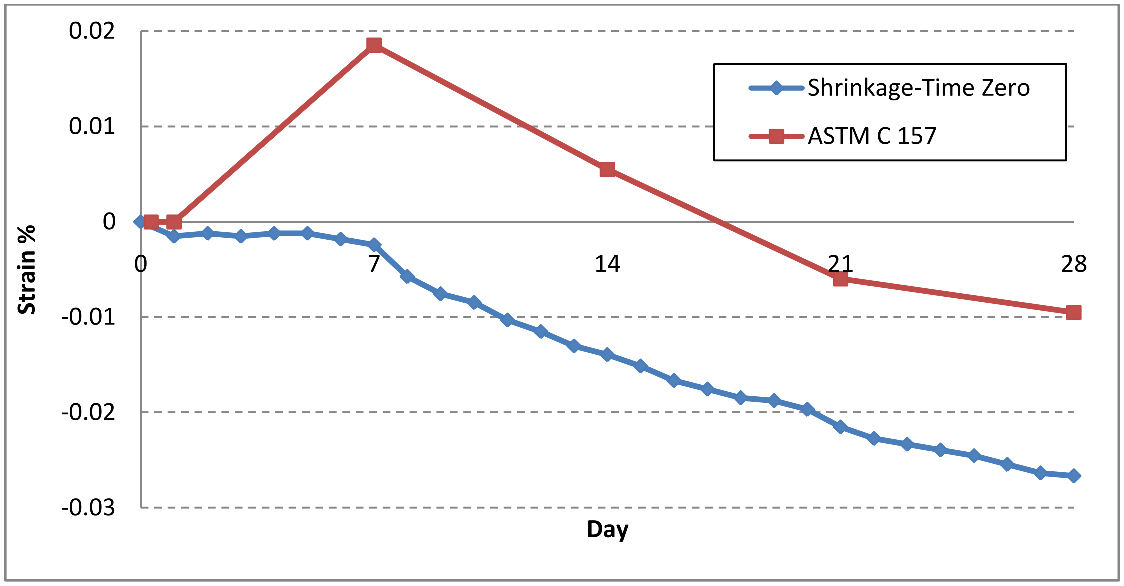

Figure 4.31 Shrinkage from time zero in compare to ASTM C 157 using PCC+Eclipse

Figure 4.32 shows 28 days test results for shrinkage from time-zero in compare to the unrestrained expansion ASTM C 157 with the same material (PCC). Results from shrinkage from time zero method shows that PCC shrinks from the early age. Also there is the same trend using the two testing methods.

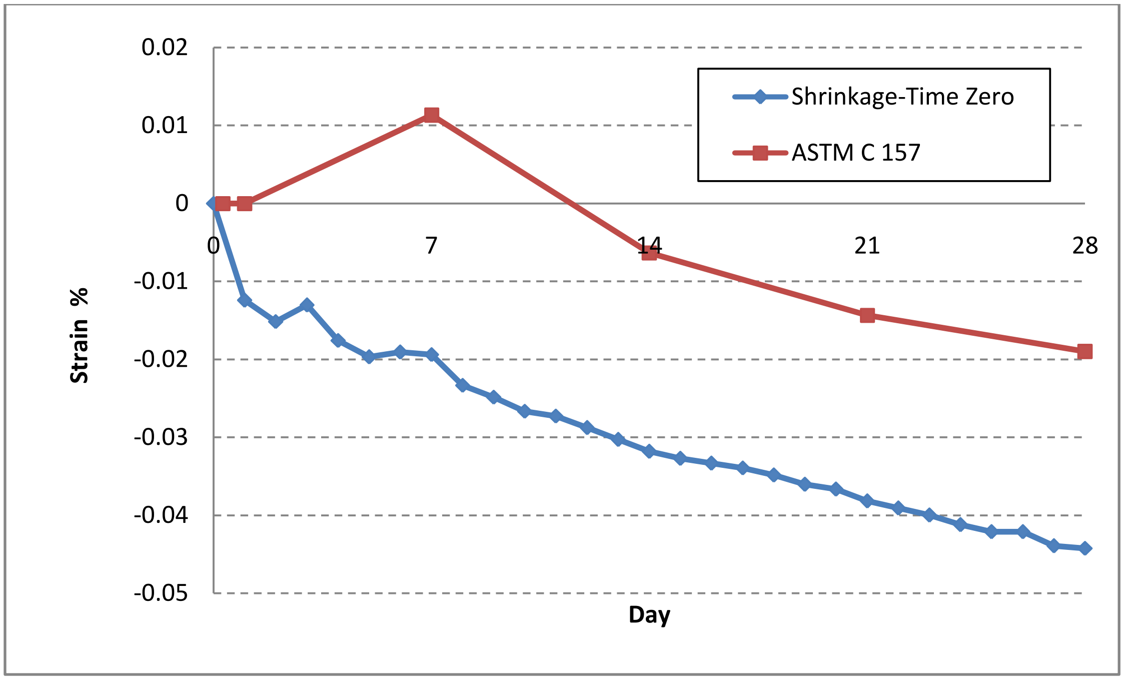

Figure 4.32 Shrinkage from time zero in compare to ASTM C 157 using PCC

Figure 4.33 shows that the results using ASTM C 878 has the same trend in compare to the resutls using shrinkage from time zero method for the concrete made with CSA. The amount of expansion is different due to the stiffness of the rod is used to restrain expansion of concrete at ASTM C 878 method in compare to the stiffness of the steel fram is used to restrain expansion of concrete at shrinkage from time zero method. Also, curing process for ASTM C 878 was different from that for shrinkage from time zero method.

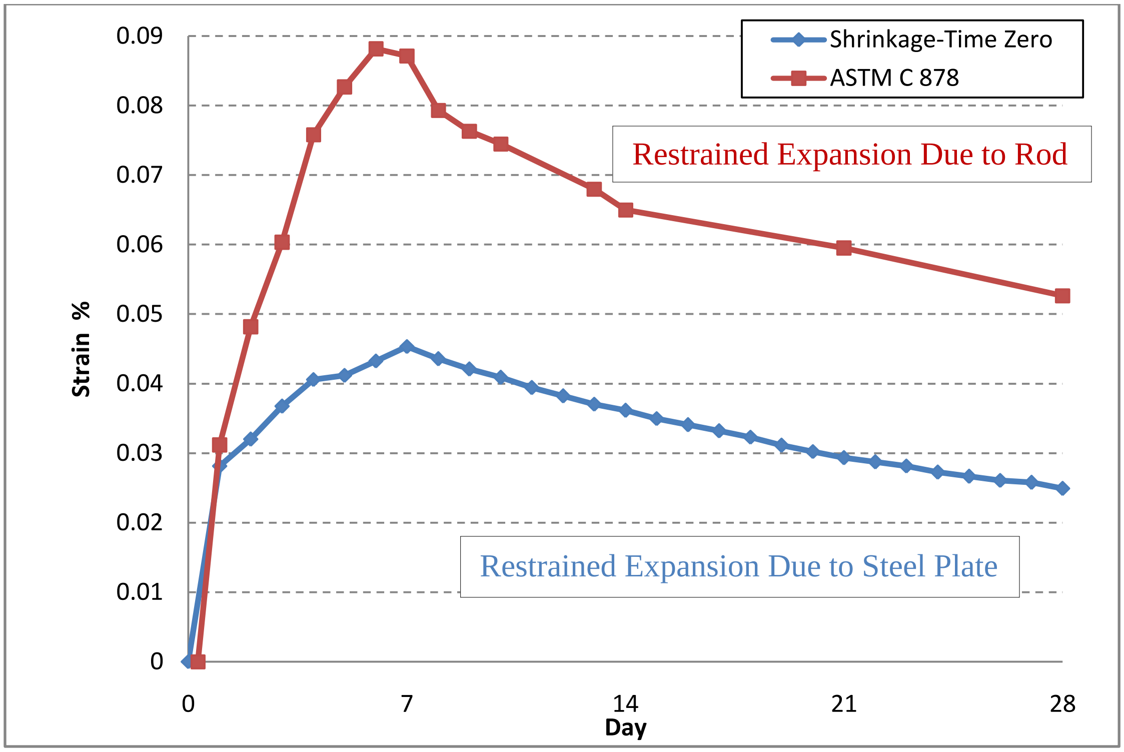

Figure 4.33 Shrinkage from time zero in compare to ASTM C 878 using CSA

Figure 4.34 presents a 110 day comparison for the shrinkage from time zero method with slab on grade behavior for the PCC mix design. Figure 4.35 shows a 110 day shrinkage from time zero with on grade slab behavior using the CSA shrinkage comp mix design. It can be seen that the results from the shrinkage from time zero test does not match the slab on grade test results. Therefore, it can be concluded that the constant moisture that is coming from underneath of the slab changes the behavior of the concrete slab. Thus, behavior of the concrete slab on grade is dependant on the moisture gradient through depth of the slab.

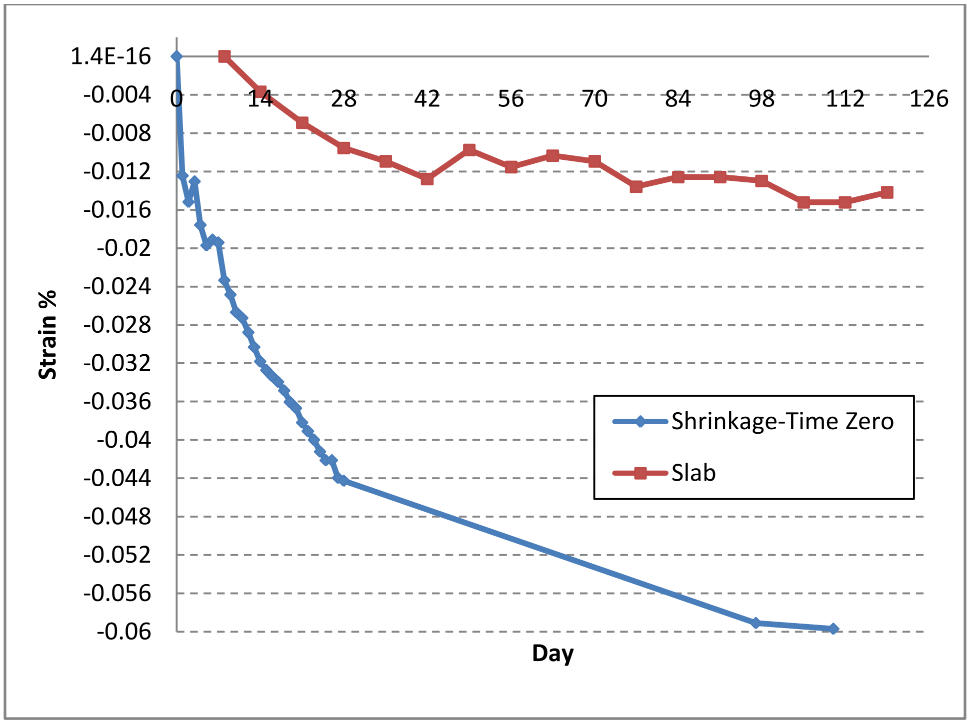

Figure 4.34 Shrinkage from time zero vs. Slab-on-Grade using PCC

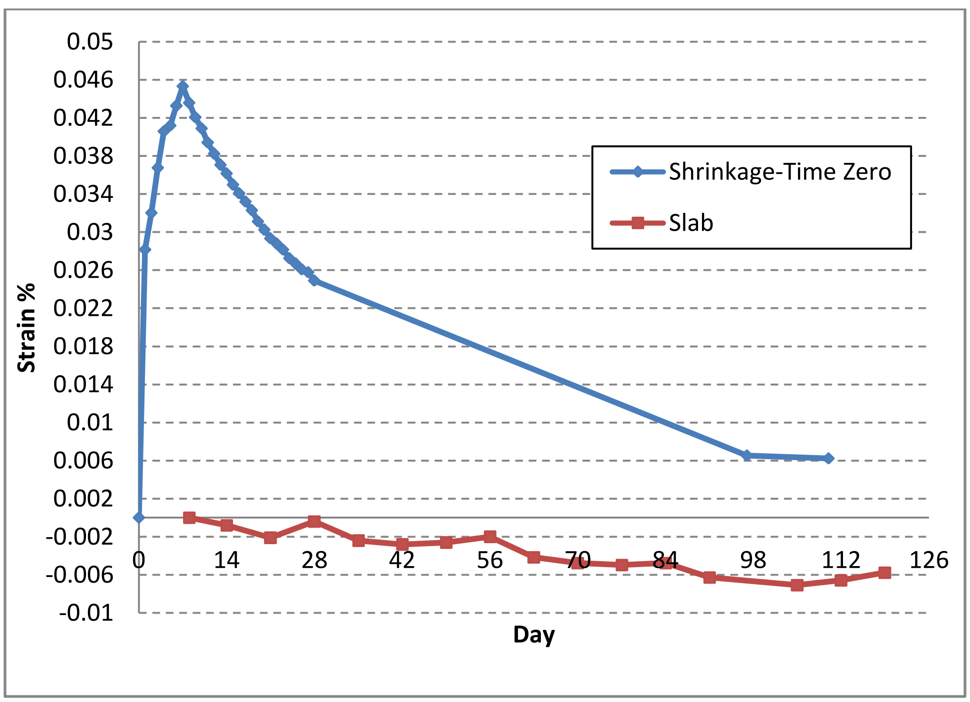

Figure 4.35 Shrinkage from time zero vs. Slab-on-Grade using CSA

CHAPTER 5

Discussion of Results

This section first analyzes the relationship between shrinkage, warping and joint opening in slabs on grade. Then, it follows a discussion of the concrete matrix effects. At the end, a discussion of additional tests results (phase IV) is presented.

Results of Phase III (Large Scale Slab)

From the data collected over 600 days at the Advanced Concrete Research lab of University of Oklahoma, the effects of shrinkage reducing admixture, shrinkage compensating concrete, high performance concrete, and conventional concrete , on shrinkage, warping and joint opening were investigated.

Tests Based on ASTM C 157 and ASTM C 878

Test results demonstrate the strain of concrete made with shrinkage compensating concrete (CSA) and concrete using shrinkage reducing admixture (SRA), suggest that strain of CSA (about 0.08%) is much greater than that for concrete using shrinkage reducing admixture (about 0.02%) (Figure 5.1). The same results can be seen from all the test specimens (expansion of CSA is much greater than other concrete mixes). Thus, it can be expected that the expansion of CSA concrete offsets the drying shrinkage at the long term and that the possibility of warping and cracking caused by drying shrinkage is reduced. Therefore, it can be concluded that CSA reduces warping of concrete slab and expansion of joint openings which are caused by drying shrinkage.

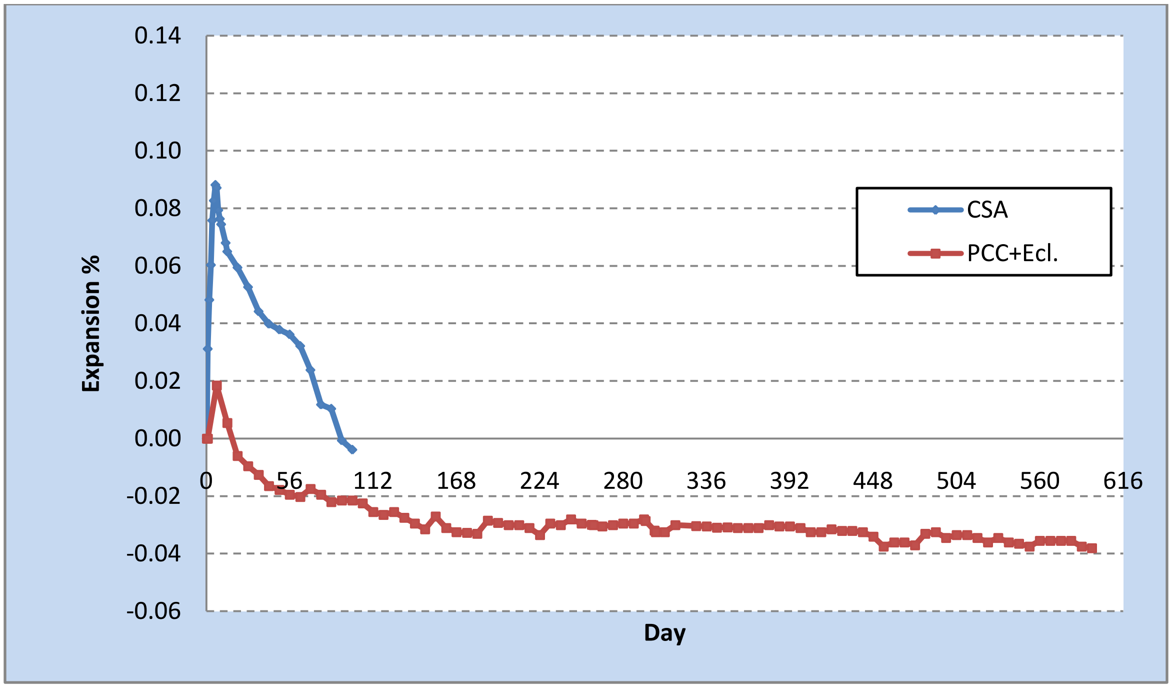

Figure 5.1 Expansion test slab using shrinkage compensating concrete vs. (PCC with Eclipse, SRA)

From ASTM C 157 test results, shrinkage reducing admixture has minimal *impact* on shrinkage at early age but not at long term. The results display that in comparison to HPC, SRA has only a minor impact on shrinkage at both short and long terms. Also, HPC showed the greatest shrinkage at both short and long terms compared to the other types of concrete mixtures used in this research. From comparison ASTM C 157 with slab test results, it can be concluded that ASTM C 157 does not match the slab on grade behavior.

Joint Opening and Surface Strain

Comparing the joint opening of shrinkage compensating cement (CSA) with that of PCC, PCC + Eclipse, PCC + Tetraguard, and HPC shows CSA has a major impact on expansion of joint openings at both short and long terms. CSA shows the smallest joint opening expansion and HPC shows the greatest joint opening expansion, which result in

CSA having the smallest shrinkage and HPC having the largest shrinkage in both short and long terms. It can be concluded that using CSA reduces warping in comparison to the other types of concrete used in this research. Also, PCC and HPC showed continuing crack growth for long term.

Interior Relative Humidity and Temperature

From the interior relative humidity of slabs, it was found that HPC has the greatest moisture gradient and slab with CSA has the least moisture gradient. Also, PCC and PCC+SRAs and RSCC moisture gradients are between CSA and HPC. This brings up two possible hypotheses. The first possible hypothesis is that the porosity of the CSA is low since it is hard for moisture to get in to the concrete from top surface of the slab and it is much easier to suck it out. Thus, the least porous material has the highest Relative Humidity at the top surface, i.e. the concrete is at equilibrium with the soil moisture for more of its depth and only a very small portion of it is drying. The second possible hypothesis is that CSA is the least porous material has the lowest Relative Humidity at the top surface i.e. the concrete is drying further into its core. These two hypotheses need further research resolve, comparing the porosity of the materials.

Phase IV Discussion

However testing specimens with shrinkage from time zero method and using CSA did not provide enough data to show the shrinkage of CSA concrete which was one of the purposes of this phase. The results from shrinkage from time zero agreed with the results from ASTM C 157 and C 878 tests. Shrinkage from time zero method shows the general trend for restrained expansion compared to the ASTM C 878 and also shows the general trend for unrestrained shrinkage when compared to ASTM C 157. In addition, shrinkage from time zero was found easier to perform in compare to the ASTM C 157 and C 878 methods.

Comparing shrinkage from time zero with slab behavior shows a poor correlation. Thus, shrinkage from time zero cannot represent the behavior of concrete slab on grade. Therefore, shrinkage from time zero cannot be used as early method to determine the behavior of the slab on grade.

CHAPTER 6

Conclusions

The main objective of this research was to perform controlled experiments to relate warping and internal strain measurements of slab strips through shrinkage from time zero, ASTM C157, and ASTM C878 drying shrinkage measurement methods, with a realistic characterization of dimensional properties for the selected concrete mixtures, CSA, PCC, HPC, SRAs, and the evaluation of their performance in slabs on grade exposed to drying conditions. The main findings from that perspective can be summarized as follows:

- Typical PCC and HPC continue to exhibit crack growth at approximately 2 years.
- Shrinkage from time zero accurately measures shrinkage when compared to ASTM C 157.
- Shrinkage from time zero follows the general trend for restrained expansion when compared to ASTM C 878.
    - The difference is due to the stiffness of the steel frame compared to the stiffness of the rod restraining the two systems.
- Shrinkage from time zero test method is easier to perform when compared to ASTM C 157 and C 878.
    - The shrinkage from time zero can accurately perform unrestrained shrinkage and restrained expansion.

- The shrinkage from time zero tests do not provide accurate results for predicting slab on grade behavior.

    - Comparing slab on grade shrinkage at mid-span with shrinkage form time zero shows significant differences in the results.

- ASTM C 157 does not provide accurate results for predicting slab behavior.

    - Comparing slab on grade shrinkage at mid-span with ASTM C 157 shows significant differences in the results.

- Based on the measured interior relative humidity of the slabs on grade, CSA are inherently less sensitive to warping than PCC or HPC.

    - CSA exhibits the lowest moisture gradient and HPC showed the greatest moisture gradient.
    - Moisture gradient causes a shrinkage gradient causes a curling moment results in warping (Carlson, 1938).

- Shrinkage compensating concrete is extremely stable, with little or no long term shrinkage, cracking or warping. This stability is noted at both early age and at approximately 2 years.

- Shrinkage reducing admixtures have a minor impact at early age but do not impact long term sectional stability.

- Shrinkage, cracking and warping are nearly similar to typical PCC but slightly better than HPC. The difference with HPC is probably due to the paste quantity in the HPC.

REFERENCES

Abdul-Wahab, H. M. S., Jaffar, A. S. (1983), "Warping of Reinforced Concrete Slabs Due to Shrinkage," ACI Journal, *Proceedings* V. 80, No. 2, pp. 109-115.

Al-Nasra, M., Wang, L. R. L. (1994), "Parametric Study of Slab-on-Grade Problems Due to Initial Warping and Point Loads," *ACI Structural Journal*, V. 91, No. 2, pp. 198-210

American Concrete Institute Committee Report (1970), Standard Practice for the Use of Shrinkage-Compensating Concrete".

American Concrete Institute Committee 223 Report (1975),"Expansive Cement Concretes-Present State of Knowledge".

American Concrete Institute (1982), "Concrete Craftsman Series: Slabs on Grade".

American Concrete Institute (1982), "Concrete Craftsman Series: Slabs on Grade, CCS-1", American Concrete Institute, Detroit, 80 pp.

American Concrete Institute 211.1-81, Revised (1984), "Standard Practice for Selecting Proportions for Normal, Heavyweight, and Mass Concrete".

American Concrete Institute Committee 302 (1989), "Guide for Concrete Floor and Slab Construction (ACI 302. IR-89)".

American Concrete Institute (1989), P.O. Box 19150, Redford Station, Detroit, MI 48219.

American Concrete Institute Committee 209 (1992), "Prediction of Creep, Shrinkage, and Temperature Effects in Concrete Structures".

American Concrete Institute Committee 360 (1992), "Design of Slabs on Grade (ACI 360R-92)," American Concrete Institute, Farmington Hills, Mich., 57 pp.

American Concrete Institute Committee 302 (1996), "Guide for Concrete Floor and Slab Construction (ACI 302. IR-96)," American Concrete Institute, Farmington Hills, Mich., 65 pp.

American Concrete Institute 224R (2001), "Control of Cracking in Concrete Structure (ACI 224R-01)".

American Concrete Institute 318 (2005), "Building Code Requirements for Structural Concrete (ACI 318-05)".

American Concrete Institute Committee 360 (2006), "Design of Slabs on Grade (ACI 360R-06)," American Concrete Institute, Farmington Hills, Mich., 74 pp.

American Society for Testing and Materials C 157-93 (1993), "Standard Test Method for Length Change of Hardened Hydraulic-Cement Mortar and Concrete".

American Society for Testing and Materials C 878-95 (1995), "Standard Test Method for Restrained Expansion of Shrinkage-Compensating Concrete".

American Society for Testing and Materials C1202 - 10 (2010), "Standard Test Method for Electrical Indication of Concrete's Ability to Resist Chloride Ion Penetration".

Annual Book of ASTM Standard (1996), Concrete and Aggregates; Sections C-33, C39, C-314, C-496, C-494, and C-494. ASTM, west Conshohocken, Pa., V. 4.02.
ASTM C 494-92 (1992), " Chemical Admixtures for Concrete".

Anon (1966), "Expansive Cement—New Approach to Reducing Concrete Cracking," *Architectural Record*, V. 140, No. 3, pp. 231-232.

Balogh, A. (1996), "New Admixture Combats Concrete Shrinkage," *Concrete Construction*.

Baron, J., Sauterey, R (1982), Le Béton Hydraulicue, Paris, Presses de l'école Nationale des Ponts et Chaussées (ENPC), 560 pp.

Bissonnette, B. (1996), "The Tensile Creep: an Important Aspect of the Problem of Concrete Repairs," *Doctoral Thesis*, Laval University, 279 pp.

Bissonnette, B., Pierre, P., and Pigeon, M. (1999), "Influence of Key Parameters on Drying Shrinkage of Cementitious Materials," *Cement and Concrete Research*, V. 29, No. 10, pp. 1655-1662.

Bissonnette, B., Attiogbe, E. K., Miltenberger, M. A., Fortin, C. (2007), "Drying Shrinkage, Curling, and Joint Opening of Slab on Ground," *ACI Materials Journal*, V. 104, No. 3.

Bondy, K. B. (2010), "Shrinkage-Compensating Concrete in Post-Tensioned Buildings," *Structure Magazine*, pp. 18-20.

Beretka, J., Sherman, N., Marroccoli, M., Pompo, A., Valenti, G.L. (1997), " Effect of Composition on the Hydration Properties of Rapid-Hardening Sulfoaluminate Cements, in: H. Justnes," *Proceedings of the 10th International Congress on the Chemistry of Cement*, Amarkai AB and Congrex, Gothenburg, Sweden, June 2-6, V. II, p.2ii029, 8 pp.

Brown, P. W., Shi, D., Skalny, J. (1991), " Porosity/Permeability Relationships," *Material Science of Concrete II, ed. Skalny, J., and Mindess, S.*, pp. 83-110.

Campbell, R. H., Harding, W., Misenheimer, E., Nicholson, L. P., Sisk, J. (1976), "Job Conditions Affect Cracking and Strength of Concrete in-Place," *ACI Journal*, American Concrete Institute.

Carlson, R. W. (1938), "Drying Shrinkage of Concrete as Affected by Many Factors," *Proceedings of the American Society for Testing and Materials*, V. 38, Part II, ASTM, West Conshohocken, Pa.

Carrier, R. E., Pu, D. C., Cady, P. D. (1975), "Moisture Distribution in Concrete Bridge Decks and Pavements," *Durability of Concrete*, SP-47, American Concrete Institute, Farmington Hills, Mich., pp. 169-192.

Cement Concrete and Aggregates (2006), "Curing of Concrete Slabs", Australia.

Chatterjee, A. K. (2002), "Special Cements, in: Bensted J., Barnes (Eds) P. ," *Structure and Performance of Cements*, E & FN Spon, London & New York, pp. 226-231.

Childs, L. D., Kapernick, J. W. (1958), "Tests of Concrete Pavements on Gravel Subbases," *Proceedings of the American Society of Civil Engineers*, V. 84, HW3.

Cohen, M. D., Mobasher, B. (1988), "Drying Shrinkage of Expansive Cements," *Journal of Materials Science*, 1988, V. 23, No. 6, pp. 1976-1980.

Cusson, D., Hoogeveen, T., Mitchell, L. (2005), "Restrained Shrinkage Testing of High Performance Concrete Modified with Structural Lightweight Aggregate", *National Research Council Canada, 7th International Symposium on Utilization of High-Strength/High Performance Concrete (Washington, D.C. June 20, 2005),* pp. 1-20.

Datasheet (2006), "Curling of Concrete Slabs," *Cement Concrete and Aggregates Australia*.

De Larrad, F., Acker, P., Le Roy, R. (1994), " Chapter 3-Shrinkage Creep and Thermal Properties" in High Performance Concrete and Applications, ed. Shah, S. P., and Ahmad, S. H., Edward Arnold, Great Britain, pp. 65-114.

Dobson, G. (1995), "Concrete Floor Slabs: Recognizing Problems before they Happen," *Concrete International*, pp. 45-47.

Duran-Herrera, A., Aitcin, P. C., Petrov, N. (2007), "Effect of Saturated Lightweight Sand Substitution on Shrinkage in 0.35 w/b Concrete," *Material Journal*, V. 104, pp. 48-52.

Fanshen, M. (2011), "Study on Effects of Admixture and Shrinkage Models on High-Performance Concrete", *Advanced Materials Research*, V. 168-170, pp. 1073-1076.

Favre, R. et al. (1983), "Fissuration et Déformations ", *Manual du Comite Ewo-International du Beton (CEB),* Ecole Polytechnique Federal de Lausanne, Switzerland, 249 pp.

Fitzpatrick, R. (1996), "Designing Durable Industrial Floor Slabs," *Concrete International*, V. 18, No. 1, pp. 38-39.

Folliard, K. J., Berke, N. S. (1997), "Properties of High-Performance Concrete Containing Shrinkage-Reducing Admixture," *Cement and Concrete Research*, V. 27, No. 9, pp. 1357-1364.

Gebler, S. H. (1982), "The Effects of High-Range Water Reducers on the Properties of Freshly Mixed and Hardened Flowing Concrete," *Research and Development Bulletin* No. RD081.01T , Portland Cement Association, Skokie, 16 pp.

Gettu, R., Roncero J. (2005), "On the Long Term Response of Concrete with a Shrinkage Reducing Admixture," *Proceedings of the International Conference on Admixtures-Enhancing Concrete Performance*, pp. 209-216.

Gilbert, R. I. (1988), "Time effects in Concrete Structures," *Elsevier Science Publishers*, Amsterdam, 321 pp.

Gilbert, R. I. (1992), "Shrinkage Cracking in Fully Restrained Concrete Members", *ACI Structural Journal*, V. 89, No. 2, pp. 141-149.

Gilbert, R. I. (2001), "Shrinkage, Cracking and Deflection-the Serviceability of Concrete Structures," *Electronical Journal of Structural Engineering*, V. 1, No. 1.

Gupta, S. M., Sehgal, V. K., Kaushik, S. K. (2009), "Shrinkage of High Strength Concrete," *World Academy of Science, Engineering and Technology 50*, pp. 264-267.

Hanson, J. A., Elstner, R. C., Clore, R. H. (1973), "Role of Shrinkage-Compensating Cement in Reduction of Cracking of Concrete," *ACI (Publ S-38)*, pp. 251-271.

Hansen, W. (1987), "Drying Shrinkage Mechanisms in Portland Cement Paste," *Journal of the American Ceramic Society*, V. 70, No. 5, pp. 323-328.

Hansen, W. (1985), "Drying Shrinkage Mechanisms in Portland Cement Paste", *Journal of the American Ceramic Society*, Department of Civil Engineering, the University of Michigan.

Harrison, P. (2003), "Looking Beyond Compressive Strength", *Concrete Producer*, V. 21, No. 5, pp. 57-59.

Hart, W. E. (1928), "The Technique Involved in Laying a Good Concrete Floor," *Engineering and Contracting*, V. 67, No. 8, pp. 393-394.

Hindy, E. E., Miao, B., Chaallal, O., and Aitcin, P. C. (1994), "Drying Shrinkage of Ready-Mixed High-Performance Concrete," *ACI Materials Journal*, V. 91, No. 3, pp. 300-305.

Holt, E. E. (2001), “Early Age Autogenous Shrinkage of Concrete”, *VTT Technical research center of Finland*.

Houst, Y. F. (1997), “Carbonation Shrinkage of Hydrated Cement Paste,” *Online Publications*.

Jeong, J. H., Zollinger, D. G. (2003), “Development of Test Methodology and Model for Evaluation of Curing Effectiveness in Concrete Pavement Construction”, *Transportation Research Record*, No. 1861, pp. 17-25.

Jeong, J. H., Zollinger, D. G. (2004), “Early-Age Curling and Warping Behavior: Insights from a Fully Instrumented Test-Slab System,” *Transportation Research Board*.

Jian- Guo, H., Pei-Yu, Y. (2006), “The Effect of Shrinkage-Reducing Admixture on Mechanical Properties and Volume Stability of Concrete”, *Key Engineering Materials*, V. 302-303, pp. 230-234.

Keene, P. W. (1961), “The Effect of Air- Entrainment of the Shrinkage of Concrete Stored in Laboratory Air,” *Magazine of Concrete Research*, V. 13, No. 38, pp. 55-60.

Keeton, J. R. (1979), “Shrinkage Compensating Cement for Airport Pavement,” *Report* No. FAA-RD-79-11, Phase 2, Federal Aviation Administration, Washington D.C.

Keith, F. R., Walker, W. W., Holland, J. A. (1996), “A Peach of a Pavement Using Shrinkage-Compensating Concrete,” *Concrete International*, V. 18, pp. 27-32.

Kesler, C. E., Seeber, K. E., Bartlett, D. L. (1973), “Behavior of Shrinkage-Compensating Concretes Suitable for Use in Bridge Decks, Interim Report, Phase I,” *T&AM Report*, No. 372, University of Illinois, Urbana, III.

Kiamco, C. (1997), “Structural Look at Slabs on Grade,” *Concrete International*, V. 19, No. 7, pp. 45-49.

Kim, S. M., Won, M. C., McCullough, B. F. (2003), “Mechanistic Modeling of Continuously Reinforced Concrete Pavement,” *ACI Structural Journal*, V. 100, No. 5, pp. 674-682.

Kosmatka, S. H., Panarese, W. C., “Design and Control of Concrete Mixtures”, 13th Edition, *Portland Cement Association*, Skokie, III, pp. 155.

Lange, D. A., Lee, C. J., Liu, Y. (2006), “Prediction of Moisture Curling of Concrete Slabs for Airfield Applications,” *ASCE*.

Lee, B. (2003), “Review of the Present Status of Optical Fiber Sensors,” *Optical Fiber Technology*, V. 9, No. 2, pp. 57-79.

Lee, P., Chui, Y. H., Smith, I., Mailvaganam, N., Pernica, G. (2002), "Prediction of Early Age Curling in Thin Topping Wood Floor Systems," *Canadian Journal of Civil Engineering*, V. 29, No. 4, pp. 622-626.

Lee, H. K., Lee, K. M., Kim, B. G. (2003), "Autogenouse Shrinkage of High-Perofrmance Concrete Containing Fly Ash," *Magazine of Concrete Research*, V. 55, No. 6, pp. 507-515.

Leonards, G. A., Harr, M. E. (1959), "Analysis of Concrete Slabs on Ground," *Journal of the Soil Mechanics and Foundations Division*, Proceedings of the American Society of Civil Engineers, pp. 35-58.

Liljestrom, W. P. (1976), "Shrinkage-Compensating Cement Concrete", *Chemically Prestressed Concrete Corporation*.

Lyse, I. (1935), "Shrinkage of Concrete, "*Proceeding of American Society for Testing and Materials*, ASTM, V. 35, pp. 383-395.

Mailvaganam, N., Springfield, J., Repette, W., Taylor, D. (2000), "Curling of Concrete Slabs on Grade," *Institute for Research in Construction*.

Mailvaganam, N. P., Wellington L., Repette, W. L., Taylor, D. A. (2002), "Curling in Concrete Floors-Causes and Repair," *The Indian Concrete Journal*.

Meininger, R. C. (1966), "Drying Shrinkage of Concrete," *Engineering Report* No. RD3 (A Summary of Joint Research Laboratory Series J-135, J-145, 173, and D-143), National Ready Mixed Concrete Association, Silver Spring, 22 pp.

Mehta, P. K. (1973), "Studies on Slump Loss in Expansive Cement Concretes," *ACI (Publ. Sp-38)*, pp. 57-68.

Mehta, P. K. (1973), "Mechanism of Expansion Associated with Ettringite Formation," Cem. Con. Res., V. 3, No. 1, pp. 1-6.

Miltenberger, M. A., Attiogbe, E. K. (2002), "Shrinkage-Based Analysis for Control-Joint-Spacing in Slabs-on-grade," *ACI Structural Journal*, V. 99, No. 3, pp. 352-359.

Nagataki, S. (1970), "Shrinkage Restraints in Concrete Pavements," *Journal of the Structural Division*, Proceedings of the American Sosiety of Civil Engineers, pp. 1333-1358.

Nassif H., Suksawang N., Mohammed M. (2003), "Effect of Curing Methods on Early-Age and Drying Shrinkage on High-Performance Concrete," *Transportation Research Record*, No. 1834, pp. 48-58.

Neal, F. A. (1996), “Concrete Industrial Ground Floors,” *ICE Design and Practice Guides*, The Institution of Civil Engineers, London, 10 pp.

Neville, A. M. (2000), “Properties of Concrete”, *Paris*, 804 pp.

Neville, A. M., Brooks, J. J. (2004). *Concrete Technology*, Prenitice Hall, Harlow.

Newberry, C. (2001), “Using Shrinkage-Reducing Admixtures to Minimize Shrinkage Cracking,” *Quality Concrete*, V. 7, No. 11-12, pp. 179-181.

Nicholson, L. P. (1981), “How to Minimize Cracking and Increase Strength of Slabs on Grade,” *Cocrete Construction*.

Nmai, C. K., Tomita, R., Hondo, F., Buffenbarger, J. (1998), “Shrinkage-Reducing Admixtures,” *Concrete International*, V. 20, No. 4, pp. 31-37.

Oldler, I. (2000), Cements Containing Calcium Sulfoaluminate, in: Bentur A., Mindess (Eds.) S., Special Inorganic Cements, E & FN Spon, London & New York, pp. 69-87.

Parrott, L. J., Hansen, W., Berger, R. L. (1980), “Effect of First Drying upon the Pore Structure of Hyrated Alite Paste,” *Cement and Concrete Research* 10[5] 647-55.

Pera, J., Ambroise, J. (2004), “New Applications of Calcium Sulfoaluminate Cement,” *Cement and Concrete Research* 34-671-676.

Perenchio, W. F. (1997), “The Drying Shrinkage Dilemma,” *Concrete Construction*.

Phelan, W. S. (2004), “Admixtures and Aggregates: Key Elements in “Athletic Concrete” Revisited”, *Concrete International*.

Phelan, W. S. (2008), “Low Shrinkage and Shrinkage Compensating Concrete Benefits,” *Structural Magazine*.

Pinkerton, J. W., Williams J., Joe, V. (1973), “Expansive Cement Concrete Paving-Taxiways,” *ACI (Publ SP-38)*, pp. 289-297.

Poppoff, M. (2008), “Standing on a Success Story”, *Concrete International*.

Portland Cement Association (1967), “Volume Changes of Concrete”.

Portland Cement Association (1983), “Concrete Floors on Ground,” 2nd Edition *Publication* No. PA 136B, Skokie, 16 pp.

Portland Cement Association (1983), “Concrete Floors on Ground,” 2nd Edition, *Publication* No. E075D, Skokie, 36 pp.

Portland Cement Association (1997), “Concrete Slab Surface Defects: Causes, Prevention, Repair,” Skokie, lll., pp. 4-5.

Powers, T. C. (1959), “Causes and Control of Volume Change,” *Journal*, PCA Research and Development Laboratories, V. 1, No. 1, pp. 29-39.

Powers, T. C. (1968), “Mechanisms of Shrinkage and Reversible Creep of Hardened Cement Paste,” *Conference Proceeding,* the Structure of Concrete and Its Behavior under Load, London.

Qi, M., Li, Z. J., Ma, B.G. (2002), “Shrinkage and Cracking Behavior of High Performance Concretes Containing Chemical Admixtures,” *Journal of Zhejinag University,* V. 3, No. 2, pp. 188-193.

Ramseyer, C. C., (1999), “Investigation of Very Early Strength Concrete with Low Shrinkage Properties”, *University of Oklahoma, Thesis,* pp. 178-179

Reiterman, R. (1996), “Why Steel Reinforcement is Needed in Concrete Slabs,” *Concrete International*.

Rixom, M. R., Waddicor, J. (1981), “Role of Lignosulfonates as Superplasticizers,” *Developments in the Use of Superplasticizers,* SP-68, American Concrete Institute, Detroit, pp. 359-379.

Rollings, R. S. (1993), “Curling Failures of Steel-Fiber-Reinforced Concrete Slabs,” *Journal of Performance of Constructed Facilities*, V. 7, No. 1, pp. 3-19.

Rubin, E. H. (1973), “Testing Agency’s Experience with Expansive Cements,” *ACI (Publ Sp-38),* pp. 341-351.

Russell, H. G. (1973), “ Design of Shrinkage-Compensating Concrete Slabs,” *ACI (Publ Sp-38),* pp. 193-226.

Schrader, E., McKinnon, R. (1989), “RCC Paving and Slabs-Deeper is Cheaper,” *Concrete International: Design and Construction*, V. 11, pp. 64-66.

Tarr, S. M., Craig, P. A., Kanare, H. M. (2006), “Concrete Slab Repair: Getting Flat is One Thing, Staying Flat is Another!” *Concrete Repair Bulletin*.

Shah, S. P., Karaguler, M. E., Sarigaphuti, M. (1992), “Effects of Shrinkage-Reducing Admixtures on Restrained Shrinkage Cracking of Concrete,” *ACI Materials Journal*, V. 89, No. 3, pp. 291-295.

Shah, S., Murphy, W. P., Weiss, W. J., Yang, W. (1997), “Shrinkage Cracking in High Performance Concrete,” *Proceeding of the PCI/FHWA International Symposium on High Performance Concrete*, pp. 148-158.

Shah, S. P., Weiss, W. J. (2000), "High Strength Concrete: Strength, Permeability, and Cracking," *Proceedings of the PCI/FHWA International Symposium on High Performance Concrete*, Orland Florida, pp. 331-340.

Shashaani, G. R., Vahman, J., Valdez, E. (2000), "24 Steps to Successful Floor Slabs", *Concrete International*, Vol. 22, No. 1, pp. 45-49.

Siddique, Z. Q., Hossain, M., Devore, J., Parcells, W. H. (2003), "Effect of Curling on As-Constructed and Early Life Smoothness of PCC Pavements," *Proceedings of the 2003 Mid-Continent Transportation Research Symposium*.

Silfwerbrand, J., Paulsson-Tralla, J. (2000), "Reducing Shrinkage Cracking and Curling in Slab-on-Grade," *Concrete International*, V. 22, No. 1, pp. 69-72.

Simms, J. F. (1996), "Expansive Cements for Crack-Resistant Concrete," *Civil Engineering (New York),* V. 36, No. 6, pp. 46-47.

Simpson, D. (2004), "Suspended Floors for Industrial Use: An Overview," *Concrete (London)*, V. 38, No. 2, pp. 16-18.

Soliman, A. M., Nehdi, M. L. (2010), "Effect of Drying Conditions on Autogenous Shrinkage in Ultra-High Performance Concrete at Early-Age," *Materials and Structures/Materiaux et Constructions*, pp. 1-21.

Spears, R. E. (1983), "The 80 Percent Solution to Inadequate Curing Problems," *Concrete International: Design & Construction*, V. 5, No. 4, pp. 15-18.

Springfield, J. (2003), "Curling of Interior Concrete Slabs-on-Grade: Cause and Repair," V. 8, No. 2, pp. 64-66.

Standards Australia, AS 1012.13 (1992), *Determination of the Drying Shrinkage of Concrete for Samples Prepared in the Field or in the Laboratory.*

Standards Australia, AS 1012.2, (1994), *Preparation of Concrete Mixes in the Laboratory*.

Standards Australia, AS 1012.16, (1996), *Determination of Creep of Concrete Cylinders in Compression.*

Standards Australia, AS 1012.8.1, (2000), *Method for making and curing Concrete-Compression and Indirect Tensile Test Specimens.*

Su, M., Kurdowski, W., Sorrentino, F. (1992), "Development in Non-Portland Cements," *Proceeding of the 9th Inernational Congress on the Chemistry of Cement*, New Delhi, India, V. 1, pp. 317-354.

Su, M., Wang, Y., Zhang, L., Li, D. (1997), Preliminary Study on Durability of Sulfo/Ferro-Aluminate Cements, in: Justnes (Ed) H., *Proceedings of the 10th International Congress on the Chemistry of Cement*, Amarkai AB and Congrex, Gothenburg, Sweden, June 2-6, Vo. IV, p. 4iv029, 12 pp.

Suprenant, B. A. (1992), "Vapor Barriers under Concrete Slabs".

Suprenant, B. A., Malisch, W. R. (1998), "Quick-Dry Concrete: A New Marker for Ready-Mix Producers," *The Concrete Producer*, pp. 330-333.

Suprenant, B. A., Malisch, W. R. (1999), "Repairing Curled Slabs," *Concrete Construction*, Copyright @ 1999 from the Aberdeen Group a Division of Hanley-Wood, Inc.

Suprenant, B. A. (2002), "Why Slabs Curl, Part I: A Look at the curling Mechanism and effect of Moisture and Shrinkage Gradients on the Amount of Curling," *Concrete International*, pp. 56-61.

Suprenant, B. A. (2002), "Why Slabs Curl, Part II: Factors Affecting the Amount of Curling," *Concrete International*, pp. 59-64.

Takahashi, T., Yamamoto, M., Loku, K., Goto, S. (1997), "Relationship Between Compressive Strength and Pore Structure of hardened Cement Paste," *Advances in Cement Research*, V. 9, No. 33, pp. 25-30.

Tremper, B., Spellman, D. L. (1963), "Shrinkage of Concrete-Comparison of Laboratory and Field Performance," *High-way Research Record No. 3*, Highway Research Board, pp. 30-61.

Troxell, G. E., Davis, H. E., Kelly, J. W. (1968), "Composition and Properties of concrete," *2nd Edition, McGrawHill Book Co. New York*, 529 pp.

Walker, W., Holland, J. A. (1999), "The First Commandment for Floor Slabs: Thou Shalt Not Curl Nor Crack… (Hopefully)," *Concrete International*, V. 21, No 1, pp. 47.

Walker, W. W., Holland, J. A. (2007), "Performance- Based Dowel Design," *Concrete Construction Magazin.*

Washa, G. W. (1955), "Volume Changes and Creep," *Significance of Tests and Properties of Concrete and Concrete Aggregates*, STP-169, ASTM, pp. 115-128.

Westergaard, H. M. (1927), "Analysis of Stresses in Concrete Roads Caused by Variations of Temperature," *Public Roads*, V.8, No. 3, pp. 54-60.

Weiss, W. J., Shah, S. P. (1997), "Recent Trends to Reduce Shrinkage Cracking in Concrete Pavements," *Proceedings of the Airfield Pavement Conference*, pp. 217-228.

Weiss, W. J., Yang, W., Shah, S. P. (1998), "Shrinkage Cracking of Restrained Concrete Slabs," *Journal of Engineering Mechanics*.

Weiss, J., Berke, N. (2003), "Early Age Cracking in Cementitious Systems", *Report of RILEM Technical Committee TC 181-EAS*, pp. 323-334.

Whiting, D. (1979), "Effects of High-Range Water Reducers on Some Properties of Fresh and Hardened Concretes," *Research and Development Bulletin* No. RD061.01T, Portland Cement Association, Skokie, 16 pp.

Wiegrink, K., Marikunte, S., Shah, S. P. (1996), "Shrinkage Cracking of High-Strength Concrete," *ACI Materials Journal*, V. 93, No. 5, pp. 409-415.

Wong, A. C. L., Childs, P. A., Terry, W., Gowripalan, N., Peng, G. (2007), "Experimental Investigation of Drying Shrinkage and Creep of Concrete Using Fiber-Optic Sensors," *Advanced in Structural Engineering*, V. 10, No. 3.

Ye, J. X, Liao, J. Q., Yang, C. H. (2009), "Influence of Fine Aggregate on Initial Shrinkage of high Performance Concrete," *Chongqing Daxue Xuebao/Journal of Chongquing University*, V. 32, No. 2, pp. 168-172.

Young, J. F. (1986), " Physical Mechanisms and Their Mathematical Descriptions," *Fourth RILEM International Symposium on Creep and Shrinkage of Concrete: Mathematical Modeling, ed. Z.P. Bazant*, pp. 44-78.

Ytterberg, R. F. (1987), "Shrinkage and Curling of Slabs on Grade: Part I-Drying Shrinkage," *Concrete International*, V. 9, pp. 22-31.

Ytterberg, R. F. (1987), "Shrinkage and Curling of Slabs on Grade: Part II-Warping and Curling," *Concrete International*, V. 9, pp. 54-61.

Ytterberg, R. F. (1987), "Shrinkage and Curling of Slabs on Grade "(Published in Three Parts), *Concrete International*, pp. 23-31; May 1987, pp. 54-61; and June 1987, pp. 72-81.

Ytterberg, R. F. (1993), "Control of Shrinkage and Curling in Slabs on Grade: Part III-How to Control Cracks," Aberdeens *Concrete International*, V. 38, pp. 42-48.

Zhang, L., Glasser, F. P. (1999), "New Concretes based on Calsium Sulfoaluminate Cement, in: R.K. Dhir, D. Dyer, T. Telford (Eds)," *Proceedings of the International Conference on Modern Concrete Materials: Binders Additions and Admixtures*, pp. 261-274.

Zhibin, Z., Lingling, X., Liang, C., Minshu, T. (2009), " Effect of Shrinkage-Reducing Admixtures on the Shrinkage and Hydration of Cement Based Materials," *American* Concrete Institute, ACI Special Publication, *9th ACI Interna*tional, No. 262 SP, pp. 309-320.

Zongjin, L., Meng, Q., Zailiang, L., Baoguo, M. (1999), "Crack width of High-Performance Concrete Due to Restrained Shrinkage," *Journal of Materials in Civil Engineering*, V. 11, No. 3, pp. 214-223.

APPENDIX A

Pre-Research (Initial) Test Results

(Phase II)

A.1. Preliminary Flow Table Tests

Table A.1 Flow table test results for PCC and CSA (type K, Komp I, and Komp II)

Cement Type	Original Diameter (in.)	Measurerd (in.)						Flow (%)
		1	2	3	4	Average		[(B-A)/A]x100
	A					B	B-A=	%
P C	4	7.95	8.50	8.50	8.15	8.28	4.28	107
Type K	4	4.80	4.70	4.60	5.20	4.83	0.83	21
Komp I	4	5.30	5.40	5.25	5.30	5.31	1.31	33
Komp II	4	5.90	5.95	5.95	6.00	5.95	1.95	49

A.2. Materials and Compressive Strength for 13 Initial Batches

Table A.2 Materials used for 13 batches

Materials per Cubic Yard	Portland Cement							Type I Cement					
	Water			2/3 Water+1/3 Ice									
	# 1	#2	#3	# 4	# 5	# 6	# 7	# 8	# 9	# 10	# 11	# 12	# 13
Komp I	100	120	140	140	140	130	120	110	100	130	120	110	100
P C	470	470	470	470	470	430	390	350	310	430	390	350	310
C. Aggregate 57	1750	1750	1750	1750	1750	1750	1750	1750	1750	1750	1750	1750	1750
Sand	1406	1361	1315	1315	1315	1315	1315	1315	1315	1315	1315	1315	1315
Water	285	295	305	335.5	323.3	296.8	270.3	243.8	217.3	308	280.5	253	225.5
MR (WRDA (oz))	47	67.6	67.6	-	-	-	-	-	-	-	-	-	-
MR (Polyheed (oz))	-	-	-	54.8	56.4	51.6	46.8	42.0	37.2	51.6	46.8	42.0	37.2
W/C ratio	0.5	0.5	0.5	0.55	0.53	0.53	0.53	0.53	0.53	0.55	0.55	0.55	0.55
Slump (in.)	2 1/4	2 3/4	3 1/4	8 1/2	9 1/6	8 3/8	7 4/7	2 1/2	1/4	7 5/6	8 3/4	3 1/4	1 3/4
Concrete Temp.											81 ºF	80 ºF	80 ºF

Table A.3 Compressive strength test results for 13 batches

Comp. Strength	#1	#2	#3	#4	#5	#6	#7	#8	#9	#10	#11	#12	#13
Day	(psi)	(psi)	(psi)	(psi)	(psi)	(psi)	(psi)	(psi)	(psi)	(psi)	(psi)	(psi)	(psi)
1	2850	2750	2350	2700	2350	2700	2700	1500	1650	1400	1900	1650	1350
3	4250	4500	4100	4100	3850	4050	4250	3000	2750	2850	3700	3300	2450
7	5050	4850	4450	5150	4800	5250	5150	4000	3700	3900	4900	4050	3600
14	5150	5400	5000	5600	5700	6050	5900	4650	5200	4950	5500	4750	4200
28	5650	6250	5650	6500	6500	6850	6650	5250	5400	5400	6200	5400	4600

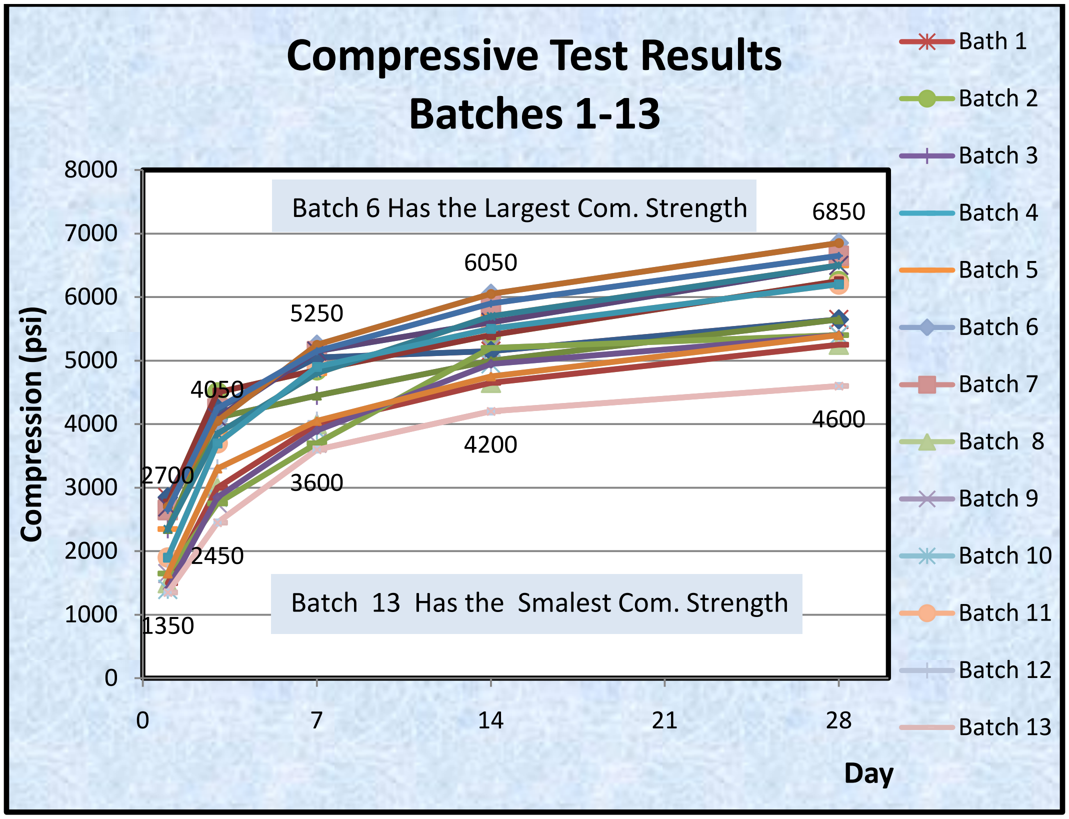

Figure A.1 Compressive Strength vs. Time for 13 initial batches

A.3. ASTM C 878 Test Results for 13 Batches

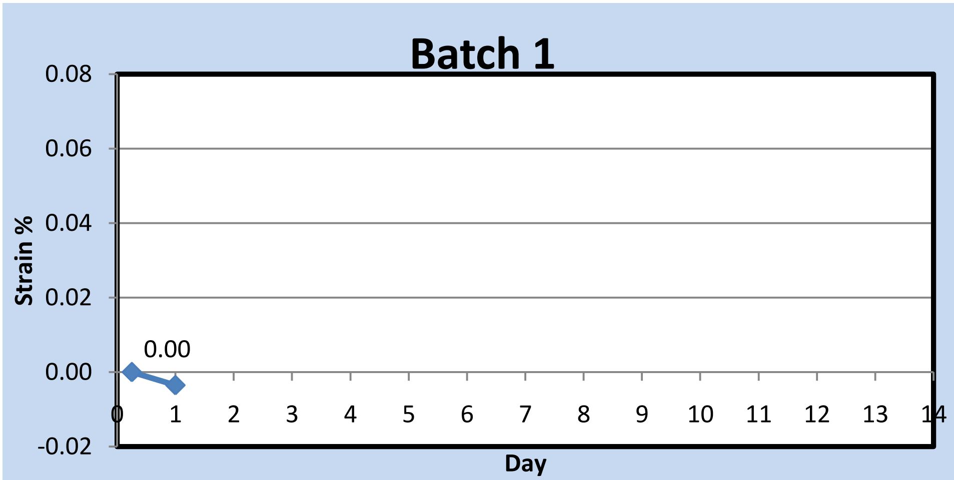

Figure A.2 ASTM C 878 Restrained Expansion vs. Time for specimen using PCC with 470 PCY cement, 100 PCY Calcium SulphoAluminate (Komp I), and 0.5 w/c ratio

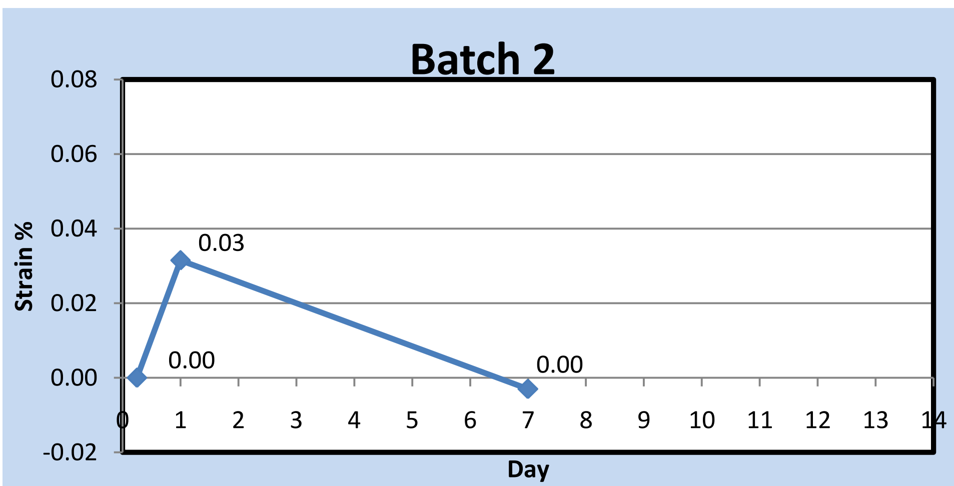

Figure A.3 ASTM C 878 Restrained Expansion vs. Time for specimen using PCC with 470 PCY cement, 120 PCY Calcium SulphoAluminate (Komp I), and 0.5 w/c ratio

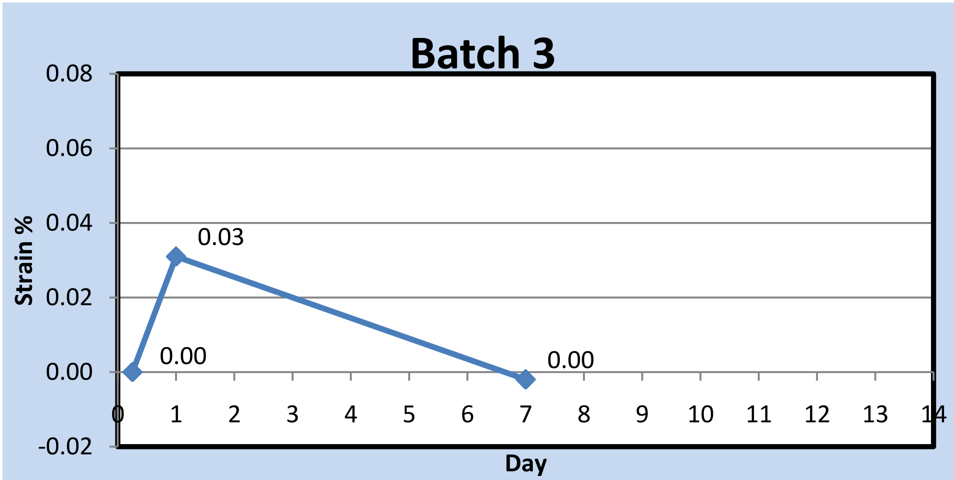

Figure A.4 ASTM C 878 Restrained Expansion vs. Time for specimen using PCC with 470 PCY cement, 140 PCY Calcium SulphoAluminate (Komp I), and 0.5 w/c ratio

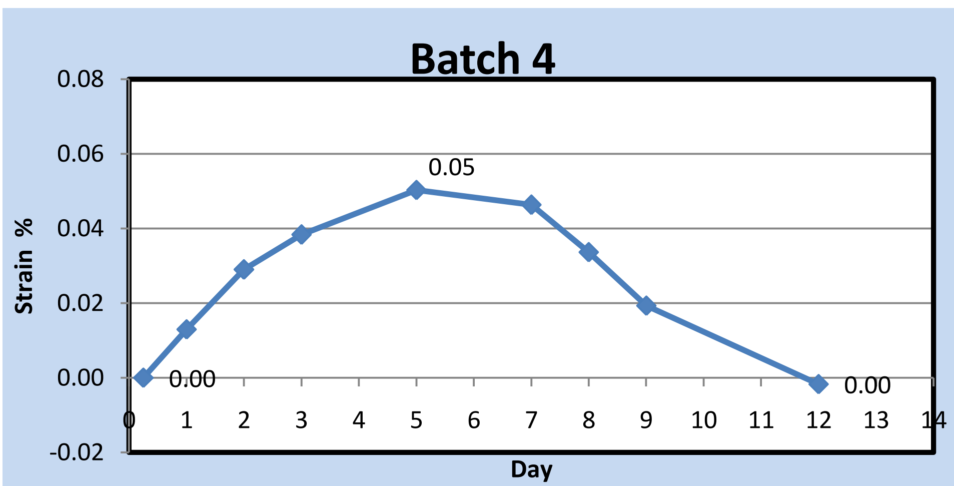

Figure A.5 ASTM C 878 Restrained Expansion vs. Time for specimen using PCC with 470 PCY cement, 140 PCY Calcium SulphoAluminate (Komp I), and 0.55 w/c ratio

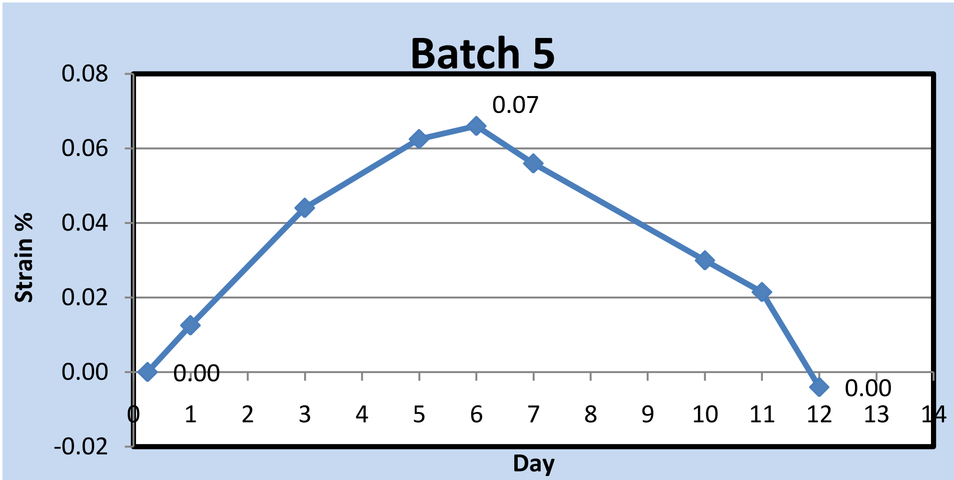

Figure A.6 ASTM C 878 Restrained Expansion vs. Time for specimen using PCC with 470 PCY cement, 140 PCY Calcium SulphoAluminate (Komp I), and 0.53 w/c ratio

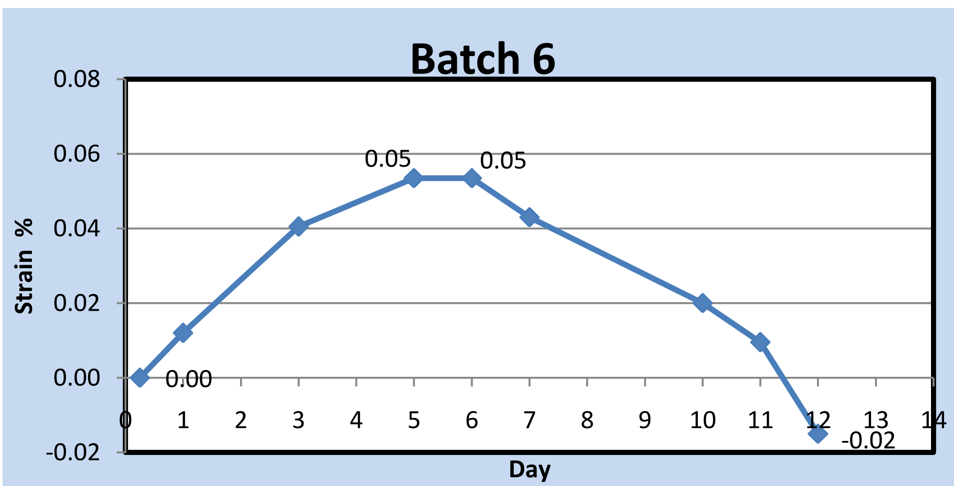

Figure A.7 ASTM C 878 Restrained Expansion vs. Time for specimen using PCC with 430 PCY cement, 130 PCY Calcium SulphoAluminate (Komp I), and 0.53 w/c ratio

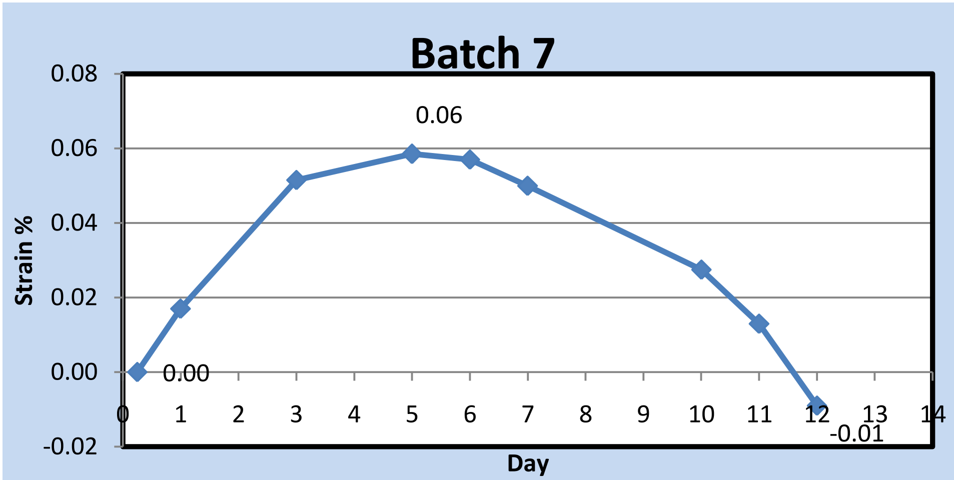

Figure A.8 ASTM C 878 Restrained Expansion vs. Time for specimen using PCC with 390 PCY cement, 120 PCY Calcium SulphoAluminate (Komp I), and 0.53 w/c ratio

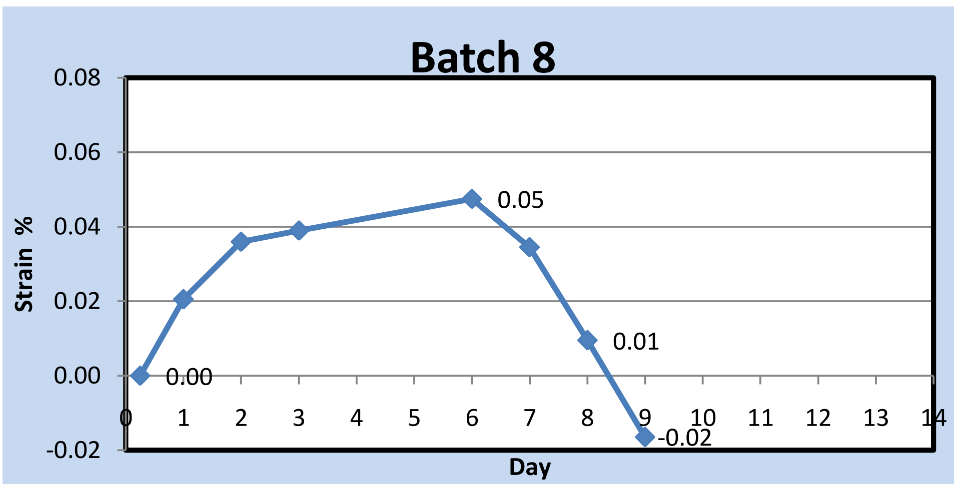

Figure A.9 ASTM C 878 Restrained Expansion vs. Time for specimen using PCC with 350 PCY cement, 110 PCY Calcium SulphoAluminate (Komp I), and 0.53 w/c ratio

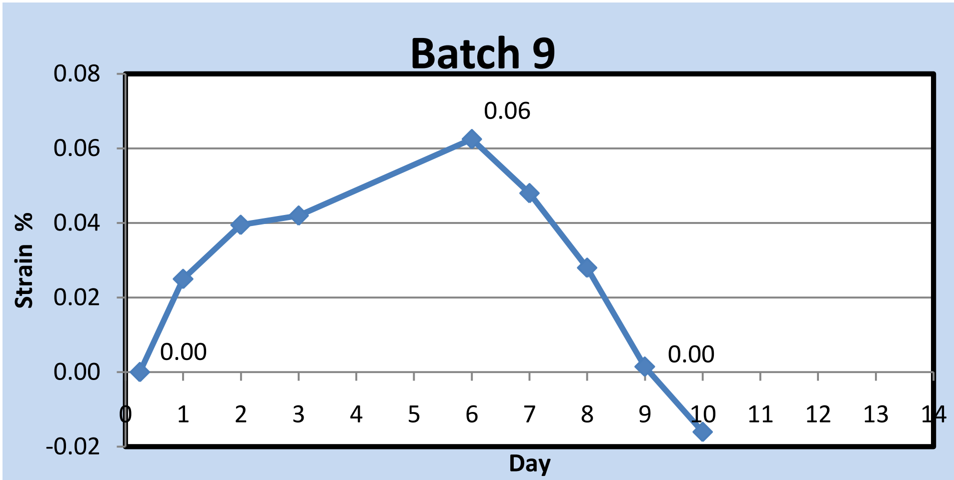

Figure A.10 ASTM C 878 Restrained Expansion vs. Time for specimen using PCC with 310 PCY cement, 100 PCY Calcium SulphoAluminate (Komp I), and 0.53 w/c ratio

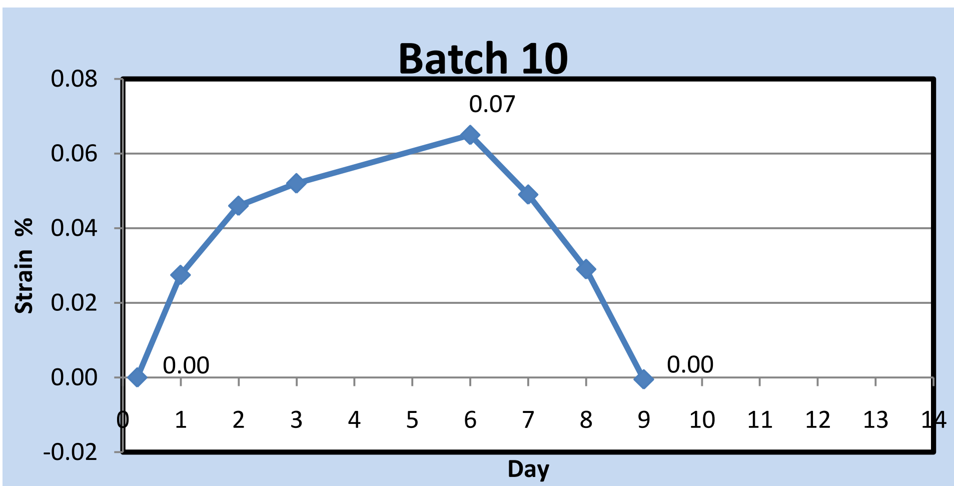

Figure A.11 ASTM C 878 Restrained Expansion vs. Time for specimen using PCC with 430 PCY cement, 130 PCY Calcium SulphoAluminate (Komp I), and 0.55 w/c ratio

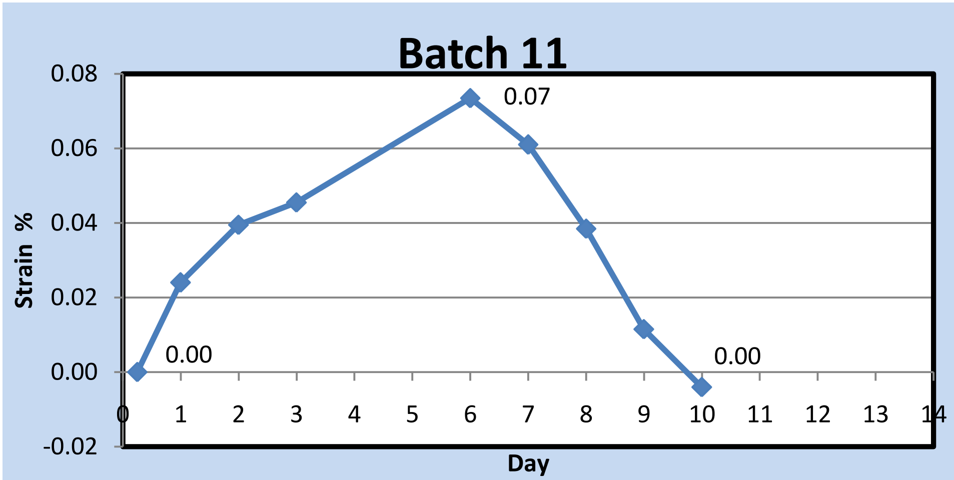

Figure A.12 ASTM C 878 Restrained Expansion vs. Time for specimen using PCC with 390 PCY cement, 120 PCY Calcium SulphoAluminate (Komp I), and 0.55 w/c ratio

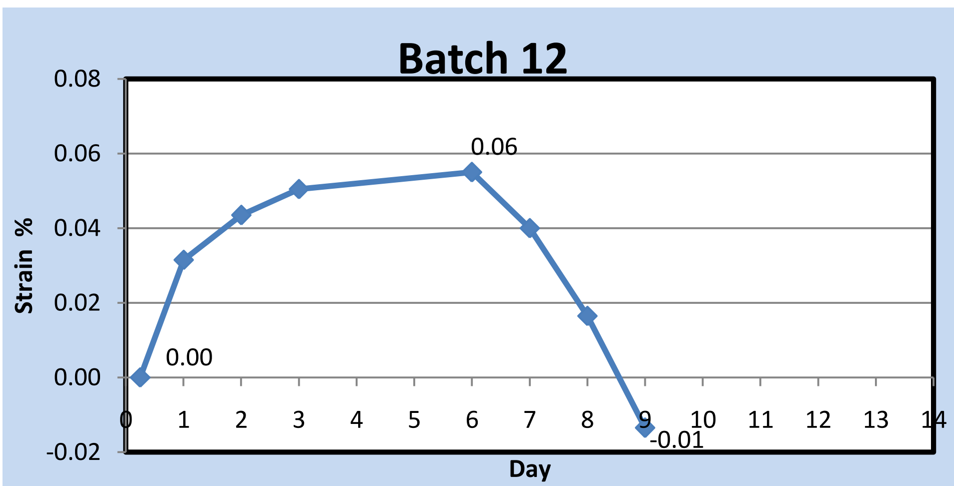

Figure A.13 ASTM C 878 Restrained Expansion vs. Time for specimen using PCC with 350 PCY cement, 110 PCY Calcium SulphoAluminate (Komp I), and 0.55 w/c ratio

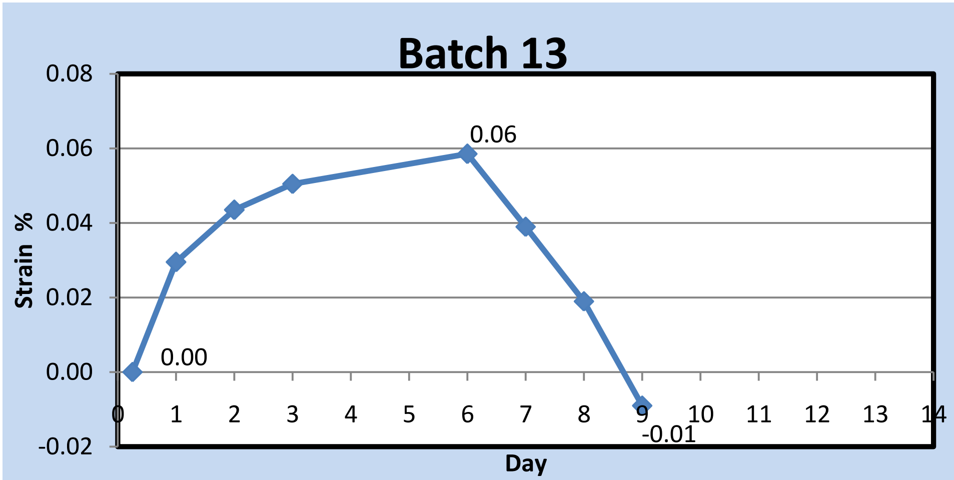

Figure A.14 ASTM C 878 Restrained Expansion vs. Time for specimen using PCC with 310 PCY cement, 100 PCY Calcium SulphoAluminate (Komp I), and 0.55 w/c ratio

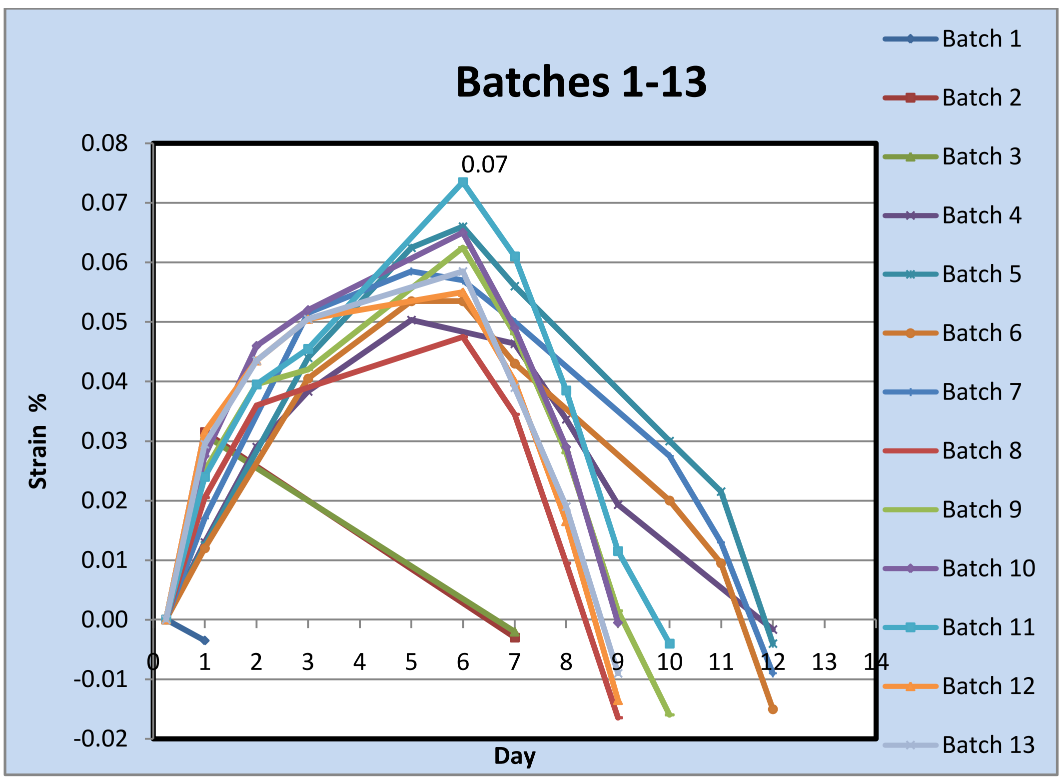

Figure A.15 ASTM C 878 Restrained Expansion vs. Time for all 13 initial tests

Tables (A.2 and A.3) and graphs (A.1 to A.15) show that batch 11 has an acceptable slump and higher expansion (0.07 %) in compare to the other batches. The results from batch 12 are very close to batch 11 with smaller slump. Batch 10 has results close to batch 11 and 12 with using more Portland cement and CSA (Komp I). Thus, batch 11 and 12 with using less Portland cement and Komp I make the mix design more economical than batch 10 with the same results. Therefore, the mix for the large scale slab specimens made with CSA (komp I) was designed based on the materials used for batches 11 and 12.

APPENDIX B

Large Scale Slab on Grade Test Results

(Phase III and V)

B.1. Materials

Table B.1 Materials used for 7 large scale slab specimens

Materials (per cubic yard)	SRA#1	SRA#2	PCC	HPC	CTS Shrinkage Compensating Cement		Rapid Set
					#1	#2	
Komp I	-	-	-	-	120	120	-
P C	356	355	355	543	370	370	-
Flyash	88	88	88	180	-	-	-
Rapid Set Cement	-	-	-	-	-	-	658
Citric Acid	-	-	-	-	-	-	5
Course Aggregate 57	1850	1850	1850	1850	1750	1750	1772
Sand	1463	1463	1463	1196	1315	1315	1307
Water	266	266	266	264	270	272	290
MR (Polyheed 1020 (oz))	-	-	-	-	64	64.6	52.6
MR (Pozzolith 80 (oz))	13	14	14	29	-	-	-
Eclipse (oz)	128	-	-	-	-	-	-
Tetraguard (oz)	-	128	-	-	-	-	-
W/C ratio	0.60	0.60	0.60	0.37	0.55	0.55	0.44

B.2. Slab Specimens Using PCC+Eclipse (SRA)

B.2.1. Compressive Strength

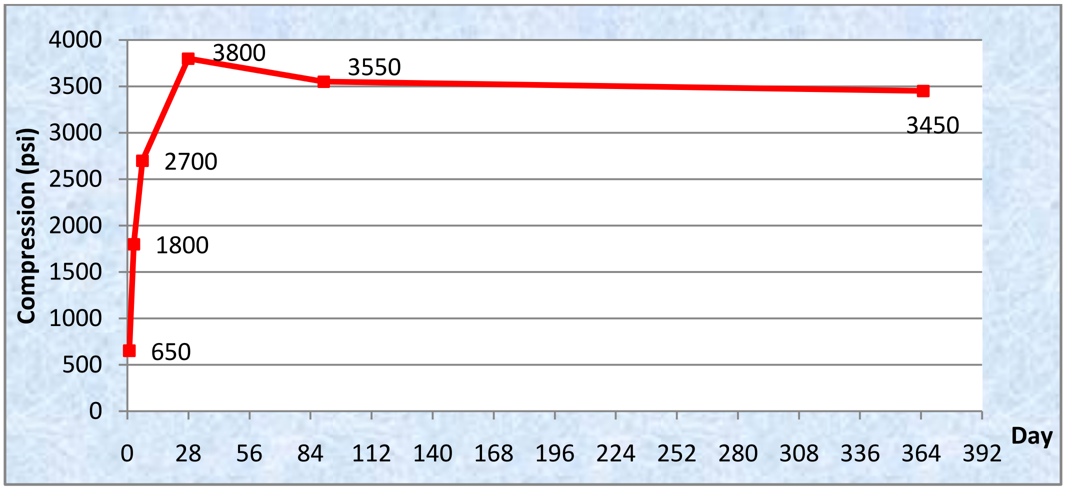

Figure B.1 Compressive Strength vs. Time for slab using PCC with Eclipse

B.2.2. Material Characterization ASTM C 157 Test Results

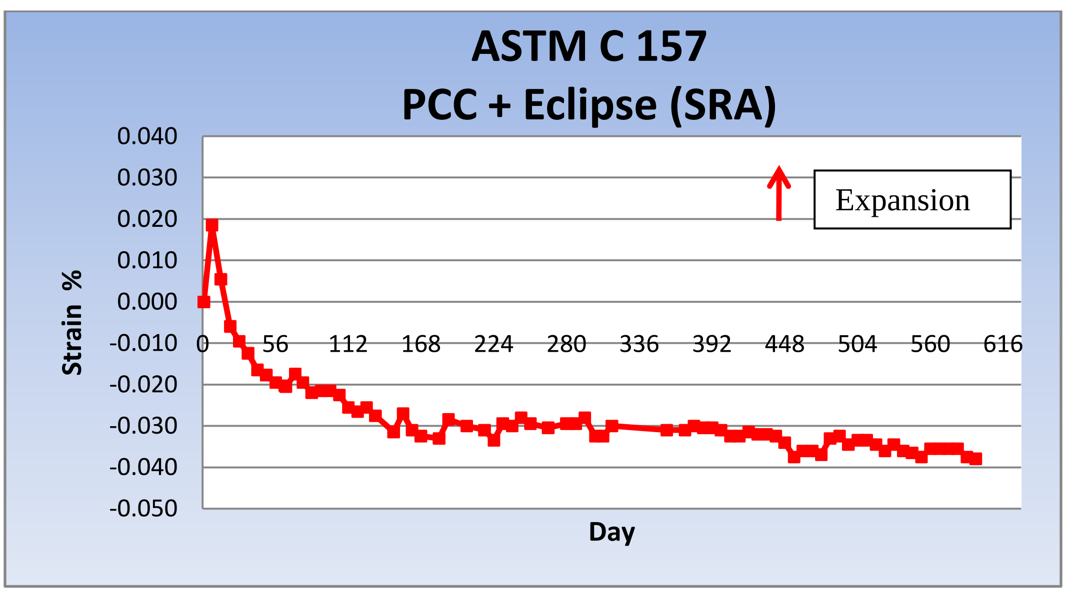

Figure B.2 ASTM C 157 Unrestrained Expansion vs. Time for slab using PCC with Eclipse

B.2.3. Behavior of Slab on Grade

B.2.3.1. Strain at Control Joints and Mid-Span

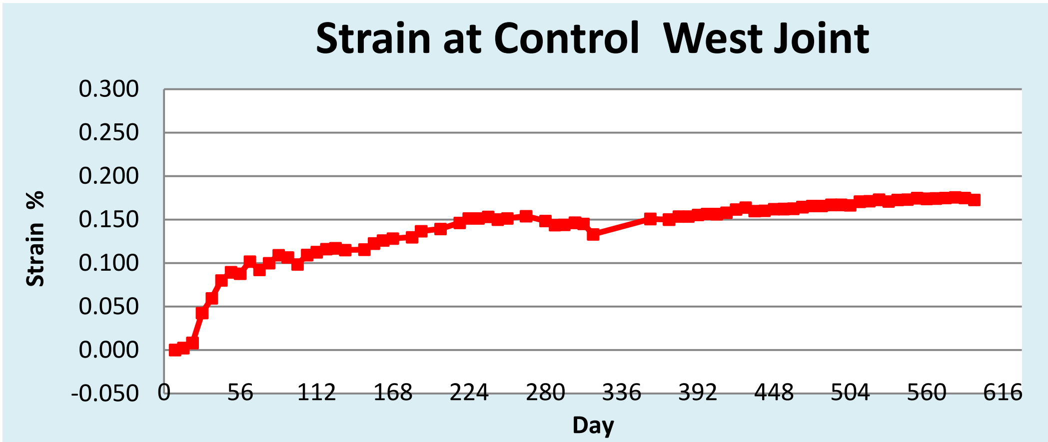

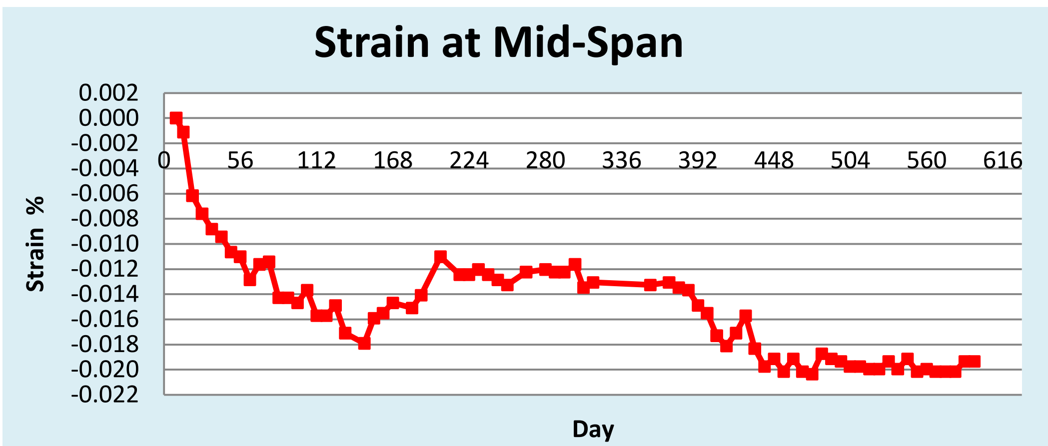

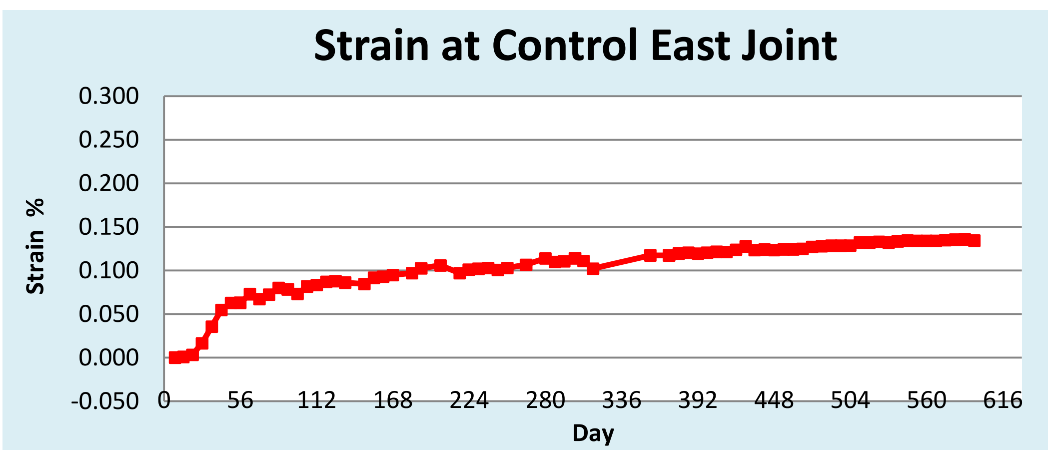

B.3 Strain at Control Joints and Mid-Span of Slab vs. Time for slab using PCC+Eclipse

B.2.3.2. Expansion or Crack at West and East Joint Openings

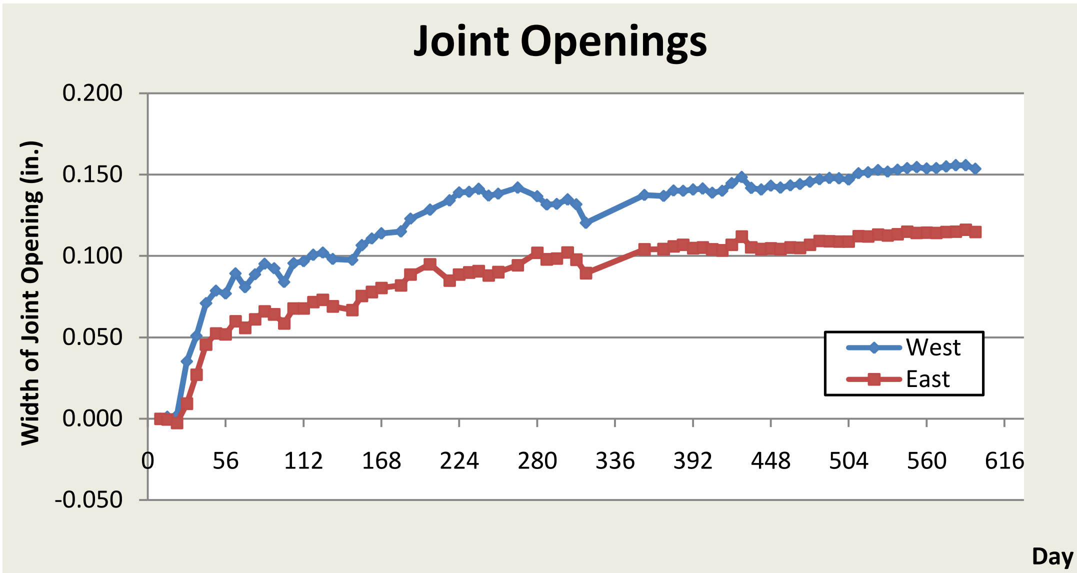

B.4 Width of Joint Openings at West and East Sides vs. Time for slab using PCC+ Eclipse

Note: shrinkage reducing admixture (Eclipse) delays crack only for few days.

B.3. Slab Specimens Using PCC+Tetraguard (SRA)

B.3.1. Compressive Strength

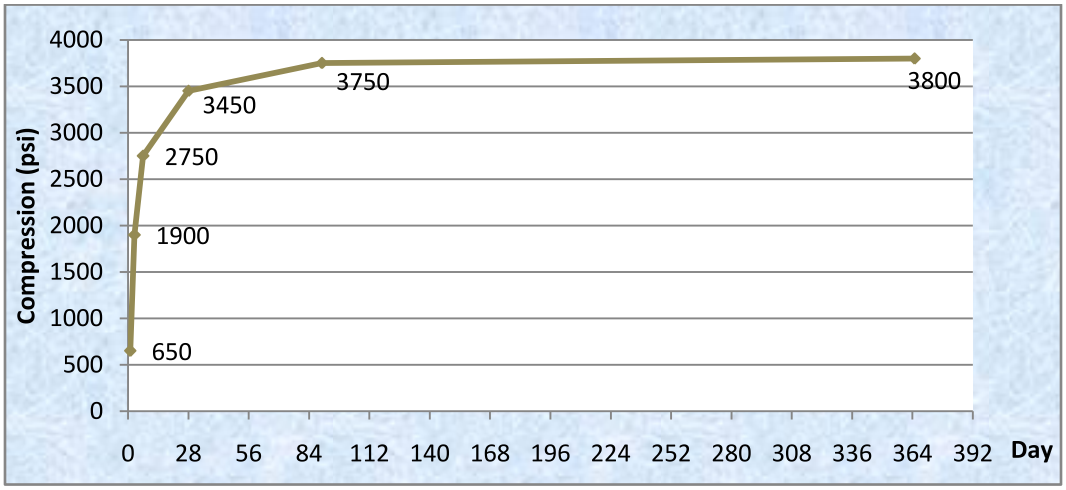

Figure B.5 Compressive Strength vs. Time for slab using PCC with Tetraguard

B.3.2. Behavior of Slab on Grade

B.3.2.1. Strain at Control Joints and Mid-Span

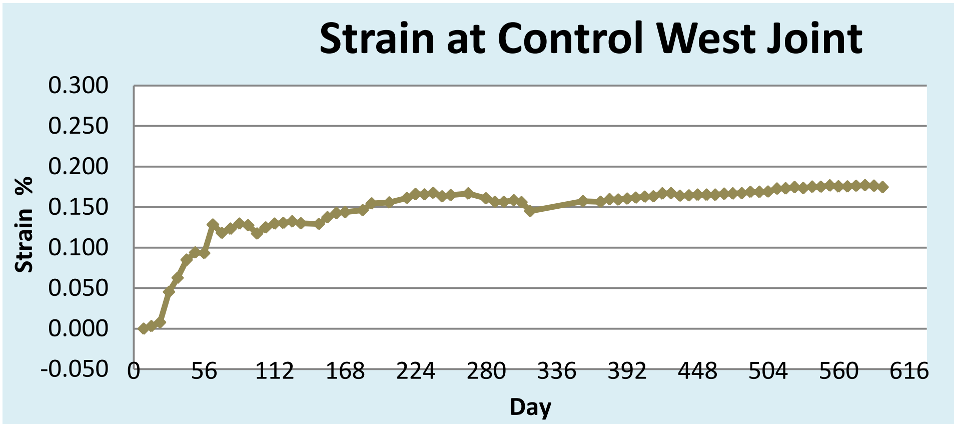

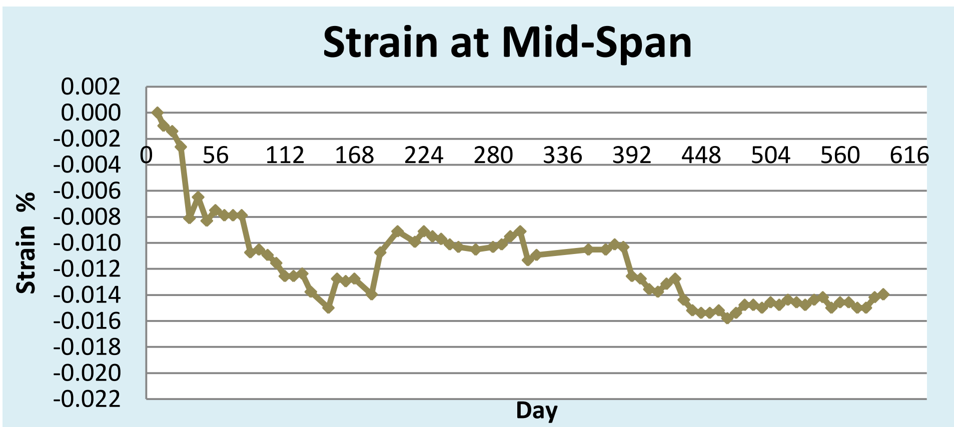

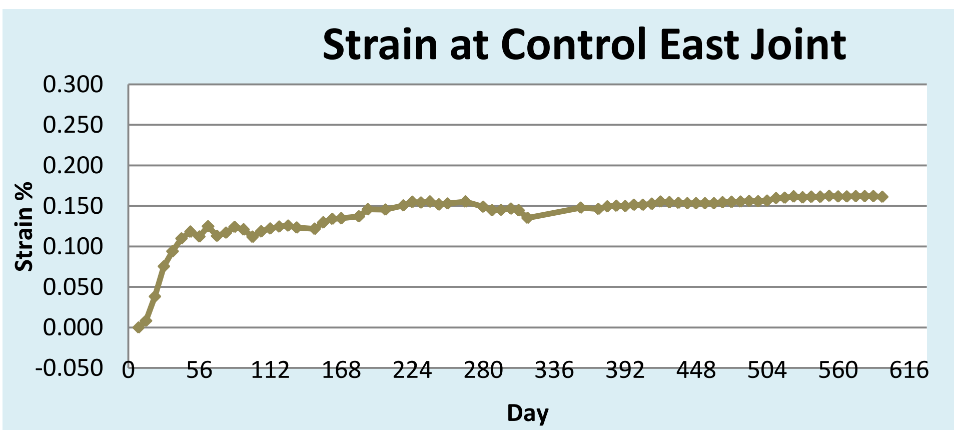

B.6 Strain at Control Joints and Mid-Span of Slab vs. Time for slab using PCC+Tetraguard

B.3.2.2. Expansion or Crack at West and East Joint openings

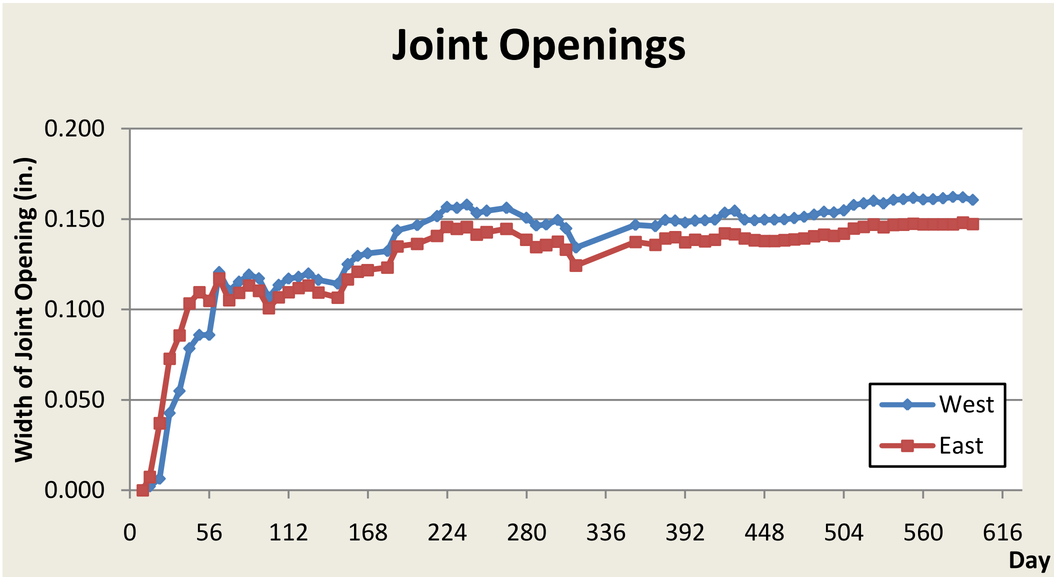

B.7 Width of Joint Openings at West and East Sides vs. Time for slab using PCC+ Tetraguard

Note: Shrinkage reducing admixture (Tetraguard) delays crack only for few days.

B.4. Slab Specimens Using PCC

B.4.1. Compressive Strength

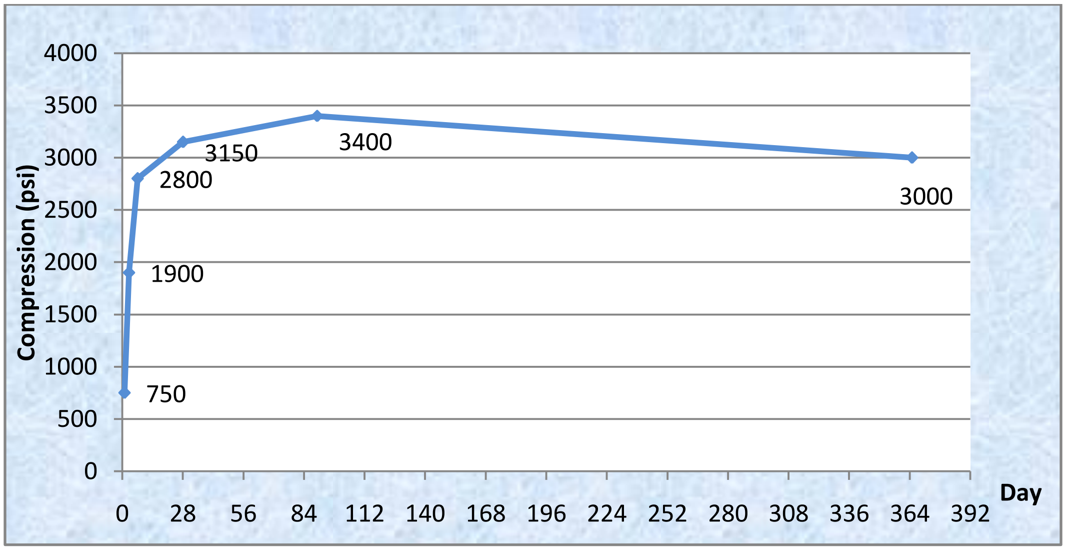

Figure B.8 Compressive Strength vs. Time for slab using PCC

B.4.2. Material Characterization ASTM C 157 Test Results

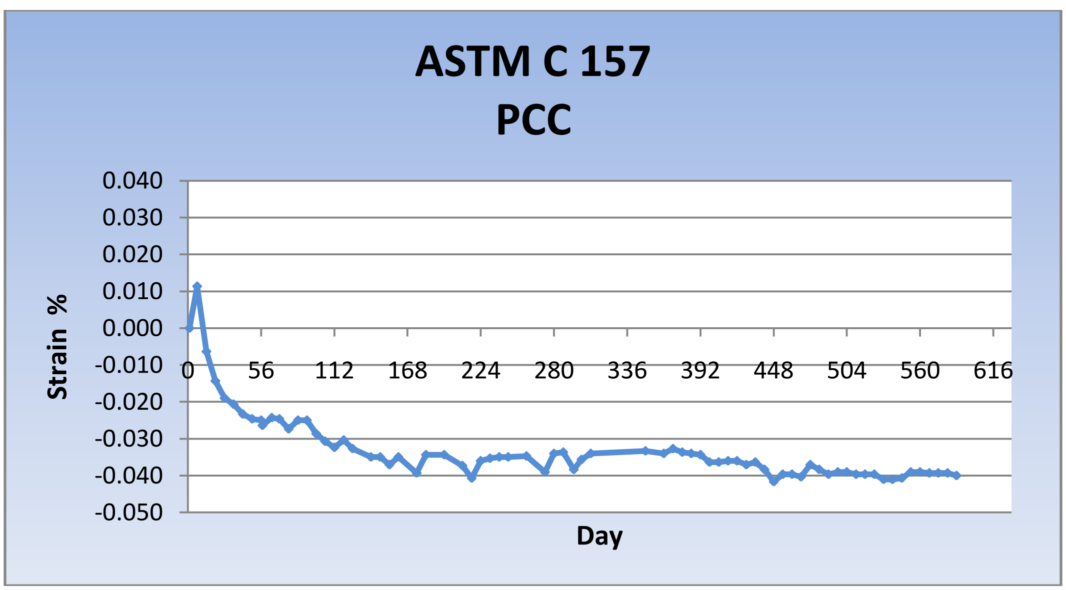

Figure B.9 ASTM C 157 Unrestrained Expansion vs. Time for slab using PCC with 355 PCY cement and 0.60 w/c ratio

B.4.3. Behavior of Slab on Grade

B.4.3.1. Strain at Control Joints and Mid-Span

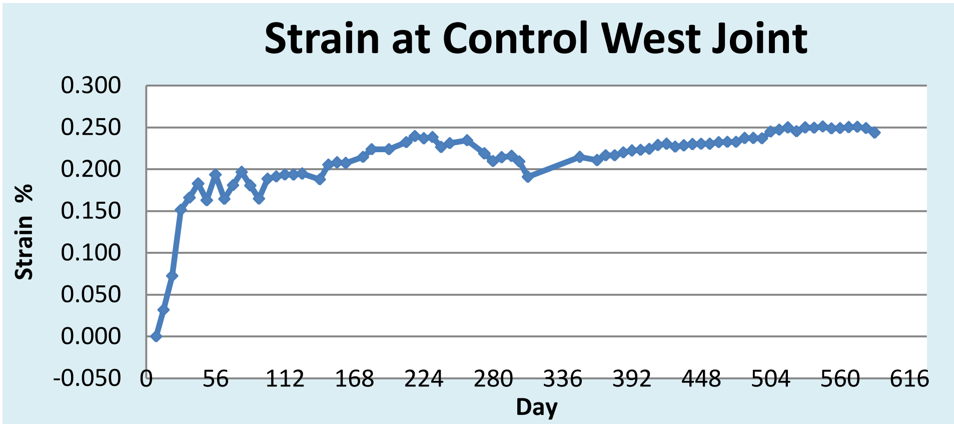

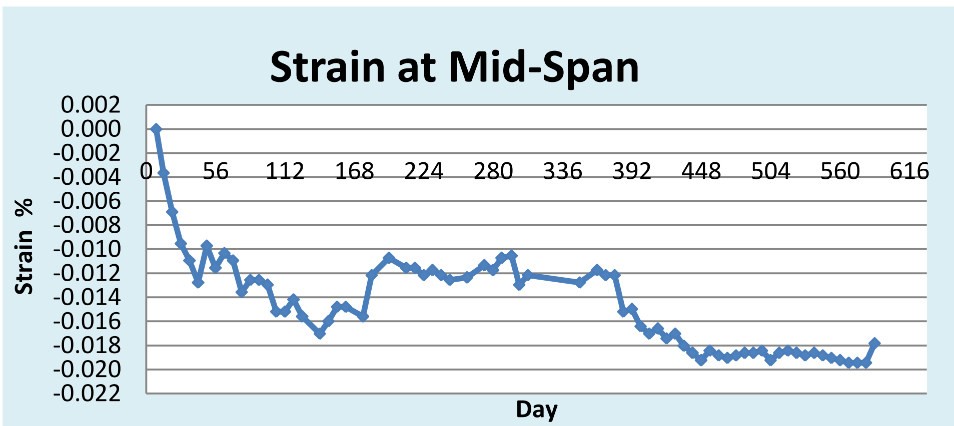

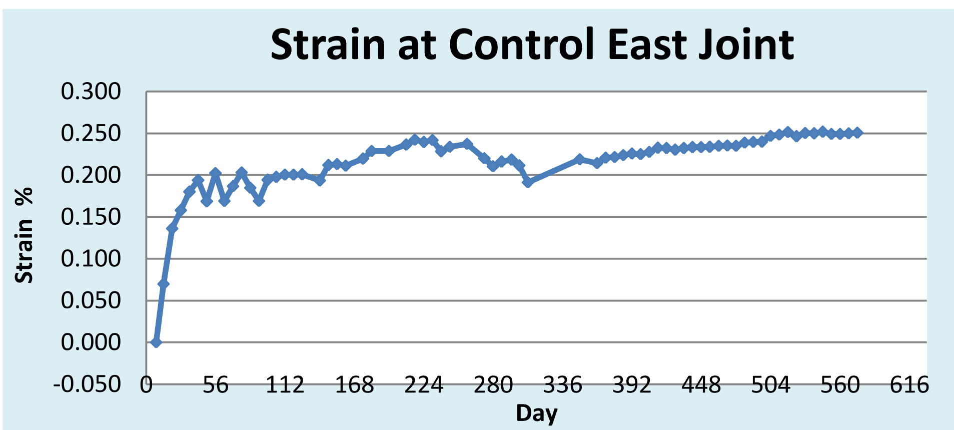

B.10 Strain at Control Joints and Mid-Span of Slab vs. Time for slab using PCC with 355 PCY cement and 0.60 w/c ratio

B.4.3.2. Expansion or Crack at West and East Joint openings

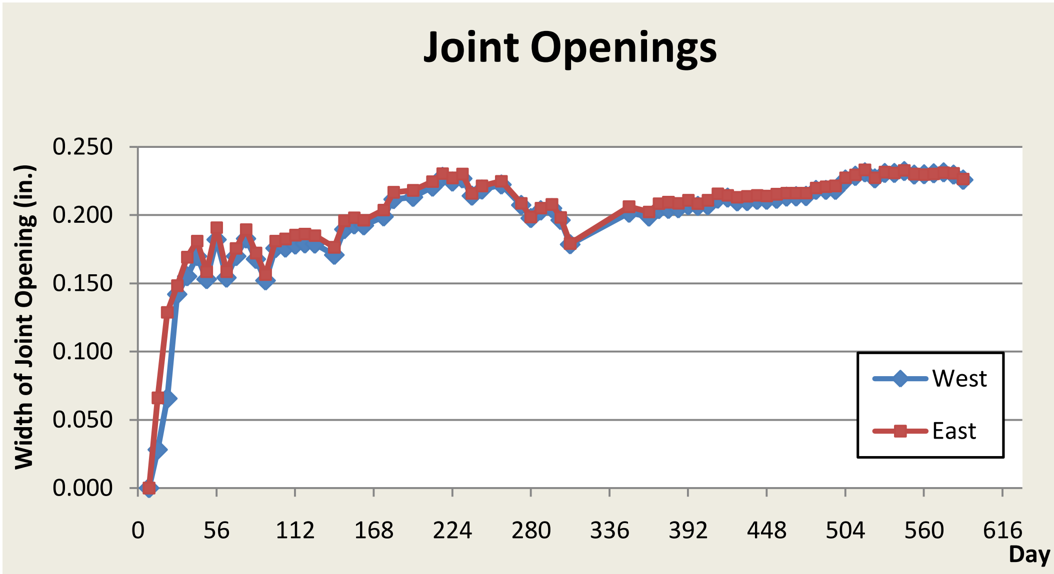

B.11 Width of Joint Openings at West and East Sides vs. Time for slab using PCC with 355 PCY cement and 0.60 w/c ratio

B.5. Slab Specimens Using HPC

B.5.1. Compressive Strength

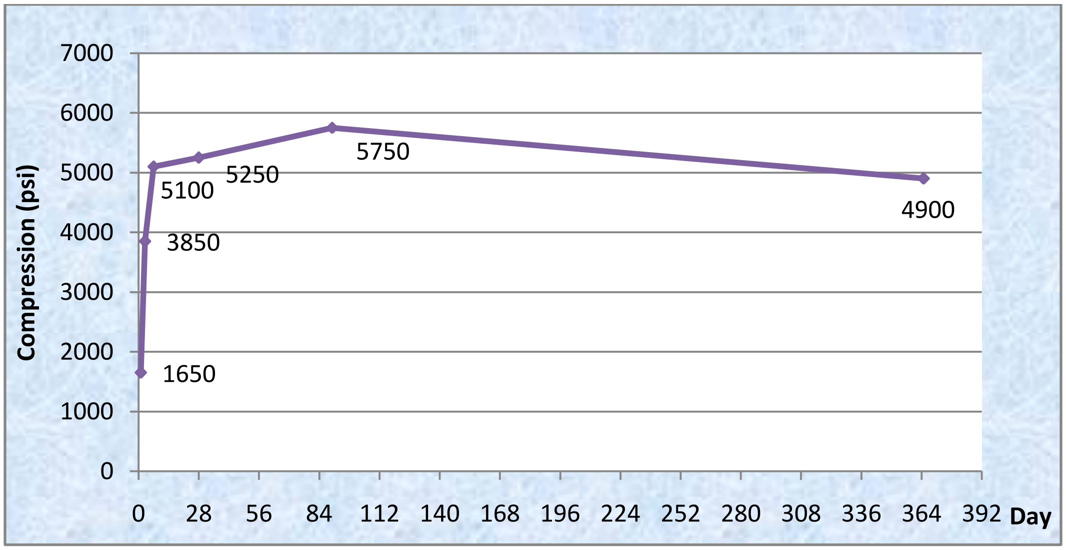

Figure B.12 Compressive Strength vs. Time for slab using HPC

B.5.2. Material Characterization ASTM C 157 Test Results

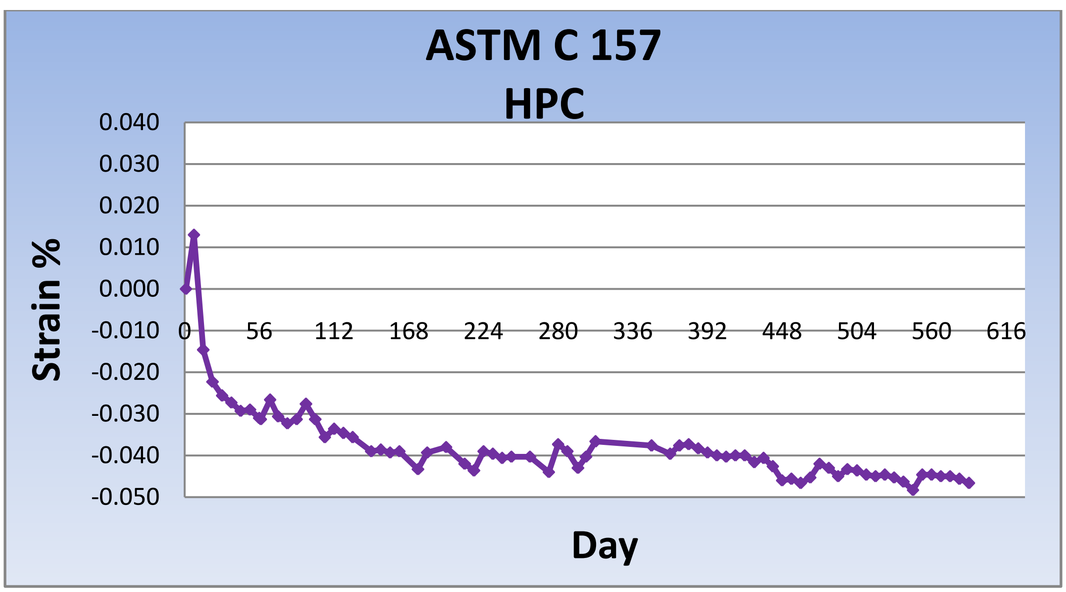

Figure B.13 ASTM C 157 Unrestrained Expansion vs. Time for slab using HPC with 543 PCY cement and 0.37 w/c ratio

B.5.3. Behavior of Slab on Grade

B.5.3.1. Strain at Control Joints and Mid-Span

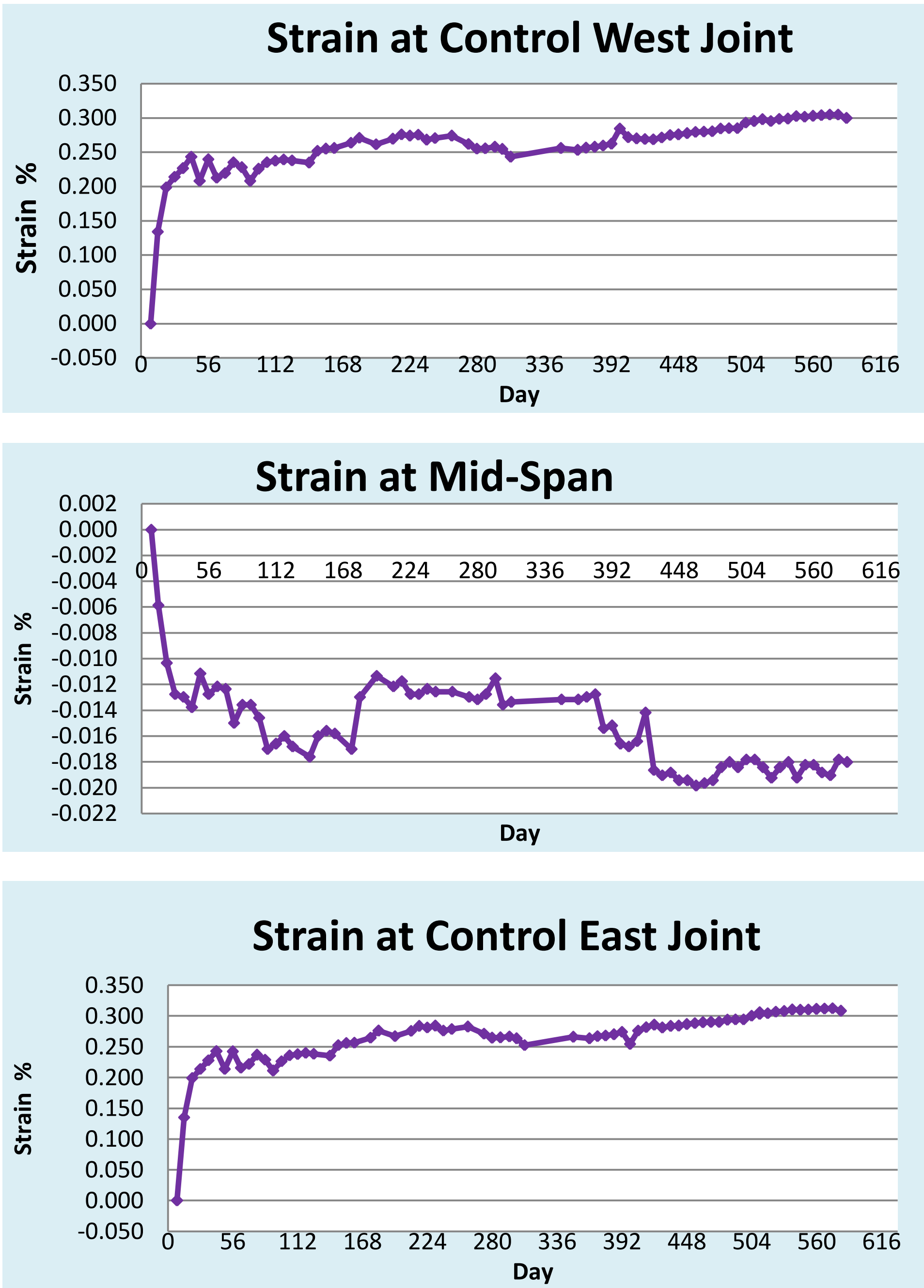

B.14 Strain at Control Joints and Mid-Span of Slab vs. Time for slab using HPC with 543 PCY cement and 0.37 w/c ratio

B.5.3.2. Expansion or Crack at West and East Joint openings

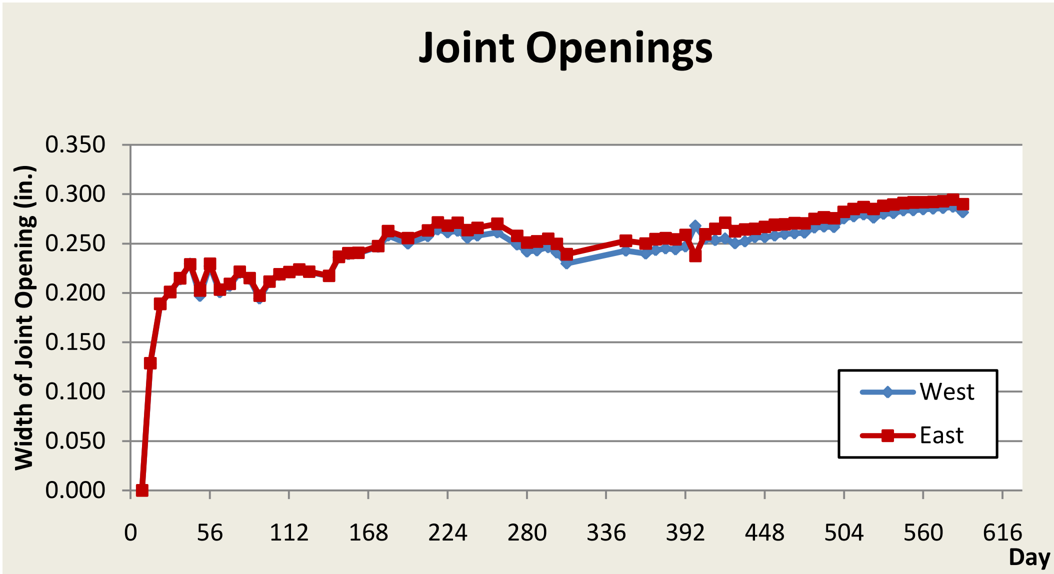

B.15 Width of Joint Openings at West and East Sides vs. Time for slab using HPC with 543 PCY cement and 0.37 w/c ratio

B.6. Slab Specimens Using CSA

Note: Two slabs have similar concrete mix using CSA, Komp I.

B.6.1. Compressive Strength

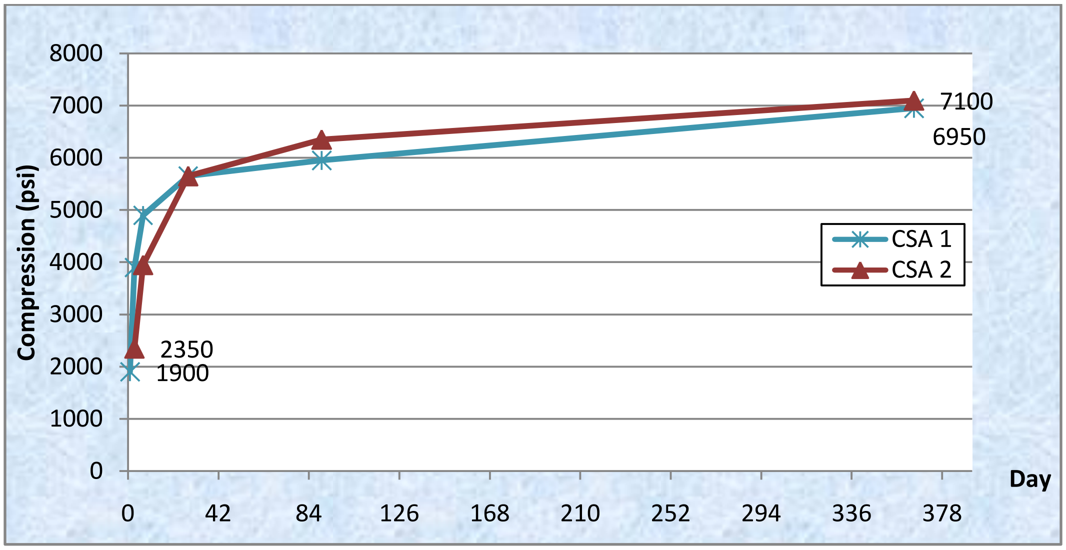

Figure B.16 Compressive Strength vs. Time for two slabs using CSA

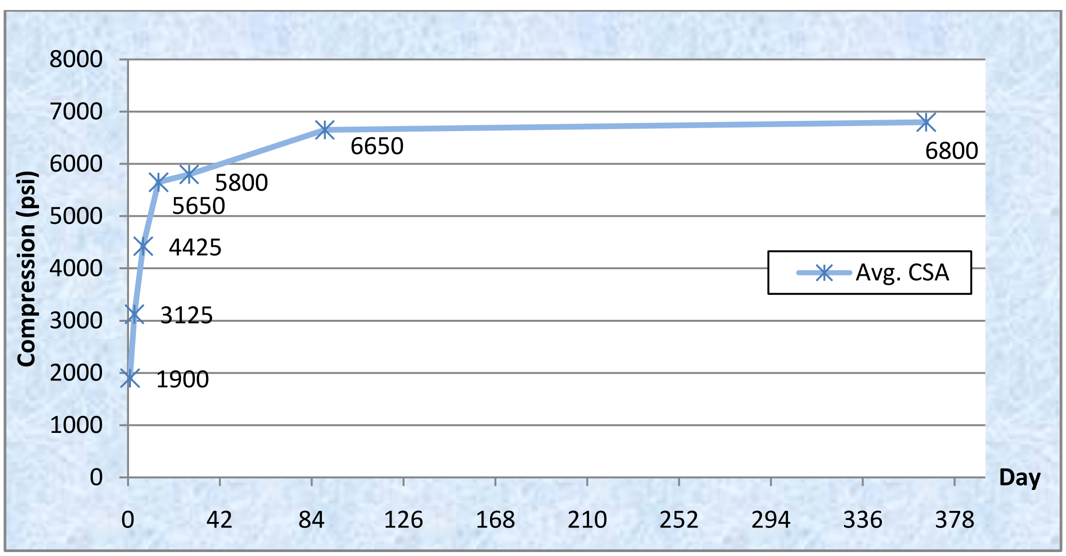

Figure B.17 Average Compressive Strength vs. Time for slabs using CSA

B.6.2. Material Characterization ASTM C 878 Test Results

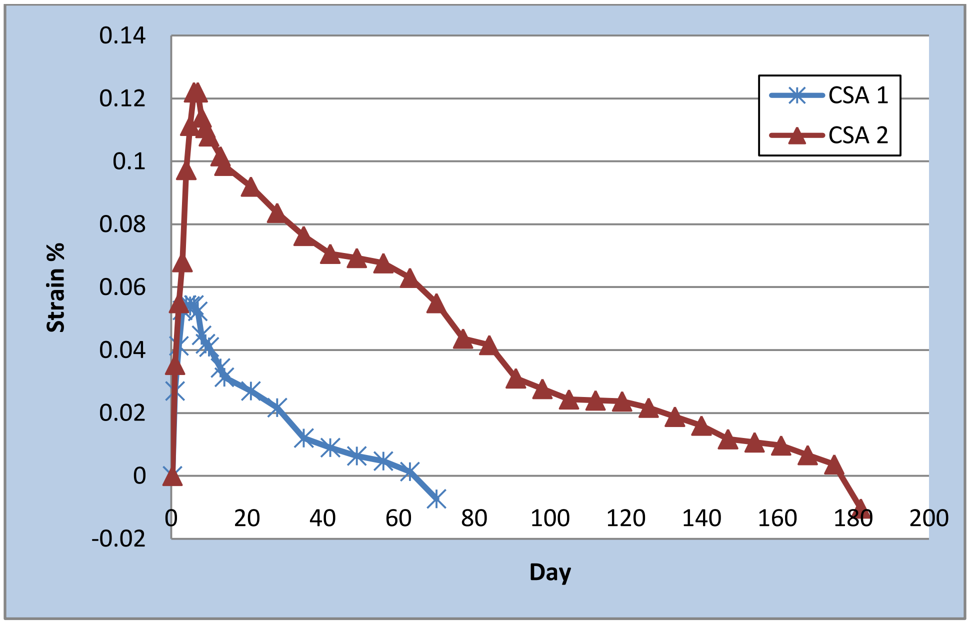

Figure B.18 ASTM C 878 Restrained Expansion vs. Time for Two slabs made with CSA

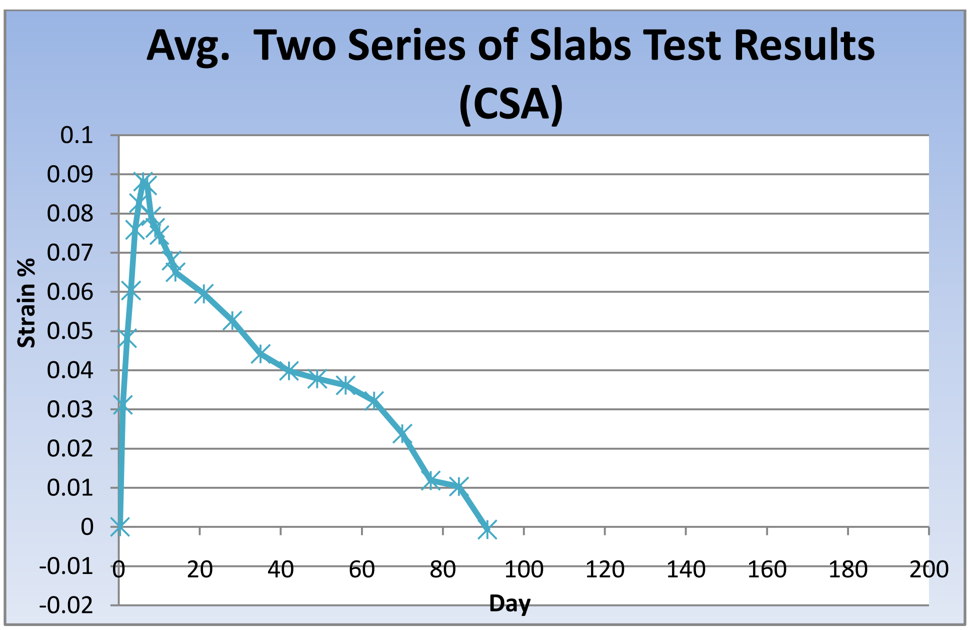

Figure B.19 ASTM C 878 Restrained Expansion vs. Time for slab using shrinkage compensating concrete (CSA), Komp I

B.6.3. Behavior of Slab on Grade

B.6.3.1. Strain at Control Joints and Mid-Span

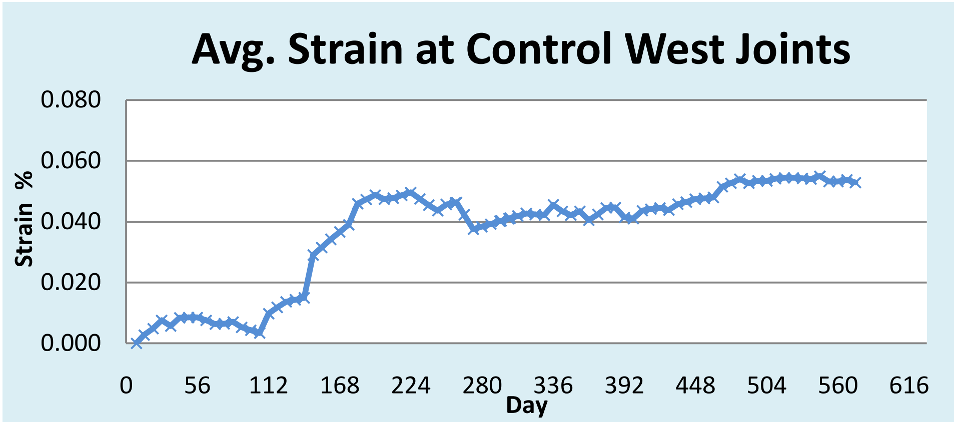

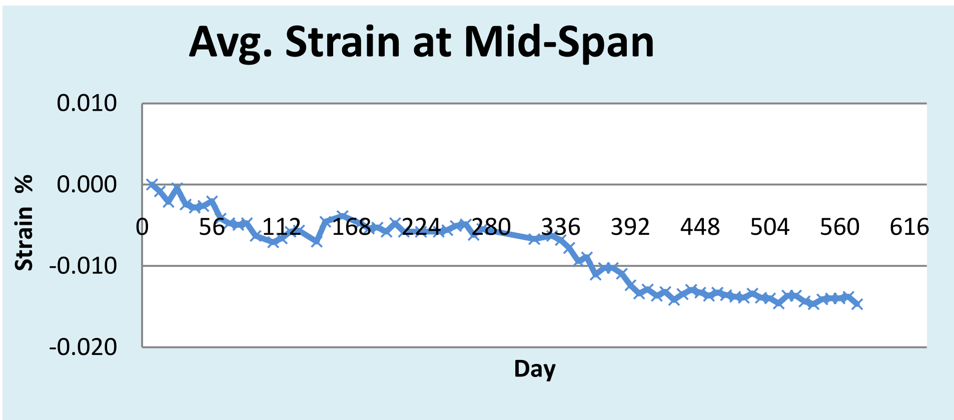

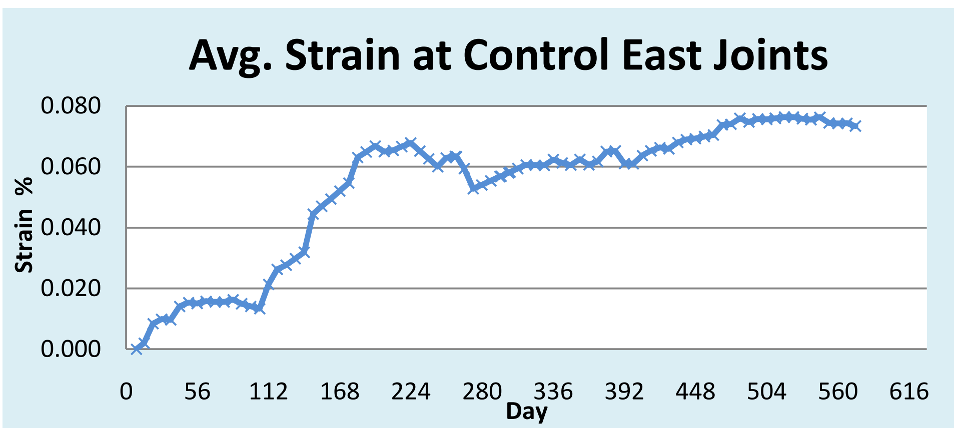

B.20 Strain at Control Joints and Mid-Span of Slab vs. Time for slab using CSA

B.6.3.2. Expansion or Crack at West and East Joint openings

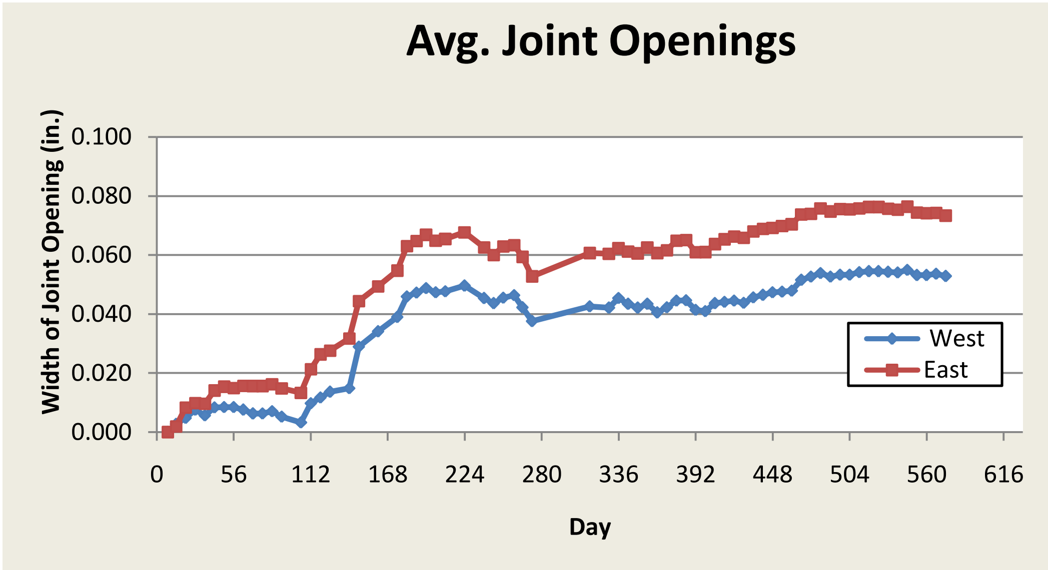

B.21 Width of Joint Openings at West and East Sides vs. Time for slab using CSA

Note: The average results for two slabs using CSA are used for the comparison with the other concrete slab results.

B.7. Slab Specimens Using RSCC

B.7.1. Compressive Strength

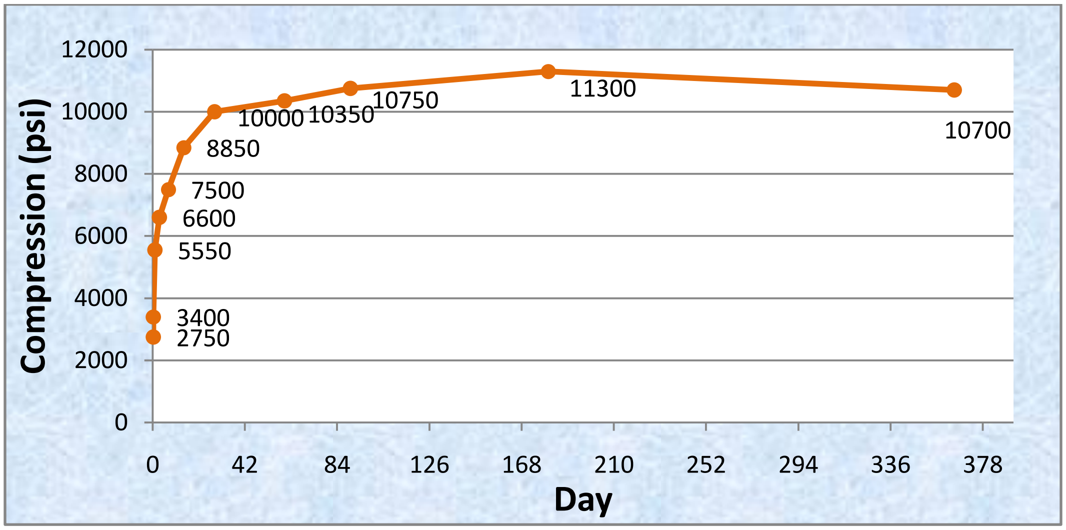

Figure B.22 Compressive Strength vs. Time for slab using RSCC

B.7.2. Material characterization ASTM C 878 Test Results

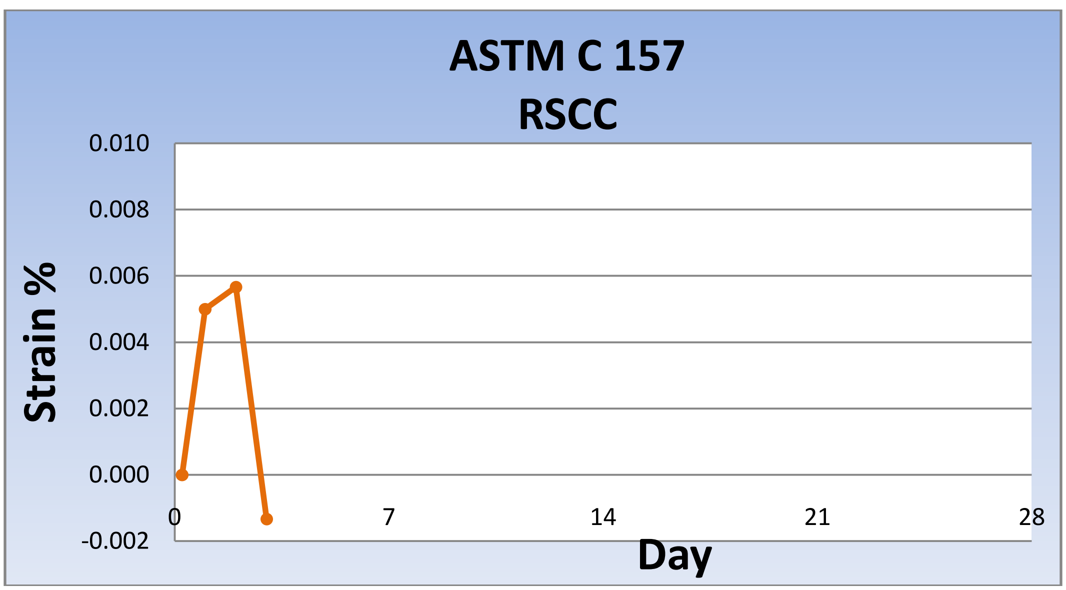

Figure B.23 ASTM C 878 Restrained Expansion vs. Time for slab using rapid set cement concrete

B.7.3. Behavior of Slab on Grade

B.7.3.1. Strain at Control Joints and Mid-Span

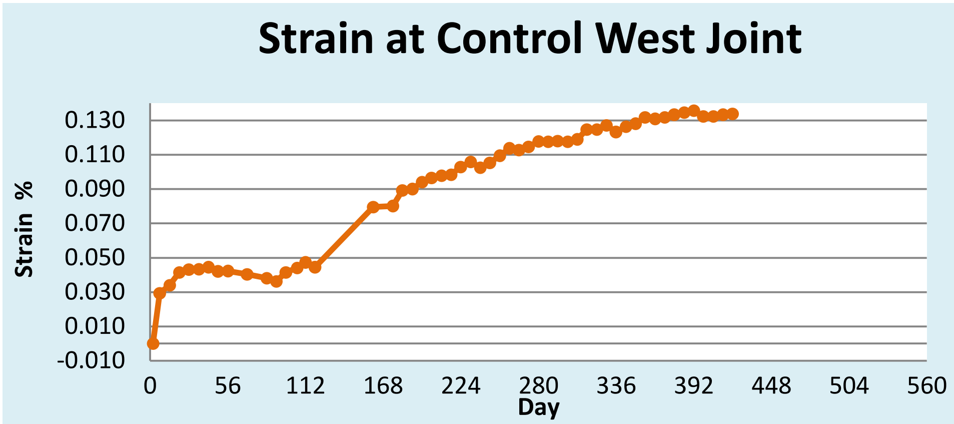

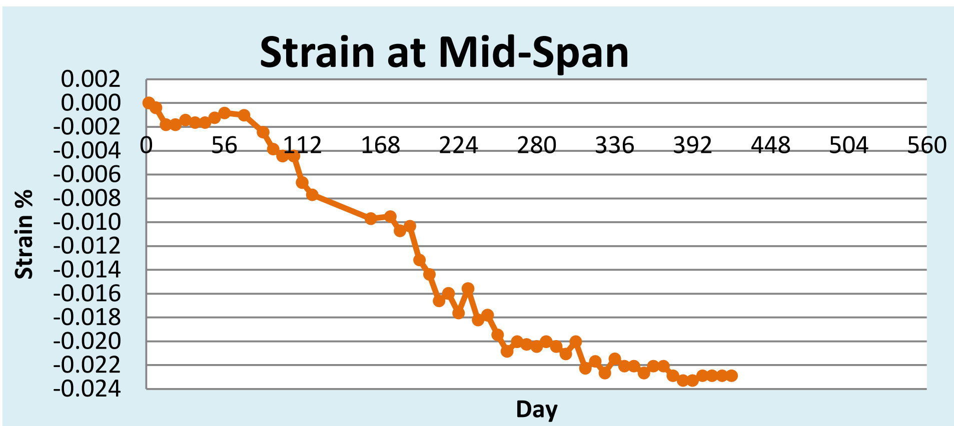

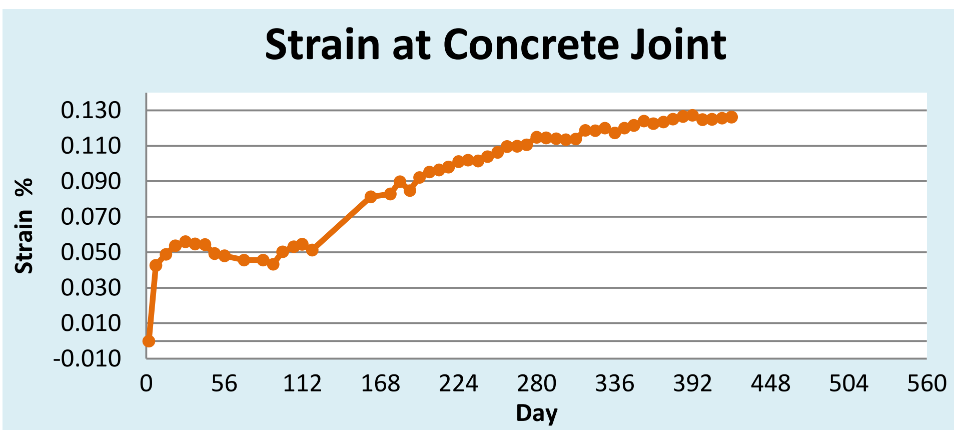

B.24 Strain at Control Joints and Mid-Span of Slab vs. Time for slab using RSCC

B.7.3.2. Expansion or Crack at West and East Joint openings

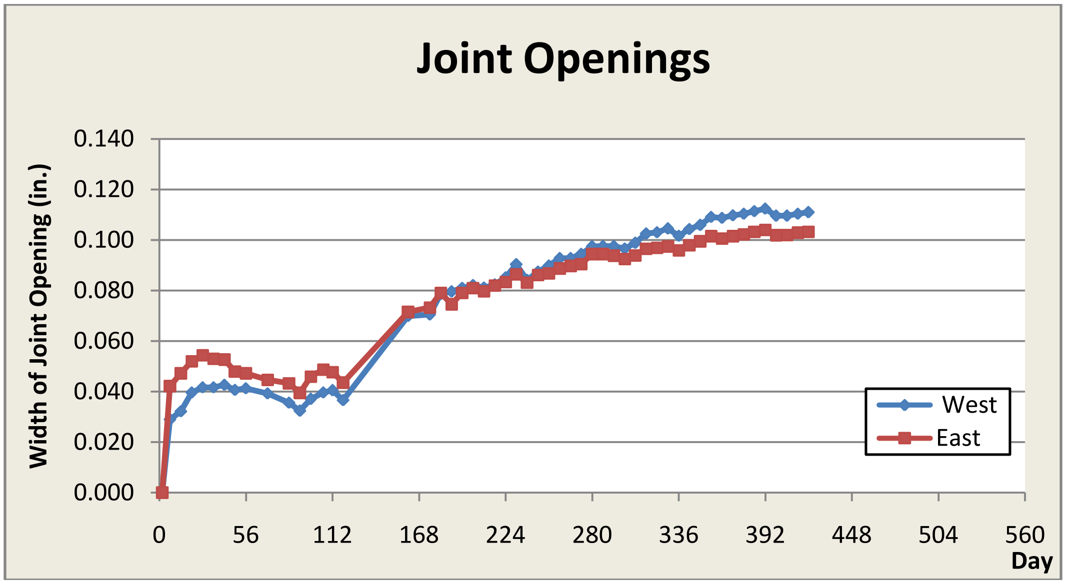

B.25 Width of Joint Openings at West and East Sides vs. Time for slab using RSCC

B.8. Comparison of Results

B.8.1. ASTM C 157 and ASTM C 878 Test Results Comparison

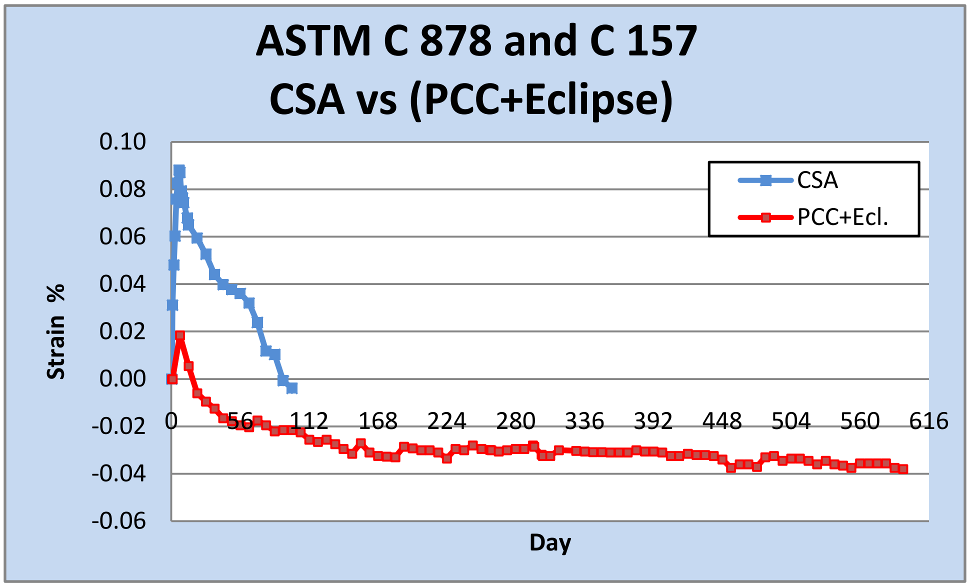

Figure B.26 Expansion Test Slab using Shrinkage Compensating Concrete (CSA) vs. PCC with Eclipse

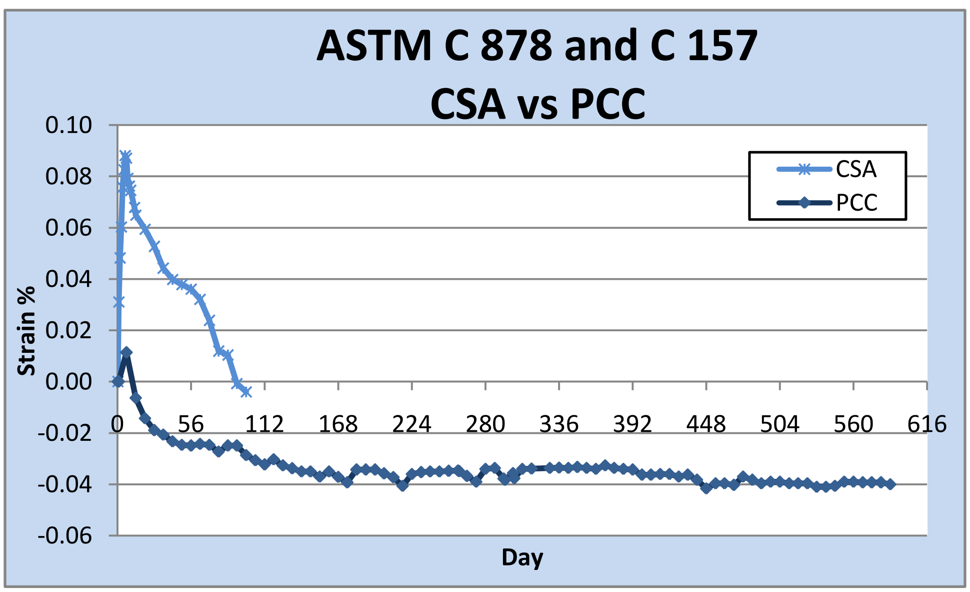

Figure B.27 Expansion Test Slab using Shrinkage Compensating Concrete (CSA) vs. PCC with 355 PCY cement and 0.60 w/c ratio

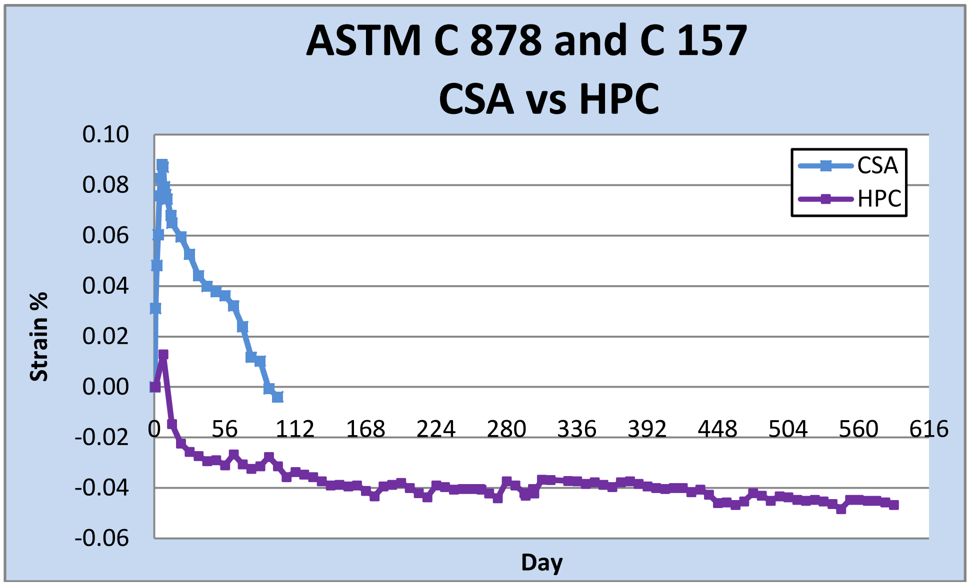

Figure B.28 Expansion Test Slab using Shrinkage Compensating Concrete (CSA) vs. PCC with 547 PCY cement and 0.37 w/c ratio

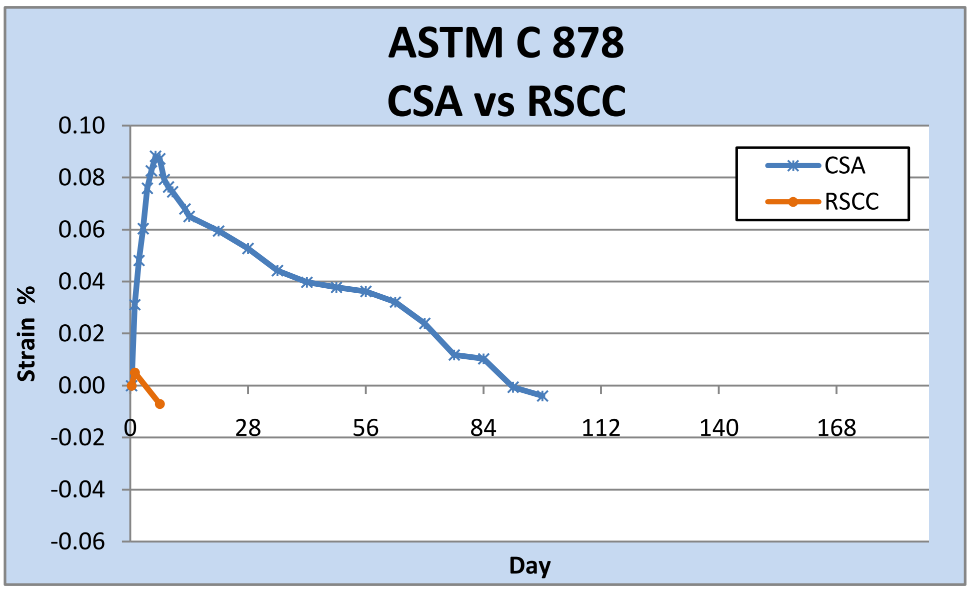

Figure B.29 Expansion Test Slab using Shrinkage Compensating Concrete (CSA) vs. RSCC

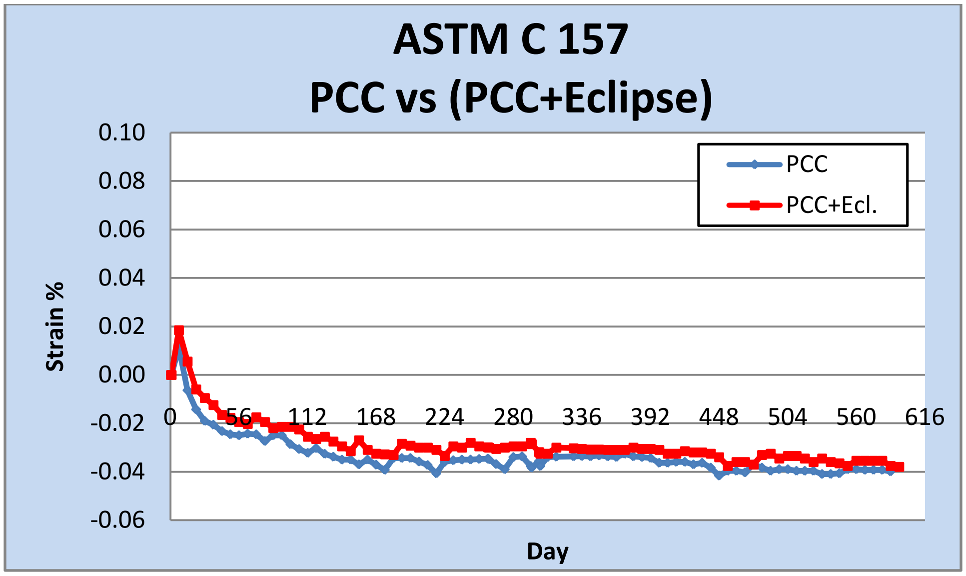

Figure B.30 Expansion Test Slab using PCC vs. (PCC+Eclipse)

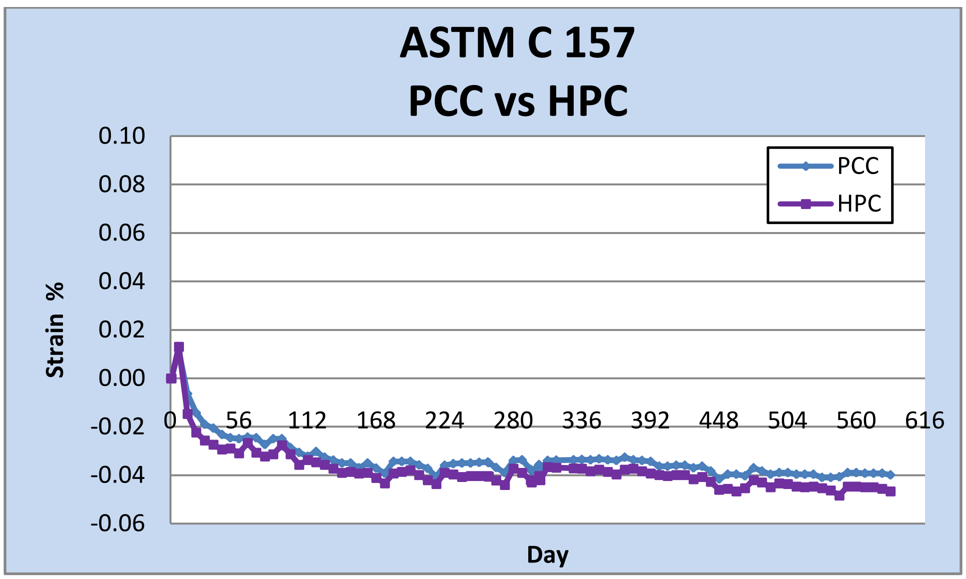

Figure B.31 Expansion Test Slab using PCC vs. HPC

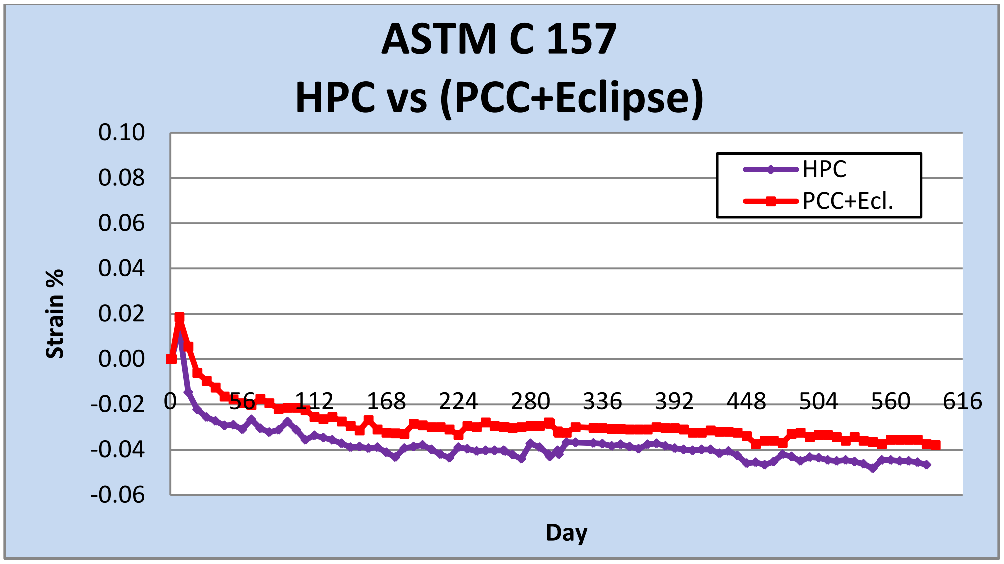

Figure B.32 Expansion Test Slab using HPC vs. (PCC+Eclipse)

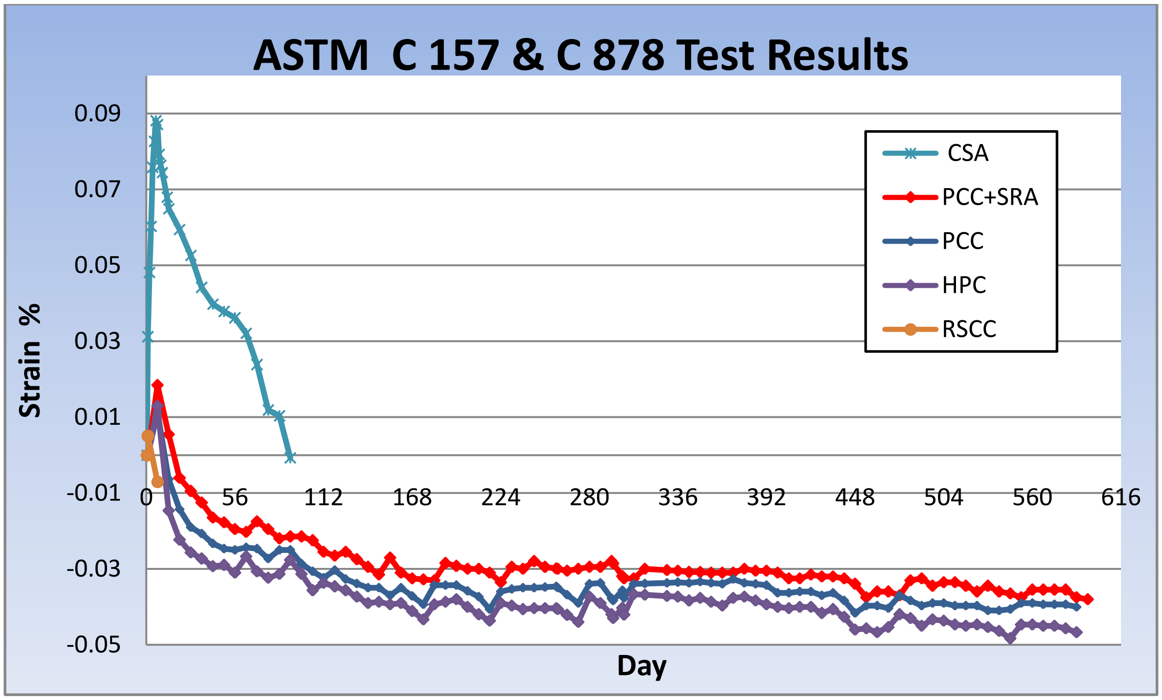

Figure B.33 Expansion Test for all of the slab specimens

B.8.2. Joint Expansion and Surface Strain

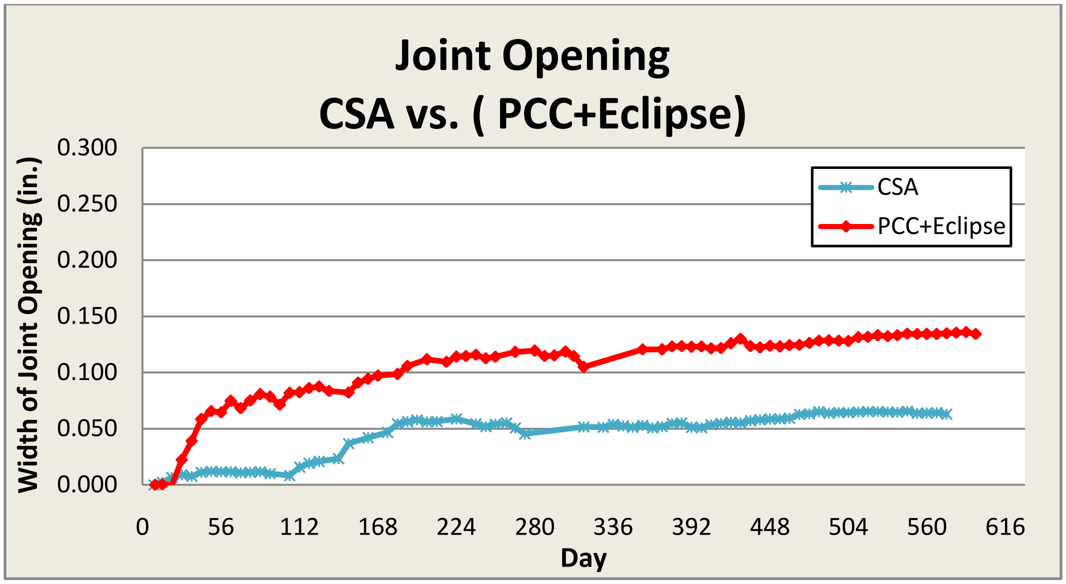

Figure B.34 Expansion of joint opening for slab using CSA vs. slab using (PCC+Eclipse)

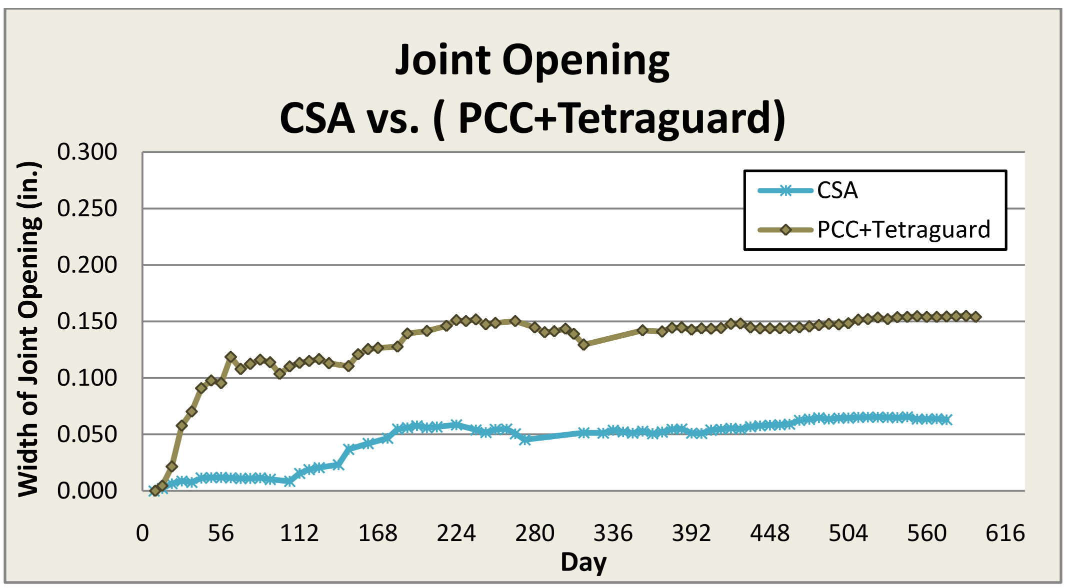

Figure B.35 Expansion of joint opening for slab using CSA vs. slab using (PCC+Tetraguard)

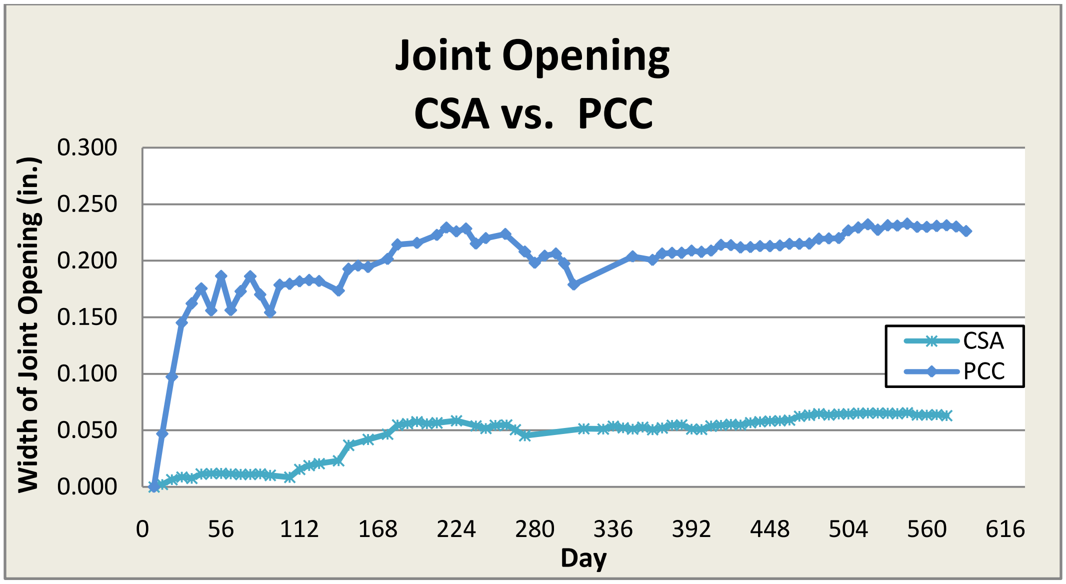

Figure B.36 Expansion of joint opening for slab using CSA vs. slab using PCC

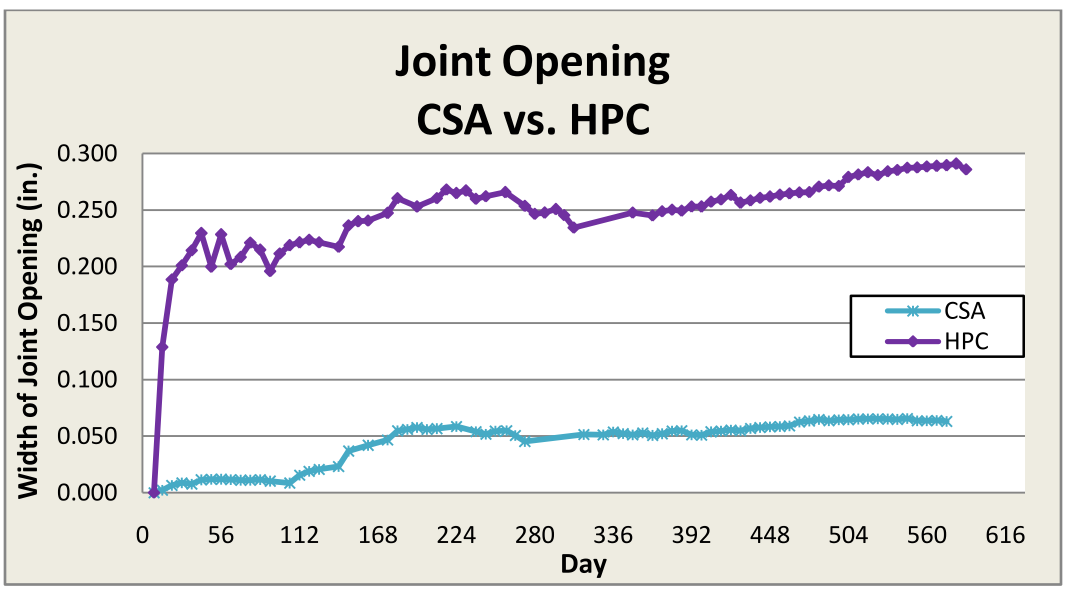

Figure B.37 Expansion of joint opening for the slab using CSA vs. slab using HPC with 542 PCY cement and 0.37 w/c ratio

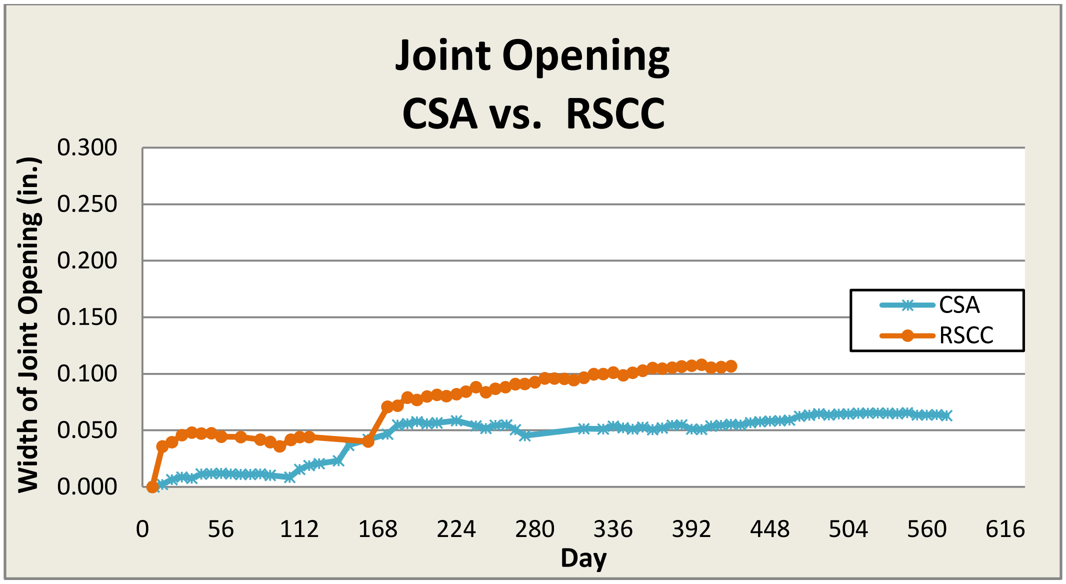

Figure B.38 Expansion of joint opening for the slab using CSA vs. slab using RSCC

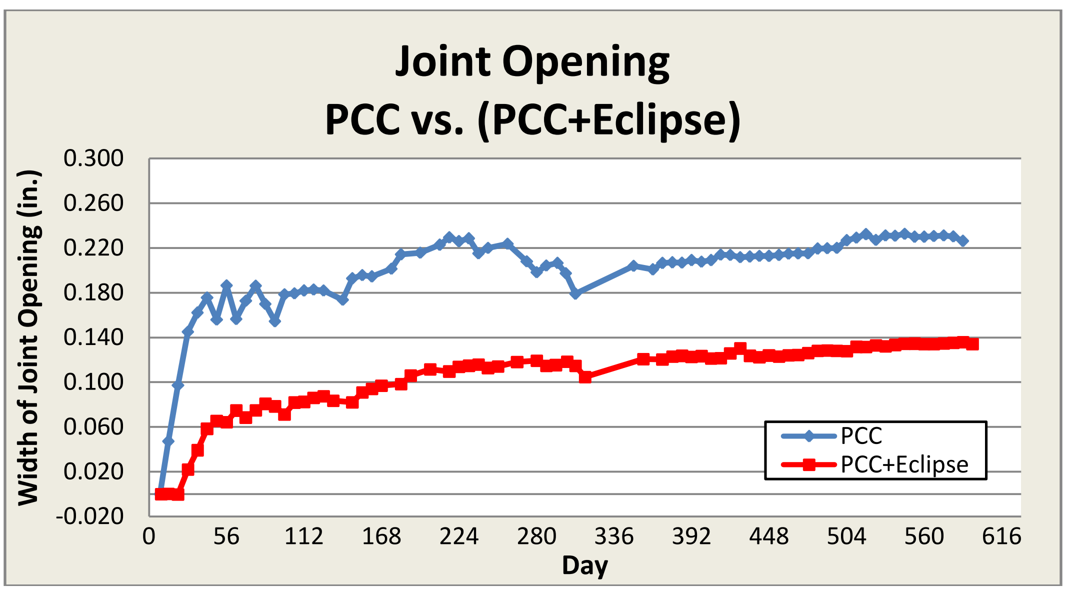

Figure B.39 Expansion of joint opening for the slab using PCC vs. slab using (PCC+Eclipse)

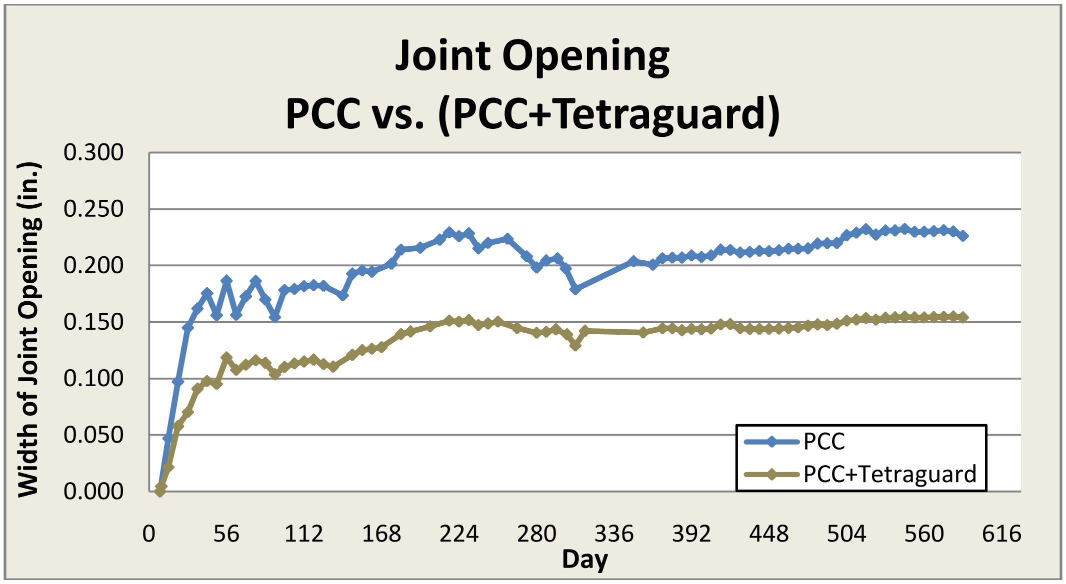

Figure B.40 Expansion of joint opening for the slab using PCC vs. slab using (PCC+Tetraguard)

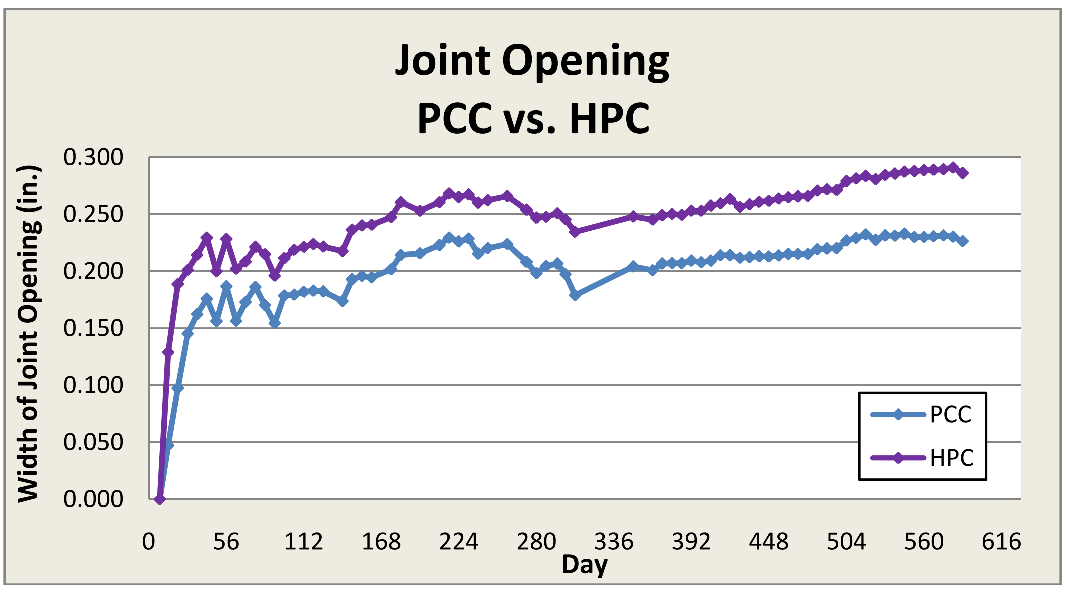

Figure B.41 Expansion of joint opening for the slab using PCC vs. slab using HPC

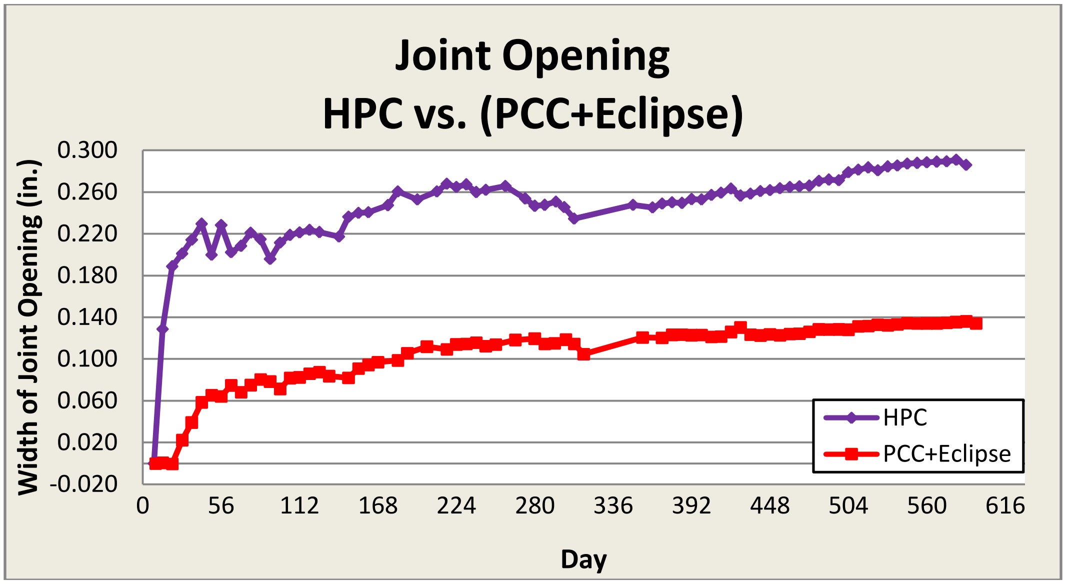

Figure B.42 Expansion of joint opening for the slab using HPC vs. slab using (PCC+Eclipse)

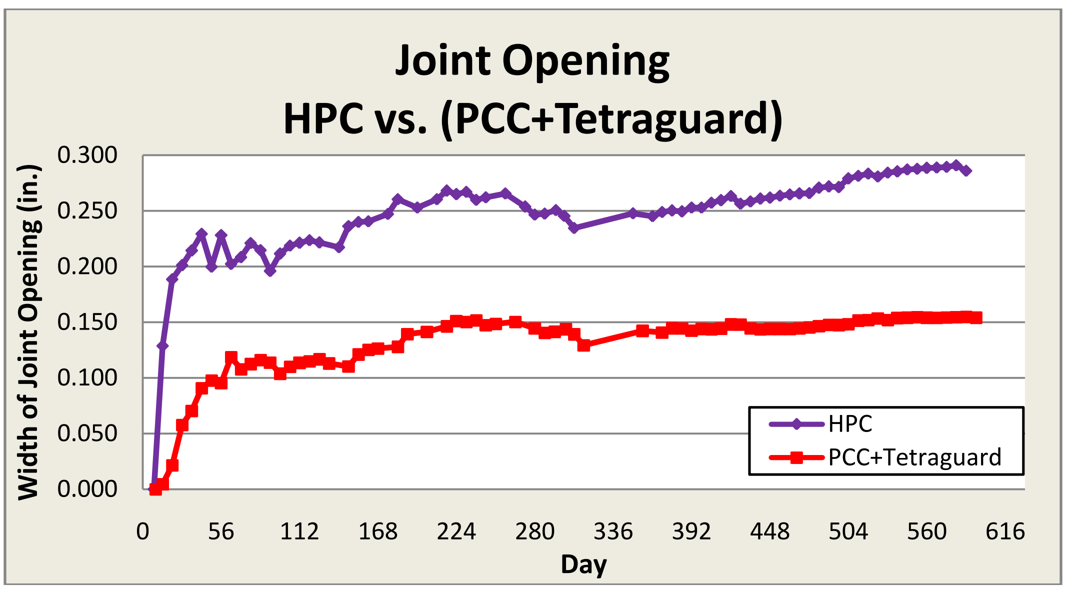

Figure B.43 Expansion of joint opening for the slab using HPC vs. slab using (PCC+Tetraguard)

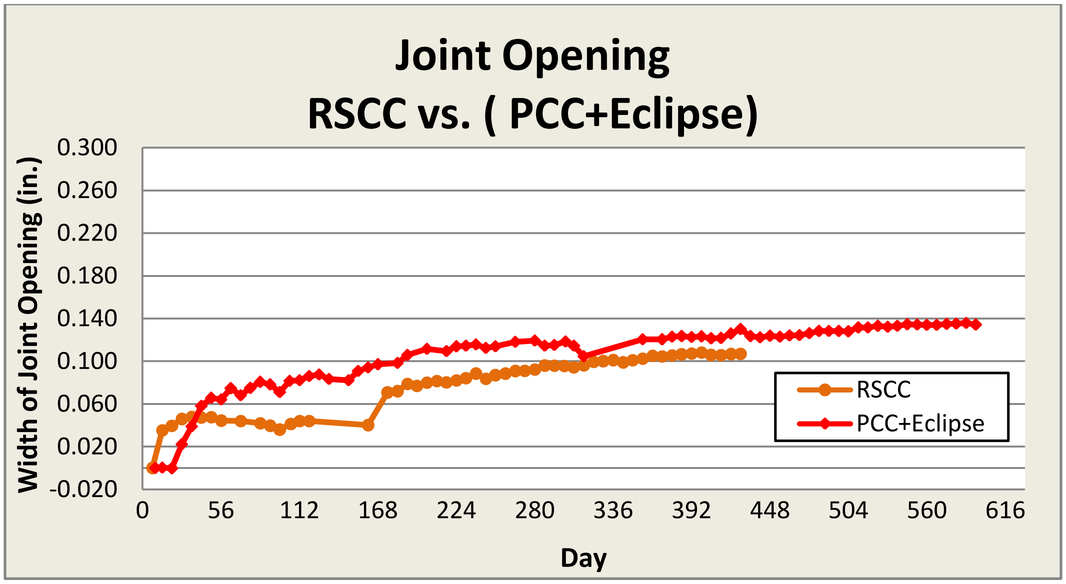

Figure B.44 Expansion of joint opening for the slab using RSCC vs. slab using (PCC+Eclipse)

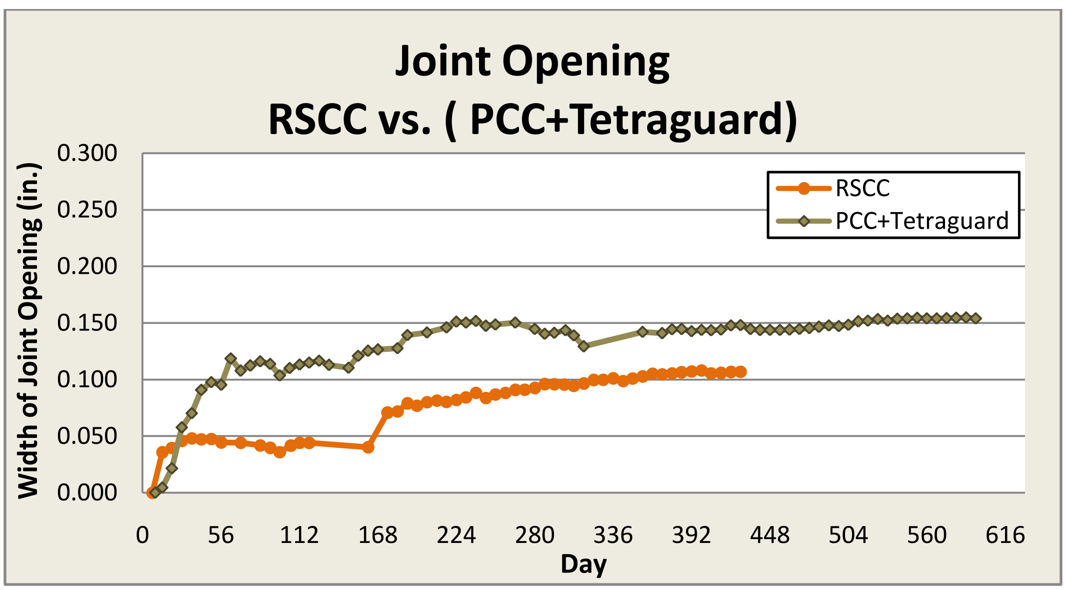

Figure B.45 Expansion of joint opening for the slab using RSCC vs. slab using (PCC+Tetraguard)

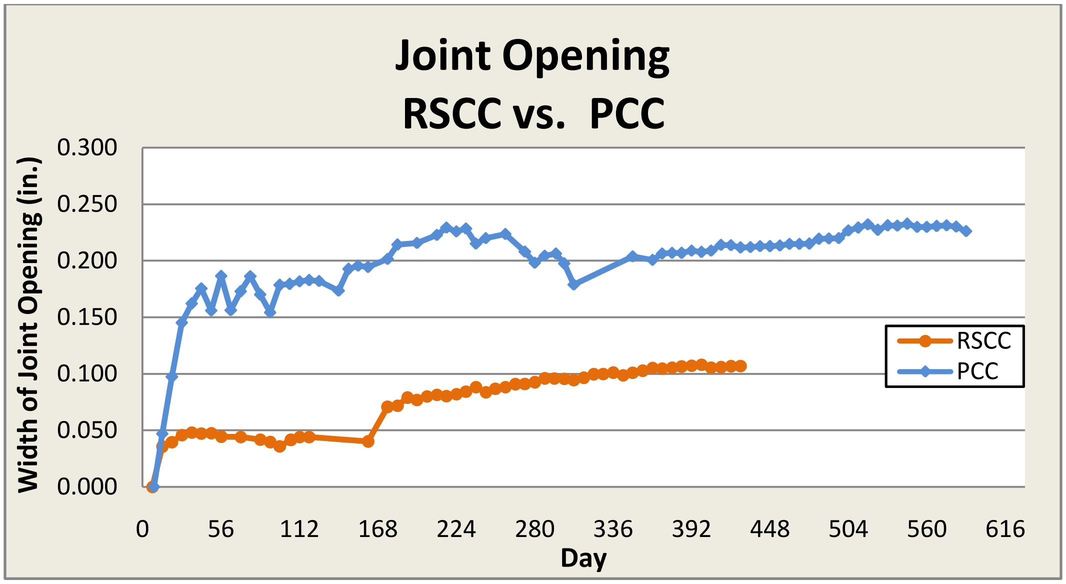

Figure B.46 Expansion of joint opening for the slab using RSCC vs. slab using PCC

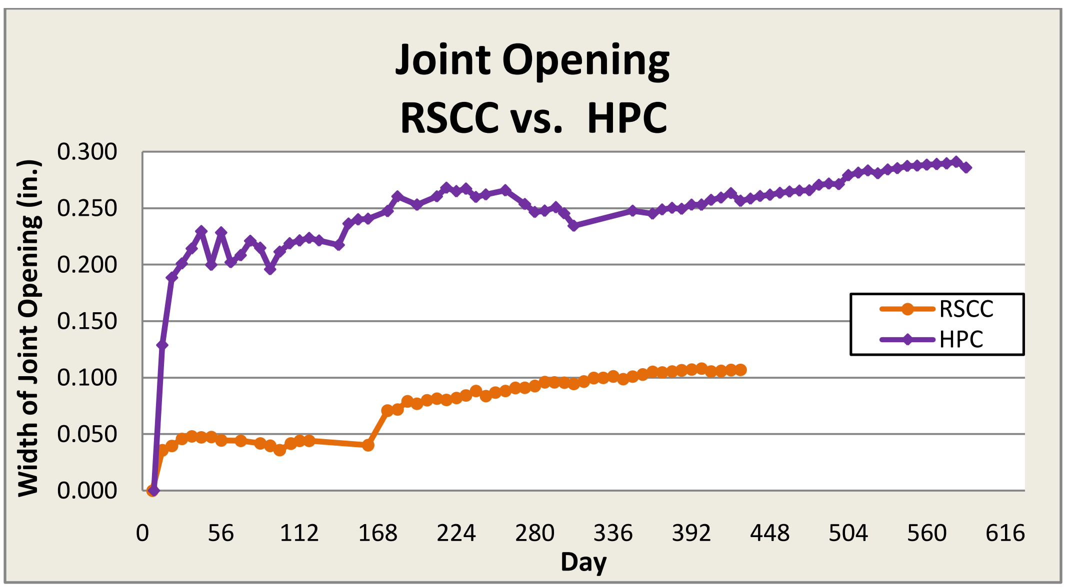

Figure B.47 Expansion of joint opening for the slab using RSCC vs. slab Using HPC

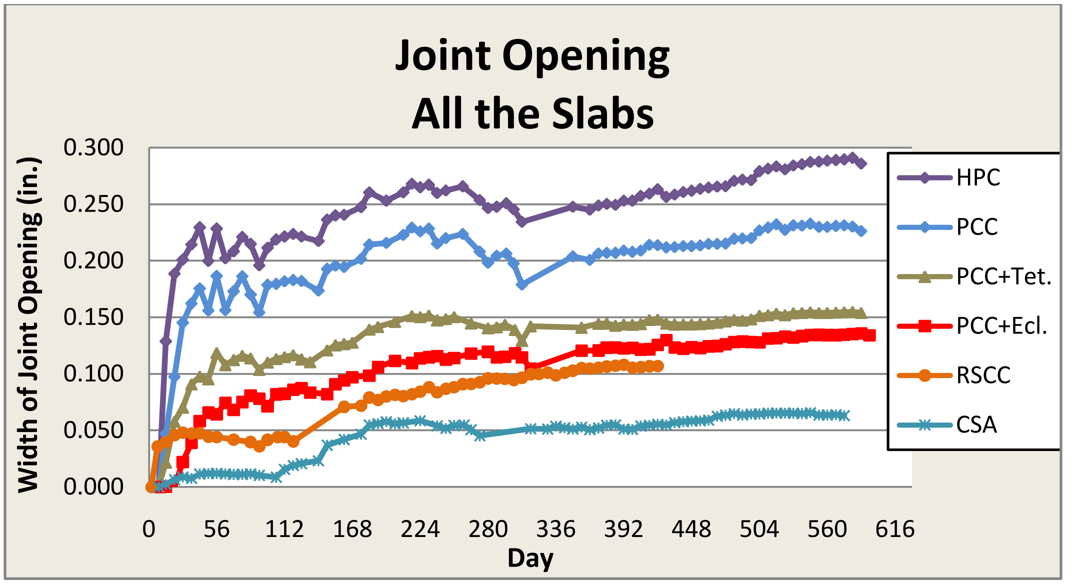

Figure B.48 Expansion of joint opening for all slab specimens

B.8.3. Comparing Strains at Mid-Span and Average Strain at Control Joints of the Slabs

Note: Strain at control joints is average of strain at west and east control joints.

B.8.3.1 Calcuim SulphoAlominate vs. PCC with Eclipse (SRA)

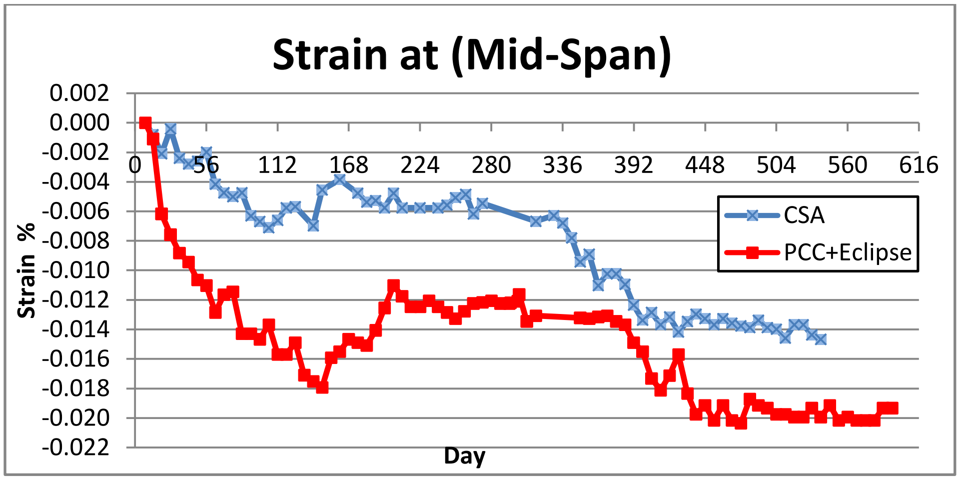

Figure B.49 Strain at Mid-Span vs. Time for slab using CSA and slab using (PCC+Eclipse)

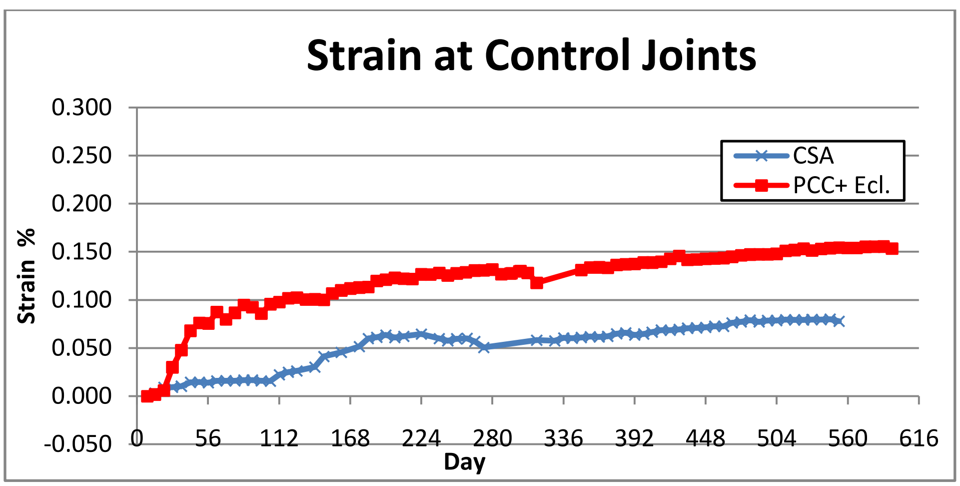

Figure B.50 Strain at Control Joint vs. Time for slab using CSA and slab using (PCC+Eclipse)

B.8.3.2. Calcuim SulphoAlominate vs. PCC with Tetraguard (SRA)

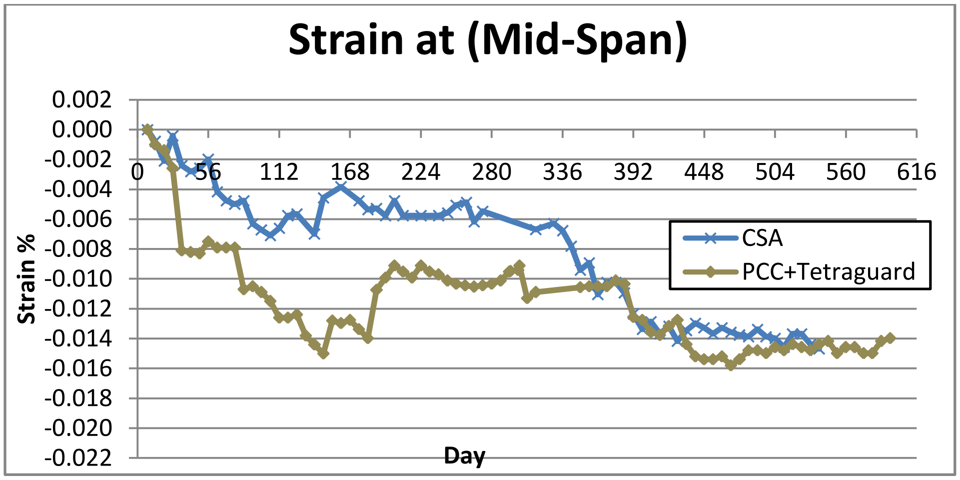

Figure B.51 Strain at Mid-Span vs. Time for slab using CSA and slab using (PCC+Tetragaurd)

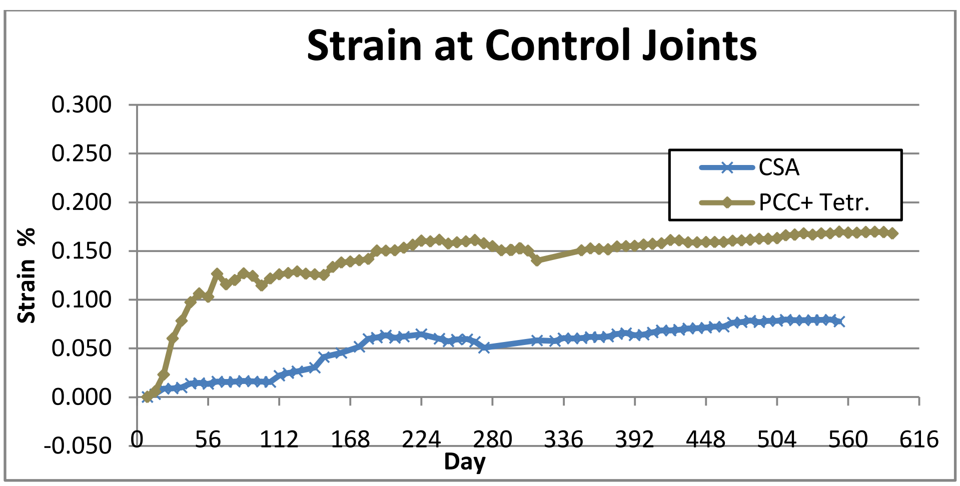

Figure B.52 Strain at Control Joint vs. Time for slab using CSA and slab using (PCC+Tetragaurd)

B.8.3.3. Calcuim SulphoAlominate vs. PCC

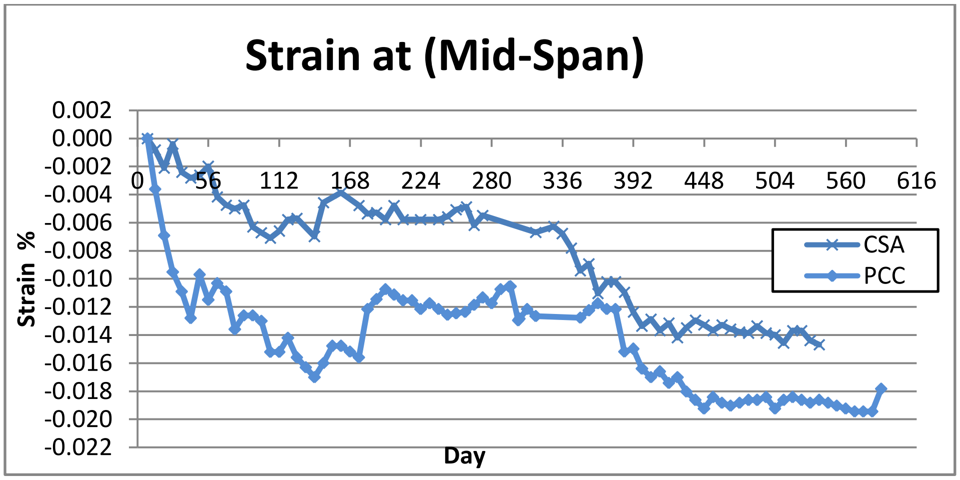

Figure B.53 Strain at Mid-Span vs. Time for slab using CSA and slab using PCC

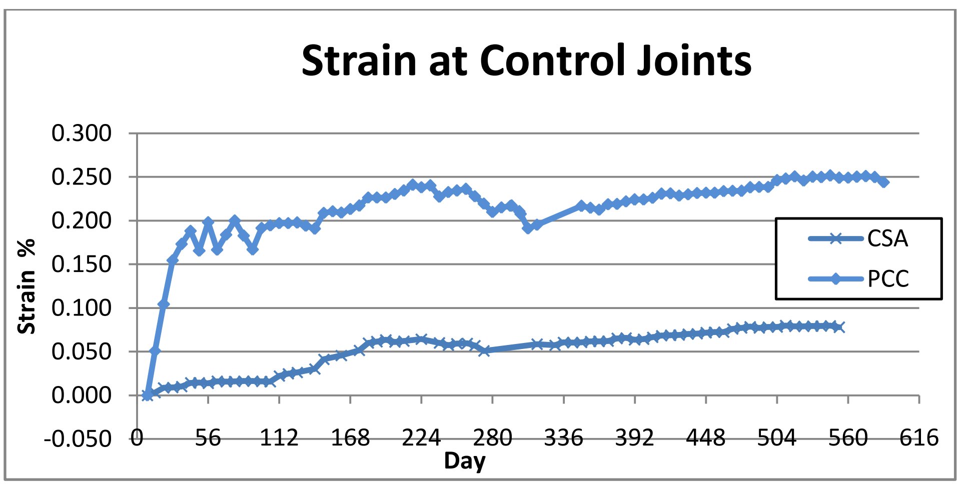

Figure B.54 Strain at Control Joint vs. Time for slab using CSA and slab using PCC

B.8.3.4. Calcuim SulphoAlominate vs. HPC

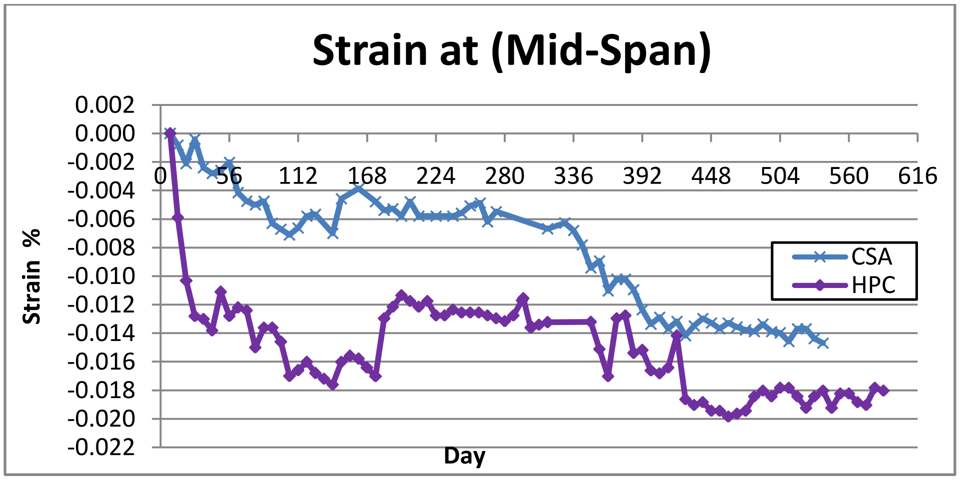

Figure B.55 Strain at Mid-Span vs. Time for slab using CSA and slab using HPC

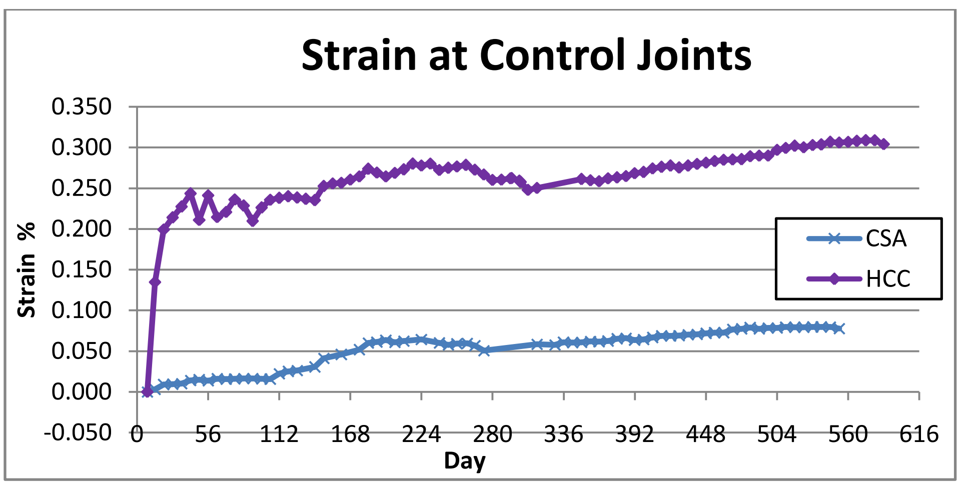

Figure B.56 Strain at Control Joint vs. Time for slab using CSA and slab using HPC

B.8.3.5. Calcuim SulphoAlominate vs. RSCC

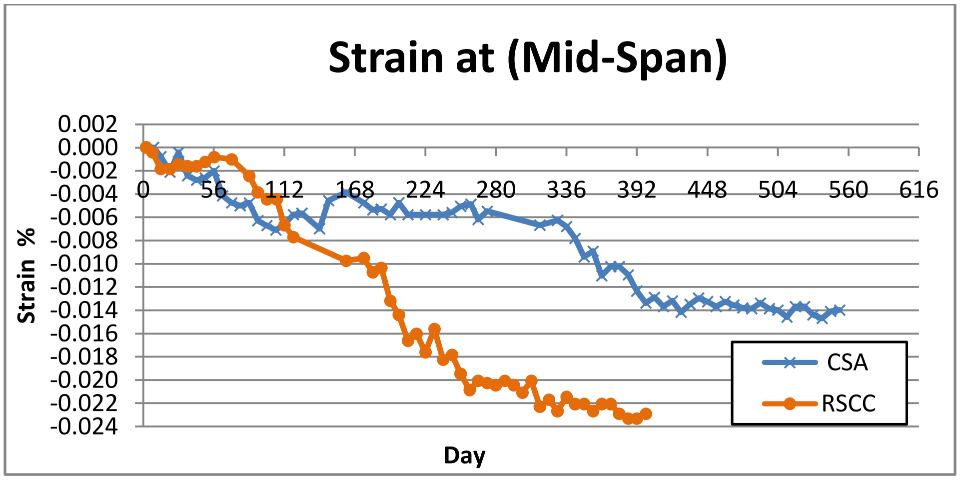

Figure B.57 Strain at Mid-Span vs. Time for slab using CSA and slab using RSCC

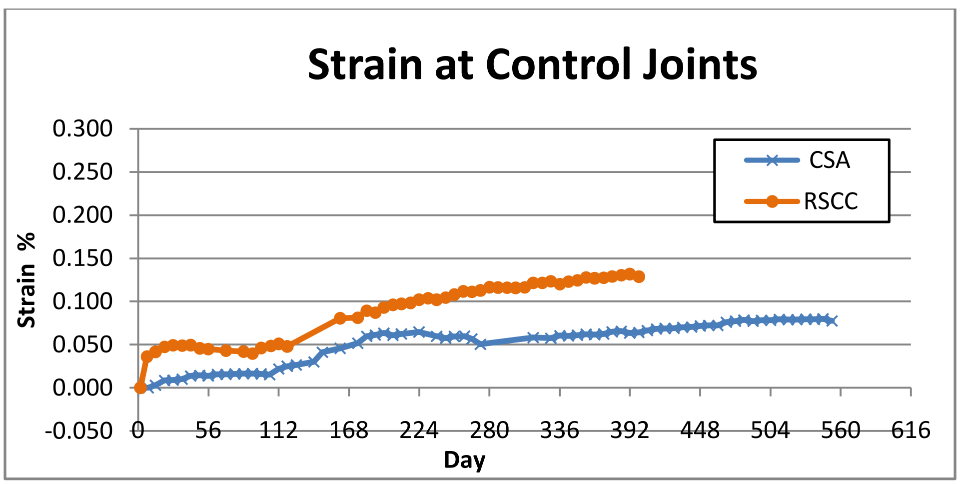

Figure B.58 Strain at Control Joint vs. Time for slab using CSA and slab using HPC

B.8.3.6. Portalnd Cement Concrete vs. PCC+Eclipse (SRA)

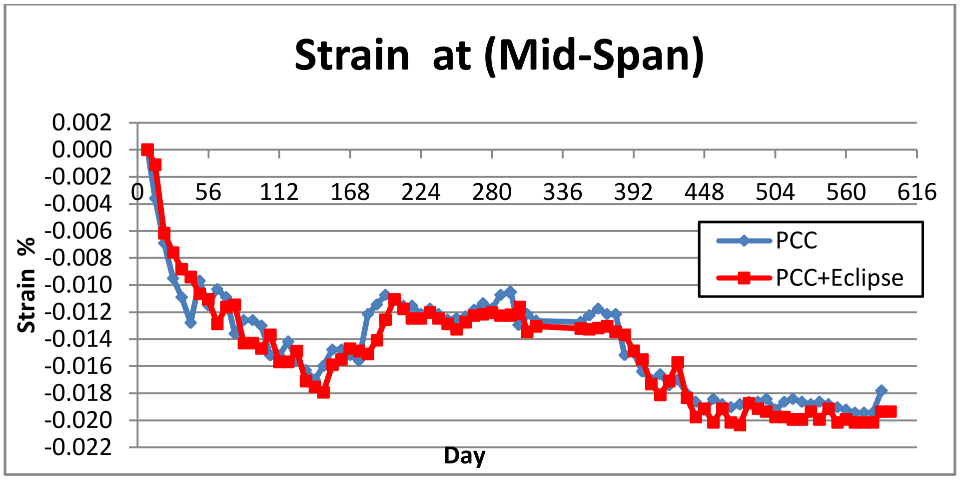

Figure B.59 Strain at Mid-Span vs. Time for slab using PCC and slab using (PCC+ Eclipse)

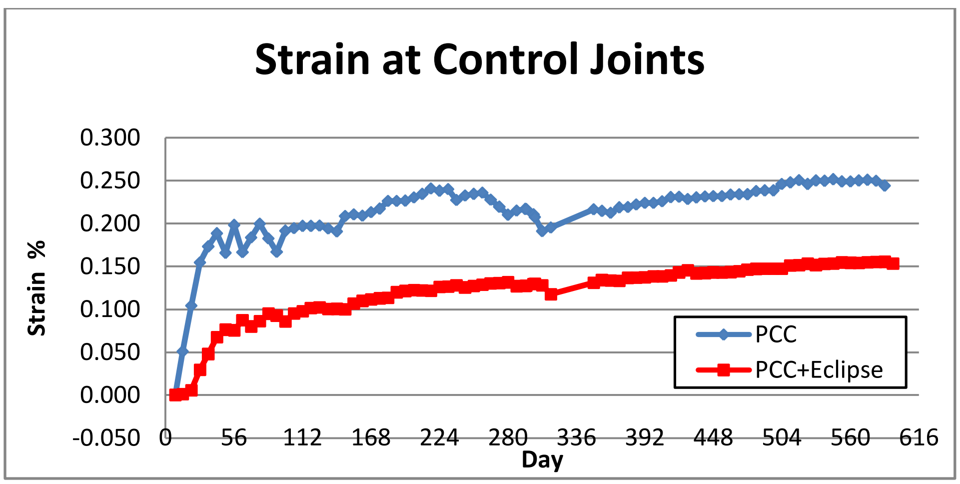

Figure B.60 Strain at Control Joint vs. Time for slab using PCC and slab using (PCC+Eclipse)

B.8.3.7. Portalnd Cement Concrete vs. PCC+Tetraguard (SRA)

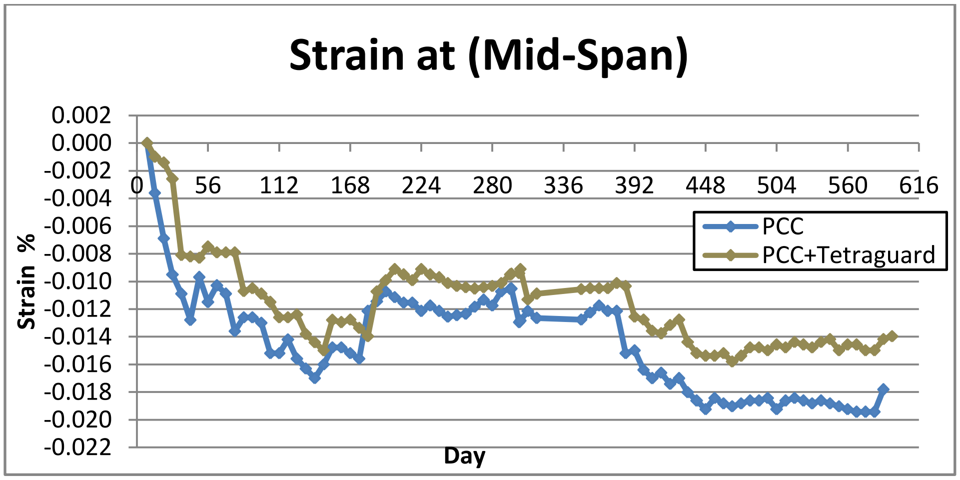

Figure B.61 Strain at Mid-Span vs. Time for slab using PCC and slab using (PCC+ Tetraguard)

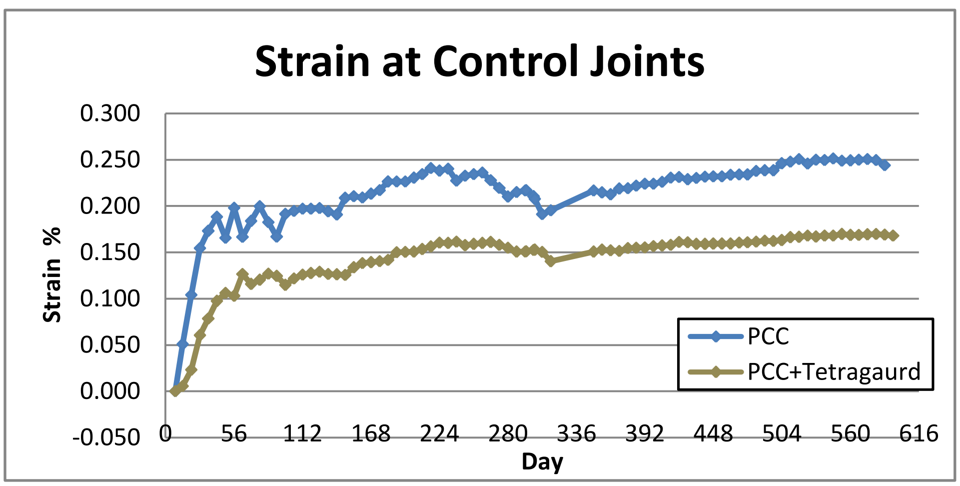

Figure B.62 Strain at Control Joint vs. Time for Slab using PCC and slab using (PCC+Eclipse)

B.8.3.8. Portland Cement Concrete vs. HPC

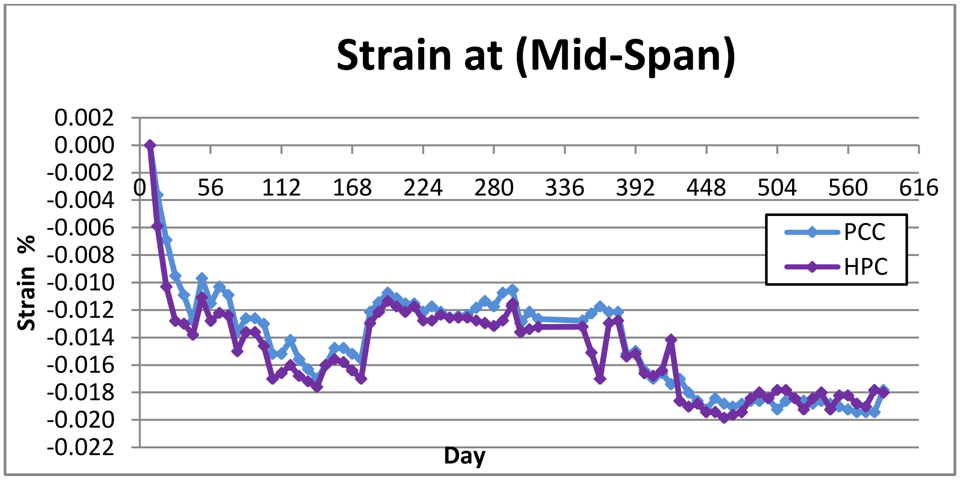

Figure B.63 Strain at Mid-Span vs. Time for Slab using PCC and slab using HPC

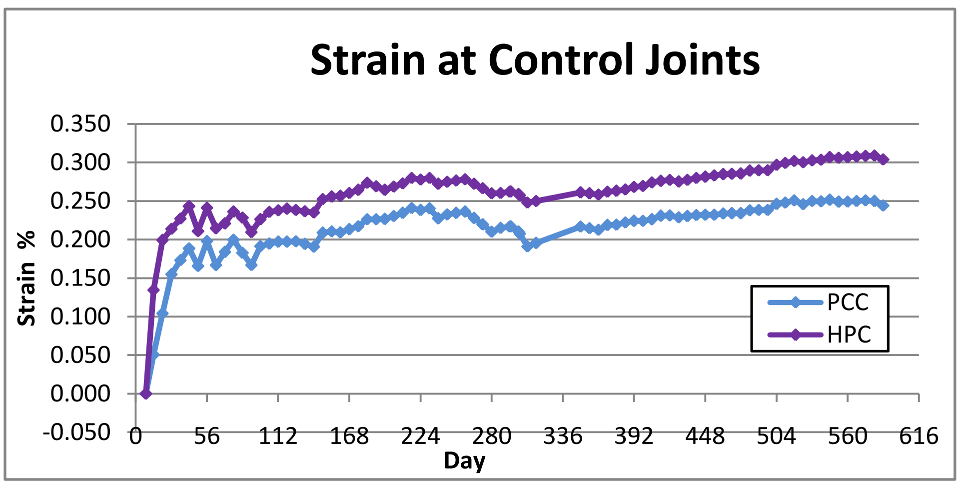

Figure B.64 Strain at Control Joint vs. Time for Slab using PCC and slab using HPC

B.8.3.9. High Performance Concrete vs. PCC+Eclipse (SRA)

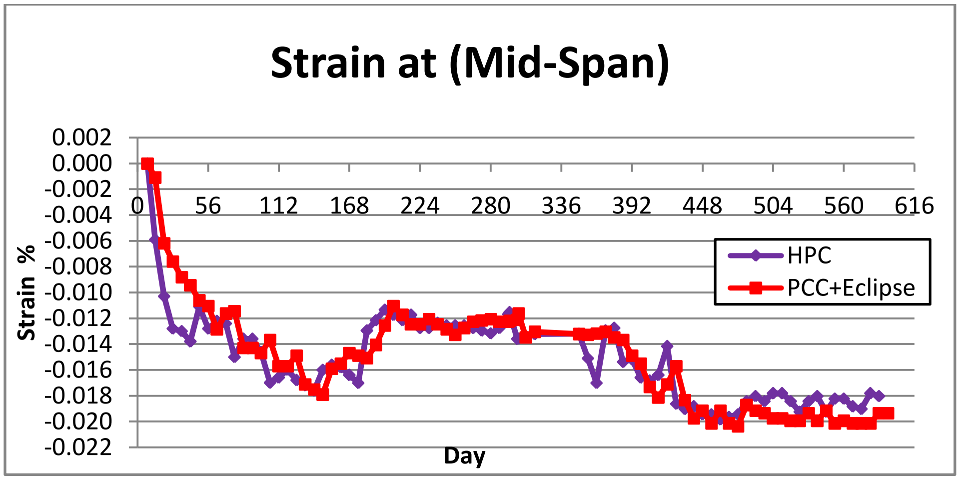

Figure B.65 Strain at Mid-Span vs. Time for slab using HCC and slab using (PCC+ Eclipse)

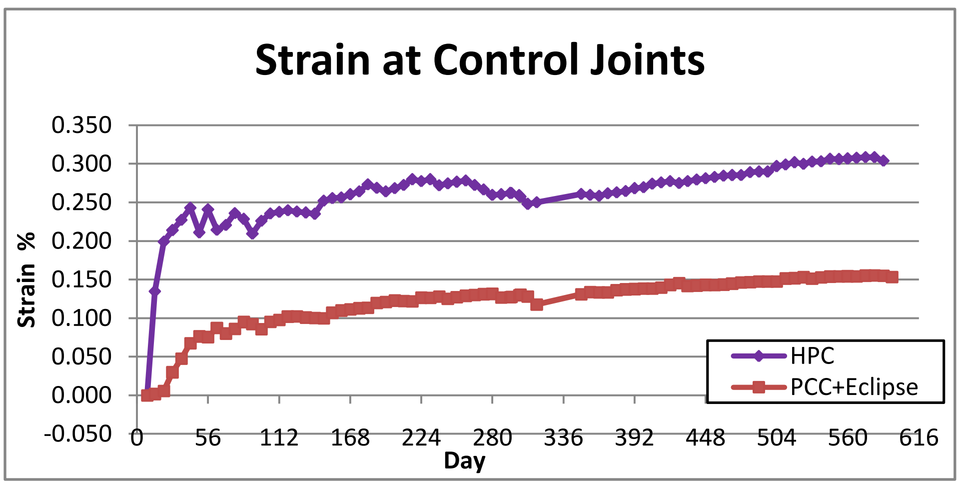

Figure B.66 Strain at Control Joint vs. Time for slab using PCC and slab using (PCC+Eclipse)

B.8.3.10. High Performance Concrete vs. PCC+Tetraguard (SRA)

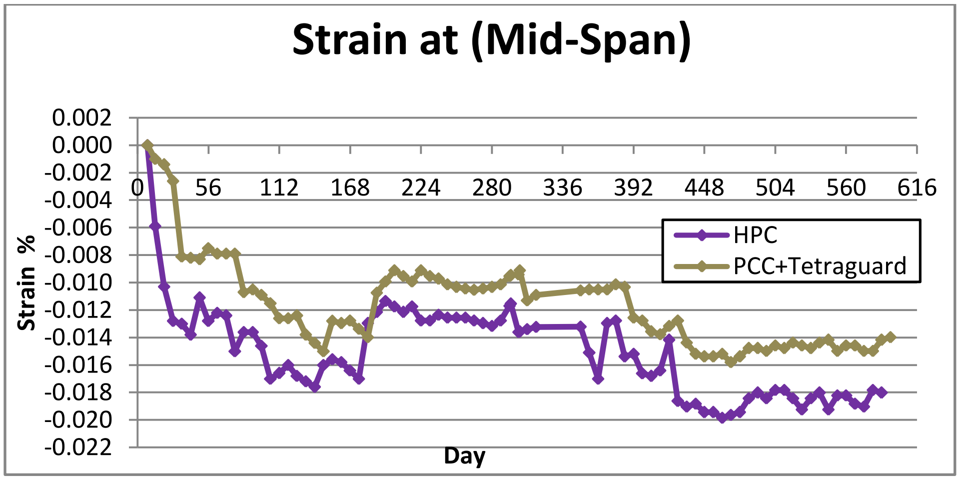

Figure B.67 Strain at Mid-Span vs. Time for Slab using HPC and slab using (PCC+Tetraguard)

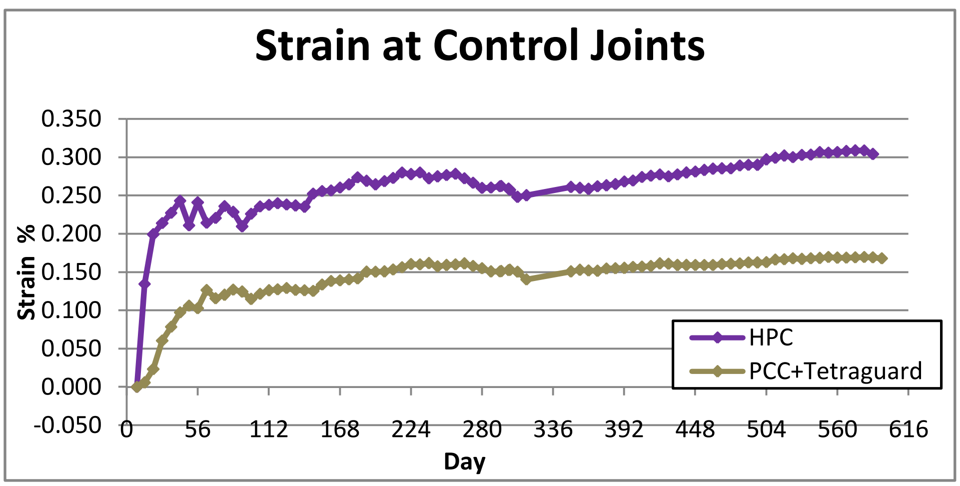

Figure B.68 Strain at Control Joint vs. Time for Slab using HPC and slab using (PCC+Tetraguard)

B.8.3.11. Rapid Set Cement Concrete vs. PCC+Eclipse (SRA)

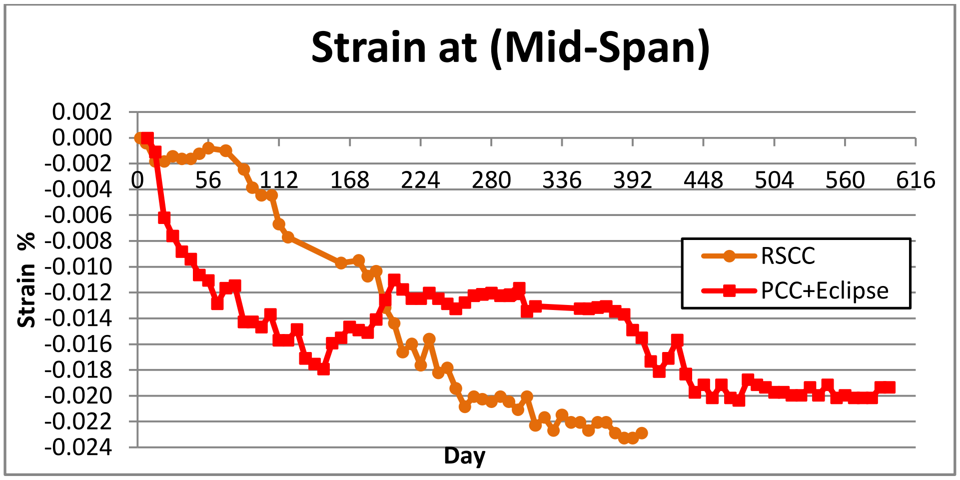

Figure B.69 Strain at Mid-Span vs. Time for slab using RSCC and slab using (PCC+ Eclipse)

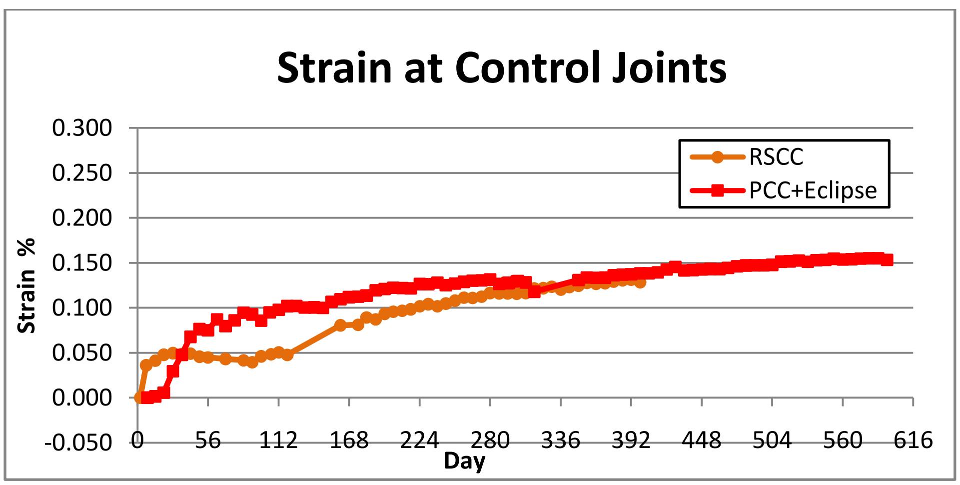

Figure B.70 Strain at Control Joint vs. Time for slab using RSCC and slab using (PCC+Eclipse)

B.8.3.12. Rapid Set Cement Concrete vs. PCC+Tetraguard (SRA)

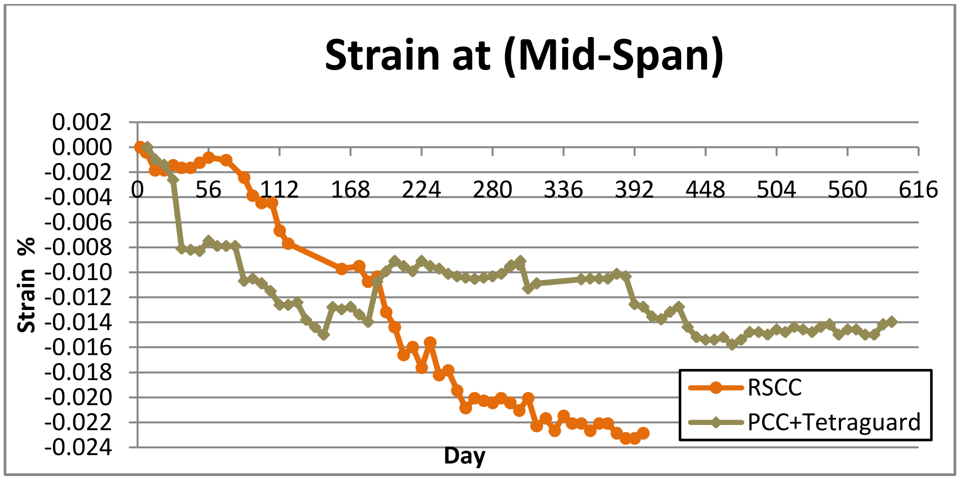

Figure B.71 Strain at Mid-Span vs. Time for slab using RSCC and slab using (PCC+ Tetraguard)

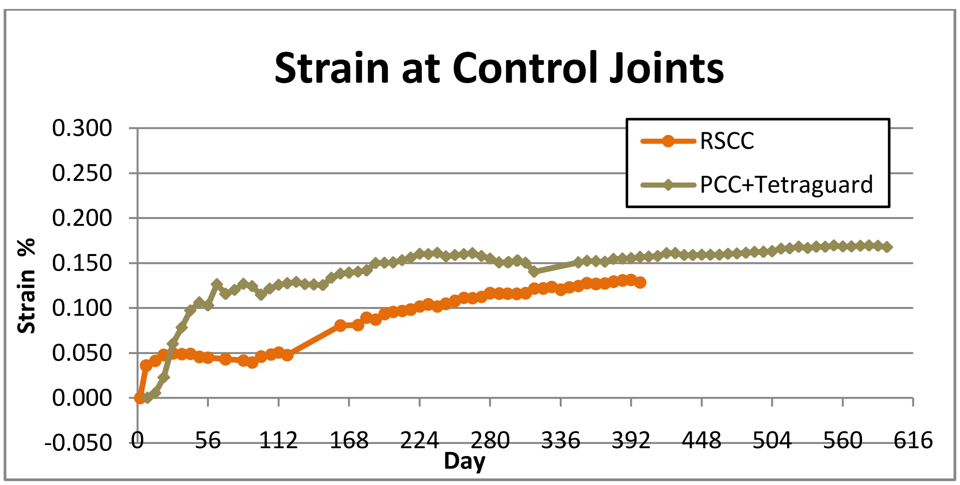

Figure B.72 Strain at Control Joint vs. Time for slab using RSCC and slab using

(PCC+Tetraguard)

B.8.3.13. Rapid Set Cement Concrete vs. PCC

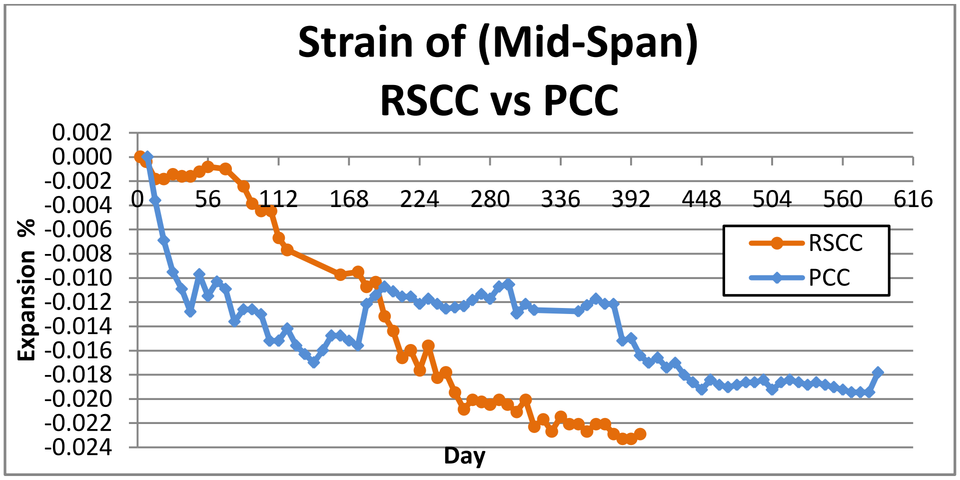

Figure B.73 Strain at Mid-Span vs. Time for slab using RSCC and slab using PCC

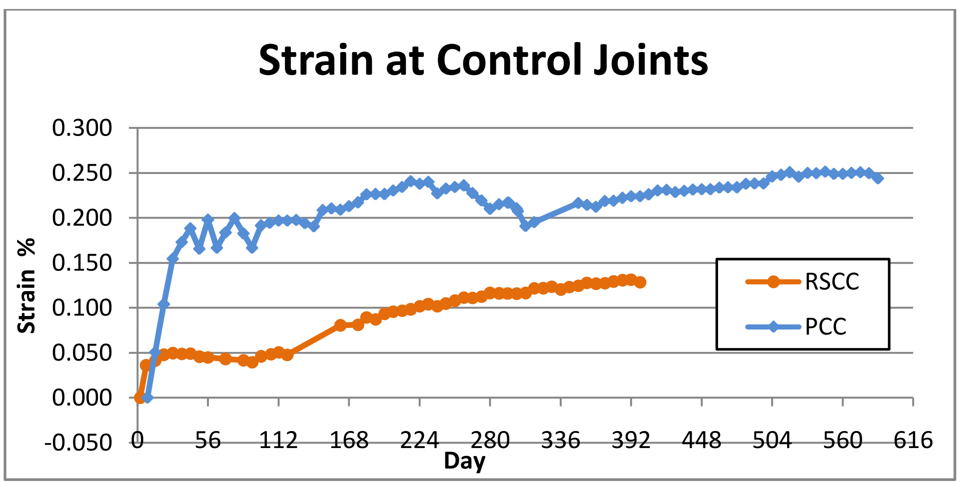

Figure B.74 Strain at Control Joint vs. Time for slab using RSCC and slab using PCC

B.8.3.14. Rapid Set Cement Concrete vs. HPC

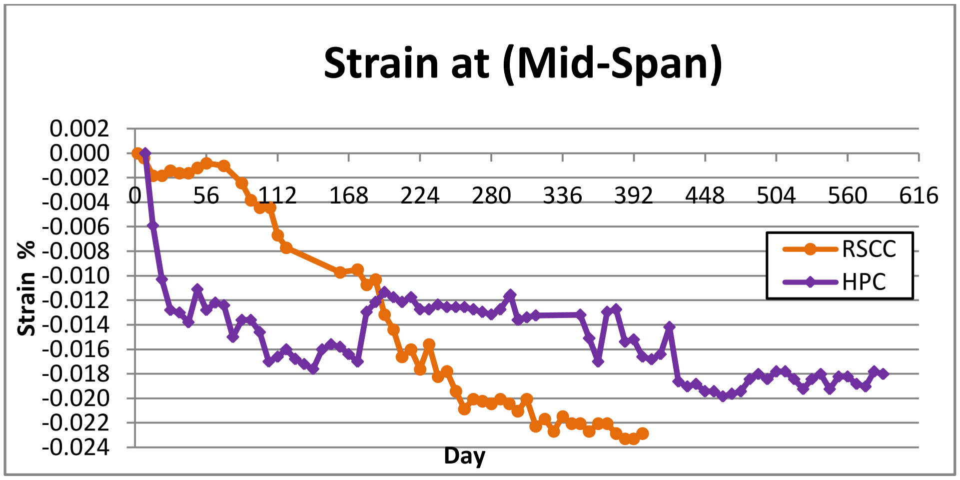

Figure B.75 Strain at Mid-Span vs. Time for slab using RSCC and slab using HPC

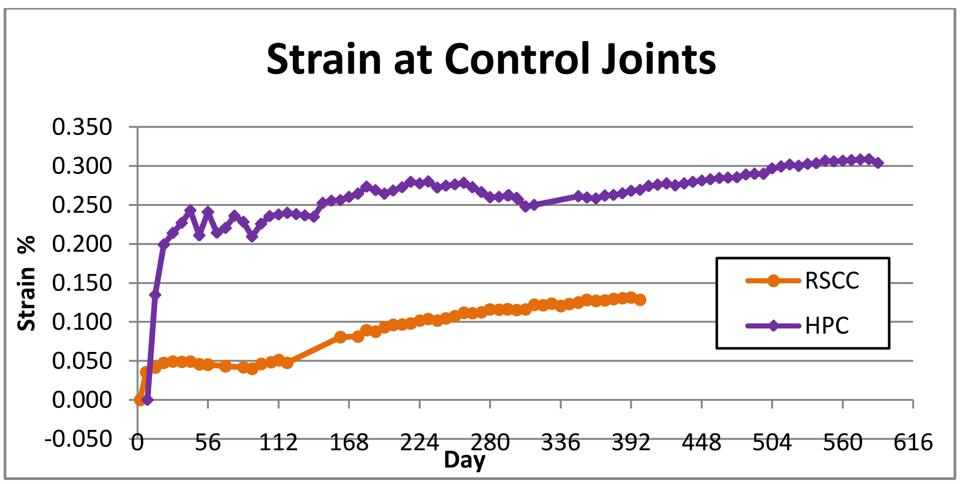

Figure B.76 Strain at Control Joint vs. Time for slab using RSCC and slab using HPC

B.8.4. Temperature through Depth of Slabs

Note: PCC+Ecl. and PCC+Tet. are abbreviations for PCC+Eclipse and PCC+Tetraguard respectively.

Table B.2 Slab temperature on 1/19/2010

1/19/2010	Slab Temperature (°F)							
Depth (in.)	PCC+Ecl.	PCC+Tet.	PCC	HPC	CSA #1	CSA#2	RSCC	Avg. CSA
0								
-0.5	70	71	71	71	70	71	75	71
-1	70	71	71	71	71	70	75	71
-1.5	70	71	70	71	70	70	75	70
-2	70	71	71	70	70	70	75	70
-2.5	70	70	70	71	70	70	75	70
-3								

Table B.3 Slab temperature on 1/26/2010

1/26/2010	Slab Temperature (°F)							
Depth (in.)	PCC+Ecl.	PCC+Tet.	PCC	HPC	CSA #1	CSA#2	Slab 8	Avg. CSA
0								
-0.5	70	71	71	71	70	71	70	71
-1	71	71	71	71	71	71	69	71
-1.5	70	71	71	71	70	71	69	71
-2	71	71	71	71	71	70	69	71
-2.5	70	71	71	71	71	71	70	71
-3								

Table B.4 Slab temperature on 2/23/2010

2/23/2010	Slab Temperature (°F)							
Depth (in.)	PCC+Ecl.	PCC+Tet.	PCC	HPC	CSA #1	CSA#2	RSCC	Avg. CSA
0								
-0.5	71	72	72	72	71	71	70	71
-1	71	72	72	72	72	72	69	72
-1.5	71	72	72	72	71	71	69	71
-2	71	72	72	72	72	71	70	72
-2.5	71	72	72	72	71	72	70	72
-3								

Table B.5 Slab temperature on 3/16/2010

3/16/2010	Slab Temperature (°F)							
Depth (in.)	PCC+Ecl.	PCC+Tet.	PCC	HPC	CSA #1	CSA#2	RSCC	Avg. CSA
0								
-0.5	71	71	71	71	71	71	70	71
-1	71	71	72	72	72	71	69	72
-1.5	71	71	71	71	71	71	69	71
-2	71	71	72	72	71	71	70	71
-2.5	71	71	71	72	71	71	70	71
-3								

Table B.6 Slab temperature on 4/20/2010

4/20/2010	Slab Temperature (°F)							
Depth (in.)	PCC+Ecl.	PCC+Tet.	PCC	HPC	CSA #1	CSA#2	RSCC	Avg. CSA
0								
-0.5	70	70	71	71	70	70	70	70
-1	70	70	71	71	71	71	69	71
-1.5	70	70	70	70	70	70	70	70
-2	70	70	71	70	70	71	69	71
-2.5	70	70	70	71	70	70	70	70
-3								

Table B.7 Slab temperature on 5/18/2010

5/18/2010	Slab Temperature (°F)							
Depth (in.)	PCC+Ecl.	PCC+Tet.	PCC	HPC	CSA #1	CSA#2	RSCC	Avg. CSA
0								
-0.5	66	67	67	66	66	66	67	66
-1	67	67	67	67	67	67	66	67
-1.5	66	66	66	66	66	66	66	66
-2	67	66	67	67	66	66	66	66
-2.5	66	67	67	67	66	66	66	66
-3								

Table B.8 Slab temperature on 6/29/2010

6/29/2010	Slab Temperature (°F)							
Depth (in.)	PCC+Ecl.	PCC+Tet.	PCC	HPC	CSA #1	CSA#2	RSCC	Avg. CSA
0								
-0.5	71	71	71	71	70	71	72	71
-1	71	71	71	71	71	71	71	71
-1.5	71	71	71	71	70	70	72	70
-2	71	71	71	71	71	71	71	71
-2.5	71	71	71	71	70	71	72	71
-3								

Table B.9 Slab temperature on 7/13/2010

7/13/2010	Slab Temperature (°F)							
Depth (in.)	PCC+Ecl.	PCC+Tet.	PCC	HPC	CSA #1	CSA#2	RSCC	Avg. CSA
0								
-0.5	71	71	71	71	70	71	72	71
-1	71	71	71	71	71	71	71	71
-1.5	71	71	71	71	70	71	71	71
-2	71	71	71	71	71	71	72	71
-2.5	71	71	71	71	71	71	72	71
-3								

Table B.10 Slab temperature on 7/20/2010

7/20/2010	Slab Temperature (°F)							
Depth (in.)	PCC+Ecl.	PCC+Tet.	PCC	HPC	CSA #1	CSA#2	RSCC	Avg. CSA
0								
-0.5	72	71	71	71	70	70	72	70
-1	72	71	71	71	71	70	72	71
-1.5	72	71	71	71	70	70	72	70
-2	72	71	71	71	71	70	72	71
-2.5	72	72	71	71	70	71	72	71
-3								

Table B.11 Slab temperature on 7/27/2010

7/27/2010	Slab Temperature (°F)							
Depth (in.)	PCC+Ecl.	PCC+Tet.	PCC	HPC	CSA #1	CSA#2	RSCC	Avg. CSA
0								
-0.5	72	72	72	72	72	74	73	73
-1	72	72	72	72	73	73	72	73
-1.5	72	72	71	72	71	72	72	72
-2	72	72	72	72	72	72	72	72
-2.5	72	72	72	72	72	72	72	72
-3								

Table B.12 Slab temperature on 8/3/2010

8/3/2010	Slab Temperature (°F)							
Depth (in.)	PCC+Ecl.	PCC+Tet.	PCC	HPC	CSA #1	CSA#2	RSCC	Avg. CSA
0								
-0.5	72	71	71	71	70	70	73	70
-1	72	71	71	71	71	70	72	71
-1.5	71	71	71	71	70	70	72	70
-2	72	71	71	71	71	70	72	71
-2.5	72	71	71	71	70	70	72	70
-3								

Table B.13 Slab temperature on 8/10/2010

8/10/2010	Slab Temperature (°F)							
Depth (in.)	PCC+Ecl.	PCC+Tet.	PCC	HPC	CSA #1	CSA#2	RSCC	Avg. CSA
0								
-0.5	72	72	71	71	70	71	73	71
-1	72	72	71	71	71	71	72	71
-1.5	72	71	71	71	70	70	72	70
-2	72	71	71	71	71	71	72	71
-2.5	72	72	71	71	71	71	72	71
-3								

Table B.14 Slab temperature on 8/17/2010

8/17/2010	Slab Temperature (°F)							
Depth (in.)	PCC+Ecl.	PCC+Tet.	PCC	HPC	CSA #1	CSA#2	RSCC	Avg. CSA
0								
-0.5	71	71	71	71	70	70	72	70
-1	72	71	71	71	71	71	72	71
-1.5	72	71	71	71	70	70	72	70
-2	72	71	72	71	71	71	72	71
-2.5	72	71	71	71	70	71	72	71
-3								

Table B.15 Slab temperature on 8/24/2010

8/24/2010	Slab Temperature (°F)							
Depth (in.)	PCC+Ecl.	PCC+Tet.	PCC	HPC	CSA #1	CSA#2	RSCC	Avg. CSA
0								
-0.5	71	71	71	71	70	71	72	71
-1	72	71	71	71	71	71	72	71
-1.5	71	71	71	71	70	70	72	70
-2	72	71	71	71	71	71	72	71
-2.5	71	71	71	71	71	71	72	71
-3								

Table B.16 Slab temperature on 8/31/2010

8/31/2010	Slab Temperature (°F)							
Depth (in.)	PCC+Ecl.	PCC+Tet.	PCC	HPC	CSA #1	CSA#2	RSCC	Avg. CSA
0								
-0.5	72	72	71	71	70	70	72	70
-1	72	72	72	71	71	71	72	71
-1.5	72	71	71	71	70	70	72	70
-2	72	71	72	71	71	71	72	71
-2.5	72	71	71	71	71	71	72	71
-3								

Table B.17 Slab temperature on 9/7/2010

9/7/2010	Slab Temperature (°F)							
Depth (in.)	PCC+Ecl.	PCC+Tet.	PCC	HPC	CSA #1	CSA#2	RSCC	Avg. CSA
0								
-0.5	71	71	71	71	70	71	72	71
-1	71	71	71	71	71	71	72	71
-1.5	71	71	71	71	70	70	72	70
-2	71	71	71	71	71	71	72	71
-2.5	71	71	71	71	70	70	72	70
-3								

Table B.18 Slab temperature on 9/14/2010

9/14/2010	Slab Temperature (°F)							
Depth (in.)	PCC+Ecl.	PCC+Tet.	PCC	HPC	CSA #1	CSA#2	RSCC	Avg. CSA
0								
-0.5	72	71	71	71	70	71	72	71
-1	72	71	71	71	71	71	72	71
-1.5	71	71	71	71	70	70	72	70
-2	72	71	72	71	71	71	72	71
-2.5	72	71	71	71	71	71	72	71
-3								

Table B.19 Slab temperature on 10/12/2010

10/12/2010	Slab Temperature (°F)							
Depth (in.)	PCC+Ecl.	PCC+Tet.	PC C	HPC	CSA #1	CSA#2	RSCC	Avg. CSA
0								
-0.5	69	69	68	68	68	68	70	68
-1	69	69	69	68	69	68	69	69
-1.5	69	68	68	68	68	68	69	68
-2	69	68	69	68	68	68	70	68
-2.5	69	69	68	68	68	68	70	68
-3								

Table B.20 Slab temperature on 11/9/2010

11/9/2010	Slab Temperature (°F)							
Depth (in.)	PCC+Ecl.	PCC+Tet.	PCC	HPC	CSA #1	CSA#2	RSCC	Avg. CSA
0								
-0.5	72	72	71	72	71	71	72	71
-1	72	72	72	72	72	71	71	72
-1.5	71	72	71	71	71	71	71	71
-2	72	71	72	71	71	71	71	71
-2.5	72	72	71	71	71	71	72	71
-3								

Table B.21 Slab temperature on 12/7/2010

12/7/2010	Slab Temperature (°F)							
Depth (in.)	PCC+Ecl.	PCC+Tet.	PCC	HPC	CSA #1	CSA#2	RSCC	Avg. CSA
0								
-0.5	71	71	71	71	71	71	71	71
-1	71	71	71	71	72	71	70	72
-1.5	71	71	71	71	71	71	70	71
-2	71	71	72	71	71	71	70	71
-2.5	71	71	71	71	71	71	70	71
-3								

Table B.22 Slab temperature on 12/14/2010

12/14/2010	Slab Temperature (°F)							
Depth (in.)	PCC+Ecl.	PCC+Tet.	PCC	HPC	CSA #1	CSA#2	RSCC	Avg. CSA
0								
-0.5	71	71	71	71	71	71	70	71
-1	71	71	71	71	72	71	70	72
-1.5	71	71	71	71	71	71	70	71
-2	71	71	71	71	71	71	70	71
-2.5	71	71	71	71	71	70	70	71
-3								

Table B.23 Slab temperature on 1/11/2011

1/11/2011	Slab Temperature (°F)							
Depth (in.)	PCC+Ecl.	PCC+Tet.	PCC	HPC	CSA #1	CSA#2	RSCC	Avg. CSA
0								
-0.5	70	71	71	70	70	70	70	70
-1	70	71	71	71	71	70	68	71
-1.5	70	71	71	70	70	70	68	70
-2	70	71	71	71	70	70	69	70
-2.5	70	71	71	71	70	70	69	70
-3								

Table B.24 Slab temperature on 2/8/2011

2/8/2011	Slab Temperature (°F)							
Depth (in.)	PCC+Ecl.	PCC+Tet.	PCC	HPC	CSA #1	CSA#2	RSCC	Avg. CSA
0								
-0.5	71	72	72	72	71	70	70	71
-1	71	72	72	72	72	71	69	72
-1.5	71	72	72	72	71	71	69	71
-2	71	72	72	72	71	71	69	71
-2.5	71	72	72	72	71	70	70	71
-3								

Table B.25 Slab temperature on 2/22/2011

2/22/2011	Slab Temperature (°F)							
Depth (in.)	PCC+Ecl.	PCC+Tet.	PCC	HPC	CSA #1	CSA#2	RSCC	Avg. CSA
0								
-0.5	72	72	72	72	72	71	71	72
-1	72	72	72	72	72	71	71	72
-1.5	71	72	72	72	71	71	70	71
-2	72	72	72	72	72	71	70	72
-2.5	71	72	72	72	72	71	71	72
-3								

Table B.26 Slab temperature on 3/15/2011

3/15/2011	Slab Temperature (°F)							
Depth (in.)	PCC+Ecl.	PCC+Tet.	PCC	HPC	CSA #1	CSA#2	RSCC	Avg. CSA
0								
-0.5	72	72	72	72	71	71	71	71
-1	72	72	72	72	72	71	71	72
-1.5	71	72	72	72	71	71	70	71
-2	72	72	72	72	72	71	71	72
-2.5	71	72	72	72	72	71	70	72
-3								

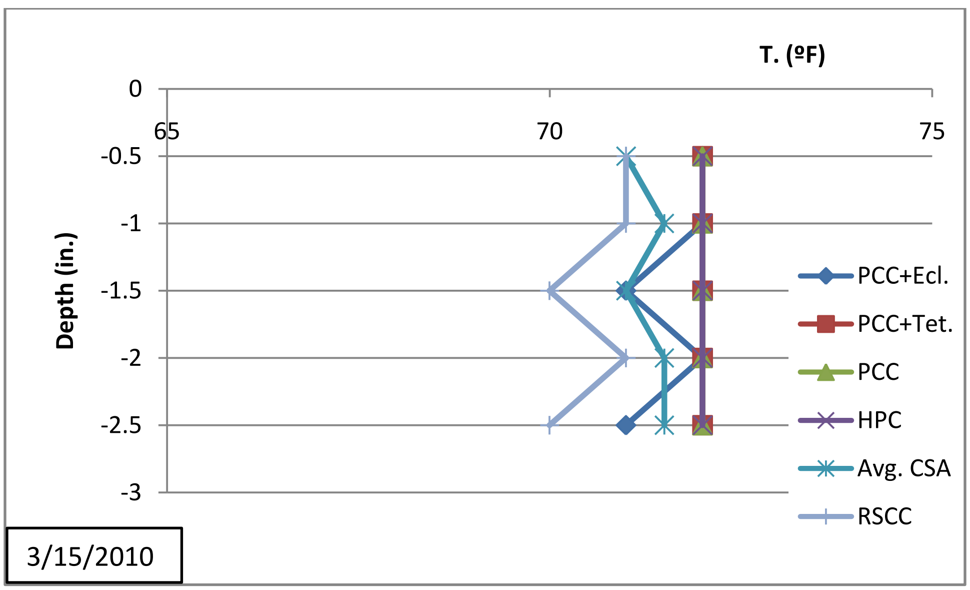

Figure B.77 Slab temperature on 3/15/2011

Note: There is *No Changes* in temperature with slab depth. This means that the ambient temperature was constant (70 ºF). Thus, only one graph is provided as a sample for the interior slab temperature on day 3/15/2010.

B.8.5. Relative Humidity through Depth of Slabs

Note: PCC+Ecl. and PCC+Tet. are abbreviations for PCC+Eclipse and PCC+Tetraguard respectively.

Table B.27 Slab relative humidity on 1/19/2010

1/19/2010	Slab Relative Humidity (%)							
Depth (in.)	PCC+Ecl.	PCC+Tet.	PCC	HPC	CSA #1	CSA#2	RSCC	Avg. CSA
0								
-0.5	77	77	74	66	86	87	93	87
-1	84	81	77	69	89	95	93	92
-1.5	94	89	87	81	94	99	92	97
-2	98	94	91	88	99	99	94	99
-2.5	99	99	96	99	99	99	94	99
-3								

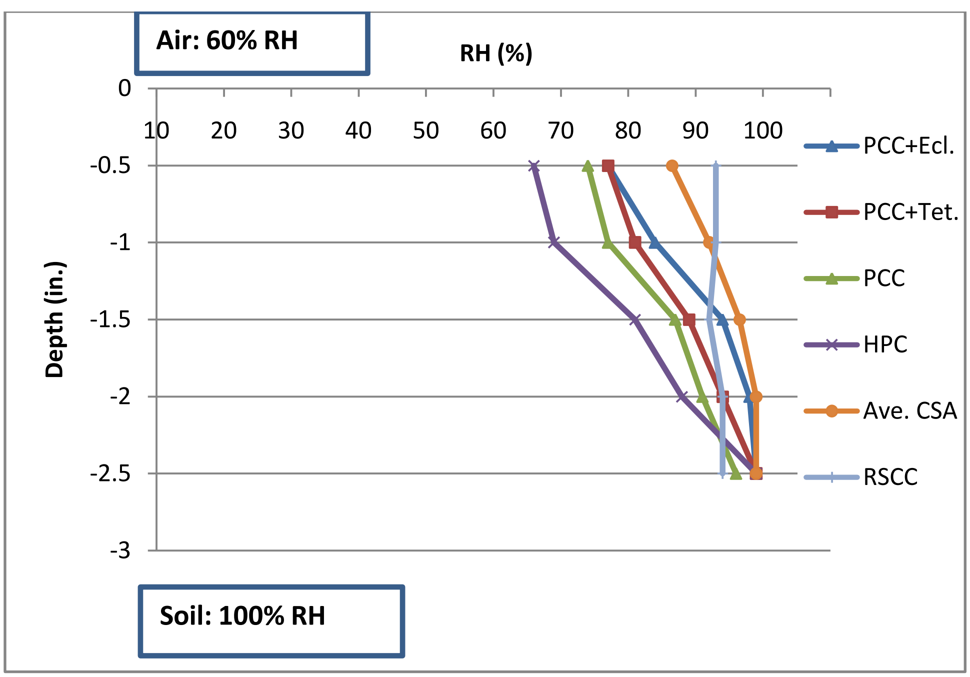

Figure B.78 Slab relative humidity on 1/19/2010

Table B.28 Slab relative humidity on 1/26/2010

1/26/2010	Slab Relative Humidity (%)							
Depth (in.)	PCC+Ecl.	PCC+Tet.	PCC	HPC	CSA #1	CSA#2	RSCC	Ave. CSA
0								
-0.5	62	69	67	48	82	82	84	82
-1	80	75	73	62	87	94	94	91
-1.5	92	87	85	78	94	98	95	96
-2	96	93	90	84	100	100	96	100
-2.5	100	99	96	100	100	100	100	100
-3								

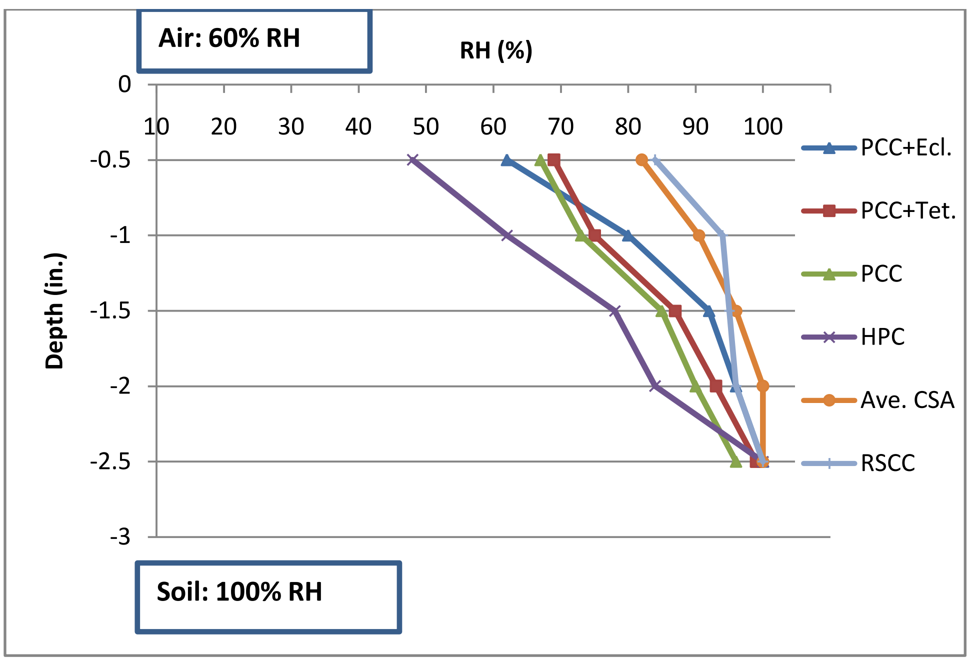

Figure B.79 Slab relative humidity on 1/26/2010

Table B.29 Slab relative humidity on 2/23/2010

2/23/2010	Slab Relative Humidity (%)							
Depth (in.)	PCC+Ecl.	PCC+Tet.	PCC	HPC	CSA #1	CSA#2	RSCC	Ave. CSA
0								
-0.5	48	56	59	41	73	75	48	74
-1	69	60	66	53	79	92	91	86
-1.5	87	80	80	70	92	97	96	95
-2	94	90	87	76	100	100	98	100
-2.5	99	97	95	100	100	100	100	100
-3								

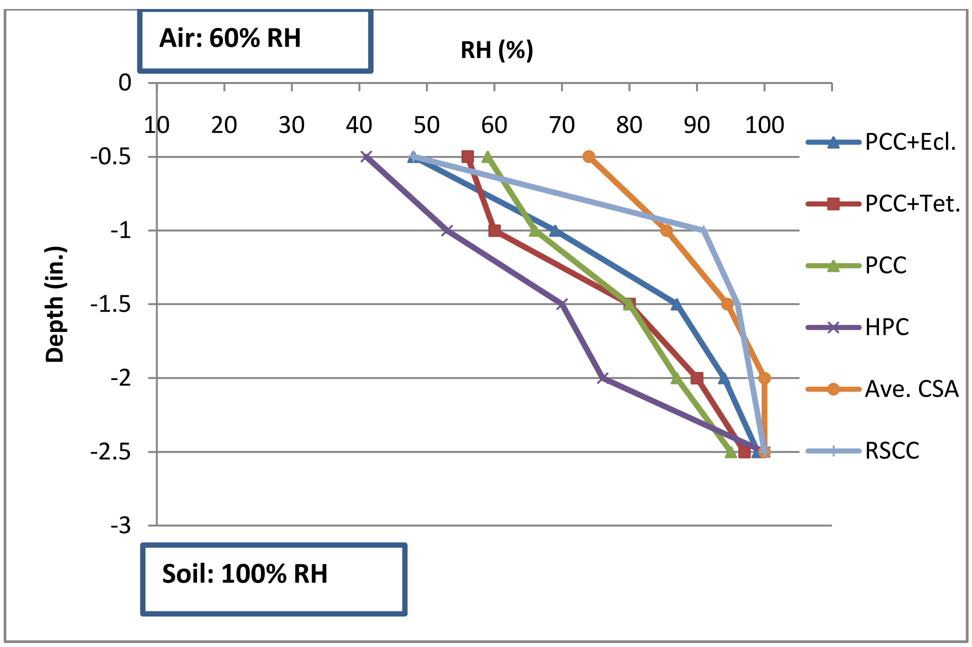

Figure B.80 Slab relative humidity on 2/23/2010

Table B.30 Slab relative humidity on 3/16/2010

3/16/2010	Slab Relative Humidity (%)							
Depth (in.)	PCC+Ecl.	PCC+Tet.	PCC	HPC	CSA #1	CSA#2	RSCC	Ave. CSA
0								
-0.5	55	61	62	48	75	77	58	76
-1	70	62	68	56	80	93	95	87
-1.5	87	79	80	70	93	98	99	96
-2	94	90	87	76	100	100	100	100
-2.5	99	97	95	100	100	100	100	100
-3								

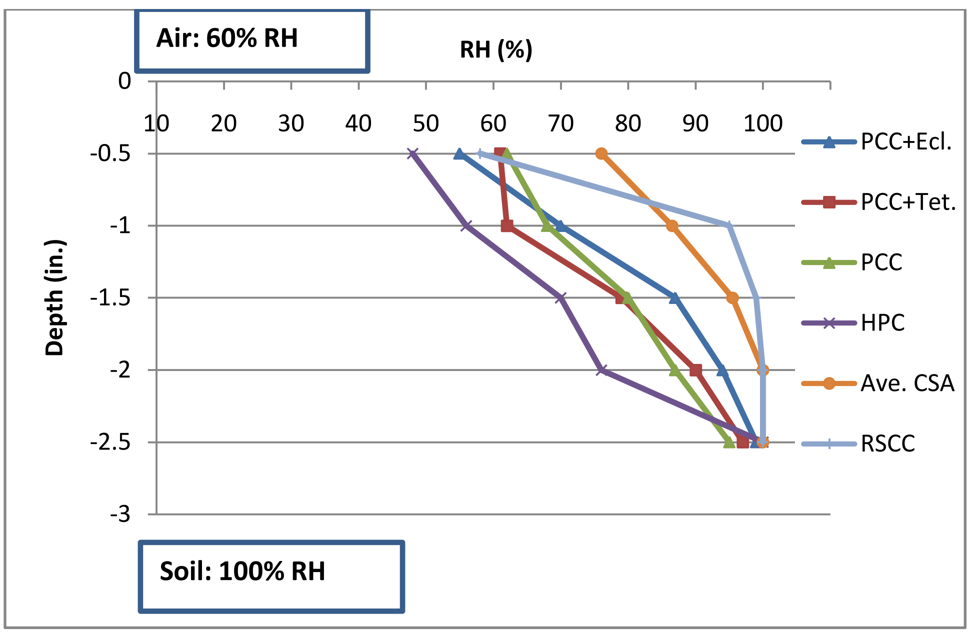

Figure B.81 Slab relative humidity on 3/16/2010

Table B.31 Slab relative humidity on 4/20/2010

4/20/2010	Slab Relative Humidity (%)							
Depth (in.)	PCC+Ecl.	PCC+Tet.	PCC	HPC	CSA #1	CSA#2	RSCC	Ave. CSA
0								
-0.5	70	72	73	64	83	85	73	84
-1	77	73	77	68	86	96	95	91
-1.5	89	83	85	77	95	100	98	98
-2	95	92	90	81	100	100	100	100
-2.5	99	98	96	100	100	100	100	100
-3	HI							

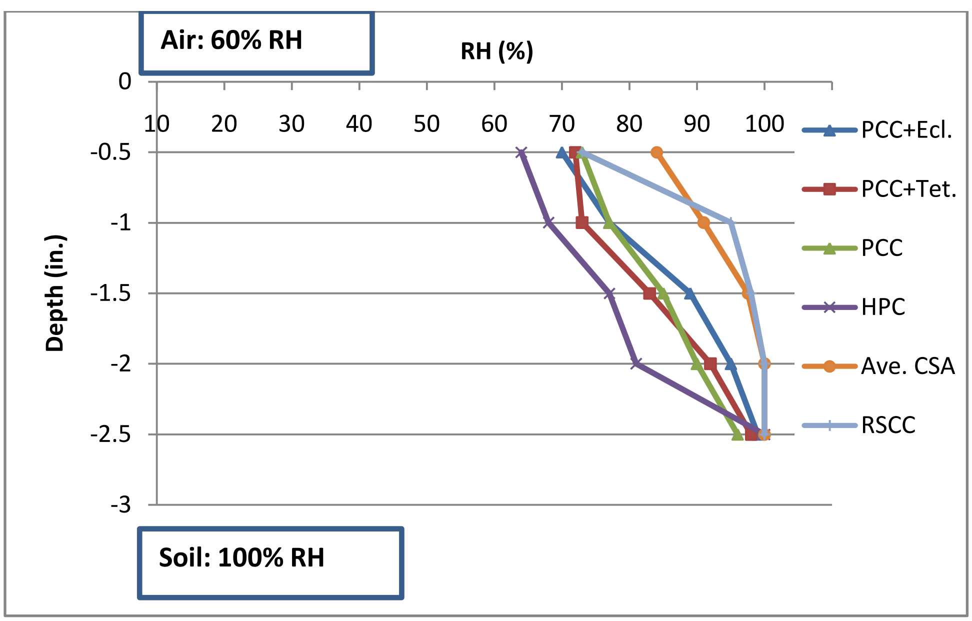

Figure B.82 Slab relative humidity on 4/20/2010

Table B.32 Slab relative humidity on 5/18/2010

5/18/2010	Slab Relative Humidity (%)							
Depth (in.)	PCC+Ecl.	PCC+Tet.	PCC	HPC	CSA #1	CSA#2	RSCC	Ave. CSA
0								
-0.5	83	83	84	80	91	93	86	92
-1	85	82	85	78	92	99	95	96
-1.5	93	89	90	83	97	100	99	99
-2	97	94	93	86	100	100	100	100
-2.5	100	99	98	100	100	100	100	100
-3								

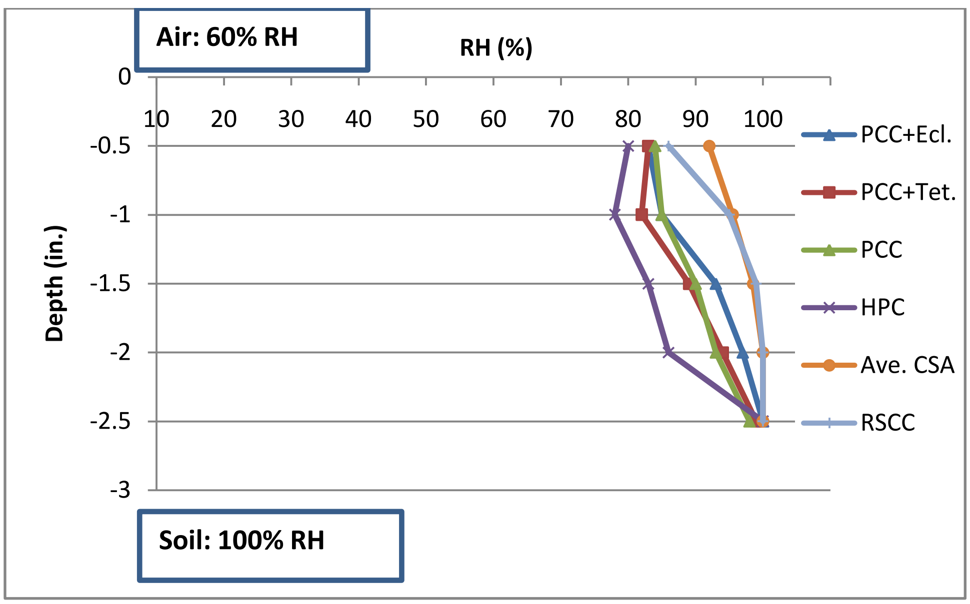

Figure B.83 Slab relative humidity on 5/18/2010

Table B.33 Slab relative humidity on 6/29/2010

6/29/2010	Slab Relative Humidity (%)							
Depth (in.)	PCC+Ecl.	PCC+Tet.	PCC	HPC	CSA #1	CSA#2	RSCC	Ave. CSA
0								
-0.5	66	69	71	61	81	77	64	79
-1	74	69	74	65	84	95	82	90
-1.5	87	81	83	74	94	99	92	97
-2	94	90	89	78	100	100	96	100
-2.5	100	97	95	100	100	100	100	100
-3								

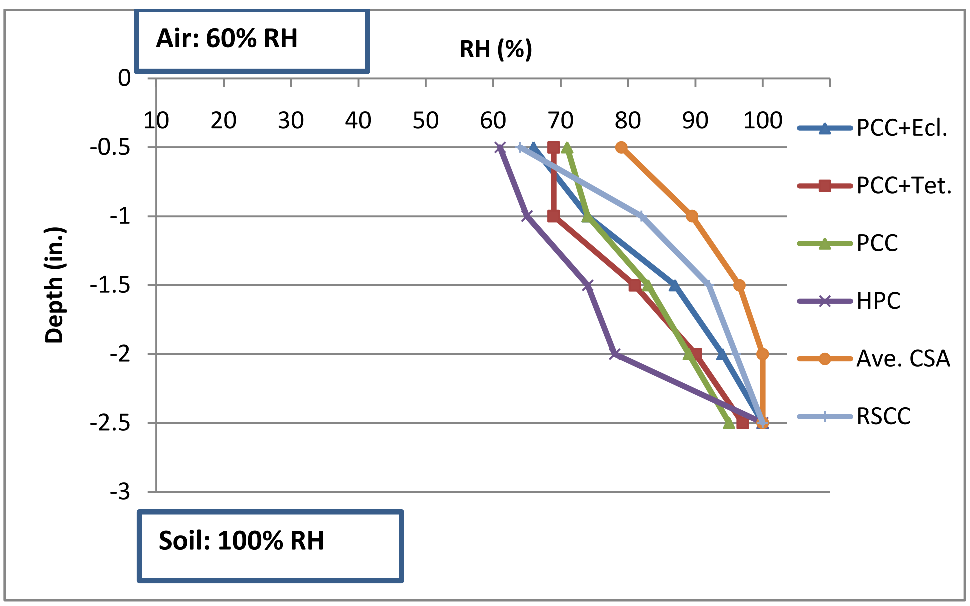

Figure B.84 Slab relative humidity on 6/29/2010

Table B.34 Slab relative humidity on 7/13/2010

7/13/2010	Slab Relative Humidity (%)							
Depth (in.)	PCC+Ecl.	PCC+Tet.	PCC	HPC	CSA #1	CSA#2	RSCC	Ave. CSA
0								
-0.5	68	70	73	63	83	79	61	81
-1	75	71	76	68	87	96	82	92
-1.5	87	82	84	76	95	99	91	97
-2	94	91	90	80	100	100	96	100
-2.5	100	97	96	100	100	100	100	100
-3								

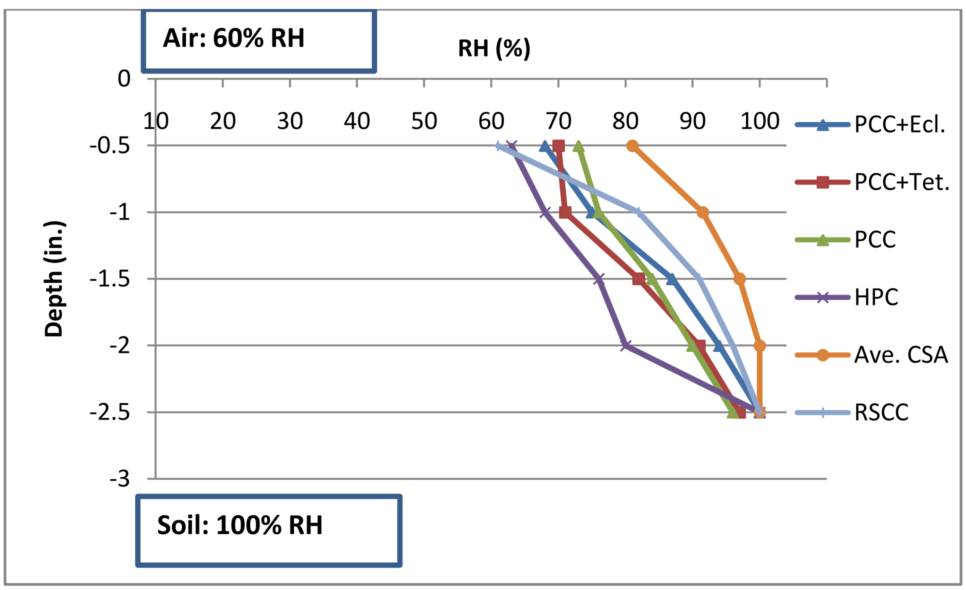

Figure B.85 Slab relative humidity on 7/13/2010

Table B.35 Slab relative humidity on 7/20/2010

7/20/2010	Slab Relative Humidity (%)							
Depth (in.)	PCC+Ecl.	PCC+Tet.	PCC	HPC	CSA #1	CSA#2	RSCC	Ave. CSA
0								
-0.5	63	67	69	60	81	3	59	42
-1	73	68	73	64	85	100	78	93
-1.5	86	80	83	74	95	100	88	98
-2	94	90	81	78	100	100	96	100
-2.5	99	96	95	100	100	100	100	100
-3								

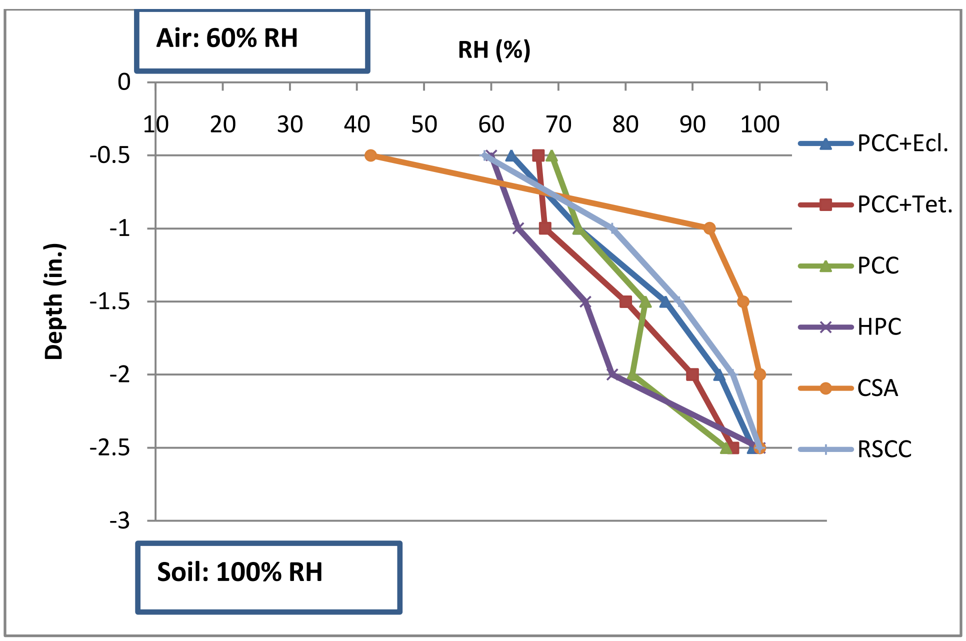

Figure B.86 Slab relative humidity on 7/20/2010

Table B.36 Slab relative humidity on 7/27/2010

7/27/2010	Slab Relative Humidity (%)							
Depth (in.)	PCC+Ecl.	PCC+Tet.	PCC	HPC	CSA #1	CSA#2	RSCC	Ave. CSA
0								
-0.5	67	69	71	66	82	5	66	44
-1	73	70	74	66	85	97	79	91
-1.5	86	80	83	74	94	100	88	97
-2	94	90	88	77	100	100	95	100
-2.5	99	96	95	100	100	100	100	100
-3								

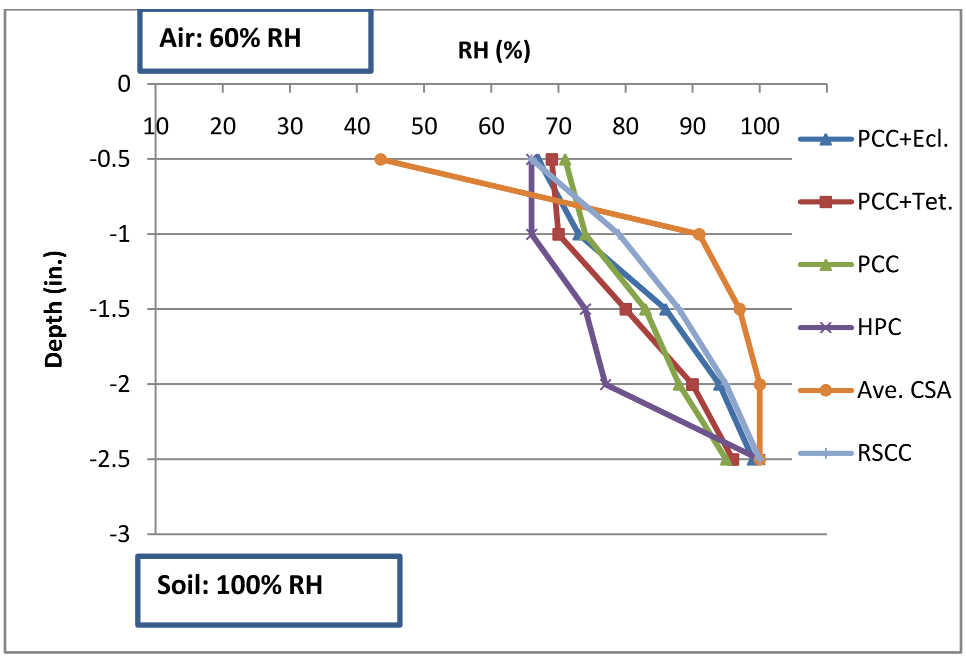

Figure B.87 Slab relative humidity on 7/27/2010

Table B.37 Slab relative humidity on 8/3/2010

8/3/2010	Slab Relative Humidity (%)							
Depth (in.)	PCC+Ecl.	PCC+Tet.	PCC	HPC	CSA #1	CSA#2	RSCC	Ave. CSA
0								
-0.5	59	63	66	55	78	5	51	42
-1	69	64	70	61	83	97	74	90
-1.5	84	77	81	71	94	100	86	97
-2	92	89	88	75	100	100	94	100
-2.5	99	96	95	100	100	100	100	100
-3								

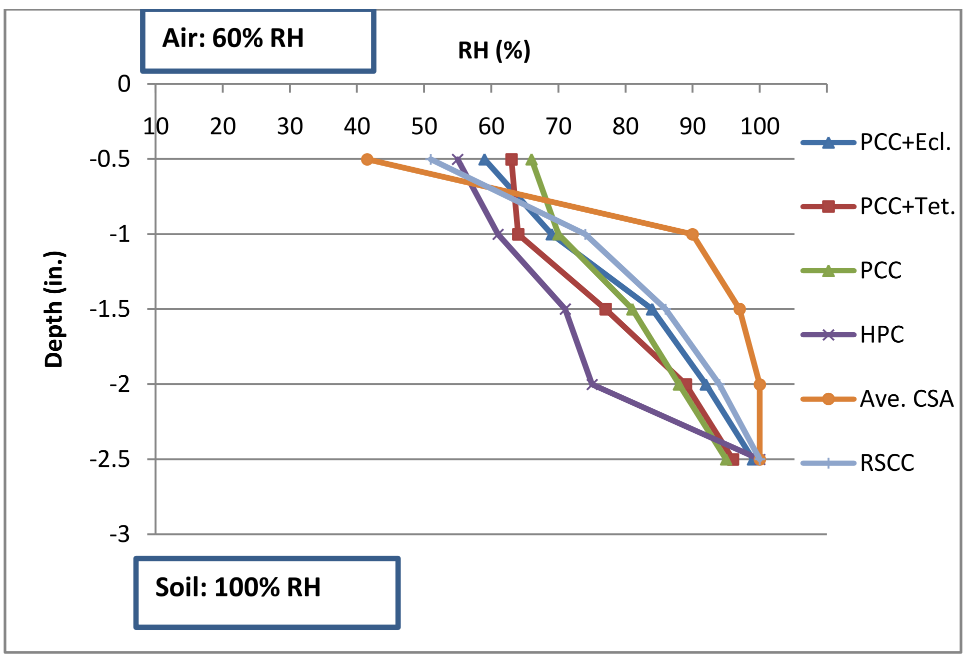

Figure B.88 Slab relative humidity on 8/3/2010

Table B.38 Slab relative humidity on 8/10/2010

8/10/2010	Slab Relative Humidity (%)							
Depth (in.)	PCC+Ecl.	PCC+Tet.	PCC	HPC	CSA #1	CSA#2	RSCC	Ave. CSA
0								
-0.5	57	62	65	54	77	6	50	42
-1	68	63	69	60	82	96	72	89
-1.5	83	77	80	70	94	100	83	97
-2	92	89	87	74	100	100	94	100
-2.5	99	96	94	100	100	100	100	100
-3								

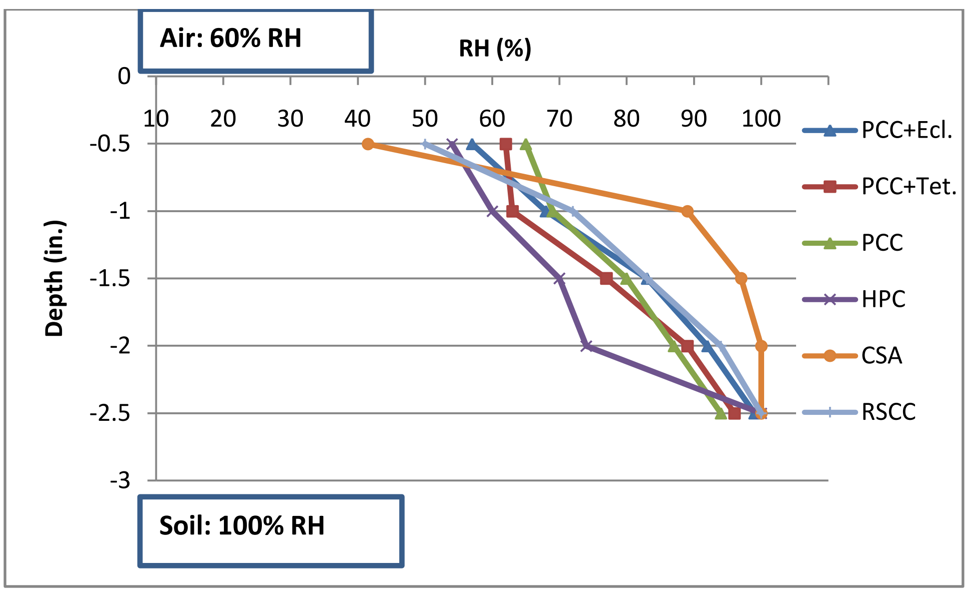

Figure B.89 Slab relative humidity on 8/10/2010

Table B.39 Slab relative humidity on 8/17/2010

8/17/2010	Slab Relative Humidity (%)							
Depth (in.)	PCC+Ecl.	PCC+Tet.	PCC	HPC	CSA #1	CSA#2	RSCC	Ave. CSA
0								
-0.5	59	63	65	55	77	4	53	41
-1	69	64	69	60	82	96	71	89
-1.5	83	77	80	70	94	100	82	97
-2	92	88	87	74	100	100	92	100
-2.5	99	96	94	100	100	100	100	100
-3								

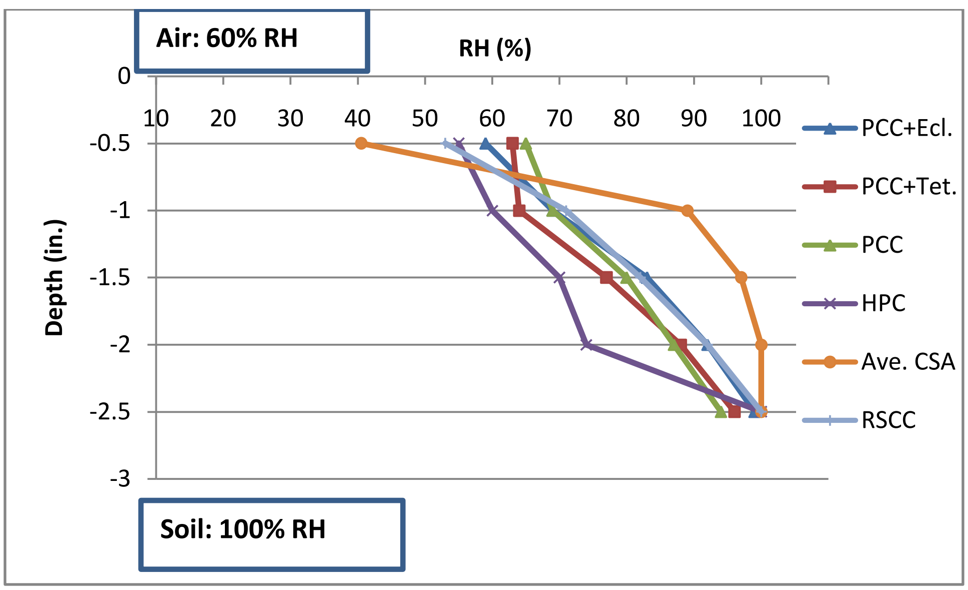

Figure B.90 Slab relative humidity on 8/17/2010

Note: Relative humidity was reduced from 60% to 30% with Dehumidifier on day 8/17/2010.

Table B.40 Slab relative humidity on 8/24/2010

8/24/2010	Slab Relative Humidity (%)							
Depth (in.)	PCC+Ecl.	PCC+Tet.	PCC	HPC	CSA #1	CSA#2	RSCC	Ave. CSA
0								
-0.5	60	64	66	57	78	3	55	41
-1	69	64	70	60	82	96	71	89
-1.5	83	77	80	69	94	100	82	97
-2	92	88	87	74	100	100	92	100
-2.5	99	96	94	100	100	100	100	100
-3								

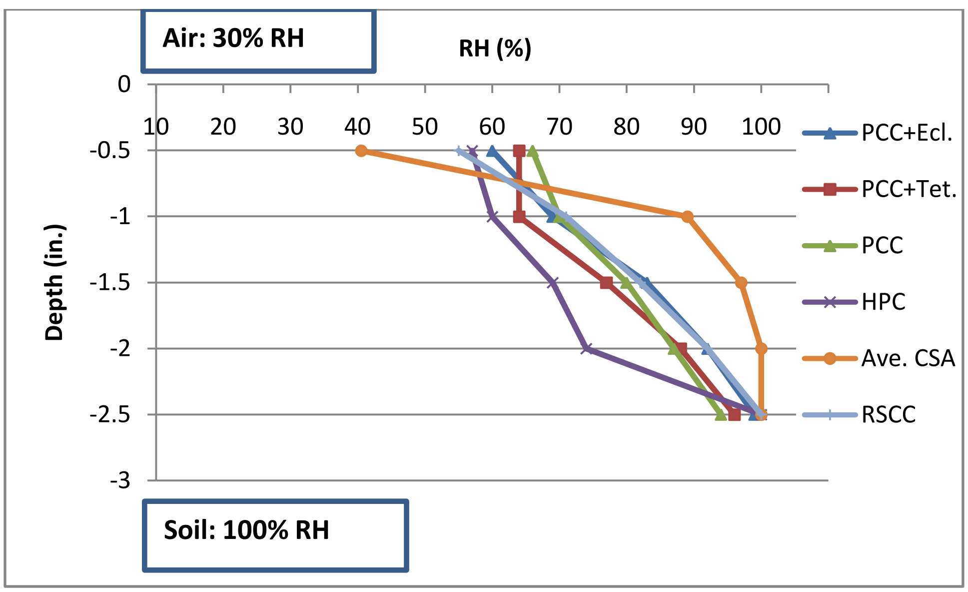

Figure B.91 Slab relative humidity on 8/24/2010

Table B.41 Slab relative humidity on 8/31/2010

8/31/2010	Slab Relative Humidity (%)							
Depth (in.)	PCC+Ecl.	PCC+Tet.	PCC	HPC	CSA #1	CSA#2	RSCC	Ave. CSA
0								
-0.5	56	60	62	52	76	12	48	44
-1	66	61	67	57	80	95	68	88
-1.5	82	75	78	68	93	100	79	97
-2	91	88	86	72	100	100	91	100
-2.5	98	95	94	100	100	100	100	100
-3								

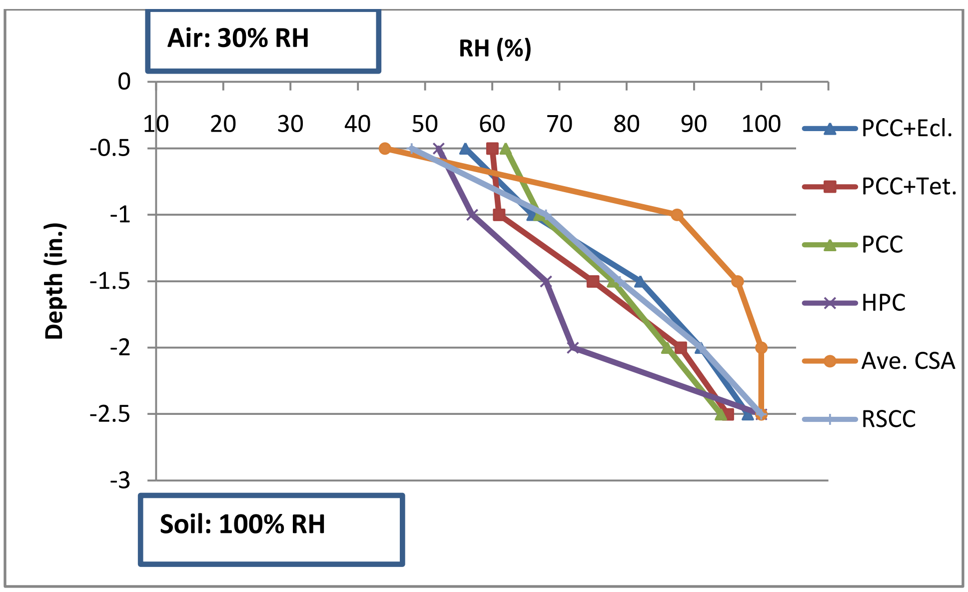

Figure B.92 Slab relative humidity on 8/31/2010

Table B.42 Slab relative humidity on 9/7/2010

9/7/2010	Slab Relative Humidity (%)							
Depth (in.)	PCC+Ecl.	PCC+Tet.	PCC	HPC	CSA #1	CSA#2	RSCC	Ave. CSA
0								
-0.5	54	58	61	49	73	23	47	48
-1	64	59	66	55	78	94	65	86
-1.5	81	73	77	66	92	99	77	96
-2	91	87	86	70	100	100	90	100
-2.5	98	95	94	100	100	100	100	100
-3								

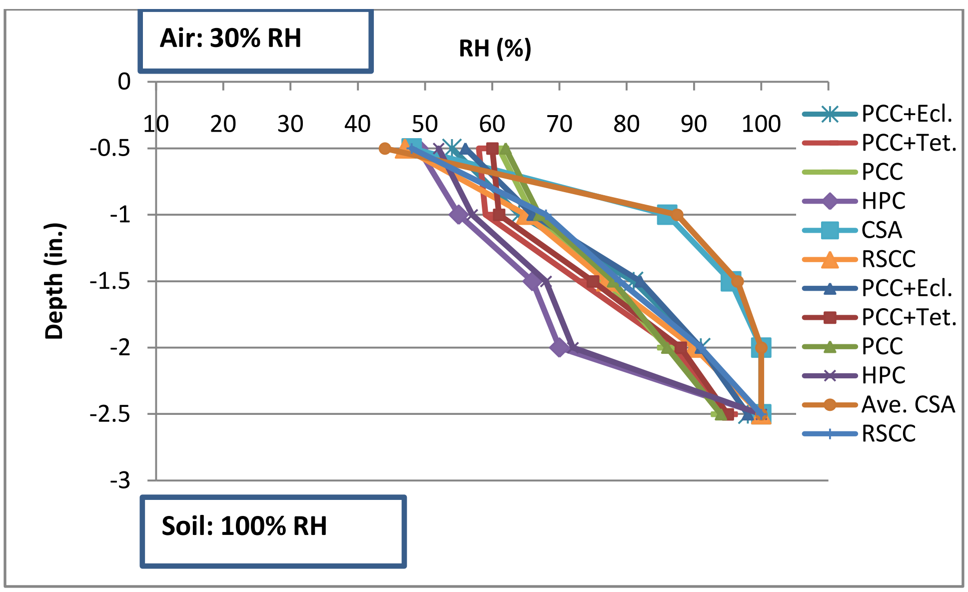

Figure B.93 Slab relative humidity on 9/7/2010

Table B.43 Slab relative humidity on 9/14/2010

9/14/2010	Slab Relative Humidity (%)							
Depth (in.)	PCC+Ecl.	PCC+Tet.	PCC	HPC	CSA #1	CSA#2	RSCC	Ave. CSA
0								
-0.5	55	59	61	51	75	14	48	45
-1	65	60	66	56	79	94	66	87
-1.5	81	73	77	67	93	99	77	96
-2	91	87	85	71	100	100	90	100
-2.5	98	95	94	100	100	100	100	100
-3								

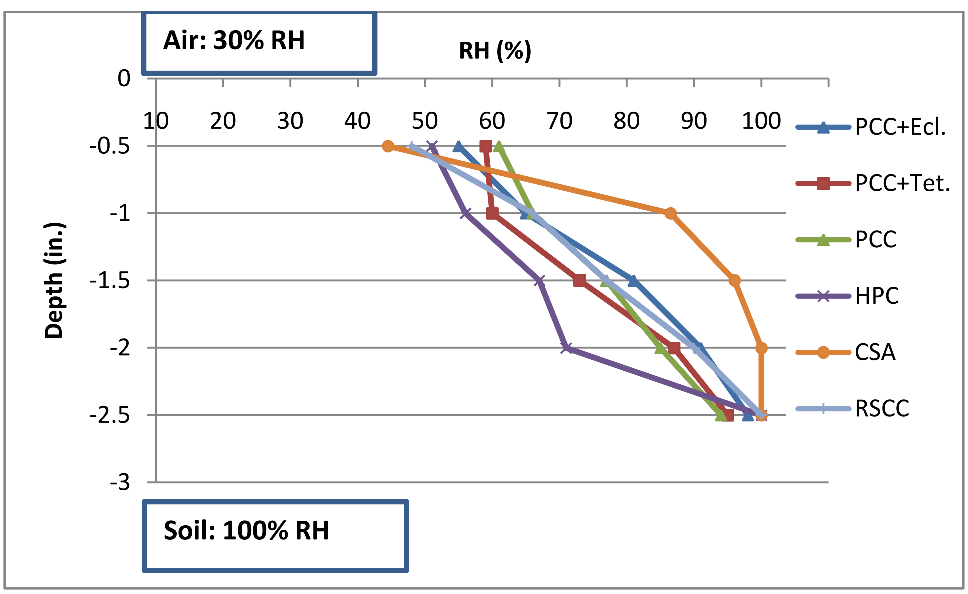

Figure B.94 Slab relative humidity on 9/14/2010

Table B.44 Slab relative humidity on 10/12/2010

10/12/2010	Slab Relative Humidity (%)							
Depth (in.)	PCC+Ecl.	PCC+Tet.	PCC	HPC	CSA #1	CSA#2	RSCC	Ave. CSA
0								
-0.5	50	55	58	46	71	46	44	59
-1	61	56	63	51	76	93	59	85
-1.5	78	70	75	62	92	99	69	96
-2	90	86	85	68	100	100	87	100
-2.5	97	94	93	100	100	100	100	100
-3								

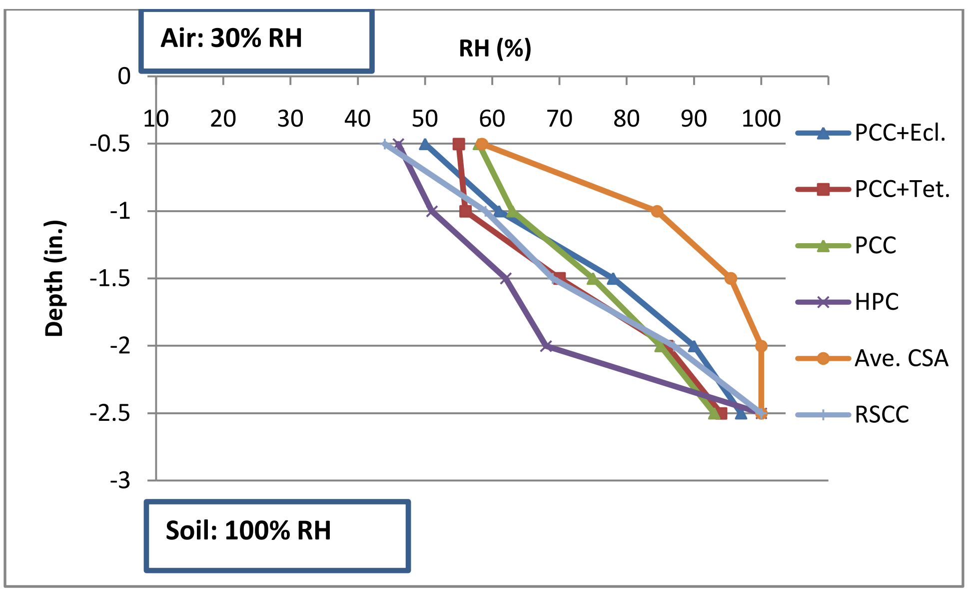

Figure B.95 Slab relative humidity on 10/15/2010

Table B.45 Slab relative humidity on 11/9/2010

11/9/2010	Slab Relative Humidity (%)							
Depth (in.)	PCC+Ecl.	PCC+Tet.	PCC	HPC	CSA #1	CSA#2	RSCC	Ave. CSA
0								
-0.5	47	50	55	43	68	57	43	63
-1	58	53	60	48	73	90	56	82
-1.5	76	67	73	60	90	96	65	93
-2	88	84	83	65	100	99	82	100
-2.5	96	92	92	100	100	99	100	100
-3								

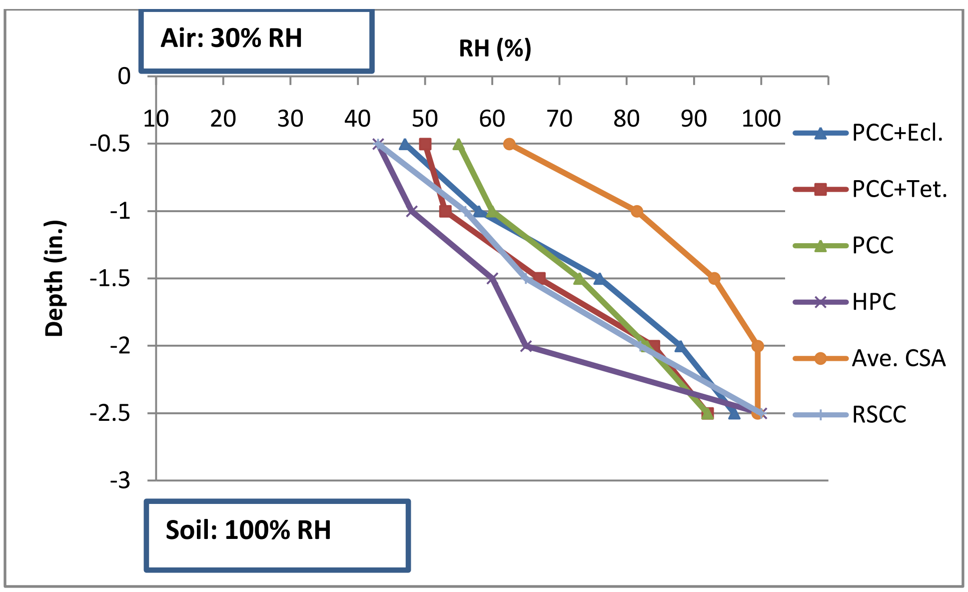

Figure B.96 Slab relative humidity on 11/9/2010

Table B.46 Slab relative humidity on 12/7/2010

12/7/2010	Slab Relative Humidity (%)							
Depth (in.)	PCC+Ecl.	PCC+Tet.	PCC	HPC	CSA #1	CSA#2	RSCC	Ave. CSA
0								
-0.5	35	37	44	30	58	50	27	54
-1	47	41	52	39	65	86	44	76
-1.5	69	59	67	52	87	95	53	91
-2	85	80	80	59	100	98	77	99
-2.5	96	91	90	100	100	99	100	100
-3								

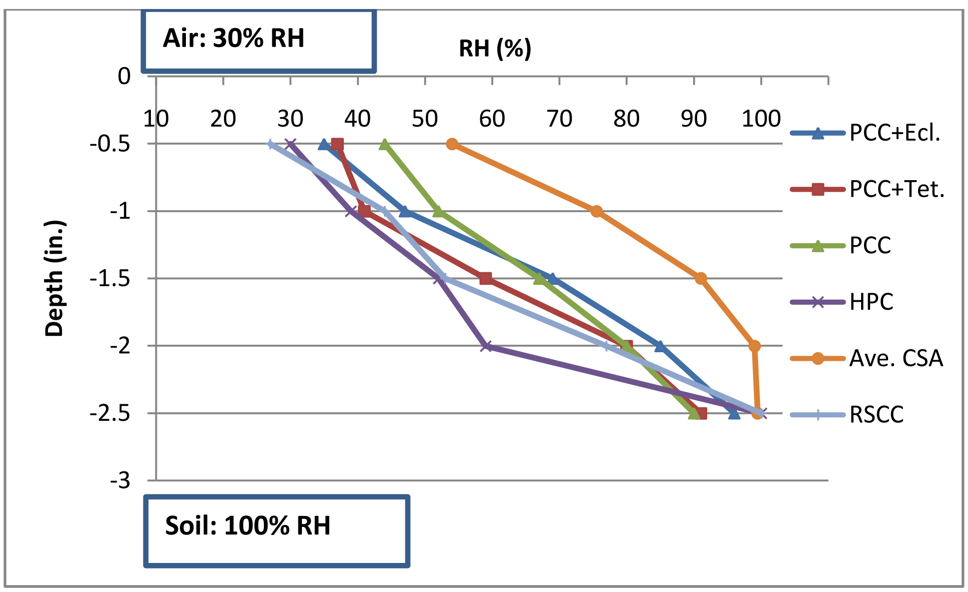

Figure B.97 Slab relative humidity on 12/7/2010

Table B.47 Slab relative humidity on 12/14/2010

12/14/2010	Slab Relative Humidity (%)							
Depth (in.)	PCC+Ecl.	PCC+Tet.	PCC	HPC	CSA #1	CSA#2	RSCC	Ave. CSA
0								
-0.5	30	33	41	27	55	46	22	51
-1	44	38	49	37	62	85	40	74
-1.5	66	56	65	50	86	94	50	90
-2	84	79	79	57	100	98	74	99
-2.5	95	90	90	100	100	99	100	100
-3								

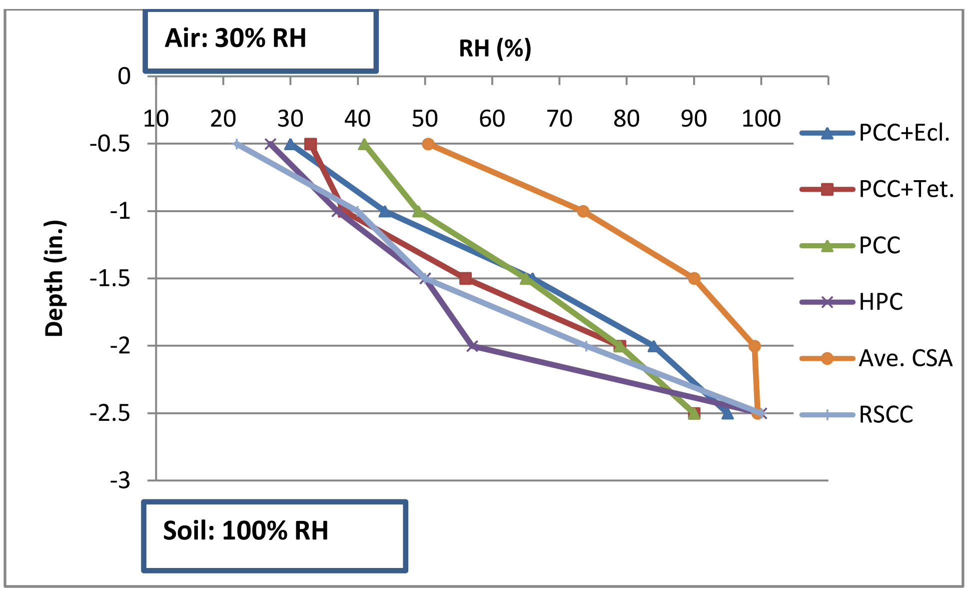

Figure B.98 Slab relative humidity on 12/14/2010

Table B.48 Slab relative humidity on 1/11/2011

1/11/2011	Slab Relative Humidity (%)							
Depth (in.)	PCC+Ecl.	PCC+Tet.	PCC	HPC	CSA #1	CSA#2	RSCC	Ave. CSA
0								
-0.5	28	31	39	24	53	45	20	49
-1	42	36	47	35	60	83	38	72
-1.5	63	54	62	47	84	94	47	89
-2	82	78	77	54	100	98	70	99
-2.5	94	90	89	100	100	98	100	99
-3								

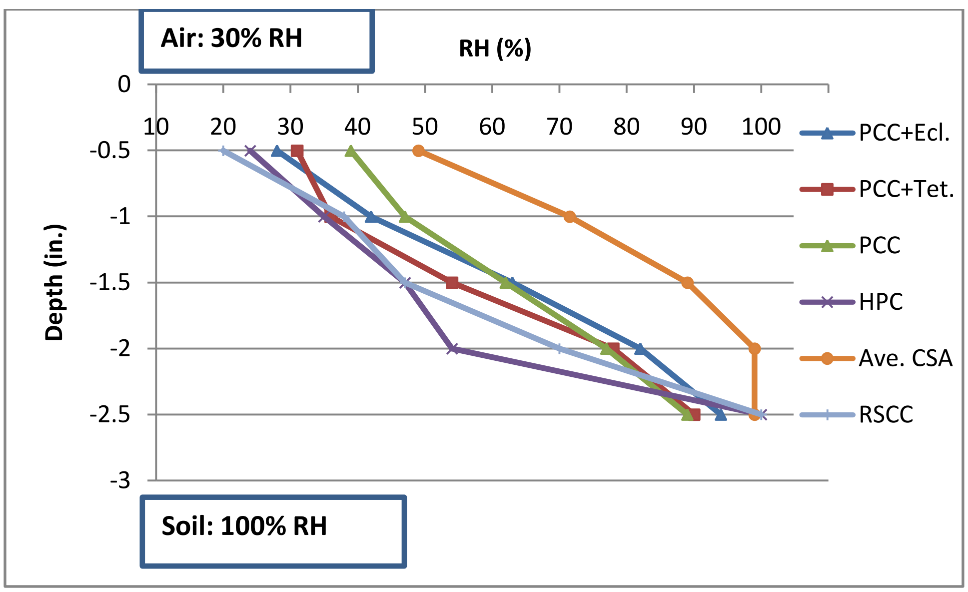

Figure B.99 Slab relative humidity on 1/11/2011

Table B.49 Slab relative humidity on 2/8/2011

2/8/2011	Slab Relative Humidity (%)							
Depth (in.)	PCC+Ecl.	PCC+Tet.	PCC	HPC	CSA #1	CSA#2	RSCC	Ave. CSA
0								
-0.5	33	35	42	29	48	48	27	48
-1	44	38	48	36	60	82	41	71
-1.5	63	54	62	47	83	93	47	88
-2	82	76	77	54	100	97	68	99
-2.5	94	89	88	100	100	98	100	99
-3								

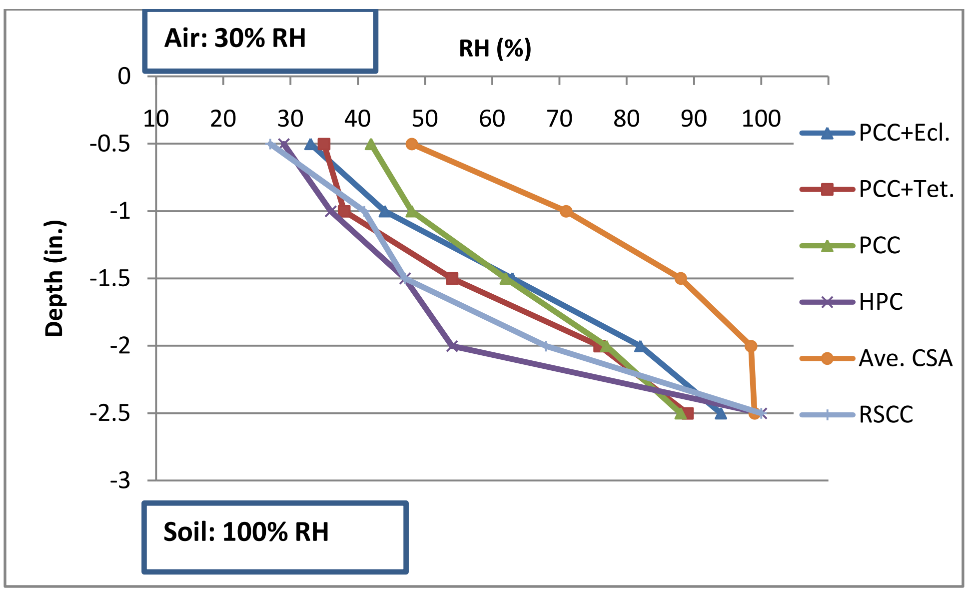

Figure B.100 Slab relative humidity on 2/8/2011

Table B.50 Slab relative humidity on 2/22/2011

2/22/2011	Slab Relative Humidity (%)							
Depth (in.)	PCC+Ecl.	PCC+Tet.	PCC	HPC	CSA #1	CSA#2	RSCC	Ave. CSA
0								
-0.5	35	37	44	31	50	50	28	50
-1	46	40	50	39	61	83	43	72
-1.5	65	56	63	51	83	93	50	88
-2	82	77	77	56	100	97	69	99
-2.5	94	88	88	100	100	98	100	99
-3								

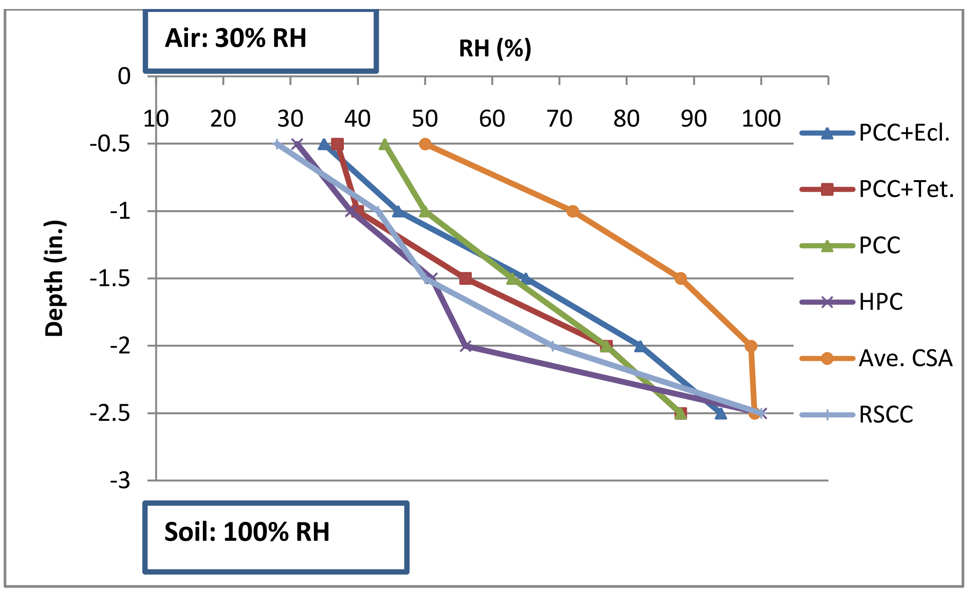

Figure B.101 Slab relative humidity on 2/22/2011

Table B.51 Slab relative humidity on 3/15/2011

3/15/2011	Slab Relative Humidity (%)							
Depth (in.)	PCC+Ecl.	PCC+Tet.	PCC	HPC	CSA #1	CSA#2	RSCC	Ave. CSA
0								
-0.5	37	39	45	33	52	52	31	52
-1	47	42	51	39	62	83	43	73
-1.5	65	57	63	50	83	93	49	88
-2	82	77	77	55	100	97	67	99
-2.5	94	89	88	100	100	98	100	99
-3								

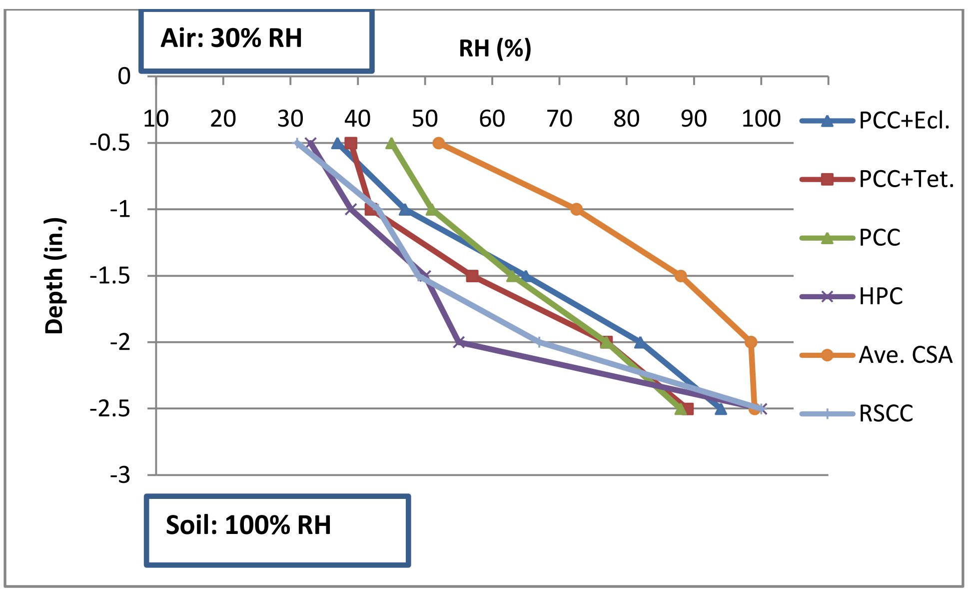

Figure B.102 Slab relative humidity on 3/15/2011

APPENDIX C

Additional Tests

Shrinkage from Time Zero Test Results

(Phase IV)

C.1. Concrete Mixes and Compressive Strength of Specimens Using "Shrinkage from Time Zero" Method

Table C.1 Materials used for the specimens

Materials (per cubic yard)	SRA#1	SRA#2	PCC	HPC	CTS Shrinkage Compensating Cement	Rapid Set
Komp I	-	-	-	-	120	-
P C	355	355	355	543	370	-
Flyash	88	88	88	180	-	-
Rapid Set Cement	-	-	-	-	-	658
Course Aggregate 57	1841	1841	1841	1841	1773	1773
Sand	1472	1472	1458	1188	1470	1293
Water	272	266	262	264	272	290
MR (Pozzolith 80 (oz))	14	14	14	29	65	52.6
Eclipse (oz)	13	-	-	-	-	-
Tetraguard (oz)	-	14	-	-	-	-
W/C ratio	0.61	0.60	0.59	0.37	0.55	0.44
Slump (in.)	3.5	4.0	2.0	0.0	2.5	1.5

Table C.2 Compressive strength

Day	SRA#1	SRA#2	PCC	HPC	Shrinkage Comp.	Rapid set
1	700	750	1000	2550	1150	5800
3	2300	2350	2550	4900	2600	6200
7	3250	3350	3250	5650	3250	6750
14	3400	3700	3750	4850	3900	6550
28	3700	4300	4100	6950	4950	6800

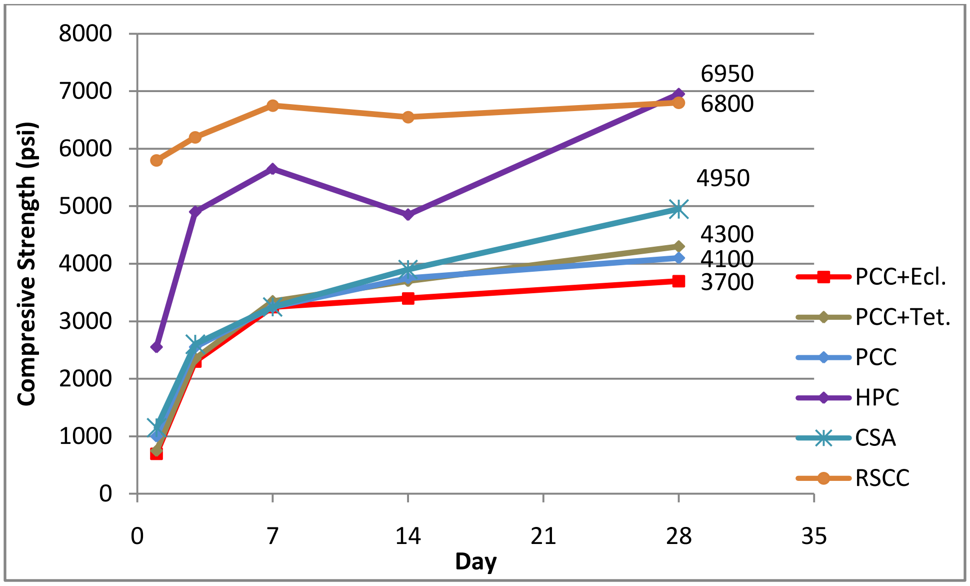

Figure C.1 Compressive strength for all specimens

C.2. Strain of Test Specimens for 28 Days Using Shrinkage from Time Zero

Note: The results are presented in two sections; results for 28 days (section C.2) and results for 110 days (section C.3). This is due to providing data for the first 28 days clearly and then for the longer period of time.

C.2.1 Strain of the Specimens Measured with Dial Gage (Dial Indicator)

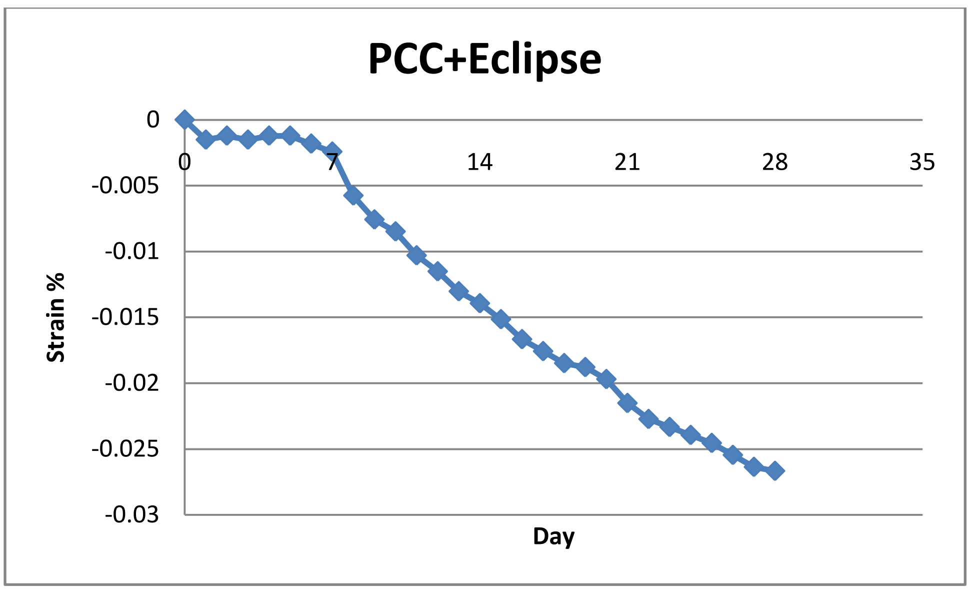

Figure C.2 Shrinkage from time zero using PCC+ Eclips (SRA)

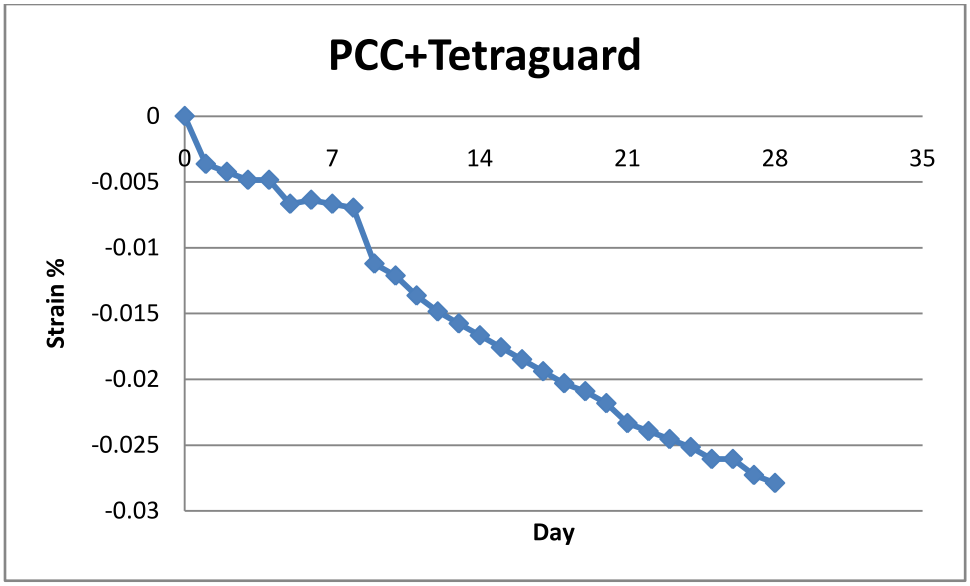

Figure C.3 Shrinkage from time zero using PCC+ Tetraguard (SRA)

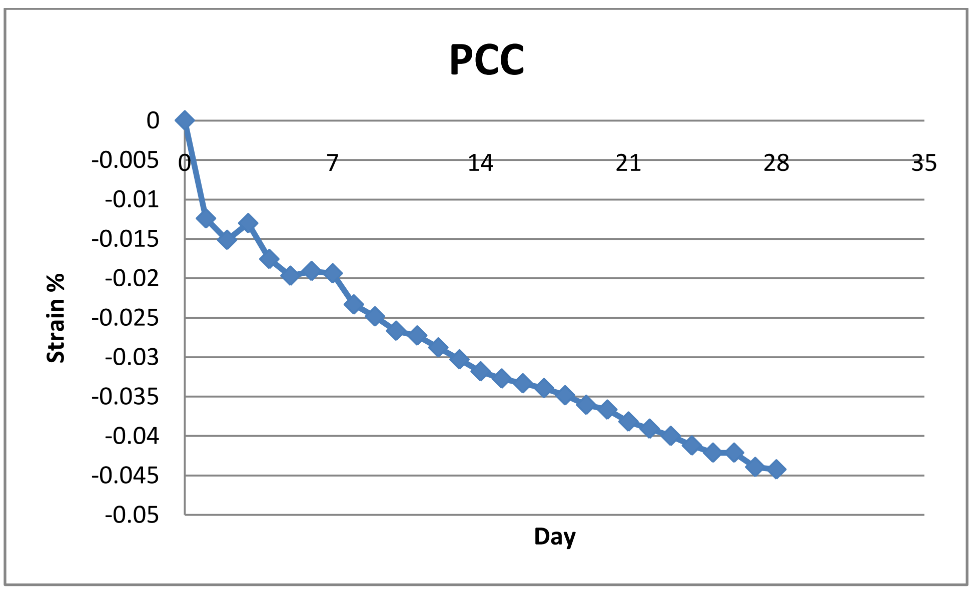

Figure C.4 Shrinkage from time zero using PCC

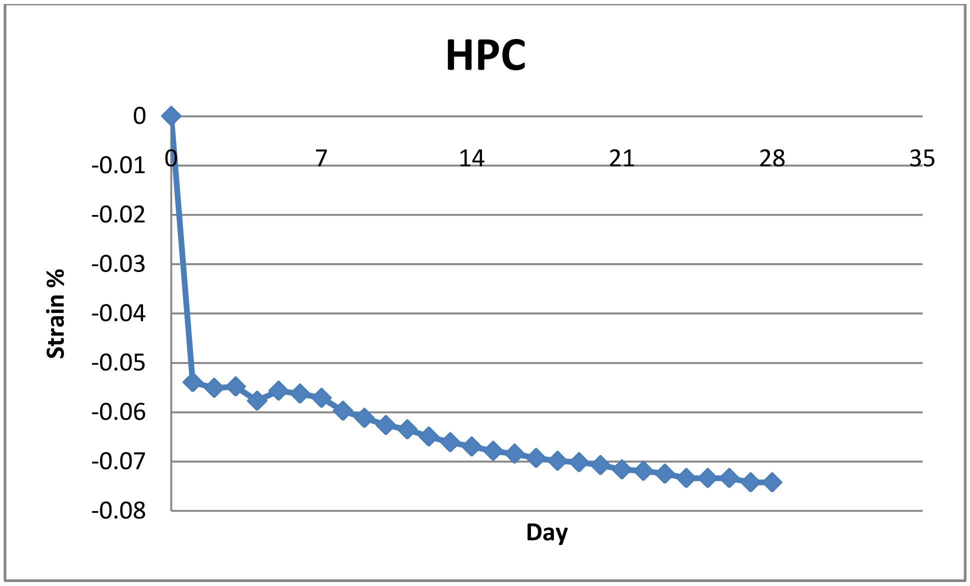

Figure C.5 Shrinkage from time zero using HPC

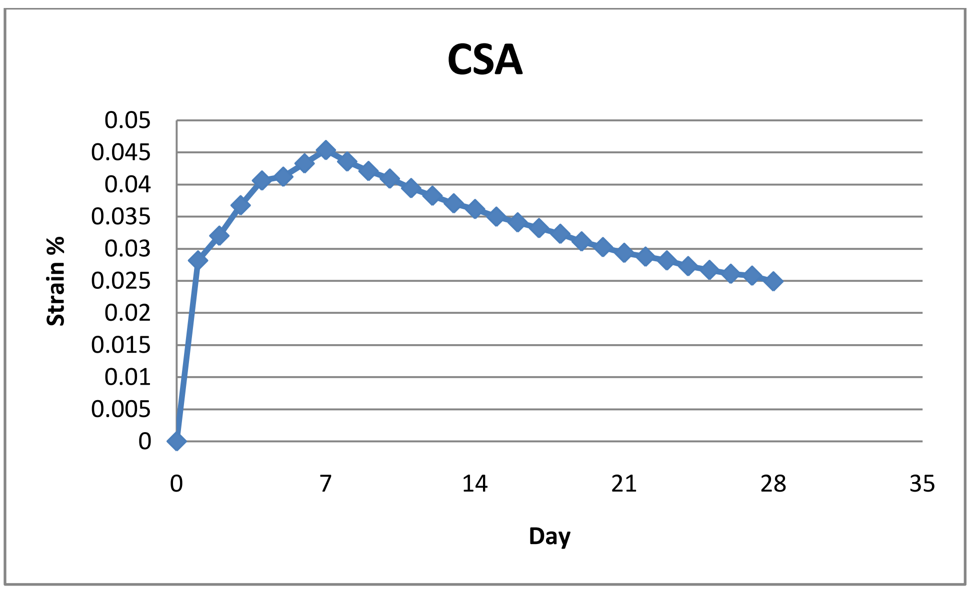

Figure C.6 Shrinkage from time zero using CSA

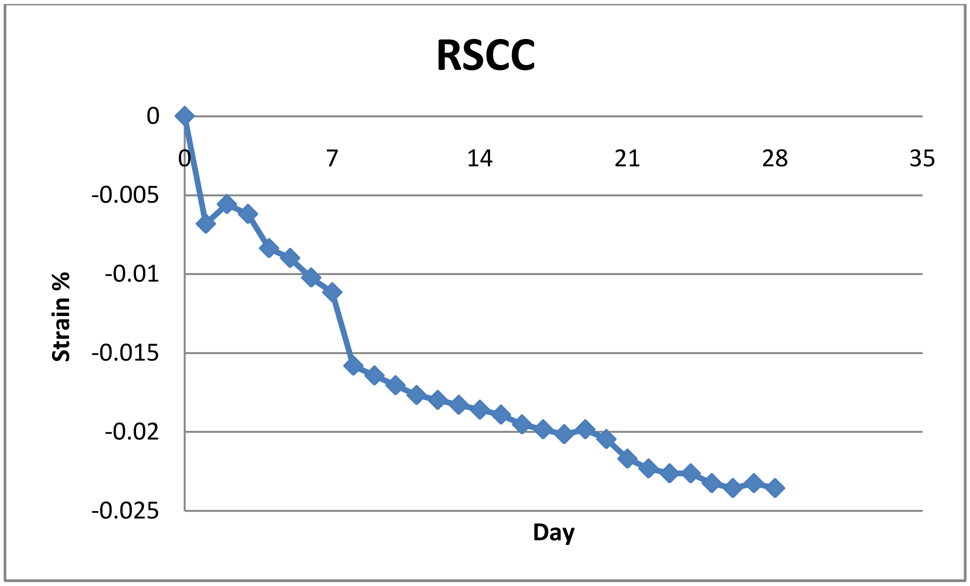

Figure C.7 Shrinkage from time zero using RSCC

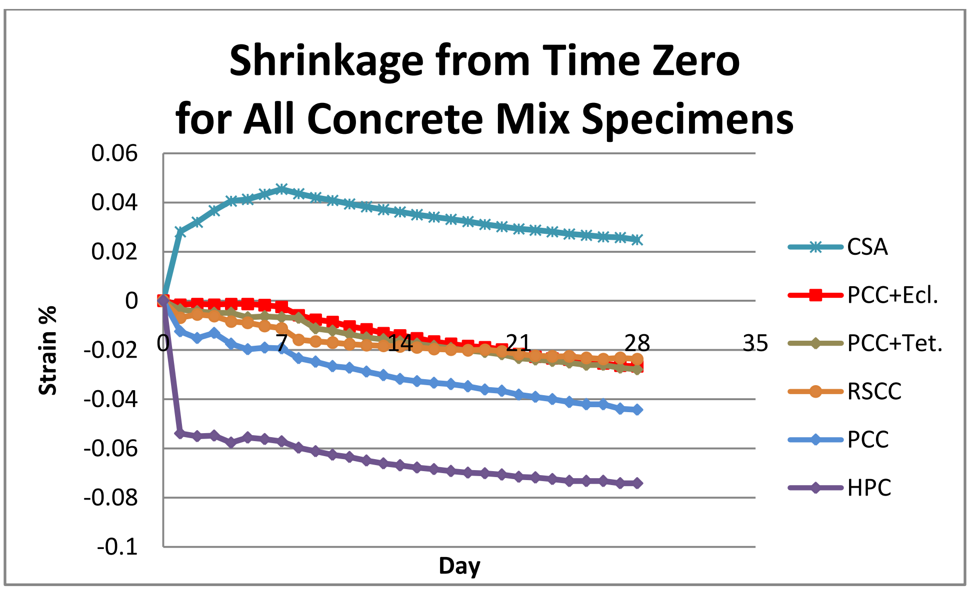

Figure C.8 Shrinkage from time zero for all specimens for 28 days

C.2.2. Two Methods Test Results Comparison (28 Days)

Note: As previously mentioned, the two methods are compared for 28 days and 110 days to provide more clear data for 28 days and then longer period of time. In this section and C.2.3, 28 days test results for shrinkage from time zero is compared with ASTM C 157, C 878 and slab on grade.

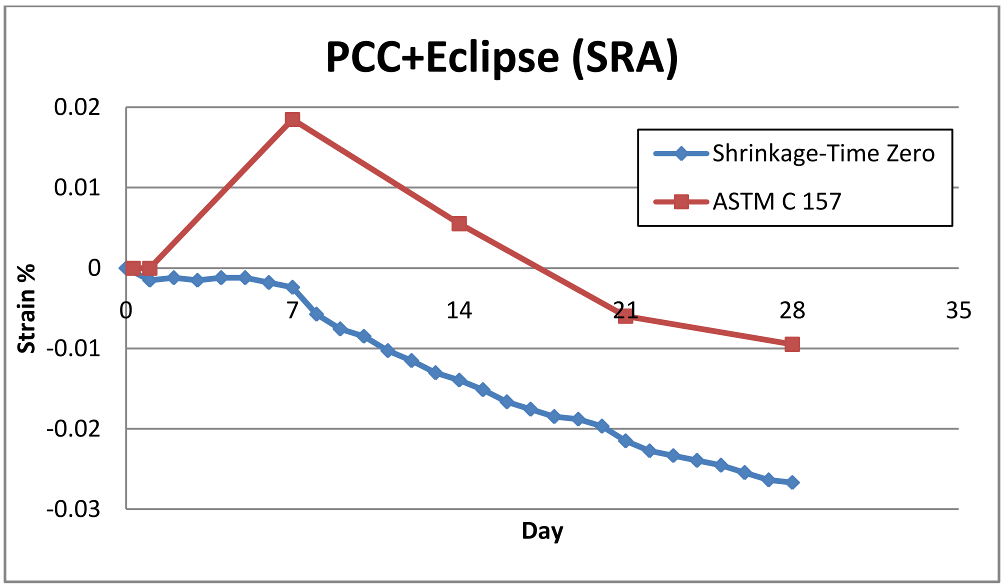

Figure C.9 Shrinkage from Time Zero vs. ASTM C 157 using PCC+Eclipse

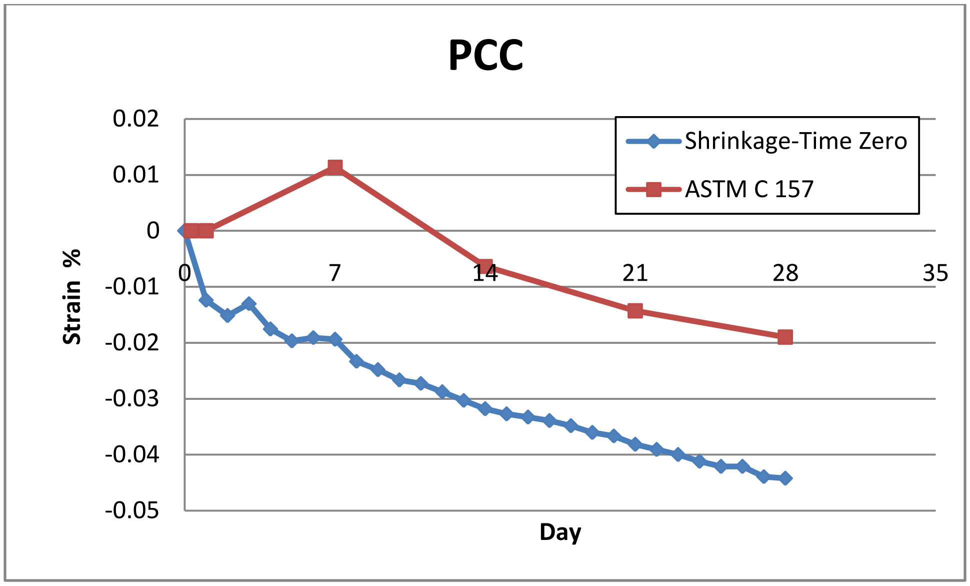

Figure C.10 Shrinkage from Time Zero vs. ASTM C 157 using PCC

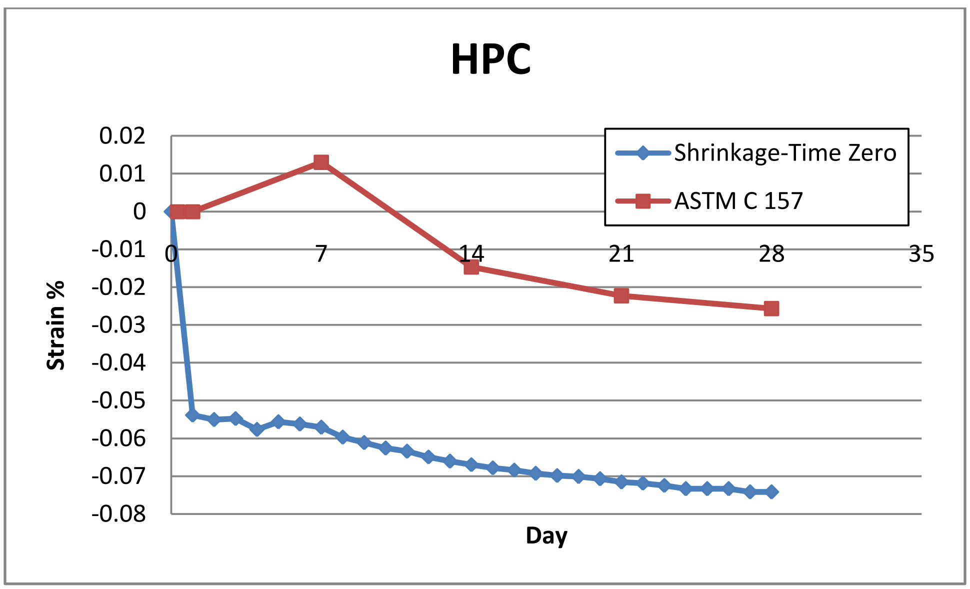

Figure C.11 Shrinkage from Time Zero vs. ASTM C 157 using HPC

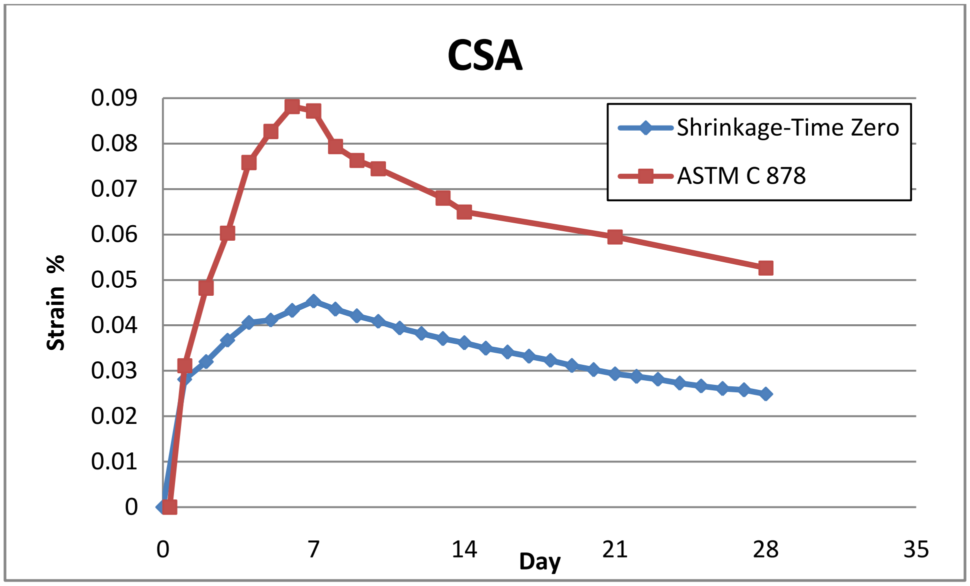

Figure C.12 Shrinkage from Time Zero vs. ASTM C 878 using CSA

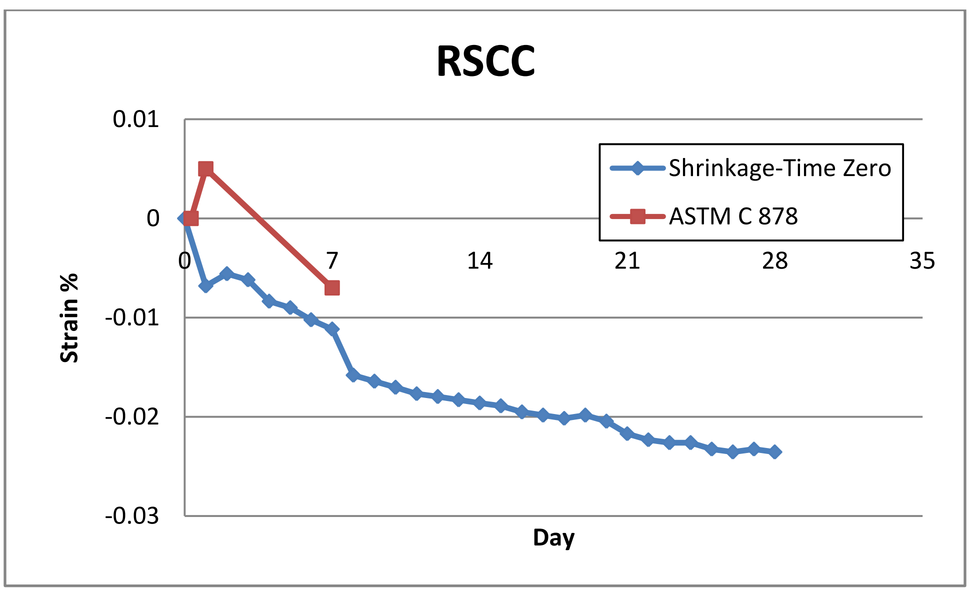

Figure C.13 Shrinkage from Time Zero vs. ASTM C 878 using RSCC

C.2.3. Comparing Shrinkage from Time Zero with Slab on Grade Test Results (28 Days)

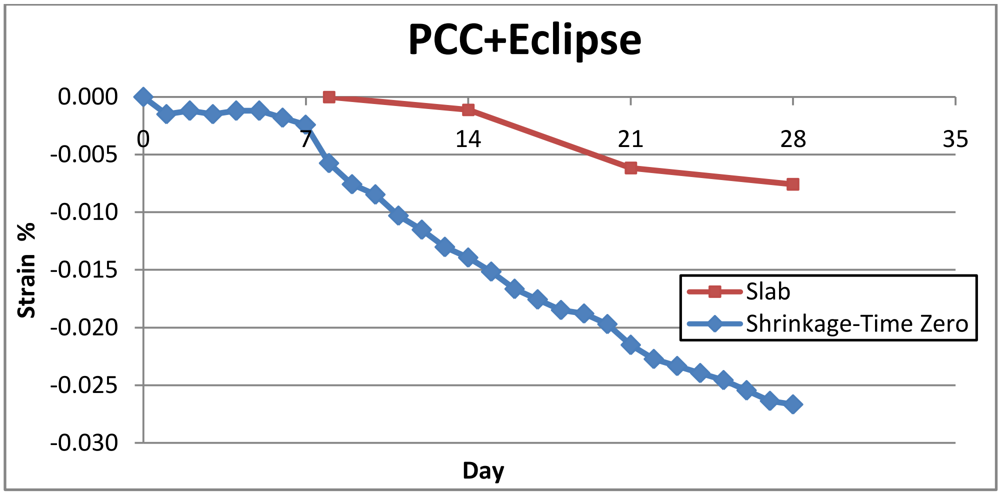

Figure C.14 Shrinkage from Time Zero vs. Slab-on-Grade using PCC with Eclipse

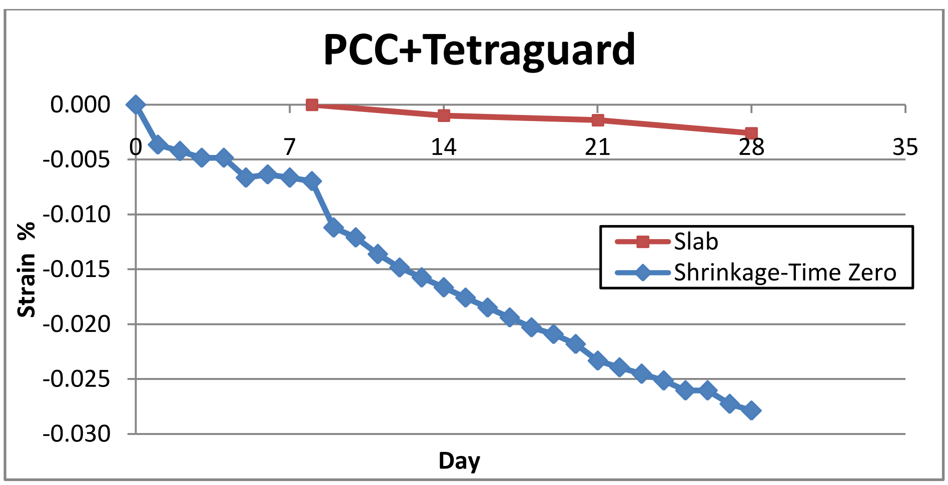

Figure C.15 Shrinkage from Time Zero vs. Slab-on-Grade using PCC with Tetraguard

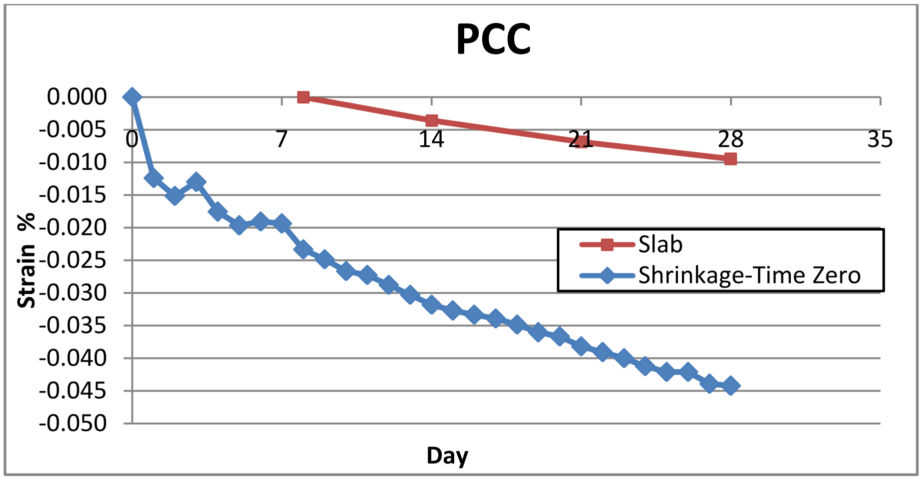

Figure C.16 Shrinkage from Time Zero vs. Slab-on-Grade using grade using PCC

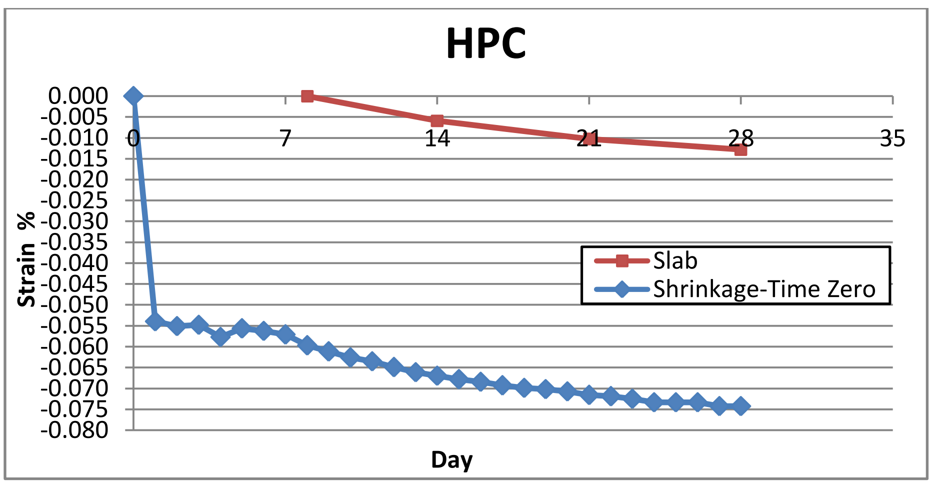

Figure C.17 Shrinkage from Time Zero vs. Slab-on-Grade using using HPC

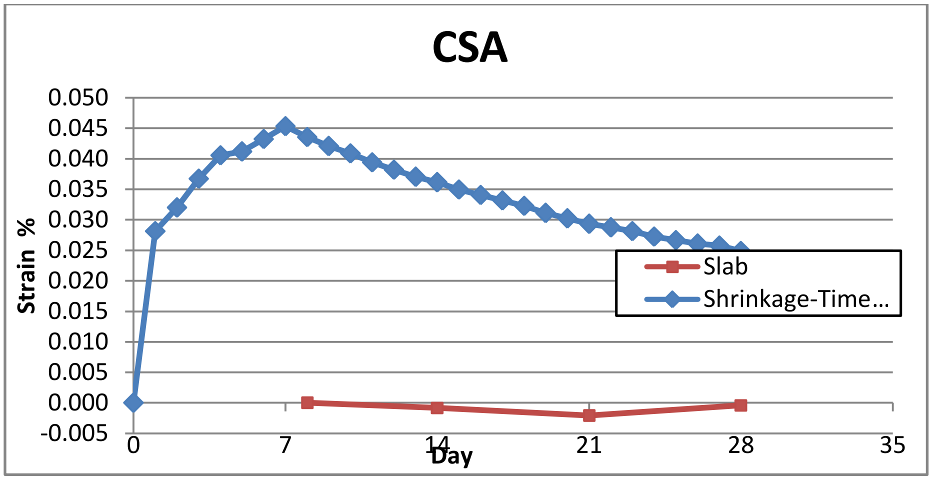

Figure C.18 Shrinkage from Time Zero vs. Slab-on-Grade using CSA

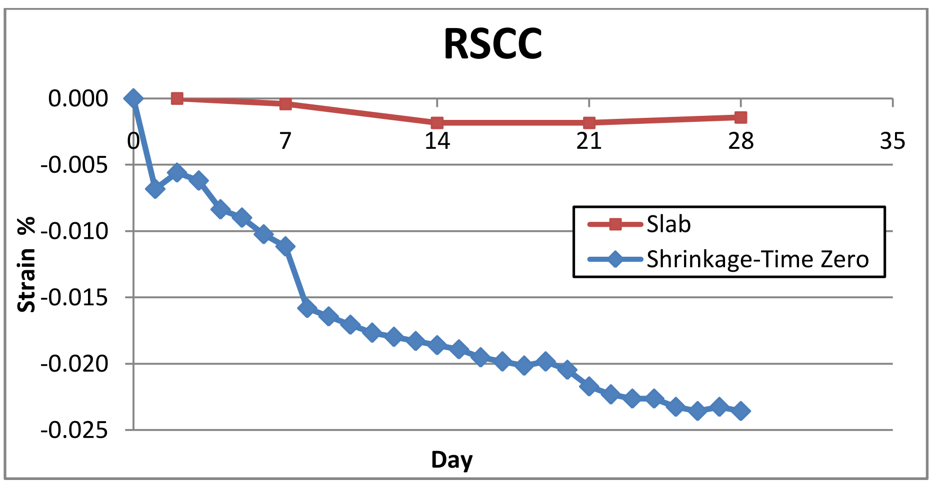

Figure C.19 Shrinkage from Time Zero vs. Slab-on-Grade using RSCC

C.3. Strain of Test Specimens for 110 Days Using Shrinkage from Time Zero

C.3.1. Strain of the Specimens Measured with Dial Gage (Dial Indicator)

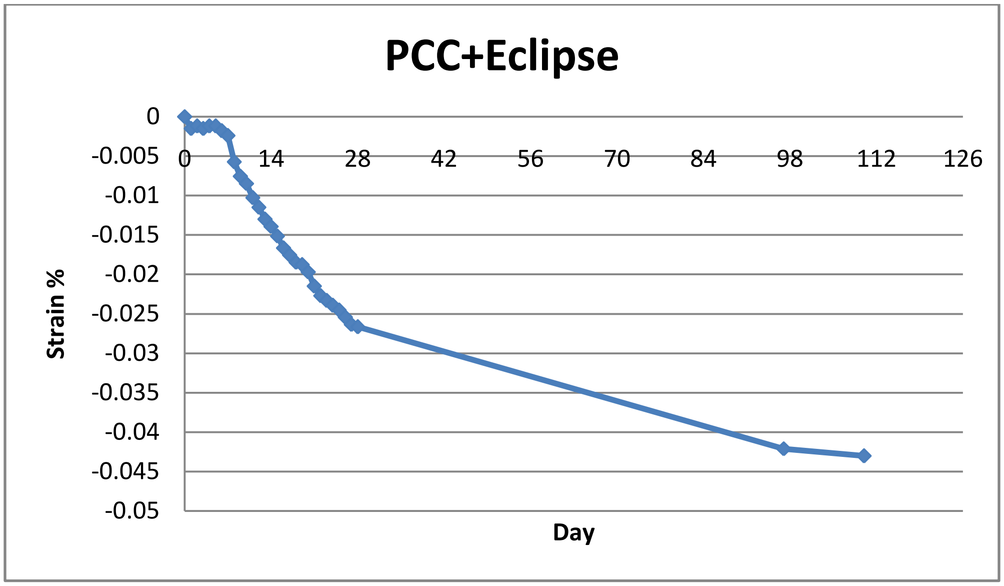

Figure C.20 Shrinkage from time zero using PCC+ Eclips (SRA)

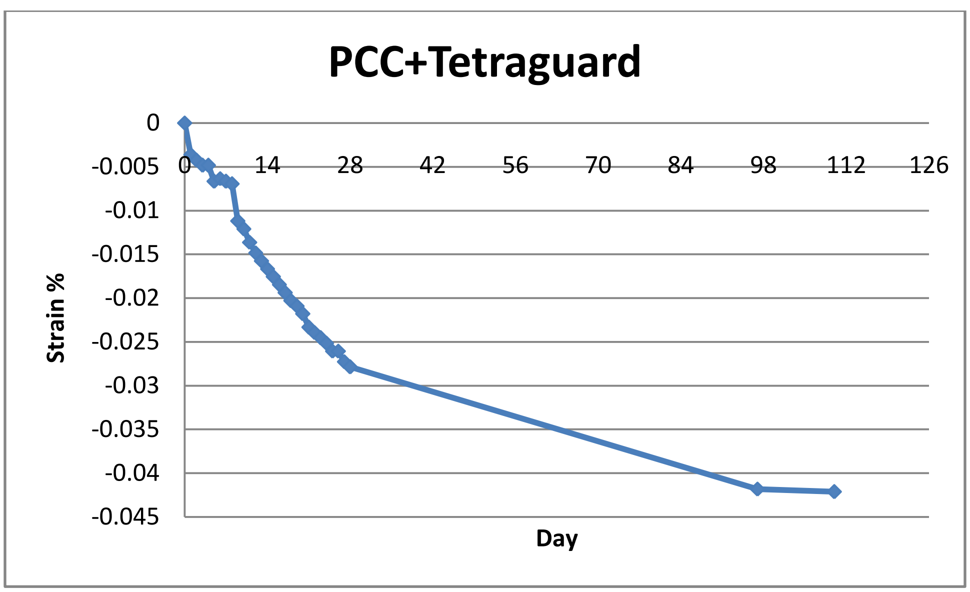

Figure C.21 Shrinkage from time zero using PCC+ Tetraguard (SRA)

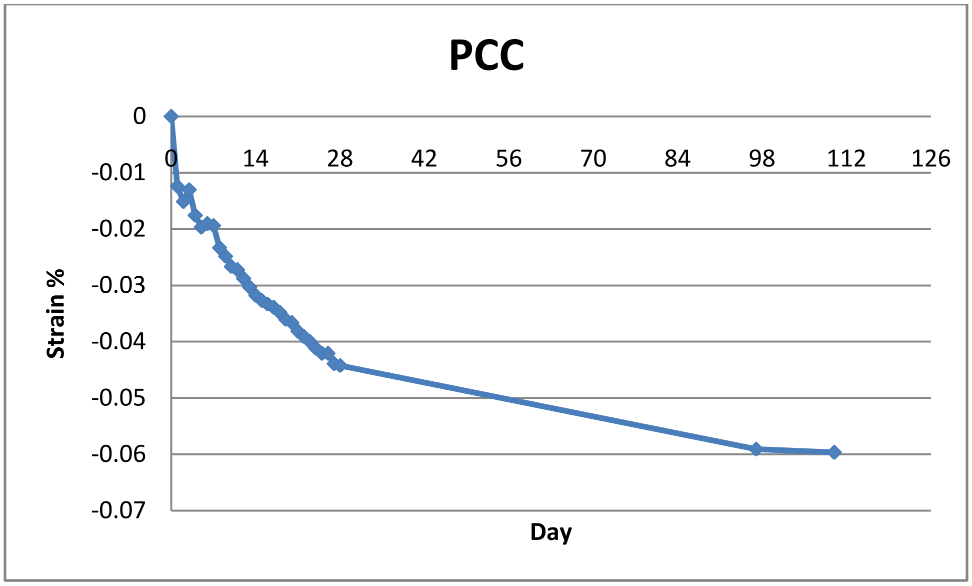

Figure C.22 Shrinkage from time zero using PCC

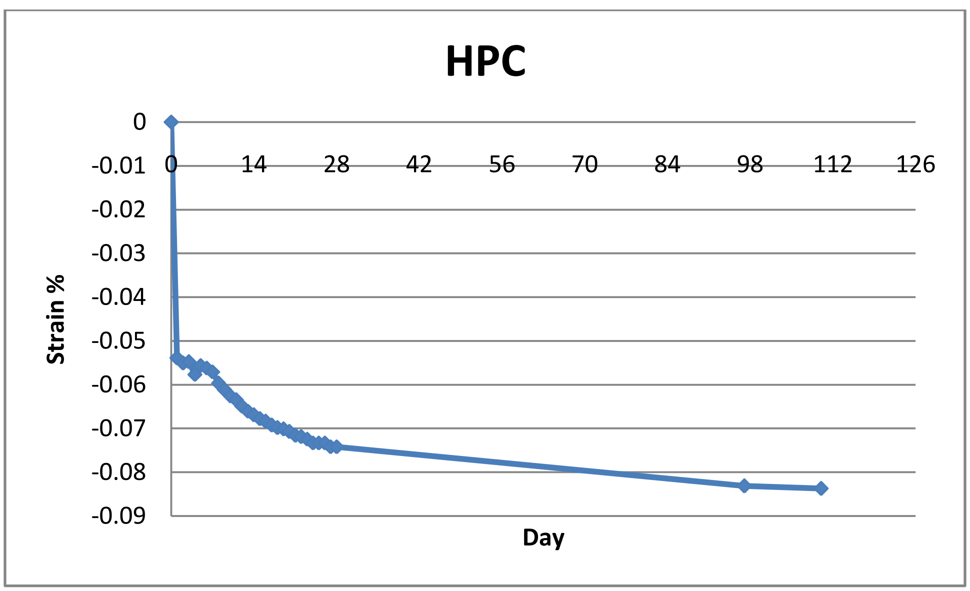

Figure C.23 Shrinkage from time zero using HPC

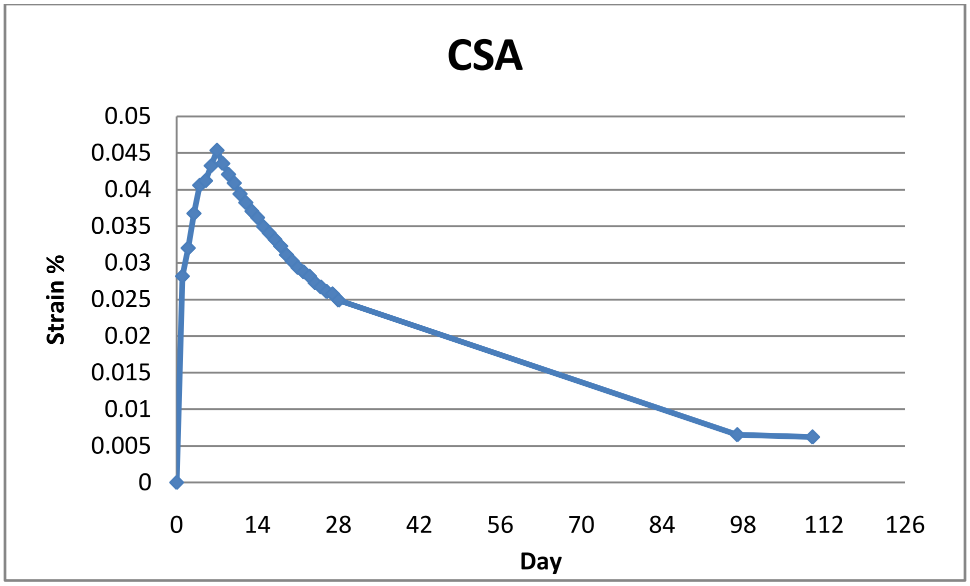

Figure C.24 Shrinkage from time zero using CSA

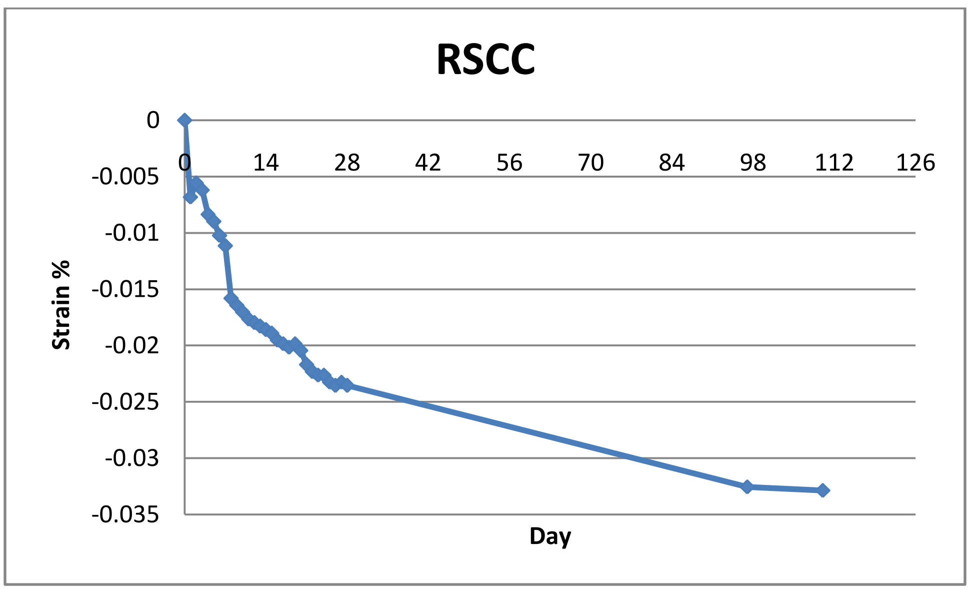

Figure C.25 Shrinkage from time zero using RSCC

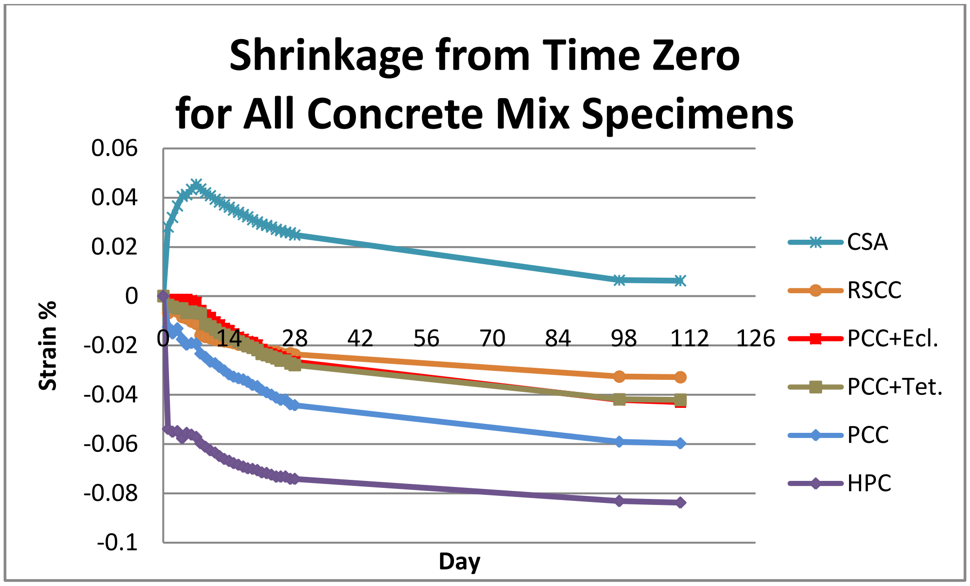

Figure C.26 Shrinkage from time zero for all specimens for 110 days

C.3.2. Two Methods Test Results Comparison (for 110 Days)

Note: In this section and and section C3.3, 110 days test results for shrinkage from time zero is compared with ASTM C 157, C 878, and slab on grade.

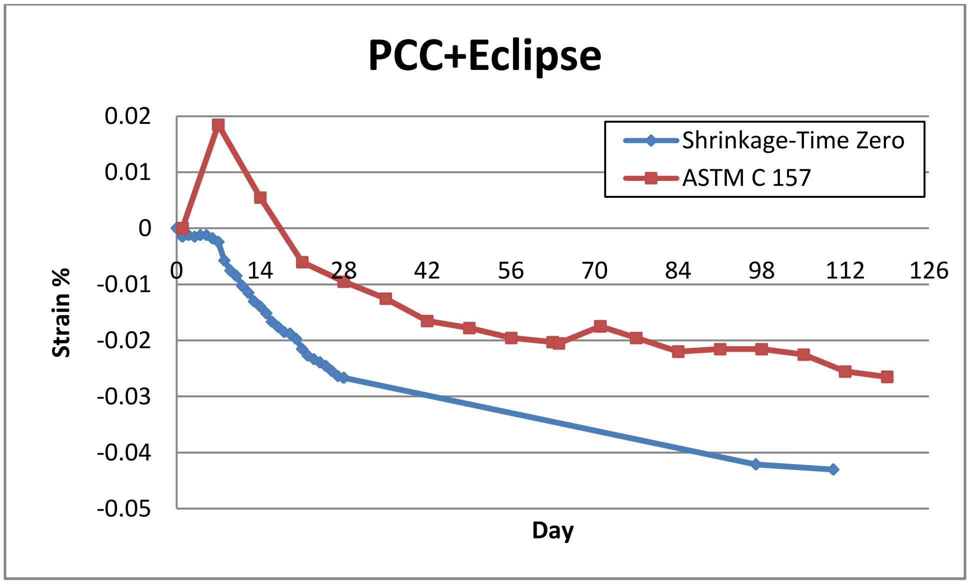

Figure C.27 Shrinkage from Time Zero vs. ASTM C 157 using PCC+Eclipse

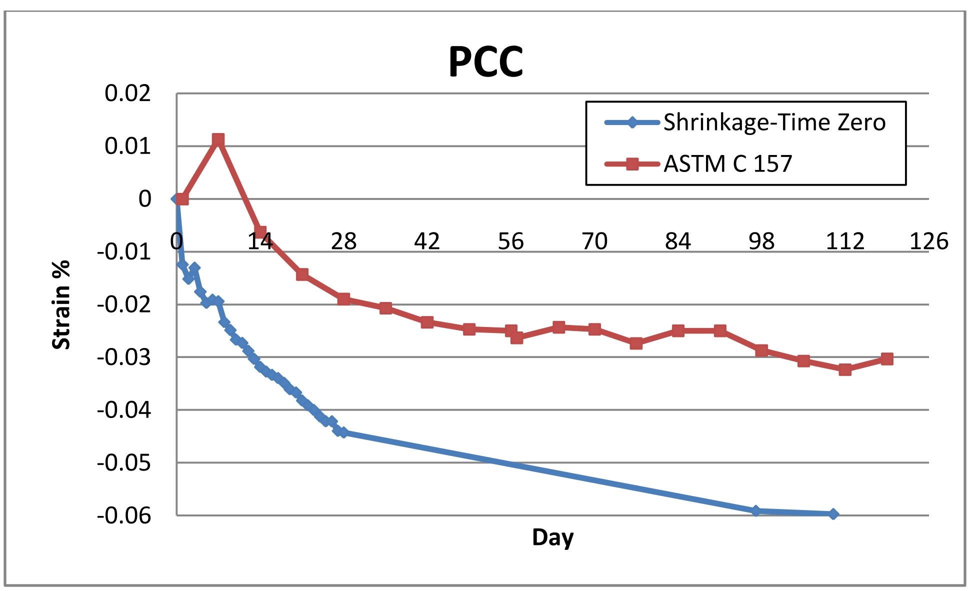

Figure C.28 Shrinkage from Time Zero vs. ASTM C 157 using PCC

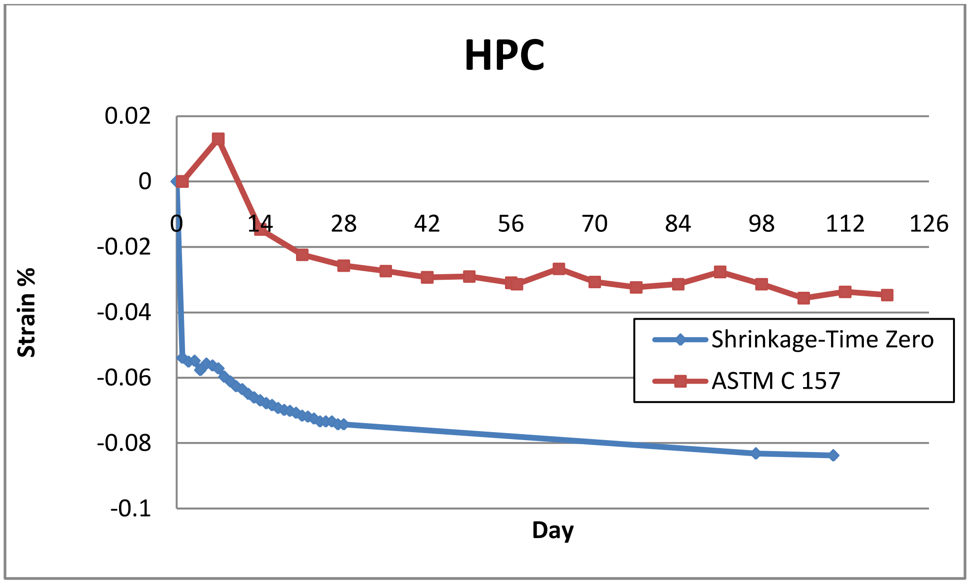

Figure C.29 Shrinkage from Time Zero vs. ASTM C 157 using HPC

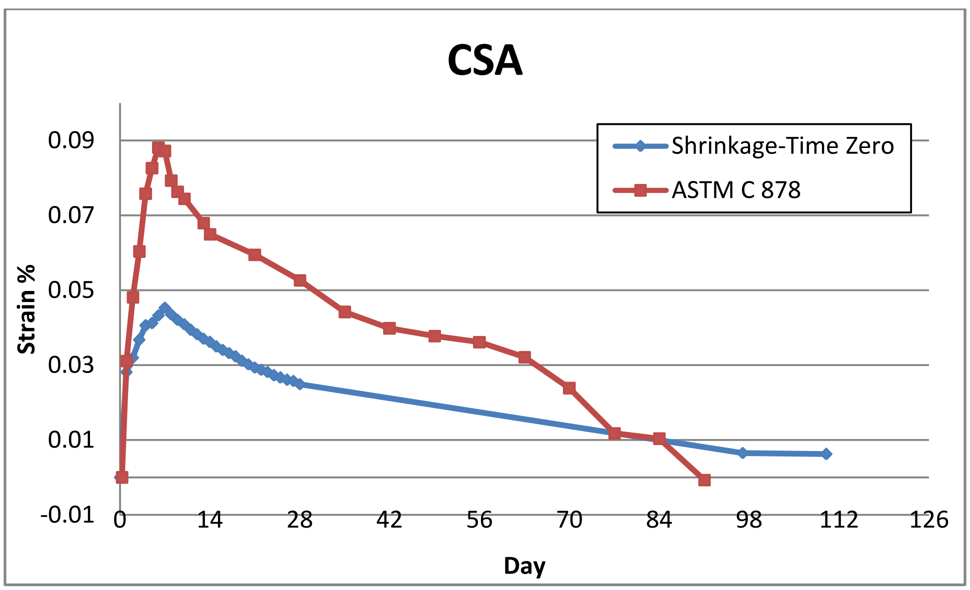

Figure C.30 Shrinkage from Time Zero vs. ASTM C 878 using CSA

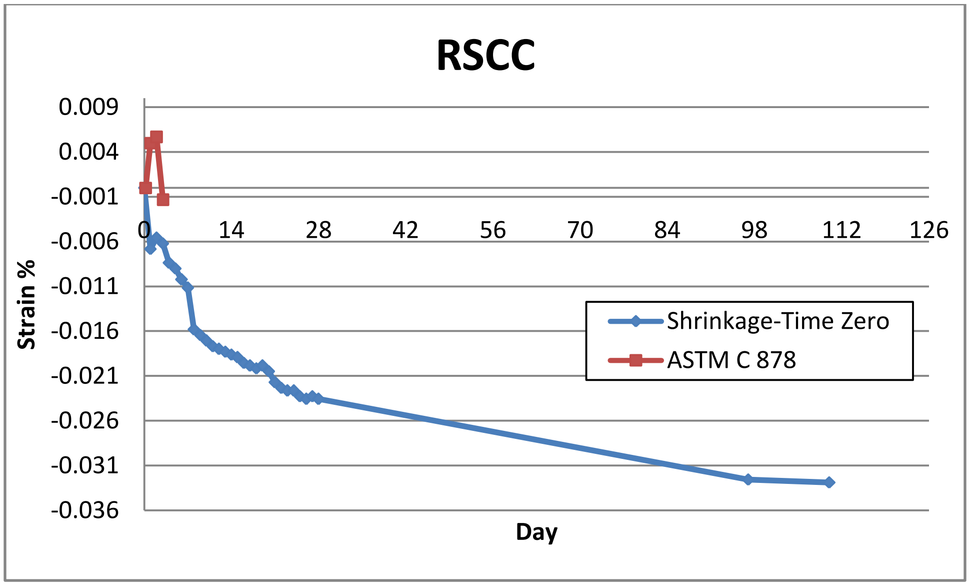

Figure C.31 Shrinkage from Time Zero vs. ASTM C 878 using RSCC

C.3.3. Comparing Shrinkage from Time Zero with Slab on Grade Test Results (110 Days)

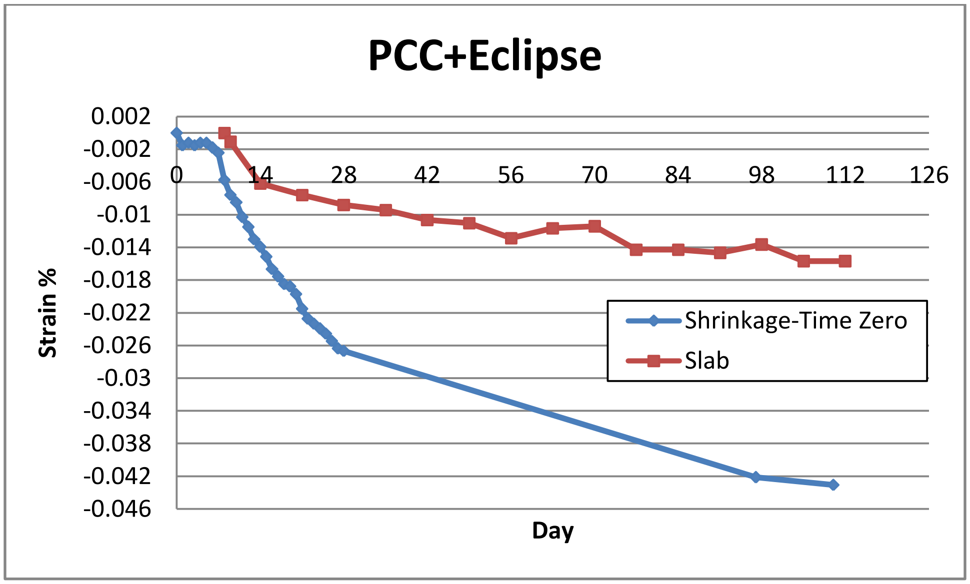

Figure C.32 Shrinkage from Time Zero vs. Slab-on-Grade using PCCwith Eclipse

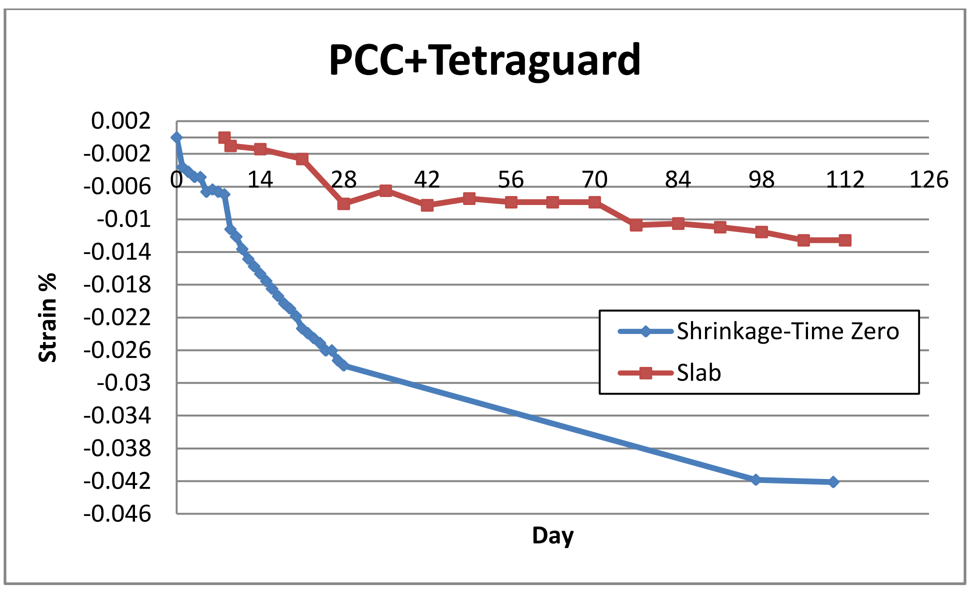

Figure C.33 Shrinkage from Time Zero vs. Slab-on-Grade grade using PCCwith Tetraguard

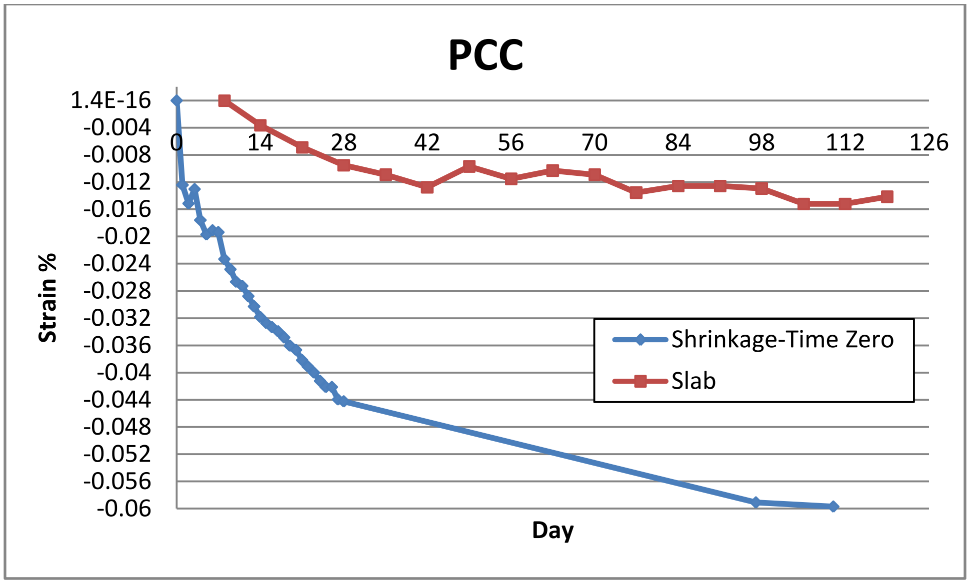

Figure C.34 Shrinkage from Time Zero vs. Slab-on-Grade using PCC

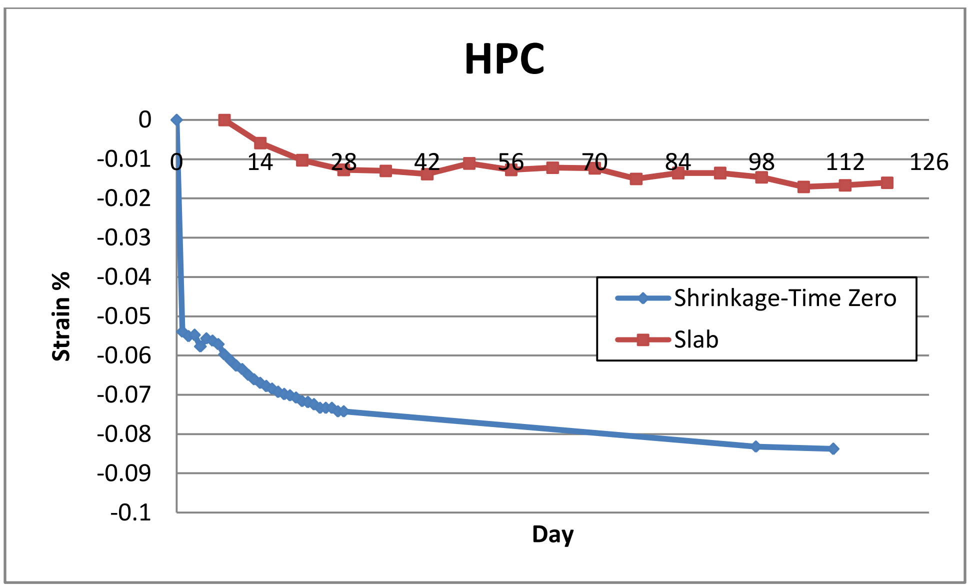

Figure C.35 Shrinkage from Time Zero vs. Slab-on-Grade using HPC

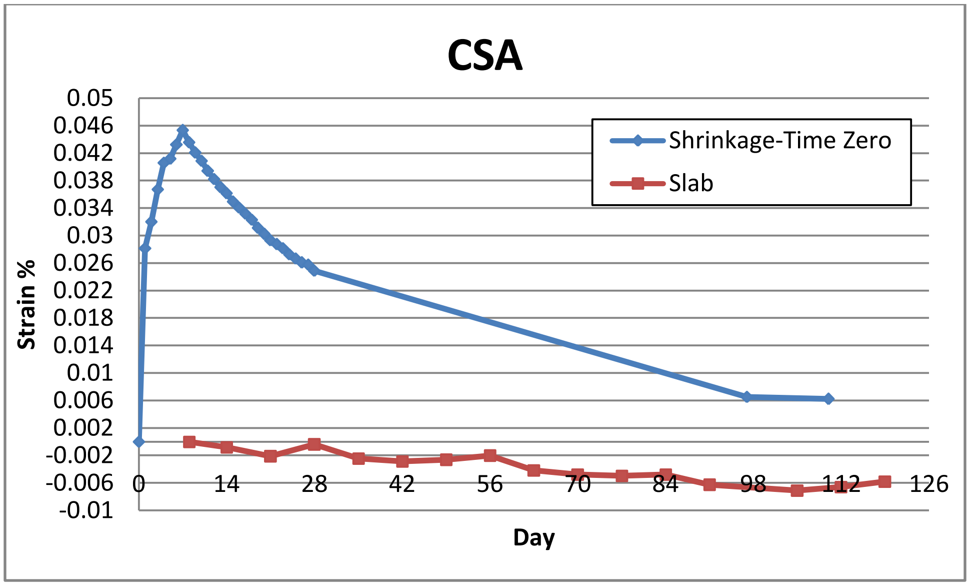

Figure C.36 Shrinkage from Time Zero vs. Slab-on-Grade using CSA

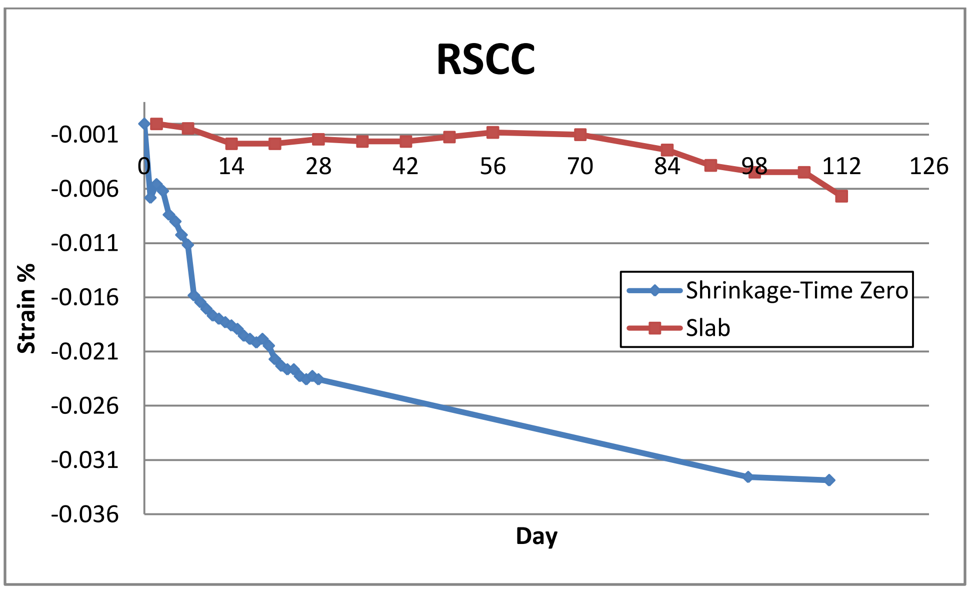

Figure C.37 Shrinkage from Time Zero vs. Slab-on-Grade using RSCC

APPENDIX D

Additional Pictures

Large Scale Slab and

Shrinkage from Time Zero Test Setup

D.1. Large Scale Slab Test Set up

Figure D.1 Making gap into the sand at the sides of the slab specimens to place the Foam around the slab specimens

Figure D.2 Placing Foam around the slab specimens

Figure D.3 Making measurement for the end of slab to provide 9 in. depth

Figure D.4 Placing bolt into the existing slab floor at the end of slab specimens

Figure D.5 Placing Plate at the ends of the slab specimens

Figure D.6 Plate at the ends of the slab specimens

Figure D.7 Fixing location of the plate at the end of the slab specimen

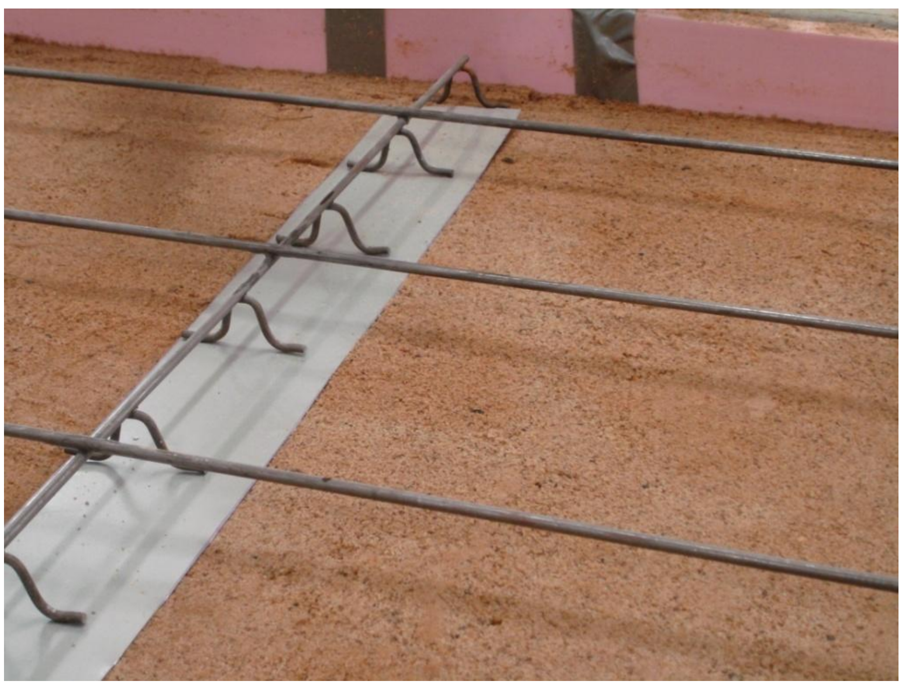

Figure D.8 Chair placed on the Aluminum sheet to prevent depressing chair into the sand

D.2. Demec Target

Figure D.9 Demec target comparator

Figure D.10 Strain gage

Figure D.11 Set of the devices used for surface strain measurements

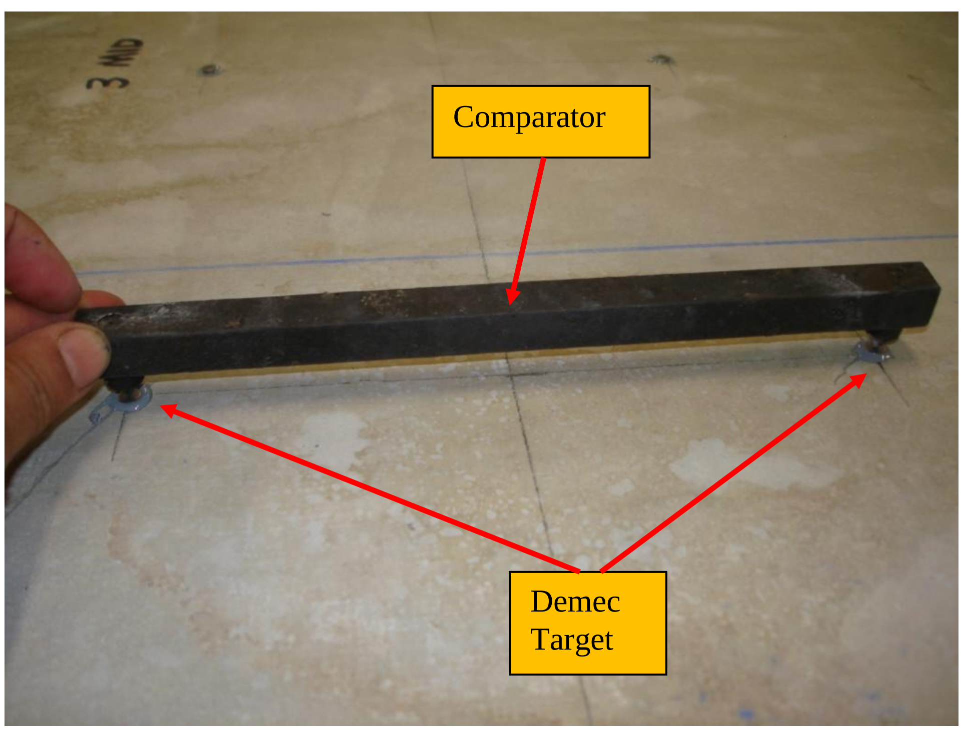

Figure D.12 Using Comparator to fix location of the Demec targets when attaching to the surface

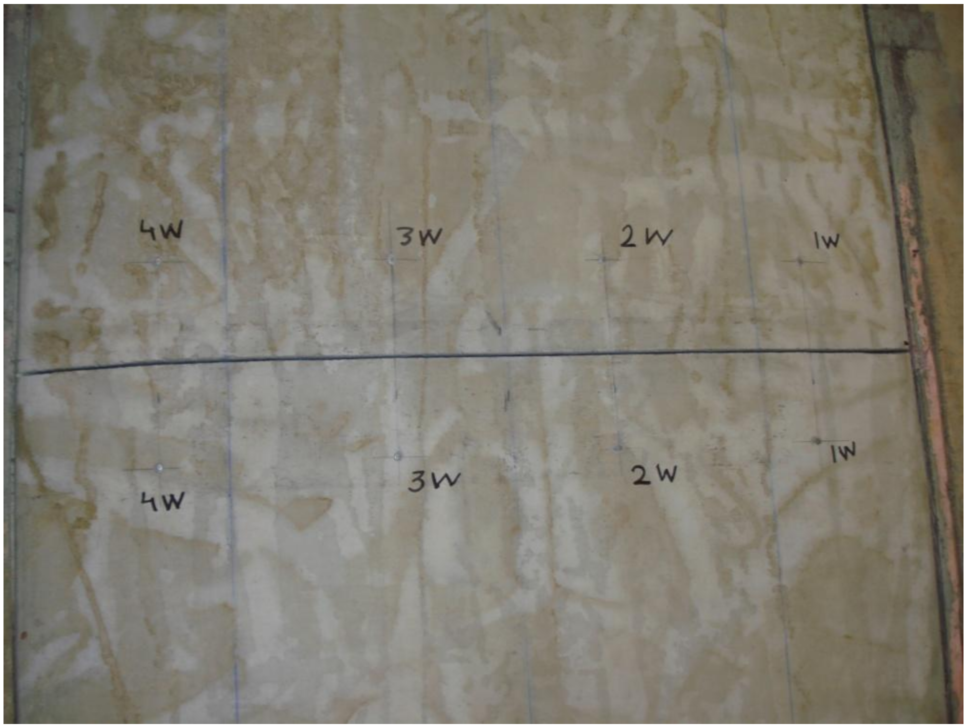

Figure D.13 Top view of control joint showing Demec targets at 1W, 2W, 3W, and 4W points

Note: for example 1W means point one of joint opening located at the west side of the slab.

D.3. Measuring Slump

Figure D.14 Slump test

Figure D.15 Concrete slump measurement

D.3. Prism Test Specimens (ASTM Method)

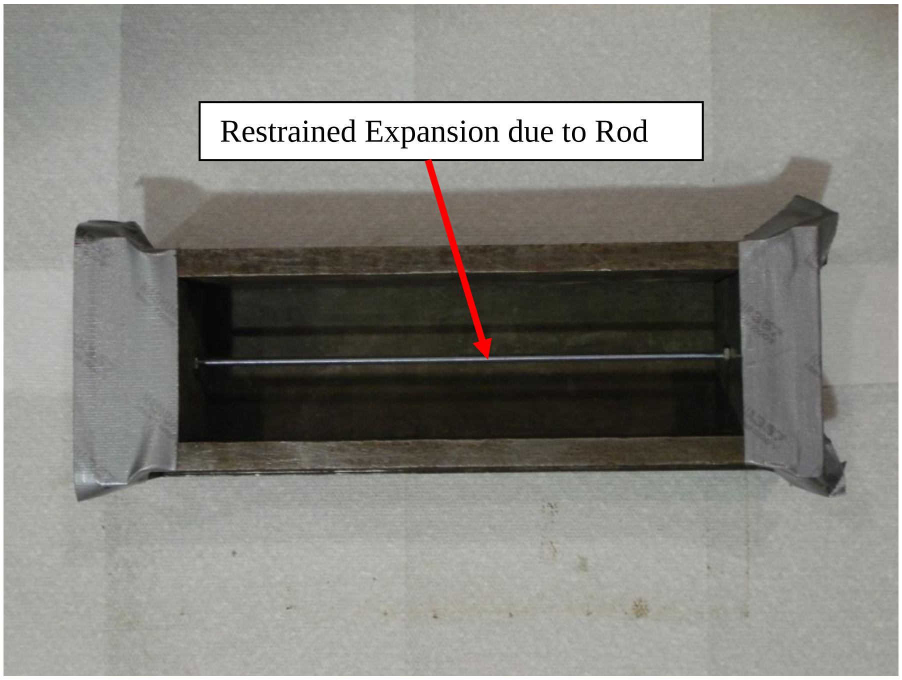

Figure D.16 Prism form was used for ASTM C 878 restrained expansion method

Figure D.17 Molded specimens

Figure D.18 Cured specimens for 7 days in water and limestone

D.3. Prism Test Specimens (Shrinkage from Time Zero Method)

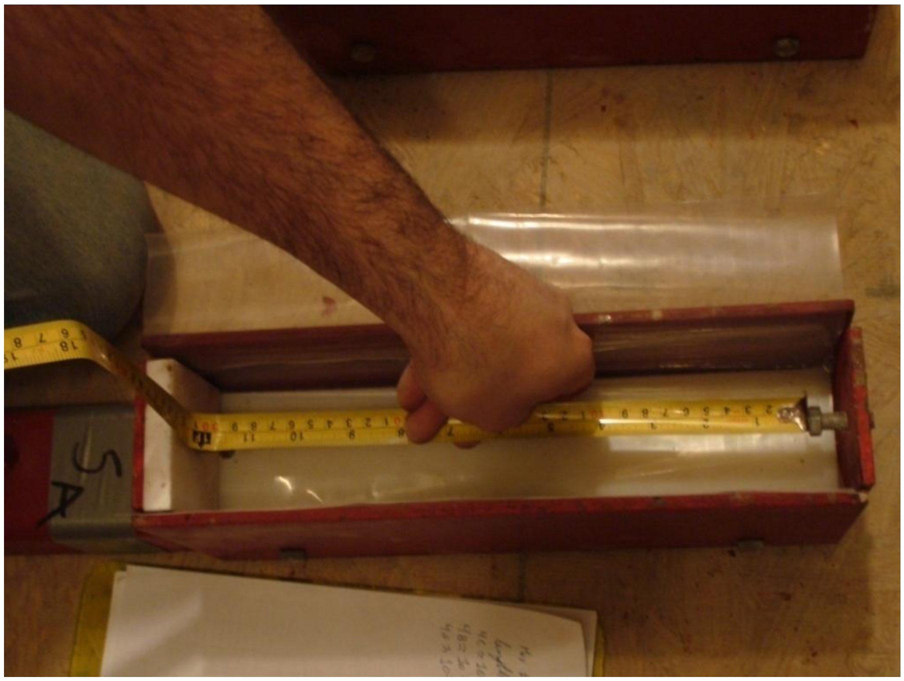

Figure D.19 Prism form was used for “shrinkage from time zero” method

D.3.1. Curing for the Specimens used for "Shrinkage from Time Zero" Method

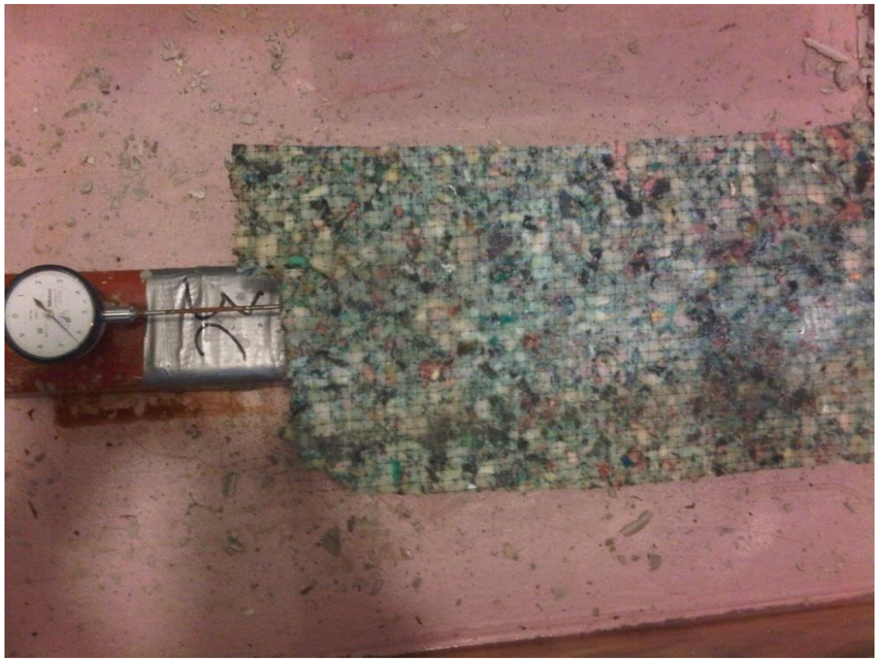

Figure D.20 Cured specimens using wet sponge

Figure D.21 Placed specimens in a closed box to keep Humidity during the curing time

APPENDIX E

Devices' Specifications

E.1. Slab Relative Humidity and Temperature Meter Specifications

	0.5 in.	1 in.	1.5 in.	2 in.	2.5 in.
PCC+Eclipse	NA	3F123BC3BD76	3F11E5C5FD76	3F8266F72D76	3F123A4A0D76
PCC+Tetraguard	3F11E6EB5D76	3F9198D1DD76	3FC1BA900A76	3F126435BD76	3F5226ECBC76
PCC	3F0266BB0C76	3F5185F2FD76	3F0225413C76	3F42659EEA76	3F8218A83A76
HPC	3FD1872D3D76	3F11A5F54D76	3F5206AF6C76	3F1225883D76	3F0266A03D76
CSA#1	3F91A537CD76	3F11E4884A74	3F5185E92A76	3F4265871D76	3F1279FE1C76
CSA#2	3F021AF00C76	3F5224133C76	3F52642E4C76	3F11E586BC76	3F5224FBED76
RSCC	3F122783ED76	3F9265AD4C76	3F5187401D76	3F1278A89A76	3E91E443BA76

E.2. Forney Machine Specifications

Forney Machine	
Model	F-600C-LCI
Serial	96054
Capacity	600,000 lbs
Voltage	115
Phaze	1